

TROPICAL CYCLONE INTENSIFICATION
FROM FINITE AMPLITUDE DISTURBANCES
or *How Hurricanes Hardly Happen*

by

MARK DAVID HANDEL

A.B.Hon. in Physics, The College, The University of Chicago (1979)
S.M. in Oceanography, Massachusetts Institute of Technology (1984)

Submitted to the Department of
Earth, Atmospheric, and Planetary Sciences
in partial fulfillment of the requirements for the degree of
DOCTOR OF SCIENCE in ATMOSPHERIC PHYSICS
at the
MASSACHUSETTS INSTITUTE OF TECHNOLOGY

February 1991

© Massachusetts Institute of Technology 1990
All rights reserved

Signature of Author _____
Center for Meteorology and Physical Oceanography
Department of Earth, Atmospheric and Planetary Sciences
13 September 1990

Certified by _____
Kerry A. Emanuel
Professor of Meteorology
Thesis Supervisor

Accepted by _____
Thomas H. Jordan
Chair
Departmental Committee on Graduate Students

MASSACHUSETTS INSTITUTE
OF TECHNOLOGY
WITHDRAWN
OCT 17 1990
Lindgren
LIBRARIES
RADIES

TROPICAL CYCLONE INTENSIFICATION FROM FINITE AMPLITUDE DISTURBANCES

or How Hurricanes Hardly Happen

by Mark David Handel

Submitted to the Department of Earth, Atmospheric and Planetary Sciences
in partial fulfillment of the requirements for the degree of
Doctor of Science in Atmospheric Physics
at the Massachusetts Institute of Technology, 13 September 1990

ABSTRACT

It has long been known that tropical cyclones depend on fluxes of heat and water vapor from the ocean surface for their primary source of energy. The same can be said of regular tropical cumulus clouds. A tropical cyclone, however, is only observed to occur when a fairly intense disturbance, started with a different energy source, is found over the oceans (though this is not a sufficient condition). There appears to be a threshold for whether or not disturbances intensify, both in the atmosphere and in numerical models. An analytic theory is provided to examine this threshold.

The model is highly simplified and uses two main layers. The boundary layer is more restricted, with fixed height and a diagnostically determined flow. It is assumed that the boundary layer is moist convectively unstable with respect to the air aloft and that deep convection occurs where there is Ekman pumping out of the boundary layer (though these assumptions are controversial). Weakly nonlinear finite amplitude techniques are applied. In the model, the impediment to linear growth is frictional, though radiative cooling contributes to damping as well.

The instability that is found is essentially a finite amplitude version of Conditional Instability of the Second Kind (CISK). Several nonlinear terms contribute: the faster than linear increase in boundary layer convergence, due to faster than linear increase of the surface drag; the advection of relative vorticity by the disturbance; and the increase in boundary layer entropy due to elevated surface fluxes of water vapor and sensible heat.

Necessary conditions for tropical cyclone intensification are discussed. Comparison is made between this Finite Amplitude CISK and the recently suggested hurricane air-sea interaction theory.

Thesis Supervisor: Kerry A. Emanuel
Professor of Meteorology

This thesis is dedicated to
the memory of my grandfather

Aaron Morris Ruby
who helped to shift my path
from firefighter to scientist.

I shall speak next of Hurricanes.

These are violent storms, raging chiefly among the
Caribee Islands; though by Relation, Jamaica has of
late been much annoyed by them; but it has been since
the time of my being there. They are expected in *July*,
August or *September*.

— William Dampier, 1699

"It seems to me that almost everything is a waste of time," he remarked one day as walked dejectedly home from school. "I can't see the point in learning to solve useless problems, or subtracting turnips from turnips, or knowing where Ethiopia is or how to spell February." And, since no one bothered to explain otherwise, he regarded the process of seeking knowledge as the greatest waste of time of all.

*Milo in
Norton Juster
The Phantom Tollbooth*

Acknowledgments

Many people have contributed to my long survival here. I would like to thank Kerry Emanuel for introducing me to the problems of hurricane dynamics, for his continued support and suggestions, and finally for the care with which he went over earlier drafts of this thesis. It is important to note that although he has served as my advisor, he has not only tolerated, but encouraged, dissent. There remain assumptions within this work with which, I know, he has substantial disagreement. Nevertheless, he has never discouraged me on the path I have taken. His objections have served as an excellent foil.

Others, both here and elsewhere, have filled in some crucial gaps. Earle Williams asked many of those simple questions which were so difficult to answer. Willem Malkus first showed me the ways of finite amplitude theory. Ronald Miller, Christopher Davis, John Nielsen, Peter Neille, Peter Stone, Chantal Rivest, Richard Lindzen, Richard Rotunno, Hugh Willoughby, and Frank Marks have all provided some grease for the brain. Early warnings and encouragement were provided by Joseph Ferretti. Comments on drafts of this work by Kerry Emanuel, Earle Williams, Frederick Sanders, and Christopher Davis were greatly appreciated.

Diana Spiegel has been a continual source of support and good will in dealing with our myriad computer systems. Jane McNabb has kept most of the bureaucracy at bay. The staffs of the MIT libraries, Lindgren and Interlibrary Borrowing in particular, and the Rare Book and Manuscript Department of the Boston Public Library, have been helpful.

James Risbey has been a gem as a friend and officemate. Our collaborations have kept me going during the past two years. As I leave here, I realize that the ease of our relationship in close quarters will be more difficult to replace than our office view. Several other people have also had to survive me as an officemate. I thank Chantal Rivest, Peter Sousounis, Xu Kuan-man, and Marilyn Wolfson (*in absentia*) for their help and forbearance.

As a friend, I have sometimes been less than fully present for some of the people closest to me; I thank William Tse and Mark Holzbach for their love and patience. Finally, I thank my parents, Irma and Mort Handel. They have helped me morally and financially over more years than we would have imagined.

The support of the Fannie and John Hertz Foundation from 1984 to 1985 is gratefully acknowledged. This research was supported by grants NSF/g 8513871-ATM and NSF 8815008-ATM. Provisions from the CMPO Fund for Potable Water and the Ladies Auxiliary of the Wave Over-Reflection Tea Society (Richard Lindzen, administrator) were essential.

An attempt has been made to keep most of this readable by my physics inclined friends who are not meteorologists (sometimes by translating meteorology into physics with footnotes). This should also help meteorology graduate students, since courses often ignore the lower latitudes. I beg the indulgence of those for whom the introductory material is “old hat”; after reading the initial paragraphs, they can charge in at chapter four, “De gustibus non est disputandum”.

Tigger

*Jamaica Plain, Massachusetts
13 September 1990*

Contents

Abstract	3
Acknowledgments	7
List of Figures	12
List of Tables	14
List of Symbols and Abbreviations	15
1 Introduction	23
1.1 Tropical Cyclones	24
1.2 Existence of a Threshold	27
1.3 The Way	30
1.4 Layout of Mathematics	32
2 Building a Tropical Cyclone	37
2.1 Structure	38
2.2 Intensification	46
2.3 Entropy and Energy	50
2.4 Angular Momentum	61
2.5 Precursors	62
3 Previous Work	65
3.1 Observations	67
3.1.1 Climatology and Composite Studies	69
3.1.2 Case Studies	73

3.2	Theory and Numerical Modelling	77
3.2.1	Early Theoretical Work	78
3.2.2	Conditional Instability of the Second Kind — CISK	82
3.2.3	Hurricane Air-Sea Interaction Theory — HASIT	86
3.2.4	Other Theoretical Work	89
3.2.5	Other Numerical Modelling Work	92
4	De Gustibus Non Est Disputandum	95
4.1	A Weak Disturbance is Not a Hurricane	95
4.2	Objections to CISK	97
4.3	Existence of CAPE (Convective Available Potential Energy)	100
4.4	Circular Disturbances	106
4.5	Ekman Layers	107
4.6	Sensitivity	110
5	Physics of the Model	113
5.1	Basic Equations	113
5.2	Expansions	125
5.3	Stationary Solutions	130
5.4	Energy Equations	132
6	Linear Theory	135
6.1	Ooyama's Linear Model	135
6.2	Linear Stationary Problem	139
6.2.1	Dissipative Linear Stationary System	139
6.2.2	Basis Functions and Nondimensionalization	143
6.2.3	Transformation to Self-Adjoint System	152
6.2.4	Calculation of the Linear Solution	155
6.2.5	Linear Solutions	160
6.3	Time Dependent Linear Problem	169
6.4	Only a Little Friction	172

7	Finite Amplitude Disturbances	175
7.1	Weakly Finite Amplitude Theory	175
7.1.1	Adjoint and Solvability Conditions	180
7.2	Amplitude of the Stationary Solutions	181
7.3	Stability of the Stationary Solutions	186
7.4	Thresholds and Growth Rates	191
7.5	Amplitude Equations and Superexponential Growth	209
8	Discussions and Conclusions	215
8.1	Discussions	215
8.1.1	Application to Real Disturbances	215
8.1.2	Disturbance Height and Vertical Instability	219
8.1.3	Development at Second Order	221
8.1.4	Our Original Questions	223
8.2	CISK vs. HASIT: Proposed Tests	228
8.3	Conclusions	231
	Epilogue	235
	Scientific Priorities	235
	Tropical Cyclone Modification	237
	References	241

List of Figures

2.1	Vertical cross section of temperature anomalies (K) for Hurricane Hilda.	39
2.2	Average relative humidity for a composite Pacific typhoon.	40
2.3	Vertical cross sections of azimuthal winds in the core of Hurricane Hilda and out to larger radius for a Pacific composite typhoon. . .	42
2.4	Averaged radial winds for a composite typhoon.	44
2.5	Averaged vertical motion for a composite typhoon.	44
2.6	Stream function for the core of a hurricane.	45
2.7	Radar reflectivity for a hurricane in plan view and cross section. .	47
2.8	Cross section of equivalent potential temperature for the core of a mature hurricane.	55
2.9	Skew-T diagram showing moist pseudoadiabats.	56
4.1	Temperature sounding for pseudoadiabatic ascent compared with virtual temperature for reversible ascent.	102
5.1	Coordinates and layers.	114
5.2	Cumulus parameterization scheme.	119
6.1	Schematic of regions and forcing.	142
6.2	Bessel and modified Bessel functions.	145
6.3	Plots of the critical value of the forcing parameter, $\eta^{(0)}$, as a function of the vertical and lateral diffusion ratios, M and K, for two values of the cooling parameter (a) B = 0 and (b) B = 0.01.	149
6.4	The squares of the nondimensional wavenumbers as a function of the forcing parameter, $\eta^{(0)}$	151
6.5	The squares of the nondimensional wavenumbers as a function of the lateral diffusion ratio, K.	152

6.6	The squares of the nondimensional wavenumbers as a function of the vertical diffusion ratio, M	153
6.7	The squares of the nondimensional wavenumbers as a function of the cooling parameter, B	153
6.8	A solution to the linear stationary problem with $M = 0.5$, $K = 0.5$, $B = 0.005$, $r_1 = 10.0$	162
6.9	Solutions to the linear problem with the same parameter values as in figure 6.8, but varying the outer radius, $r_1 = 6.0, 14.0$	164
6.10	Solution to the linear problem with $M = 0.2$, $K = 0.5$, $B = 0.005$, $r_1 = 10.0$	166
6.11	Solution to the linear problem with $M = 0.5$, $K = 0.2$, $B = 0.005$, $r_1 = 10.0$	166
6.12	Variations in the neutral forcing parameter, $\eta^{(0)}$, and the updraft extent, r_0 , for linear stationary solutions as a function of vertical diffusion ratio, M	167
6.13	Variations in relative anticyclone strength, R_2 , and relative inflow strength, R_3 , for linear stationary solutions as a function of vertical diffusion ratio, M	167
6.14	Solution to the linear problem with $M = 0.5$, $K = 0.2$, $B = 0.050$, $r_1 = 6.0$	168
6.15	Growth rate as a function of the square of the nondimensional cylindrical wavenumber.	172
7.1	The function $\Phi_1^{(1)}(r)$ for the solution in figure 6.14.	189
7.2	First order variations of the boundary layer and upper layer entropy, $\chi_0^{(1)}$ and $\chi_2^{(1)}$, respectively.	194
7.3	First order variation of the forcing parameter due to entropy changes, i.e. $\eta_r^{(1)}$, based on the $\chi_j^{(0)}$ of figure 7.2.	194
7.4	Second order correction to Ekman pumping, $w^{(2*)}$	196
7.5	Orbits for the quadratic amplitude equation.	210
7.6	Orbits for the cubic amplitude equation.	211
8.1	Schematic of the regions of decaying and growing states as a function of disturbance amplitude and ambient forcing parameter. . .	217

List of Tables

6.1	Properties of stationary solutions.	165
7.1	Values of parameters kept fixed in the following calculations. . . .	192
7.2	Evaluation of integrals.	197
7.3	Variations in finite amplitude instability criteria with variations in quadratic bulk momentum diffusion coefficient, C_D	202
7.4	Variations in finite amplitude instability criteria with variations in quadratic bulk entropy diffusion coefficient, C_E	202
7.5	Variations in finite amplitude instability criteria with variations in Coriolis parameter.	203
7.6	Variations in finite amplitude instability criteria with variations in the lateral diffusion coefficients.	204
7.7	Variations in finite amplitude instability criteria with proportional variations in the linear boundary layer diffusion coefficient k_s and the vertical diffusion coefficient μ	204
7.8	Variations in finite amplitude instability criteria with variations in overall disturbance size, r_1	205
7.9	Variations in finite amplitude instability criteria with variations in the upper level lateral diffusion.	207
7.10	Variations in finite amplitude instability criteria with variations in the lower level lateral diffusion.	207
7.11	Variations in finite amplitude instability criteria with variations in the internal vertical diffusion.	208
7.12	Variations in finite amplitude instability criteria with variations in the linear drag coefficient.	208

Lists of Symbols and Abbreviations

Symbols

Certain conventions have been followed in choosing symbols. Standard meteorological conventions have been used where possible. In many cases the notation of Ooyama 1969 has been adopted. In general the following rules hold. Subscripts of 0, 1, or 2 on many variables refer to a specific layer, with a generic subscript of j implying that the expression applies in all layers. Superscripts in parentheses refer to terms in an amplitude expansion, with the superscript (0) labeling quantities that are constants for the rest state, the superscript (1) applying to the lowest order solutions of motion, etc. [the superscript (2*) has a special meaning, see p. 129]. An overbar indicates a steady quantity, while a tilde indicates a time dependent quantity (often infinitesimal). Variables with a plus or minus superscript are nonnegative, with plus signs associated with upward motion and minus signs associated with downward motion. Primes are used to distinguish closely related symbols and are not operators of any sort; they are also used for solutions of amplitude a' (see p. 178). A superscript of T indicates a transpose and a superscript of \dagger indicates an adjoint; sometimes these operations are equivalent. Bold faced lower case symbols are vectors and bold faced upper case symbols are matrices (all square). If a symbol exists in related italic and roman faces, the roman faced symbol is nondimensional. Following an entry are units of measure, in brackets, according to the the *Système Internationale*, and the page number where the symbol is introduced. Some symbols used only in a single location are not included in this list.

- a = nondimensional amplitude of a solution; p. 125. [N.B. the symbol a , with various subscripts, is also used as a generic coefficient in contexts local to expressions that are not needed elsewhere, i.e. it serves as a dummy variable.]
- \bar{a} = nondimensional amplitude of a stationary solution; p. 125.
- \tilde{a} = nondimensional amplitude of a time dependent solution, usually infinitesimal; pp. 125, 212.

- a_{crit} = critical amplitude for unstable stationary solutions; p. 186.
- \mathbf{A} = coefficient matrix for linear stationary problem in self-adjoint form [m/sec]; p. 154.
- \mathbf{A}' = coefficient matrix for linear stationary problem [m/sec]; p. 141.
- b = radiative cooling constant [sec/m]; p. 123.
- B = $\frac{bf^2k_2^{(0)}}{k_s^2}$, nondimensional cooling parameter; p. 146.
- \mathbf{B} = coefficient matrix for linear stationary problem in self-adjoint form [m³/sec]; p. 154.
- \mathbf{B}' = coefficient matrix for linear stationary problem [m³/sec]; p. 141.
- c_p = specific heat of dry air at constant pressure [J kg⁻¹ K⁻¹]; p. 123.
- c_j = coefficient in an amplitude equation of term proportional to a^j [dimensions depend on value of j]; p.209. Also used as arbitrary constants.
- C_D = (quadratic) drag coefficient; p. 116.
- C_E = bulk surface moisture transfer coefficient; p. 124.
- f = Coriolis parameter (assumed constant) [sec⁻¹]; p. 61.
- g = acceleration of gravity [m sec⁻²]; p. 116.
- G = $\frac{g(1-\epsilon)k_s^2}{f^3k_2^{(0)}}$, nondimensional acceleration of gravity; p. 171.
- h_j = thickness of layer j (0, 1, 2) [m]; p. 114.
- H = $\frac{f}{k_s}\epsilon_j h_j$, nondimensional layer thickness p. 171.
- i = the imaginary number $\sqrt{-1}$; p. 150. Also subscript indicating an inviscid solution; p. 131. Also used as a dummy index.
- I_0 = modified Bessel function of the second kind, zeroeth order; p. 144.
- I_1 = modified Bessel function of the second kind, first order; p. 143.
- j = generic layer subscript, in the set (0, 1, 2); p. 114. Also also used as a dummy index.
- J_0 = Bessel function of the first kind, zeroeth order; p. 144.
- J_1 = Bessel function of the first kind, first order; p. 143.
- k_s = linear drag coefficient [m/sec]; p. 116.
- k_χ = boundary layer eddy diffusivity for entropy [m³/sec]; p. 124.

- k_j = layer integrated lateral eddy diffusion coefficient of angular momentum for layer j (1, 2) [m^3/sec]; p. 116.
- K = $k_1^{(0)}/k_2^{(0)}$, ratio of internal dissipation coefficients; p. 146.
- K_0 = modified Bessel function of the first kind, zeroeth order; p. 144.
- K_1 = modified Bessel function of the first kind, first order; p. 144.
- l = basis function subscript (1, 2, ..., 9); p. 155. Also used as a dummy index.
- L = length scale [m]; pp. 125, 144.
- \mathcal{L} = linear differential operator; p. 176.
- \mathcal{L}^\dagger = differential operator adjoint to \mathcal{L} ; p. 177.
- m = Bessel function wave number or sinusoidal wavenumber [m^{-1}]; p. 137.
- m = nondimensional wave number; p. 144.
- M = μ/k_s , ratio of middle level to surface friction coefficients; p. 146.
- M_j = absolute angular momentum density of layer j (0, 1, 2) [m^2/sec]; pp. 61, 115.
- $\mathcal{M}'^{(2)}$ = nonhomogeneous terms in linear stationary equation (vector) [m^2/sec^2], pp. 178, 183.
- $\mathcal{N}'^{(2)}$ = nonhomogeneous terms in time dependent equation (vector) [m^2/sec^2], pp. 179, 189.
- p_j = pressure in layer j (0, 1, 2) [kPa]; p. 116.
- p_{0j} = average pressure for layer j (1, 2) [kPa]; p. 123.
- p_{00} = reference pressure, 100 kPa; p. 123.
- Q = $Q^+ - Q^-$ = interlayer mass flux between layers 1 and 2 [m/sec]; p. 114.
- Q^- = downwards interlayer mass flux (nonnegative) [m/sec]; p. 114.
- Q^+ = upwards interlayer mass flux (nonnegative) [m/sec]; p. 114.
- r = radial coordinate [m]; p. 113.
- r = nondimensional radial coordinate; p. 155. Also r_0 and r_1 are the nondimensional symbols corresponding to r_0 and r_1 , respectively.
- r_0 = first radius dividing ascent from descent regions; [m]; p. 142.

- r_1 = limiting radius of the domain [m]; p. 141.
 R_j = $|\max(v_j)/\max(v_1)|$ for j in (2, 3); p. 165.
 s_{jl} = coefficients for obtaining v_j from the basis functions X_l ; p. 156.
 S = matrix containing the matching and boundary equations of the linear system; p. 157.
 S' = modified version of S ; p. 159.
 t = time [sec]; p. 114.
 T = as superscript indicates a transpose; p. 178.
 T = transformation matrix; p. 154.
 u_j = radial velocity (positive outwards) in layer j (0, 1, 2) [m/sec]; p. 114.
 \mathcal{U} = kinetic energy density [(m/sec)²]; p. 132.
 v_j = azimuthal velocity in layer j (0, 1, 2) [m/sec]; p. 113.
 $v_{3,4}$ = transformations of $\psi_{1,2}$ [m/sec]; p. 139.
 $v_j^{(1)}$ = solution to the first order linear system with normalized amplitude; p. 125.
 $\bar{v}_j^{(1)}$ = $\bar{a}v_j^{(1)}$ = solution to the stationary first order linear system; p. 129.
 $\tilde{v}_j^{(1)}$ = $\tilde{a}v_j^{(1)}$ = solution to the slowly varying first order linear system; p. 129.
 $v_j^{(2)}$ = solution to the second order system with normalized amplitude; p. 125.
 $\bar{v}_j^{(2)}$ = $v_j^{(2h)} + v_j^{(2)}$ = solution to the second order stationary system; p. 182.
 $\tilde{v}_j^{(2)}$ = $v_j^{(2h)} + v_j^{(2)}$ = solution to the second order time dependent system; p. 187.
 $v_j^{(2)}$ = particular solution to the inhomogeneous second order stationary system; p. 129.
 $v_j^{(\tilde{2})}$ = particular solution to the inhomogeneous second order time dependent system; p. 129.
 $v_j^{(2h)}$ = solution to the homogeneous part of the second order stationary system, proportional to $v_j^{(1)}$; p. 182.

- $v_j^{(2h)}$ = solution to the homogeneous part of the second order time dependent system, proportional to $v_j^{(1)}$; p. 187.
- \mathbf{v} = vector of (v_1, v_2, v_3) [m/sec]; p. 141.
- V = dimensional amplitude of velocity solutions [m/sec]; p. 125.
- w = $w^+ - w^-$ = vertical velocity at the top of the boundary layer [m/sec]; p. 114.
- w^- = downward vertical velocity at the top of the boundary layer (non-negative) [m/sec]; p. 114.
- w^+ = upward vertical velocity at the top of the boundary layer (non-negative) [m/sec]; p. 114.
- W_l = cylindrical derivatives of X_l , i.e. $\frac{drX_l}{rdr}$; p. 157.
- X_l = Bessel basis functions; p. 155.
- \mathbf{y} = vector function of r , usually a solution to the linear homogeneous adjoint problem; p. 177.
- Y_0 = Bessel function of the second kind, zeroeth order; p. 144.
- Y_1 = Bessel function of the second kind, first order; p. 143.
- z = vertical coordinate [m]; p. 113.
- Z_s = vertical flux of angular momentum between the surface and boundary layer [m³/sec²]; p. 115.
- Z_{ij} = vertical flux of angular momentum between layers i and j [m³/sec²]; p. 115.
- α_l = coefficients of the Bessel functions X_l ; p. 156.
- α = vector of the α_l ; p. 157.
- β = cooling constant [m sec⁻¹ K⁻¹]; p. 122.
- γ = exponential growth rate [sec⁻¹]; p. 126.
- Γ = an integral of second order terms; p. 190.
- Γ_i = an integral of one of the six second order terms in Γ ; p. 198.
- ϵ = ratio of the density of layer 2 to layer 1; p. 113.
- ϵ_j = ratio of the density of layer j to layer 1; p. 116.
- ζ_j = total vorticity [sec⁻¹]; p. 118.
- $\zeta_j^{(0)}$ = f = planetary vorticity, lowest order term [sec⁻¹]; p. 128.
- $\zeta_j^{(1)}$ = first order relative vorticity [sec⁻¹]; p. 128.

η	= entrainment parameter; used as the forcing parameter; p. 119.
η_a	= ambient value of forcing parameter; p. 150.
η_c	= perturbation to forcing parameter required by solvability condition; p. 126.
η_e	= effective value of η including first order constant term; p. 148.
η_r	= perturbation to forcing parameter from motion dependent terms; p. 126.
$\eta^{(0)}$	= lowest order value of η for solutions satisfying the linear system, including boundary conditions; p. 126.
$\eta_{crit}^{(0)}$	= critical value of $\eta^{(0)}$ for the existence of real solutions to linear equation; p. 146.
θ	= potential temperature [K]; p. 38.
θ_e	= equivalent potential temperature [K]; p. 54.
θ_e^*	= saturation equivalent potential temperature [K]; p. 120.
θ_m	= mean potential temperature of a column [K]; p. 122.
λ_j	= lateral eddy diffusivity of angular momentum for layer j (1, 2) [m ² /sec]; p. 116.
Λ_j	= lateral eddy flux of angular momentum of layer j (0, 1, 2) [m ⁵ sec ⁻²]; p. 115.
μ	= coefficient of friction between layers 1 and 2 [m/sec]; p. 116.
ν	= coefficient of friction between layers 0 and 1 [m/sec]; p. 116.
ξ	= a dimensionless length parameter; p. 137.
Ξ	= ratio of the saturation equivalent potential temperature perturbations to the potential temperature perturbations in the upper layer; p. 124.
π_j	= function of pressure; p. 123.
ρ	= reference density [kg/m ³]; p. 113.
ρ_j	= density of layer j (0, 1, 2) [kg/m ³]; p. 113.
Σ	= an integral of second order terms; p. 184.
Σ_i	= an integral of one of the nine second order terms in Σ ; p. 196.
τ_s	= surface stress [(kg/m ³)(m ² /sec ²)]; pp. 108, 116.
Υ	= nondimensional growth rate; p. 171.

- ϕ_j = geopotential perturbation in layer j (0, 1, 2) [m^2/sec^2]; p. 117.
 Φ = an integral of the geopotential perturbation; [m^4/sec^2]; p. 188.
 χ_j = moist entropy of layer j (0, 1) [K]; p. 120.
 χ_2 = saturation moist entropy of the upper layer [K]; p. 120.
 χ_s = moist entropy of parcel saturated at sea surface temperature [K];
p. 124.
 ψ_j = inward radial mass flux in layer j (0, 1, 2) [m^3/sec]; p. 114.
 Ω = an integral of second order terms; p. 184.
 $\square^2 v$ = $\frac{\partial^2 v}{\partial r^2} + \frac{1}{r} \frac{\partial v}{\partial r} - \frac{v}{r^2}$, operator similar to the radial part of a cylindrical
Laplacian [m^{-2}]; p. 127.
 \square^2 = nondimensional version of \square^2 ; p. 150.

Abbreviations

- CAPE = convective available potential energy
CISK = conditional instability of the second kind
GARP = Global Atmospheric Research Programme
GATE = GARP Atlantic Tropical Experiment
HASIT = hurricane air-sea interaction theory
ITCZ = inter-tropical convergence zone
SST = sea surface temperature
TUTT = tropical upper tropospheric trough

J'ai de sérieuses raisons de croire que la planète d'où venait le petit prince est l'astéroïde B 612. Cet astéroïde n'a été aperçu qu'une fois au télescope, en 1909, par un astronome turc.

Il avait fait alors une grande démonstration de sa découverte à un Congrès International d'Astronomie. Mais personne ne l'avait cru à cause de son costume. Les grandes personnes sont comme ça.

Heureusement pour la réputation de l'astéroïde B 612 un dictateur turc imposa à son peuple, sous peine de mort, de s'habiller à l'Européenne. L'astronome refit sa démonstration en 1920, dans un habit très élégant. Et cette fois-ci tout le monde fut de son avis.

Antoine de Saint Exupéry
Le Petit Prince

Chapter 1

Introduction

Tropical cyclones are amongst the most damaging and well studied phenomena in meteorology.¹ They are capable of great intensification into the extreme examples known either as hurricanes or typhoons.² Despite the scrutiny under which these disturbances have come, surprisingly little recent work has been done on the intensification process using analytic methods. This thesis will concentrate on the processes that lead to the formation of a tropical storm from a large scale, weak, tropical disturbance. In particular, I will analyze the observed threshold for the development of intense tropical cyclones from the far more frequent, weaker disturbances. The approach will be mostly mathematical, using the techniques of weakly finite amplitude stability theory.

The instability found in this thesis is essentially a finite amplitude version of Conditional Instability of the Second Kind (CISK). For a given amount of Convective Available Potential Energy (CAPE), of parcels in the lower boundary layer with respect to air aloft, a threshold amplitude for intensification is found. That amplitude might be measured in terms of windspeed, pressure anomaly, vorticity, or temperature, at some given level; I argue later that surface vorticity is the best choice. Disturbances of greater amplitude are unstable and will continue

¹However, they are far less studied than midlatitude cyclones.

²In unimaginative places like Australia, they simply remain “tropical cyclones”.

to grow, while lesser ones will decay. For the concept of a threshold to make sense, the mechanism that supplies the initial disturbance must be distinct from the mechanism for later development. Until now, there have been no analytic theories which exhibit a threshold for intensification. A greater understanding of the features that distinguish between weak tropical disturbances that will become great storms from those that will not, may someday help our ability to forecast storm intensity. This would be especially useful for cyclone formation forecasts in regions such as the Bay of Bengal and the Gulf of Mexico, where warning times can be quite short.

1.1 Tropical Cyclones

... I know of no difference between a Hurricane among the Carribee Iflands in the *West Indies*, and a Tuffoon on the Coast of *China* in the *East Indies*, but only the Name: And I am apt to believe that both Words have one signification, which is a *violent Storm*. (Dampier 1699, Part 3, p. 71f.)

The International Meteorological Vocabulary (WMO 1966) defines:

tropical cyclone

Cyclone of tropical origin of small diameter (some hundreds of kilometres) with minimum surface pressure in some cases less than 90 kPa,³ very violent winds, and torrential rain; sometimes accompanied by thunderstorms. It usually contains a central region, known as the “eye” of the storm, with diameter of the order of some tens of kilometres, and with light winds and more or less lightly clouded sky.

If a tropical cyclone reaches hurricane intensity, it will have gone through several named stages. These are presented by Elsberry (1987) as:

Tropical disturbance: A region of organized convection with diameter of 200–600 km having a non-frontal migratory character.

³The normal atmospheric surface pressure is about 102 kPa.

Tropical depression: A weak tropical cyclone with a definite closed surface circulation and highest sustained wind speeds (averaged over one minute or longer period) of less than 17 m sec^{-1} (34 kts).

Tropical storm: A tropical cyclone with closed isobars and highest sustained wind speeds of 17 to 32 m sec^{-1} (34 to 63 kts) inclusive.

Typhoon/hurricane: A tropical cyclone with highest sustained winds of 33 m sec^{-1} (64 kts) or more.

The winds used are *surface* winds, usually estimated for the “standard” anemometer height of 10 m. Though tropical cyclones are usually described as mesoscale features, with the area of violent winds mostly within 100 km of the center, the disturbances are noticeable beyond a radius of 1000 km of the center, or greater. (This is still significantly less than the Rossby radius of deformation in the tropics.) For full hurricanes, the Saffir-Simpson Hurricane Scale (R. Simpson 1974) provides finer distinctions within the last category, for purposes of providing public warnings. However, most cyclones reach their maximum possible intensity, given their environment, without ever reaching category 5, labeled “devastating”. Other intensity definitions sometimes use the sea level pressure at the center of the disturbance. The breakpoints between categories are somewhat arbitrary, and are of more use for warning humans of impending danger than for providing physical insight. No clues to the dynamics are found here, nor are there any hints of what determines whether or not any given disturbance will progress up the intensity ladder.

A dynamical definition concentrates on very different features. Most noticeably, tropical cyclones are *warm core disturbances* over their entire depth. They form only over large bodies of water. During the early part of the intensification there is no observed large scale descent, with adiabatic warming⁴ from compres-

⁴By *warming* we mean changes in temperature at fixed points in space, i.e. $\frac{\partial \theta}{\partial t}$. The term *heating* will refer to changes in the sensible heat content of a parcel, i.e. $\frac{d\theta}{dt}$. These are usually not equivalent. In a vertically stable atmosphere, adiabatic sinking of parcels leads to warming without heating. In a saturated moist neutral atmosphere, lifting results in heating without warming. Alas, no similar linguistic distinction is available for changes of the opposite sign, i.e. those involving cooling.

sion, in the core region. The primary energy source is heat from the upper layer of the ocean transferred to the atmosphere in the form of latent heat, by evaporation, and later released aloft through condensation. Some of this transfer occurs before the start of the cyclone and is reflected in the potential instability of boundary layer air with respect to the air aloft. The storms are of such great intensity, and the core is of such great relative warmth, that they cannot be formed by simply lifting a set of parcels from the boundary layer under normal conditions. An essential part of the development process is increasing the entropy of the boundary layer.

This dynamical definition might then lead to the inclusion of some systems that are not tropical. In particular, polar lows may be dynamically quite similar to hurricanes. This has been discussed in detail by Rasmussen (1985, 1979), by Emanuel and Rotunno (1989), and the works cited therein. Both Rasmussen, and Emanuel and Rotunno, find the dynamics of these high latitude storms to be similar to that of hurricanes, but believe that different mechanisms are responsible (see Rasmussen and Lystad 1987). Comma clouds over the ocean at high latitudes are often grouped with polar lows, but maintain their frontal character; deep convection and ocean surface fluxes may be important for the rate of development and final intensity of these storms (Reed and Blier 1986). Midlatitude baroclinic cyclones can also extract heat from the ocean. In several well studied cases (e.g. Gyakum 1983a, b; Bosart and Lin 1984) rapid intensification of such disturbances has been observed when they move over the ocean. A similar case has been described that occurred entirely over the ocean (Reed and Albright 1986). Gyakum (1983b) explicitly calls on a CISK-like mechanism to explain development. The theory presented in this thesis for tropical cyclones may also apply to these other types of storms in various degrees, but the analogies will not be discussed in any detail.

Though one could ask many detailed or esoteric questions about tropical cyclones, there are still many simple sounding ones that have not been satisfactorily answered. I will concentrate on two:

1. *How do hurricanes happen?* and
2. *Why don't they occur more often?*

The first question will be examined in chapter two; we turn now to the second.

1.2 Existence of a Threshold

At least as far back as the 1930s, the *infrequency* of tropical cyclones was vexing to those attempting to develop an explanation for these intense storms (see the discussion following Durst and Sutcliffe 1938). Hurricanes do not regularly erupt like the frequent tropical cumulus clouds, or even the occasional cumulonimbus. In the course of a year, there are many thousands of cloud clusters over the tropics (McBride 1981a). Few of these will grow to be classified as tropical depressions. Only a small fraction of the tropical depressions will become hurricanes (about a third, based on the data in N. Frank and Hebert 1974). Of those that reach tropical storm status, about two-thirds will reach hurricane intensity (Gray 1975). In a study of west Atlantic hurricane formation Riehl (1948b) stated that

deepening began, without exception, in pre-existing perturbations....
There was no evidence of spontaneous formation due to convection over an overheated tropical ocean. [Emphasis in original.]

As Palmén (1956) noted:

In spite of the fact that the necessary climatological-geographical conditions for the formation of tropical cyclones prevail over large areas of the earth during certain seasons, the actual appearance of cyclones of hurricane strength is a relatively rare phenomenon. According to statistics, only about 50 tropical cyclones are observed per year over the entire globe.⁵ This indicates that there must be a

⁵This estimate is now considered too low. Gray (1975) estimated that there are nearly 100 per year. Satellite reconnaissance is largely responsible for the fact that it is now almost impossible for a tropical cyclone to remain undetected.

rare coincidence of circumstances before a cyclone of hurricane intensity can develop.

There are no claims for a radically different vertical structure of soundings on the days before tropical cyclone development compared with days exhibiting the more usual isolated cumulus clouds or tropical cloud clusters.

R. Simpson and Riehl (1981, p. 7) noted that

The main reason for the high frequency of extratropical, compared to tropical, cyclones is thought to lie in the fact that the energy source is drawn from *preexisting* temperature differences across latitude circles, whereas the main part of the temperature difference must be *created* in the tropical weather systems for a hurricane circulation to become possible [emphasis in original].

The differences between tropical and midlatitude cyclogenesis are still not fully understood. Three distinctions stand out. The intensity of the sustained winds in strong marine nonfrontal storms in the tropics is usually greater than that for strong landbased midlatitude storms. The storm has a warm core for the entire depth of the troposphere, as opposed to the more baroclinic structure of most landbased storms. Also, there is an apparent amplitude threshold for the, usually slow, development of the intense, long-lived, tropical storms, with weak disturbances failing to intensify. Once mature, tropical cyclones remain intense until reaching land or high latitude cold water. Midlatitude disturbances occur more frequently, rapidly intensify and can decay nearly as rapidly as they form (for an observational example see Randel et alii 1987; for a theoretical discussion see Farrell 1988). *It is because of this threshold that tropical cyclones are infrequent.*

Riehl (1954, p. 326) noted that one of the requirements for cyclogenesis was “an initiating mechanism (starter) with an independent energy source”. Even some of those workers (e.g. Charney and Eliassen 1964b, Ooyama 1964) applying linear theory to the problem of tropical cyclone intensification realized the need for finite amplitude theories and the particular inadequacies of assuming growth from infinitesimal perturbations. The requirement that a rather intense disturbance, within some limited range of configurations, is needed for intensification

has appeared in some numerical models (e.g. Rotunno and Emanuel 1987; De-Maria and Pickle 1988; Tuleya 1988; Emanuel 1989a, b). Numerical models that produce hurricane like disturbances with tiny perturbations are linearly unstable and unrealistic, at least with respect to their initial conditions (e.g. Anthes 1972, Yamasaki 1977).

Older theories of tropical cyclone development were primarily trying to explain the observed length scales and energetics of the cyclones. The threshold for formation was ignored, not because it was unknown, but probably because traditional mathematical techniques were incapable of reflecting such behavior. Analytic finite amplitude methods are still slightly esoteric, but are coming into more frequent use.

Kleinschmidt (1951) thought that rapid intensification began when the anti-cyclone aloft became inertially unstable, which implies finite amplitude behavior. A trigger point based on the magnitude of the nonlinear momentum advection terms was proposed by Shapiro (1977). Emanuel (1989a, b) has recently suggested a possible cause for the threshold behavior. In contradistinction to the work presented here, he claims that Ekman pumping must perform work against a stable gradient, presenting a threshold to be overcome, and that development only occurs if the vortex is strong enough and lasts long enough to increase the moist entropy of the lower troposphere and the boundary layer. So far this theory has only been examined in the context of a simple numerical model. This explanation for a threshold is strongly tied to Emanuel's theory for hurricane formation, which we will refer to as Hurricane Air-Sea Interaction Theory (HASIT). These works will be discussed in more detail in section 3.2.3, but are not central to this thesis.

At present, the most commonly held theories of hurricane formation are variation of linear CISK, which provides no explanation for a development threshold; there are a few adherents of HASIT, and large numbers of sceptics waiting in the wings. CISK relies on a "cooperation" between deep cumulus convection and the much larger scale vortex through convergence in the boundary layer due to surface friction. More complete explanations of CISK are in sections 2.2, 3.2.2, and 4.2.

Previously, it has only been presented in linear formulations or, less clearly, in numerical models. Linear works cannot, of course, exhibit finite amplitude threshold behavior. I will extend a CISK type theory to higher order in an amplitude expansion, and show that it can yield a threshold for growth. The threshold in this work is tied to overcoming dissipation.

1.3 The Way

This work consists of a synthesis of earlier work on tropical cyclones formation and a nonlinear theory to explain why these intense storms are not more frequent. The synthesis will examine the mechanisms for providing energy, entropy, angular momentum, and organization for tropical cyclones. The nonlinear theory is based on the CISK type model of Ooyama 1969. Nonlinear theory is used, not because the amplitudes are so large that linear theory is no longer quantitatively correct (though that is the case) but rather, because linear theory is fundamentally incapable of examining the qualitative threshold behavior I wish to study.

Analyses of the CISK mechanism were first presented by Ooyama (1964) and by Charney and Eliassen (1964a). Ooyama later (1969) derived his linear version of the theory as an inviscid approximation of a more general set of equations that he integrated numerically. I will treat Ooyama's more general system up to second order with the inclusion of dissipation. The basic feature that deep convection and net heating aloft are in phase with mass convergence in the boundary layer is retained. Some of the mechanisms called upon in HASIT will also appear here at second order, in particular the increase in boundary layer entropy, due to vortex wind enhanced moisture fluxes from the sea surface.

The mathematical technique used here is not a simple application of existing method. Several complications are treated that have not previously been included in analytic studies of finite amplitude problems. They include changes in the basic forcing by perturbations at second order (rather than third order), nonlinear

matching between regions with different governing equations for the linear stationary state, and contributions by the nonlinear advective terms at second order (rather than third) as in many convection problems.

This thesis is not intended to be the *ne plus ultra* of tropical cyclone dynamics. The treatment of the cloud physics is downright simplistic. However, the techniques of weakly finite amplitude stability theory, as demonstrated here, can be applied later with perhaps wiser parameterizations for cumulus heating and dissipation. I expect that someone will bring them to bear on a model with better internal physics in the near future.

The remainder of this chapter provides an outline of the mathematical procedures used in the central part of the thesis. In the next chapter, I discuss the dynamic and thermodynamic requirements of tropical cyclones. Chapter three is a review of the published literature on tropical cyclone intensification. That chapter concludes with an examination of prior theoretical work on tropical cyclone intensification, with sections devoted to both CISK and HASIT. Objections to CISK, replies to those objections, and other odd preliminary material are in chapter four. Included is a discussion of observations of the vertical structure of the tropical atmosphere relating to the existence of CAPE. Chapter five introduces the physics of the model being used. It closely follows the model described in Ooyama 1969. A linear analysis of the model is presented in chapter six, preceded by a recapitulation of the linear theory presented by Ooyama. The linear solutions are then used in chapter seven, where the weakly finite amplitude theory is developed. First the amplitude of the linear solutions is determined and the stability of those solutions is then examined. Following that is a chapter of discussion and conclusions, including a comparison of Finite Amplitude CISK and HASIT. The epilogue contains remarks of a more speculative or political nature, including discussions of intended and unintended tropical cyclone modification. Chapters have been held to digestible sized pieces.

For additional background, monographs are available which provide an introduction to the dynamics and effects of tropical cyclones. The book by Anthes (1982) provides an excellent overview and is easily obtained. Elsberry et alii 1987

is more recent and contains more references, but may prove difficult to locate. A comprehensive, but less technical presentation is provided by R. Simpson and Riehl (1981). There will be great reliance on the model framed by Ooyama (1969) and the mathematical techniques presented clearly by Krishnamurti (1968).

1.4 Layout of Mathematics

Of necessity, tropical cyclone theory quickly becomes more complicated than one might wish. Much can be simplified if one ignores the closing of the secondary circulation (as was done in Emanuel 1986) or not allow any steady states except the trivial one (as was done in Ooyama 1969). Neither of these routes is taken here. Many pieces that come from what are often distinct lines of research must be brought together. At the minimum one starts with the equations for a gradient wind balanced vortex (see Eliassen 1951). To that must be added dynamics for the boundary layer which controls most of the energetics of a tropical storm development. For steady solutions in the presence of a secondary circulation, momentum diffusion must be included. The heating aloft, which is necessary for development of the cyclone, is tied to deep cumulus convection, which is parameterized. Closing the circulation with a descending return branch, requires either the presence of radiative cooling or that the flow be nonhydrostatic. Radiative cooling has been chosen because it is also necessary for steady solutions in the presence of diabatic heating. Since all of these processes need be treated simultaneously, they will all be treated simplistically.

As noted above, I will use weakly nonlinear theory to analyze the problem of tropical cyclone intensification. For standard linear theory, an imposed stationary basic state is assumed and the evolution of infinitesimal perturbations with exponential time dependence is studied. The “growth rate” (which in general can be complex), is an eigenvalue of the system and is determined after the boundary conditions are imposed. Dispersion relations between growth rate and wavelength, are the standard results of this analysis. However, this technique is only relevant

to systems where small perturbations actually grow. The observations of tropical cyclones demonstrate that this is not the case, so linear theory will be inadequate.

Weakly nonlinear theory assumes that the amplitude of a disturbance, a , is not infinitesimal, but that it remains small enough that an expansion in powers of the amplitude remains well ordered, i.e. terms proportional to a^2 are much less than terms proportional to a . A detailed description of the procedures will be presented in section 7.1. This approach will be quantitatively stretched even for feeble disturbances as the local vorticity approaches the rather weak planetary vorticity in the tropics. For a full hurricane, the dominant balances that will be assumed here simply no longer apply.

The weakly nonlinear technique used here was pioneered by W. Malkus and Veronis (1958).⁶ They used an amplitude expansion and the solvability condition at second order to determine the amplitude of the linear solutions for Rayleigh-Bénard convection in terms of a forcing parameter. The solvability condition for the resulting inhomogeneous boundary value problem is in some ways akin to the familiar eigenvalue determination in a homogeneous linear boundary value problem and in other ways akin to a domain integrated energy equation. Schlüter et alii (1965) built on the technique further by looking at the stability of stationary solutions (ones with no time dependence, not necessarily no motion) determined as W. Malkus and Veronis had described. Krishnamurti (1968) generalized the technique slightly and provided a more readable exposition than that of Schlüter et alii.

I will take as an article of faith that cyclone scale oscillations are not an essential part of the intensification process. No observational or theoretical studies have yet claimed otherwise. Asymmetric structures may be an important part of the environment that affects intensification, but these will not be considered necessary for intensification, though some workers have taken a contrary position (e.g. Molinari and Vollaro 1989, Challa and Pfeffer 1990, Merrill 1988b, and the

⁶They credit Lindstedt in 1883 with a similar idea.

references cited therein). Asymmetries in the upper level will only be considered helpful in the development process to the extent that they encourage momentum mixing aloft within the anticyclone, but not as an “outside” influence.

The weakly nonlinear method has several well defined steps. After laying out the basic equations, the system is linearized and the linear eigenvalue problem solved. The first order linear system is homogeneous. Only the stationary case result is needed, otherwise the solution would be dominated by the first order time dependence.⁷ Moist convection provides a major complication in even linear problems. The thermodynamics of updrafts and downdrafts are different, so matching conditions at the dividing location(s) must be met in addition to the boundary conditions. The domain location(s) separating these regions must be solved for as an eigenvalue. This eigenvalue problem is nonlinear, so even though the system appears piecewise linear there is a fundamental nonlinearity. The inclusion of dissipation, which is necessary for nontrivial stationary solutions, leads to much higher order equations than in the earlier CISK theories.

Expansion of the basic equations to second order results in a system that is linear and inhomogeneous. The associated homogeneous system is identical to the first order system, and the inhomogeneous terms are functions of the first order solutions. Inhomogeneous two point boundary problems do not in general have solutions; one point boundary, or initial, value problems are more amenable to solution. Ince (1926) provided a detailed theoretical analysis of the algebraic properties of such differential systems. The solvability condition for the two point inhomogeneous case provides a relation between the amplitude of the first order solutions, which are used in the inhomogeneous terms, and the forcing parameter. The forcing parameter is based on the relative stability of the layers, which is closely tied to the CAPE. Over the domain, the solvability condition enforces

⁷There is an example where a second order expansion was performed on slowly decaying solutions with quite interesting result. Orszag and Patera (1983) found rapidly growing three dimensional instabilities on Poiseuille flow with decaying two dimensional perturbations.

energy conservation for the second order terms. In problems such as Rayleigh-Bénard convection, a steady balance is maintained by increases in convection amplitude accompanying increases in the forcing (Rayleigh number). This is the result obtained by W. Malkus and Veronis (1958), though in that problem the solvability condition at second order is trivially satisfied and resonance occurs at third order. The problem at hand is quite different. Steady state balance requires that increases in amplitude, though only in the cyclonic sense, be matched by *decreases* in the forcing parameter. With sufficient amplitude for a disturbance, steady state can be maintained with the forcing parameter less than the critical value for linear instability. Existence of a stationary solution is no guarantee of its stability. In fact, it would be a great disappointment if the stationary solution was found to be stable.

Next, equations are derived for perturbations to the steady solutions. This also generates a bounded inhomogeneous system with a solvability condition. Since the relation between amplitude and the forcing parameter has already been determined, this second solvability condition then determines the growth rate for a perturbation. The form of any unstable perturbation is also important if it is to be possibly viewed as leading to intensification. This is a slightly different objective from than the goals of previous examinations of the stability of weakly finite amplitude stationary solutions. Demonstration that the steady solutions are unstable, with a forcing parameter less than critical for linear instability, and unstable in a manner that resembles an intensifying vortex, completes the calculation.

These concepts are difficult to digest if one has not actually performed calculations using the techniques. Elaboration and review of the procedures just outlined are provided in later chapters to assist rumination.

[Those readers already well versed in tropical cyclone dynamics may skip to chapter four.]

*And in smaller letters at the bottom it concluded:
"Results are not guaranteed, but if not perfectly satisfied, your wasted
time will be refunded."*

*Norton Juster
The Phantom Tollbooth*

Chapter 2

Building a Tropical Cyclone

The story of how a hurricane comes to be, is the story of how a weak disturbance, often called a cloud cluster, concentrates large quantities of angular momentum and develops a deep warm core. Several components are needed to breed a healthy tropical cyclone: an energy source, an angular momentum source, and the right type of initial disturbance. Many workers (including me) believe that some of the energy is already in the atmosphere as convective available potential energy of moist but unsaturated boundary layer air. Most of the energy comes from the ocean. It is transferred in the form of latent heat from water vapor evaporated at the sea surface while cooling the ocean mixed layer. This heat is later released in the middle and upper troposphere by deep cumulus convection. Angular momentum is advected into the cyclone. The initial reservoir of angular momentum is that of parcels rotating with the earth. The inward advection occurs in the boundary layer because of friction and in middle levels as a response to the heating from cumulus convection. However, only certain types of disturbances are able to extract these resources. We will examine each of these requirements after describing the basic structure of a tropical cyclone.

2.1 Structure

It has become a regular practice to describe a mature tropical cyclone before describing a growing disturbance, even if one wishes to analyze the process of development (e.g. Riehl 1950, Palmén and Newton 1969, Anthes 1982); I will follow this tradition. In some sense a mature hurricane is “simpler” than a growing disturbance, even if the former is unavoidably nonlinear. The most obvious simplifications are that a mature cyclone is nearly steady state, and also when mature it is far closer to axisymmetric than when in its formative stages. Further, near steady state the secondary circulation and cumulus convection are weaker than during periods of rapid intensification. Some of the better case studies of mature storm structure were presented by Hawkins and Rubsam (1968b), Hawkins and Imbembo (1976) and Jorgensen (1984a, b). Since data tend to be sparse, composites have been assembled for structural analyses, such as those by W. Frank (1977a, b; 1984). Holland (1987) provided an excellent review, discussing structure, structural change, and structural variability.

The field with the most symmetrical perturbation is the mass field. This is equally evident in both the temperature and pressure distributions. Figure 2.1 shows a cross section of temperature perturbations from Hurricane Hilda (Hawkins and Rubsam 1968b). The temperature perturbation is greatest at high levels. Since low pressure is in phase with high temperature, the potential temperature¹ perturbation is even larger than the temperature anomaly shown. This figure is for a mature, very intense storm, so the perturbations are comparatively large. The perturbation has a maximum near 30 kPa and decays, but does not change sign, towards both the surface and tropopause. Not only is the potential temperature

¹The potential temperature, θ , is the temperature a dry parcel of air would have if it were brought adiabatically to a reference pressure of 100 kPa. A dry parcel lifted adiabatically cools about 1 K every 100 m, due to the pressure drop and the accompanying expansion. Hence, the atmosphere can cool with height and still be stable (unlike a pot of water). Comparing the potential temperatures of a parcel and a possible environment at another pressure level allows one to directly determine the buoyancy of the parcel at that level. Complications involving water will be discussed in section 2.3.

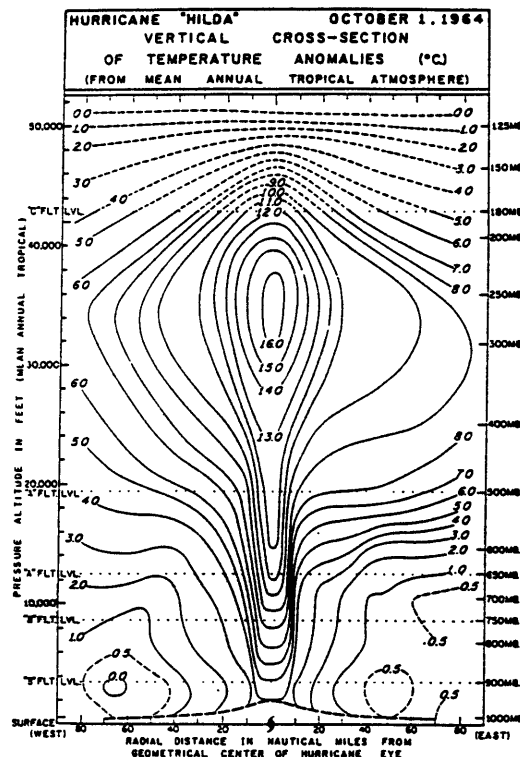


FIGURE 9.—Vertical cross section of temperature anomaly prepared from the soundings presented in figure 8.

Figure 2.1: Vertical cross section of temperature anomalies (K) for Hurricane Hilda (deviations from mean annual tropical temperature) [from Hawkins and Rubsam 1968b].

high in the storm center, but so is the relative humidity. Figure 2.2 shows a highly averaged relative humidity cross section for a composite typhoon for a large area. (N.B. the figures included here vary wildly in the choice of units and horizontal scale.) The values at large radius may be viewed as representing mean tropical conditions for the region.

The *primary* circulation of a tropical storm is also known as the “azimuthal” or “tangential” circulation. It is strongly cyclonic² near the surface and decreases in strength at higher levels. At upper levels in the troposphere, the flow is anticy-

²Cyclonic circulations are counterclockwise in the northern hemisphere and clockwise in the southern hemisphere, looking down at the earth. Cyclonic shear indicates winds becoming more westward as one moves away from the equator.

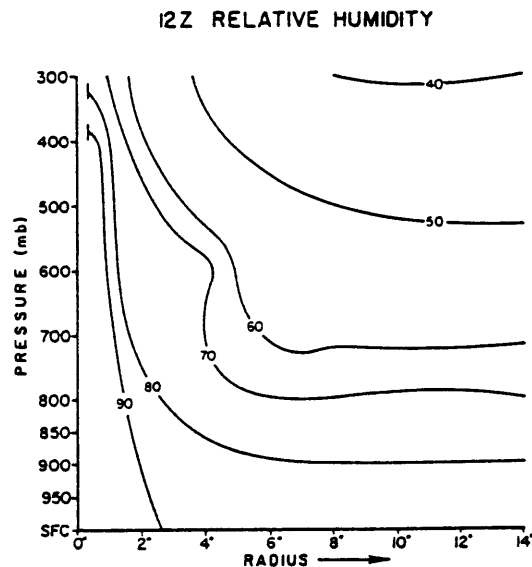


FIG. 5. Relative humidities of mean steady-state typhoon at 1200 GMT (~ 2200 LT).

Figure 2.2: Average relative humidity for a composite Pacific typhoon [from W. Frank 1977a].

clonic at a distance away from the storm axis.³ Maximum cyclonic winds of about

³In response to a question from a friend, I came up with a simple analogy to “explain” the anticyclone aloft without just mumbling “conservation of angular momentum”. Most of us are familiar with the description of an ice skater who spins faster when she pulls her arms in and slows down when she sticks her arms out. If the skater were not spinning, no change in motion would be visible as she lifted or dropped her arms.

Let us now imagine a skater at the center of an icy, spinning turntable and we are sitting at the edge of the turntable. If the skater is not spinning with respect to the turntable, and our viewing position, then she is spinning with respect to someone just off of the turntable (or absolute space). Let her start with her arms at about 45° from her body. If she then drops her arms she will be seen by us on the turntable to begin spinning and by observers off the table as just increasing her rate of spin. If she then lifts her arms away from her body, the observers not on the table see her slow down, but those of us watching from on the table see her spin *backwards*. She has not reversed her direction of spin with respect to absolute space, but she has reversed her spin from the perspective of those with her on the turntable. The anticyclone aloft is like the skater lifting her arms; as air flows outward from the center, it starts spinning backwards for those travelling with it on earth, but has the same rotational direction with respect to absolute space. Figuring out how this works away from the center of the turntable, in a fluid with pressure forces, is left as an exercise for the reader.

50 m/sec are usually found just above the surface at a radius between 20 to 50 km. The anticyclonic maximum is usually at a height of about 15 km and a radius of say 800 km with winds of about 20 m/sec. Cross sections of azimuthal wind for Hurricane Hilda (Hawkins and Rubsam 1968b), just illustrating the central core, and for a composite of a larger area (W. Frank 1977a) are shown in figures 2.3. The diagram of the core region does not cover a sufficiently large area to show the anticyclone aloft; the composite smears out and distorts the high gradient region in the core. The wind field exhibits more asymmetries than the temperature field, especially at upper levels in the outflow region (Black and Anthes 1971).

In a mature storm, the gradients of temperature, pressure, and wind are very sharp, and are strongest in the eyewall, where the most intense convection is located. Despite the small central region with large gradients, the outer circulation that can be clearly associated with the hurricane disturbance usually extends more than 1000 km from the center (see figure 2.3b), especially in the upper troposphere.

The *secondary* circulation consists of vertical winds and radial flow toward or away from the central axis of the cyclone. In older literature it is occasionally called the “solenoidal” circulation (e.g. Palmén 1948). Radial flow is also sometimes referred to as “meridional” (in the general mathematical sense of the term, rather than along longitude lines of the Earth), but this will not be used here. Though the velocities of the secondary circulation are considerably smaller than those of the primary circulation, the secondary circulation is essential for the time dependent development of the storm. Averaged radial velocities are shown in figure 2.4. Inflow extends from the surface up to about 40 kPa. In the boundary layer, inflow is a response to momentum losses due to surface friction. In the middle troposphere, heating in the core drives inflow. (Cooling may also drive middle level inflow, but this just weakens the lower level inflow and does not provide a net contribution to cyclone development.) Outflow is confined mostly to a layer between 30 kPa and the tropopause at about 10 kPa. There can be large variations around a single storm and between storms in the level dividing inflow and outflow. The outflow is usually highly asymmetric and often concentrated in

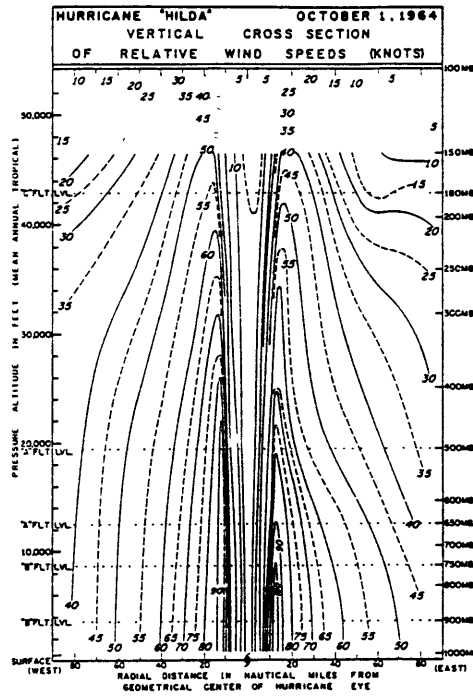


FIGURE 11.—Vertical cross section of wind speeds relative to the moving hurricane eye.

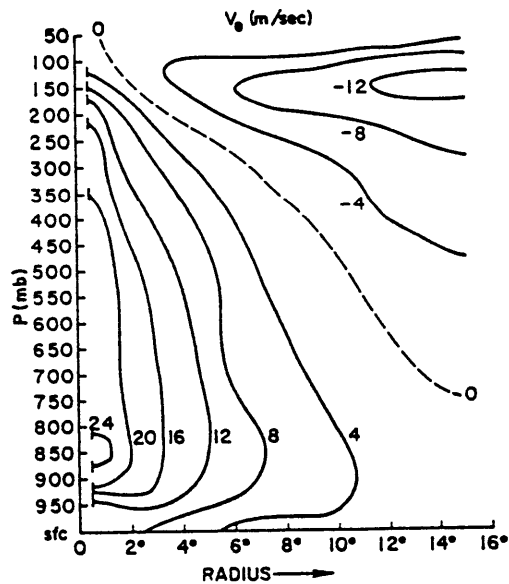


FIG. 9. Two-dimensional cross section of V_θ (m s^{-1}) in stationary (NAT) coordinates. Positive numbers denote cyclonic flow.

Figure 2.3: Vertical cross sections of azimuthal winds: (a) in the core of Hurricane Hilda [from Hawkin and Rubsam 1968b] and (b) out to larger radius for a Pacific composite typhoon [from W. Frank 1977a].

either one or two narrow jets (Merrill 1988a, and references therein). The large azimuthal gradients resulting from such structures may lead to stronger momentum mixing aloft than at lower inflow levels.

The vertical velocity field is quite noisy (see Jorgensen et alii 1985). At the top of the surface boundary layer, weak vertical velocities in the mean are forced due to the divergence of the frictionally induced inflow down the pressure gradient, usually called Ekman pumping. On average these are of order 1 cm/sec, but can exceed 10 cm/sec in high gradient regions even in very early stages of development. Large vertical velocities, exceeding 10 m/sec are found in deep convective cells (Burpee et alii 1989). Convective cores in hurricane cumulus clouds are much larger, frequently greater than 6 km across, than updraft cores for more usual tropical convection (for observations during the GATE, see Jorgensen et alii 1985). The eyewall is dominated by upward motion and dense clouds. Weak downdrafts over a large area are driven in response to convection through the continuity equation and by Ekman suction in regions with low level negative relative vorticity. More intense and narrow downdrafts are caused by evaporative cooling from rainfall into unsaturated air, by melting and sublimation of ice, and by liquid water or ice loading. Radiative cooling forces slow downward motion throughout the domain. An average of these conflicting motions is shown in figure 2.5.

If one assumes axisymmetry, or examines an azimuthal mean, one can construct a stream function for the secondary circulation. An example of such a field for the core of a hurricane is shown in figure 2.6. At steady state, the angular momentum transport associated with this flow must be balanced by diffusive processes. For development, this flow provides the crucial angular momentum supply, in excess of losses to diffusive transports.

The rainfall is one of the tropical storm's least symmetrical fields, though it is quite organized. Awareness of the asymmetries goes back to at least the first half of this century (see Deppermann 1939b). W. Frank (1977a) has found that the mean precipitation for a Pacific cyclone is 9.5 cm/day for the inner⁴ 222 km and

⁴Some work used degrees latitude as a length scale. One degree is about 111 km.

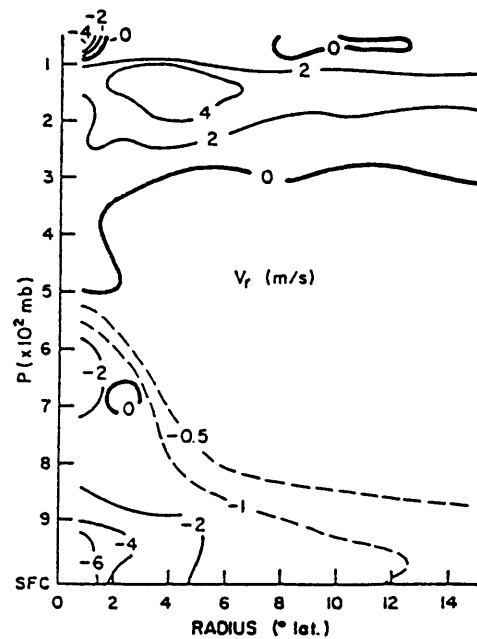


Figure 47. Two-dimensional cross-section of radial winds, V_r , for the mean steady-state typhoon.

Figure 2.4: Averaged radial winds for a composite typhoon [from Gray 1979].

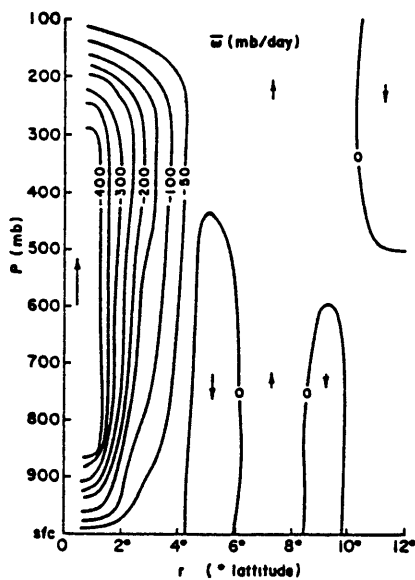


FIG. 19. Vertical motion (mb day^{-1}) from $0.7\text{--}12^\circ$ for mean steady-state typhoon.

Figure 2.5: Averaged vertical motion for a composite typhoon [from W. Frank 1977a].

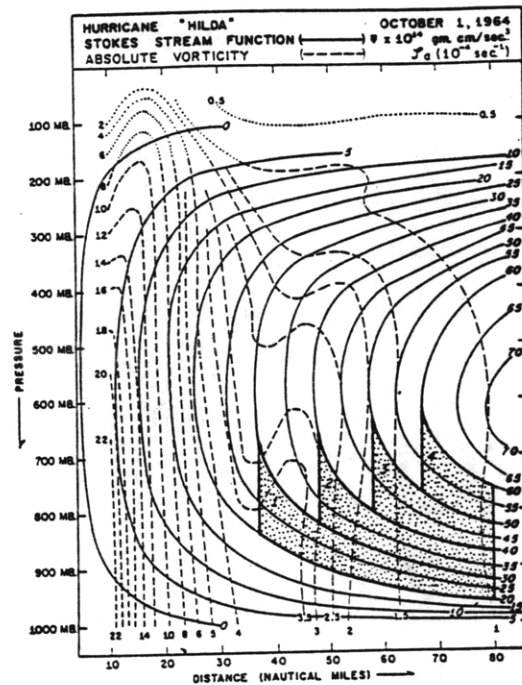


FIGURE 16.—Solid lines are Stokes' stream function superimposed on (dashed) lines of absolute vorticity. Selected streamtubes are indicated by 1, 2, etc.

Figure 2.6: Stream function for the core of a hurricane [from Hawkins and Rubsam 1968b].

about 3.5 cm/day in the ring from 222–444 km. The variations between quadrants in the composite were about 20%. A snapshot from a radar plan view provides a very different picture (see figure 2.7), where the lack of cylindrical symmetry is obvious. Rainbands other than the eyewall usually exist. Sometimes these are spiral, sometimes convective cells form an arc nearly concentric with the eyewall, and occasionally they are too fragmentary to determine an orientation. Willoughby et alii (1984b) analyzed several different patterns of rainbands. Occasionally, intense, long-lived, nearly symmetric storms develop a second eyewall, concentric with and outside of the primary eyewall. This secondary ring of convection often contracts in a manner similar to normal eyewall formation, with an accompanying decrease in convective intensity for the primary eyewall. Eventually the primary eyewall may dissipate, the secondary become primary, and the storm reintensify (Willoughby et alii 1982). Whether the formation of a secondary eyewall is akin

to the initial formation of the cyclone remains unknown, but it would not be surprising if the processes proved similar.

There are large variations between storms with respect to size, maximum intensity, and overall strength. Further, these measures of a cyclone do not correlate very well. Discussions of the variations can be found in Merrill 1984; and Weatherford and Gray 1988a, b; but it is worth noting that size and intensity are only poorly correlated (Merrill). Asymmetric features are discussed in detail by Weatherford and Gray (1988a, b); W. Frank (1984); and Shea and Gray (1973).

2.2 Intensification

We will distinguish between genesis and intensification. The creation of a large, organized, initial disturbance, by any means, will be referred to as *genesis*. Many such disturbances occur or move over the oceans. Some of these are called easterly waves, others apparently begin as instabilities of the intertropical convergence zone (ITCZ) or along the southern monsoon shear line. Most of these do not succeed in reaching any great strength. A small fraction, however, are thought by some workers (including me) to *intensify* by organizing deep convective activity, forcing unsaturated air up and out of the boundary layer so that it saturates and becomes convectively unstable, and by extracting heat from the ocean surface; all leading to the development of a very warm core. The processes leading to genesis will, on the whole, be ignored in this work, which concentrates on intensification. It has so far proven difficult to determine whether or not any given disturbance will intensify, based on observations early in its life cycle.

In section 1.2, it was noted that there is observational evidence of a threshold for intensification. The physical causes of this have proven elusive. For a growing linear mode, with exponential time dependence, it is a truism that all terms maintain the same proportional relationship throughout development. So if initially, the driving terms exceed dissipative ones, intensification occurs. Conversely, if initially dissipation exceeds driving, the mode decays. (The balances are more

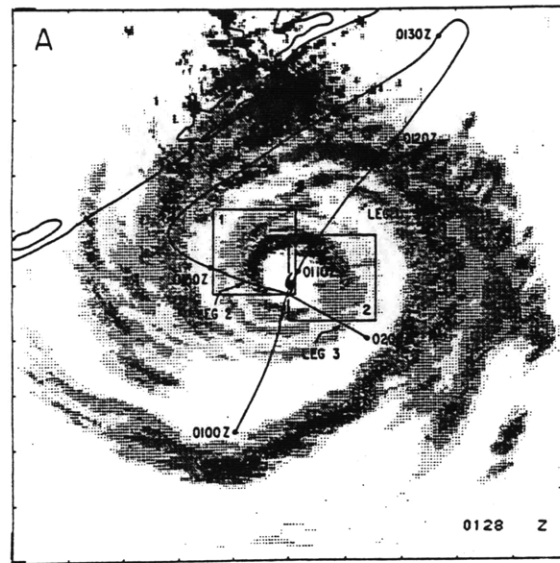


FIG. 1. (a) Horizontal distribution of reflectivity in Hurricane Alicia from the National Weather Service WSR-57 (10 cm) radar at Galveston, Texas, at 0128 UTC, 18 August 1983. Reflectivity contours are for 20, 25, 30, 35, and 40 dBZ. The aircraft flight track from 0100–0200 UTC is indicated by the solid line, and the analysis boxes, denoted by the thick solid line, are labeled 1 and 2.

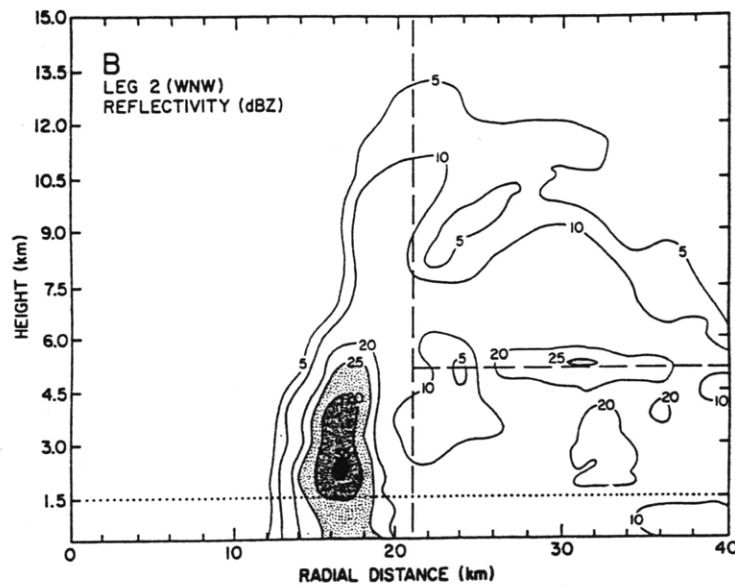


FIG. 3. Radius-height cross sections of reflectivity [dB(Z)] from the tail radar for (b) leg 2a. The aircraft flight level is depicted by the horizontal dotted line.

Figure 2.7: Radar reflectivity for a hurricane in (a) plan view and (b) cross section [from Marks and Houze 1987].

complicated with complex growth rates, but the simplified system we will examine does not have unforced oscillatory solutions.) Nonlinear systems are not so constrained, since the ratios of the terms are not fixed.

It is reasonable to ask how one distinguishes between systems where strong cyclones develop out of tiny perturbations (linear instability) and those systems where a finite amplitude perturbation is required. If one had complete and perfect data over the lifetime of a system, the order of relative importance of the dominant energy source terms would change at the threshold, if one existed. Such a data set does not exist, nor anything even close to it. However, for at least some disturbances, the Atlantic easterly waves, the disturbances begin in a region of barotropic instability over land, yet intensify over the water in a region with little barotropic or baroclinic energy supply (available kinetic energy), indicative of a change in energy source (Reed and Recker 1971, Burpee 1972).

Not only does the energetic balance change at the threshold, but it may change again in later development. It is important to distinguish between overcoming the threshold for intensification and the later intensification into a mature tropical cyclone. Some have made the leap that since there is insufficient CAPE and insufficient boundary layer entropy for mature storms of the intensity observed, therefore the boundary layer entropy (Emanuel 1985) or the middle troposphere entropy (Emanuel 1989b) must be greatly increased for intensification to *begin*. Though I can not rule out that they might some day be proved correct, the logical leap is not justified. This presents one of the divisions between CISK and HASIT. CISK requires that at least some intensification occur using existing CAPE before transformation of the boundary layer. HASIT relies entirely on transformation of the boundary layer.

In 1964, Ooyama, and Charney and Eliassen put forward theories for the development of tropical cyclones involving “cooperation” between the gross circulation of the cyclone and the smaller scale moist convection. Charney and Eliassen named the process Conditional Instability of the Second Kind (CISK).⁵ The en-

⁵The crisp acronym may have provided an important boost for the successful prop-

ergy source was the same as for moist convective instability, which implicitly was the first kind of conditional instability. The dynamics, however, were quite different. Their major contribution was to show that mass convergence in the frictional surface boundary layer can organize convection on a large scale; this is the central argument of CISK.⁶ These authors recognized that the perturbation must be finite amplitude to dominate the small scale convections, which have the fastest growth rates in the simplest analyses, but they were unable to treat this aspect of the problem.

The organized convection is, in turn, responsible for the organized midlevel inflow. This inflow drives a concentration of angular momentum. At the same time, the convection warms the upper troposphere in the inner core. If a warm core were created without convergence of angular momentum, gravity waves would eventually return the flow to near gradient wind balance⁷ at significant energy cost. Conversely, if angular momentum symmetrically converged (by some odd happenstance), gravity waves would restore the balance through subsidence warming by lowering the isopycnals at energetic cost and with some dispersion of the angular momentum (like the surface dropping in the center as one stirs a glass of chocolate milk). Schubert et alii (1980) in an examination of the geostrophic adjustment problem have shown that convection is far more efficient at driving a

agation of the theory and later corruption of the name.

⁶Ooyama (1982) has sometimes defined CISK more generally so the cooperation between the large scale flow and the convection could be through any dynamical means, rather than just frictional convergence. This redefinition will not be adopted here.

⁷For the time independent, inviscid flow of a vortex, the radial angular momentum equation has three basic terms: the Coriolis acceleration, the centripetal acceleration, and the pressure gradient. *Geostrophic* balance is a dominance by the Coriolis and pressure terms; this is the norm for large scale midlatitude weather systems. *Cyclostrophic* balance is between the centripetal acceleration and the pressure gradient; this applies to tornadoes, the hurricane core, and the vortex in a stirred bucket of water. *Gradient wind* balance, or simply “balanced flow”, indicates all three terms are of the same order of magnitude; this holds over a large fraction of a tropical cyclone. (See Holton 1979, p. 56ff.)

vortex through vorticity import than through direct heating. Tropical cyclone intensification is somewhat efficient in that the same convective processes drive the development of both the temperature and momentum fields in the same direction as required by the gradient wind balance. The works of Ooyama, and Charney and Eliassen will be examined in more detail in section 3.2.2.

Several objections have been made to CISK theory (Emanuel⁸ 1989a, b). The strongest objection has been the claim that the atmosphere in the region of hurricane development is so close to moist neutral that almost no energy is released when air is forced out of the boundary layer and begins to convect. The existence, or lack of existence, of such a reservoir of potential energy will be examined in section 4.3. Other objections will be discussed in section 4.2. The budgets of entropy, energy, and angular momentum will be discussed in the following sections. These are the keys to intensification. They are also the keys to the limits on intensification.

2.3 Entropy and Energy

Tropical cyclones are unusual not only for their intensity and infrequency, but also for their basic energetics. Continuing the quote from Palmén 1956 just where we left off (on p. 28):

On the other hand, experience has shown that once a tropical cyclone has formed it is a very persistent phenomenon as long as it remains over the waters of the hurricane regions. This indicates a fundamental difference between tropical and extratropical cyclones, namely, that of their sources of energy. Most extratropical cyclones remain for only a short time at the maximum energy level, degenerating almost as rapidly as they formed. This leads one to conclude that extratropical cyclones derive their energy from a source that soon becomes exhausted.

⁸Though Kerry Emanuel has served as my advisor during preparation of this thesis, he disagrees with several crucial assumptions of the model presented here. Also see the comment in the Acknowledgments, p. 7.

The persistence of the tropical cyclones on a constant energy level for a period of several days indicates that once the cyclone circulation is induced it in some way maintains its own source of energy. This energy must be easily utilised once the process is started, but there must exist some initial resistance against the development. The rapid decay when a cyclone moves out of the hurricane belts also gives important clues concerning the nature of the energy source.

Energy for the cyclone scale disturbance is needed in the form of potential energy for the sloping isentropes and kinetic energy for the primary azimuthal circulation. The kinetic energy of the storm winds totals about 10^{18} J. The “available potential energy” (in the sense of Lorenz 1955, though this energy is not available for conversion to the kinetic energy of the primary circulation), from the sloping pressure surfaces in gradient balance with the winds, is about an order of magnitude larger (Takahashi et alii 1951). A hurricane with a mean precipitation rate of 5 cm/day over a radius of 400 km (W. Frank 1977a) releases latent heat at a rate of nearly 10^{15} W. However, almost all of this energy is incapable of doing any work, though it does lead to a net warming of the atmosphere. We will now examine how energy is provided to the cyclone.

The ultimate energy source for tropical cyclones, as for most atmospheric motion, is the sun. However, neither contemporaneous solar heating nor ambient potential energy in the atmosphere is sufficient for full development. It is generally agreed, as Riehl (1954) suggested, that the upper ocean provides much of the energy through evaporation. Solar radiation is absorbed by the ocean. Water evaporates, cooling the ocean and moistening the boundary layer. A smaller amount of heat is transferred to the atmosphere by radiation and diffusion. Cumulus convection transfers this energy aloft along with some water vapor, since not all of the vapor condenses and some reëvaporates after mixing with drier air. The fraction of the condensate that returns to the ocean, is the “precipitation efficiency”. This is representative of the amount of heating from cumulus convection, since little liquid water is retained in the atmosphere for long periods of time.

Moist convective instability was first described by J. P. Espy in 1835. This was the seed for the development of the thermal theory of cyclones (see Kutzbach

1979, ch. 2), in which Espy played an important role. Upon learning that heat was released when water vapor condensed, he realized that a dogma of his time, that lifted parcels that became cloudy with condensate must be heavier than their surroundings, was not correct.⁹ For the condition where the lapse rate is less than the dry adiabatic lapse rate (subadiabatic) but greater than the moist saturated adiabatic lapse rate¹⁰ (super-moist-adiabatic), the atmosphere is referred to as

⁹Conditional instability is one of those wonderful phenomena that are obvious after one already knows about them, but difficult to discover. A parcel that rises, or is lifted, adiabatically cools as the pressure drops and it does work on its surroundings. Cooling the parcel decreases the local saturation vapor pressure for water. Once the parcel is saturated, continued cooling forces condensation and the release of latent heat of vaporization. This latent heat warms the parcel. If the parcel is then less dense than its surroundings it continues to rise, hence it continues to cool, the saturation vapor pressure continues to drop forcing more condensation and hence more heating. Unless the region is very steeply stratified, this increases the buoyancy of the parcel with respect to its surroundings, so it continues upwards. Eventually the environment becomes so stably stratified that the parcel loses its relative buoyancy. Once it is understood that a parcel's relative buoyancy can increase while its temperature drops, the rest is easy.

Reflecting on this discover Espy, (1841, p. iii) wrote:

It had long been known that vapor is lighter than air, and it was inferred from this, that when a portion of atmospheric vapor is condensed into cloud, the air in the cloud becomes specifically heavier than it was before. This doctrine I received as an axiom, and I never for a moment doubted it, until it occurred to me to calculate the effect which the evolution of the latent caloric produces, during the formation of cloud.

The result was an instantaneous transition from darkness to light. The moment I saw that a rapidly forming cloud is specifically lighter in proportion as it becomes darker, a thousand contradictions vanished, and the numerous facts, "a rude and undigested mass," which had been stowed away in the secret recesses of my memory, presented themselves spontaneously to my delighted mind, as a harmonious system of fair proportion.

¹⁰The *lapse rate* is the negative of the change in temperature with respect to height, usually expressed in Kelvin per kilometer. The *dry adiabatic* lapse rate is the lapse rate for a parcel lifted adiabatically without condensation (about 10 K/km) and the *moist adiabatic* lapse rate is the lapse rate for a saturated parcel lifted adiabatically while condensing out its water vapor (as low as about 4 K/km).

conditionally unstable. A parcel lifted to the level where it had cooled sufficiently to become saturated, would be convectively unstable.

An *unsaturated* conditionally unstable region of the atmosphere is, nevertheless, *linearly stable*. Disturbances of sufficiently great magnitude may set off this potential instability. Despite the need for a finite amplitude perturbation for initiation, linear instability theory can still be applied to this situation from the point where a parcel becomes saturated. The horizontal spatial scale of the updraft region in convective cells from this process is usually of order 10 km, with individual updrafts usually only a few hundred meters across. Small scale downdrafts occur within the cloud, but if there is precipitation and a net warming, there is also descent on a much larger scale. This can be explained on simple theoretical grounds. Upwards motions for saturated parcels provide energy to power the convective cell. The dry adiabatic descent in a subadiabatic region requires the expenditure of energy. This expenditure is minimized by having a small vertical extent for any sinking over as large an area as possible. The mass flux must be approximately balanced between the updrafts and downdrafts. This analysis was first provided by Bjerknes (1938). Individual convective cells usually die in less than an hour because they exhaust their supply of convective available potential energy or they create a stable layer that prevents the release of any remaining potential energy.

When parcels change pressure or height, their energy is not conserved. So entropy, which is conserved, is frequently used when examining parcel motion. More than one way of thinking about entropy has been presented in the past century and a half. Entropy is often referred to as a measure of the “disorder” of a system. In statistical mechanics it is proportional to the logarithm of the number of allowed quantum mechanical states for the system. However, the usefulness of entropy in this work here goes back to its earliest thermodynamic usage as a state variable conserved in adiabatic processes.¹¹

¹¹Argument over the primacy of these two definitions continues to this day (e.g. Buchdahl 1989).

Entropy is a state function equal to the integral of sensible heat flow into a system divided by the temperature of the system at which the heat is input, $S = \int \frac{dQ}{T}$. In this context, unlike in statistical mechanics, the zero of the function is arbitrary. Derivations of this expression can be found in any elementary textbook on thermodynamics (e.g. Sears and Salinger 1975, ch. 5, and also see section 11-8). In any adiabatic¹² process, there is no heat flow ($\Delta Q = 0$) so entropy is conserved. To a good approximation, moist parcel movements in the atmosphere are adiabatic. The important diabatic processes are precipitation, radiative heat transfer, and evaporation from the ocean.

Meteorological practice complicates the matter through the use of potential temperature and equivalent potential temperature as measures of entropy. (These are measured in Kelvin, rather than the standard units of $\frac{\text{energy}}{\text{temperature} \cdot \text{mass}}$ for an intensive measure of entropy). This provides information on the relative buoyancies of parcels. One definition of equivalent potential temperature, θ_e , is the temperature that a moist parcel would have if it was lifted high enough for “all” of the water vapor to condense (or sublime) and fall out as precipitation, with the latent heat released being used to heat the air, and the parcel was then brought to a standard reference pressure, usually 100 kPa. This, however, is not an adiabatic process since the water substance is not conserved; this hypothetical process is usually referred to as “pseudoadiabatic”. This measure is conserved for a moist rising parcel in the absence of diffusion and radiative effects. The difference in latent heat released between condensation to liquid water and sublimation to ice is significant, but it has not always been treated carefully. A cross section of θ_e for the core of a mature hurricane is shown in figure 2.8. A detailed discussion of these issues can be found in Iribarne and Godson 1981.

¹²Many authors (the names will be omitted to protect the guilty) refer to heating from condensation in cumulus convection as “diabatic”. This is incorrect. Unless there is heat flow or mass flow (e.g. precipitation) across the boundary of a parcel, the process is not diabatic. The misconception stems from studies where the temperature change from any process other than *dry* adiabatic pressure change is treated, as if it were from some diabatic process, imposed *deus ex machina*.

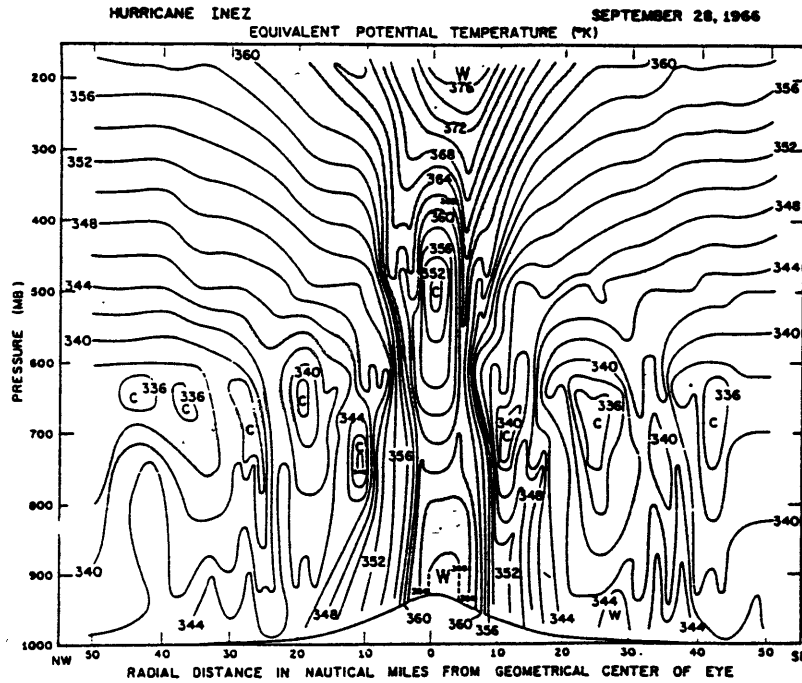


FIG. 16. In moist adiabatic ascent, the equivalent potential temperature should remain constant with height. Traces of such a regime were evident in the eye wall and rain bands.

Figure 2.8: Cross section of equivalent potential temperature for the core of a mature hurricane [from Hawkins and Imbombo 1976].

The complications involving water, in its various phases, are severe and cannot be ignored. Since entropy is measured in temperature units for relative buoyancy calculations, note that the simplification is not entirely successful. Water vapor is less dense than dry air, so a moist parcel is less dense than a dry one at the same temperature and pressure. The amount of liquid water or ice retained by a parcel after condensation greatly affects its relative buoyancy, but there is yet no simple way to predict this. Inclusion of these effects is accounted for in such measures as virtual temperature and virtual potential temperature. The treatment of these differences is at the heart of the disagreements over the amount of CAPE in the tropical atmosphere. These issues will be discussed further in section 4.3.

If the boundary layer provided moist air at its mean humidity indefinitely, which then saturated upon rising, though moist convection would occur driving

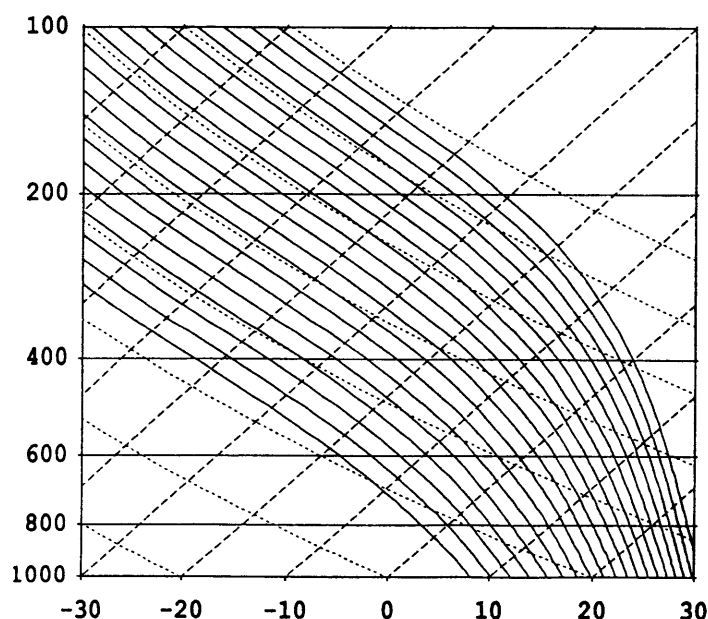


Figure 2.9: Skew-T diagram showing moist pseudoadiabats from 300 K to 390 K with 5 K intervals. The left axis is pressure in mb, the bottom axis and the long dashes are for temperature in $^{\circ}\text{C}$ with a 10°C interval, and the short dashes are for potential temperature with a 20 K interval.

secondary motions, nothing as ferocious as a hurricane or typhoon would result. The mixed layer usually has a mean relative humidity of 80% and a depth of about 500 m. Below it, the surface layer has a strong moisture gradient which saturates at the sea surface. (The surface layer also has a steep unstable potential density gradient.) A parcel of air at 298 K (25°C) and 1000 mb if at 80% humidity would have an equivalent potential temperature, θ_e , of 344 K (using the formulae from Bolton 1980). If the parcel were saturated, θ_e would be 356 K, showing the strong sensitivity to water vapor content. At constant relative humidity, small changes in temperature lead to much larger changes in equivalent potential temperature. For a temperature of 300 K (27°C) θ_e for 80% humidity is 352 K, while for a saturated parcel it is 365 K. Figure 2.9 is a skew-T diagram with several pseudoadiabats shown. What appear as small differences in the boundary layer, manifest themselves as large temperature perturbations aloft. This becomes more true as the surface temperature increases, with a 30 K increase in θ_e for a saturated parcel as the temperature increases from 25°C to 30°C .

The warming process from moist rising parcels is not simple. McBride (1981b) noted some of the steps involved:

Gray (1973), Lopez (1973) and Yanai *et al.* 1973 have shown that the latent heat released goes primarily into potential energy gain and increasing the temperature of the rising air parcel to that to the environmental temperature. The small extra (above environment) temperature increase of 1–2°C of the rising cumulus or Cb [cumulonimbus] parcel which is required for buoyancy does not warm the environment unless it directly mixes out from the cloud at a higher temperature. It appears that the rising cumulus parcel typically continues rising until it loses its buoyancy and temperature excess. It then mixes with its environment at a temperature little different to [sic] (or even lower than) that of the environment. Any heat transports out from the rising cloud are overcome by evaporation of the residual liquid-water particles as the clouds die. Although heavy rainfall may have occurred, there is typically no local region warming; instead there is often a local cooling of the immediate environment. This assessment has been substantiated in an observational study by Grube (1979).

In terms of a vertically integrated heat budget over a volume including the cloud cluster, the latent heat released in non-precipitating clouds does not increase the heat content of the volume, as it is counteracted by reevaporation within the same volume. The latent heat released as precipitation, however, does act as an energy source for the volume.

Most of the actual warming occurs through subsidence. However, on a practical level, when examining flows with a much larger scale than individual clouds, one can simply view warming as accompanying precipitating convection. Net warming of the atmosphere results even if the convection is forced and parcels experience no buoyancy, as long as the precipitation efficiency is greater than zero. If the precipitation efficiency is greater than zero, but there is no buoyancy for rising parcels, i.e. the fluid is absolutely stable in the vertical, there is still a net warming of the atmosphere; however, the energetic cost of forcing the upwards condensation causing motions, is greater than the resulting creation of available potential energy.¹³

¹³A few *gedanken* experiments can make of some of the transformations that occur for various types of circulation with different stratification more clear. Maintenance of

appropriate stratification; prevention of precipitation, diffusion, and radiation; driving of desired circulations; and violations of physical law on demand; are provided by a daemon named after Espy.

Gedanken Experiment 1. Start with air that is saturated with water and moist neutrally stratified for parcels lifted adiabatically, retaining all their liquid water that condenses. The air is also then very stably stratified with respect to downward adiabatic motion. Espy's Daemon forces a small amount of closed circulation, preventing all irreversible processes.

The entropy of the system is unchanged; there has been no heat flow in or out of any parcel. In the ascending branch, the density profile remains unchanged, though the potential temperature of individual parcels increases (while the temperature decreases). The descending branch experiences an overall warming due to adiabatic compression. Warming occurs not at the locations of condensation and latent heat release, but in the descending regions with dry thermodynamics. The available potential energy of the system is increased, as a lateral temperature gradient develops where none existed previously.

The resulting buoyancies and pressure forces oppose the direction of this (indirect) circulation. This increase in energy cannot be provided by the heat releasing moist processes, but must come from the Daemon or some other outside forcing.

Gedanken Experiment 2. Start with air that is saturated and neutrally stratified for dry adiabatic descent. The fluid is then quite unstable for upward motions with condensational heating. Espy's Daemon again provides a small amount of closed circulation, while preventing all irreversible processes (and runaway instability).

As before, the entropy of the system is unchanged. In the descending branch the density profile remains unchanged. In the ascending branch, the overall profile warms as the latent heat release more than compensates for the stratification.

Now the resulting buoyancies and pressure forces would drive the (direct) circulation in the direction it has been disturbed, indicating the basic state is unstable.

Actual conditions in the summertime tropics are not as extreme as either of these examples. The moist updrafts are only slightly unstable and there is always an energetic cost in forcing dry subsidence.

Gedanken Experiment 3. Start with a parcel of air near the lower boundary that is just slightly substaturated. The overlying atmosphere up to say 10 km is stratified more than moist neutral and less than dry neutral, i.e. conditionally unstable to upwards motion of saturated parcels but stable for dry dynamics. Above

When parcels ascend, the largest share of the energy released is used simply to increase the potential temperature of the air up to that of its new surroundings, hence it creates no potential energy and it is unavailable for conversion to kinetic energy. If there is sufficient latent heat release (or sufficiently weak stratification) to provide positive buoyancy, a parcel will accelerate upwards. Most of the kinetic energy directly generated as vertical velocities, by buoyant accelerations down the vertical pressure gradient, is eventually dissipated once parcels pass their level of neutral buoyancy. There are still additional ways for a cyclone to lose energy. Momentum dissipation provides a sink for kinetic energy provided by any means. Some energy is also radiated away by gravity waves to the surrounding atmosphere and heat is lost as electromagnetic radiation to space.

The generation of kinetic energy, as opposed to just moving it around, usually requires flow down a pressure gradient. As already noted, this occurs for ascending parcels, but most of this energy is radiated away by gravity waves or more usefully returned as potential energy as a small amount of warming from frictional dissipation. *The primary kinetic energy source is from the radial inflow in the lower level cyclone. The inflow is forced by the net convective heating and the upward acceleration of convecting parcels with the requirements of the continuity equation.* Budgets of these processes for developing storms are given by McBride (1981b).

10 km this atmosphere is set very stable, even to saturated surface parcels. Espy's Daemon now forces the slightly subsaturated parcel up to where it saturates, and becomes unstable to upwards perturbation. The Daemon gives the parcel a slight upwards kick, and enforces the prohibition on thermodynamically irreversible processes.

The parcel takes off, accelerating until it reaches the stable layer, decelerates, and then oscillates indefinitely. Some descent occurs in the neighborhood of the ascent region as required by continuity. There is a warming in response to this descent because of the static stability to dry descent. The total amount of warming is approximately equal to, though slightly less than, the amount of latent heat released by the condensation in the rising parcel. Though both precipitation and evaporation have been prevented by the Daemon, this scenario in many ways approximates how the actual atmosphere warms due to cumulus convection.

The potential energy increase is also caused by convection, as already noted, by subsidence closing the convective circulations. Anthes and Johnson (1968) discuss the generation of available potential energy. They note that this requires heating (cooling) at the high (low) pressure locations of a dry entropy (θ) surface. This is more usually (and equivalently) thought of as heating (cooling) at the high (low) dry entropy areas on a pressure surface; i.e. heat where it is hot and cool where it is cold to power the system. A corollary of this is that *heating at the radius of maximum winds, where the thermal gradient is largest (rather than where the thermal perturbation is largest), will weaken a cyclone.*¹⁴

There have been many studies of the energy fluxes and balances of mature hurricanes. Most workers have assumed that the cyclone has reached steady state. Energy budgets have been calculated by J. Malkus and Riehl (1960), Riehl and J. Malkus (1961), W. Frank (1977b, c), and Takahashi et alii 1951, amongst others. The energy balance in numerical models has been discussed by Kurihara 1975 and Lord et alii 1984, amongst others. A highly simplified picture of the energetics, examining thermodynamic requirements and efficiency can be found in Emanuel 1986. Some workers have attempted to measure the balance in growing disturbances, such as McBride (1981b), Riehl and J. Malkus (1961), and Yanai (1961a).

¹⁴The gradient wind relation for a balanced vortex can be expressed as $(f + \frac{v_1}{r}) v_1 = \frac{\partial \phi}{\partial r}$ [see eq. (5.15)]. Taking a radial derivative of this and noting that at maxima (and minima) in v_1 , where $\frac{\partial v_1}{\partial r} = 0$ we have $\frac{\partial p}{\partial r} = -(\frac{v}{r})^2 < 0$. If we now assume a cyclonic vortex, where $\frac{\partial p}{\partial r} > 0$ and $\frac{\partial p}{\partial r} \Big|_{r=0, r \rightarrow \infty} = 0$, the radius of maximum winds occurs at greater radius than the inflection point of the pressure profile. Heating concentrated at this radius, that does not extend to the center nor approach a spike profile, will tend to spread out the pressure gradient and hence decrease the maximum wind strength.

2.4 Angular Momentum

To spin up a tropical cyclone a source of angular momentum is required, in addition to the energy source discussed above. The source resides in the angular momentum a parcel has by rotating along with the spinning earth. Parcels very close to the equator have almost none of the necessary component of angular momentum normal to the earth's surface. This is why tropical cyclones do not form within 5° of the equator. For convenience, the term “angular momentum” will be slightly misused, in a manner that is traditional for meteorologists. The quantity used will be the scalar angular momentum density (i.e. velocities rather than momenta are used) in the vertical direction only.¹⁵

A process that forces a parcel toward the central axis does not exert a torque about that axis,¹⁶ so the angular momentum is conserved and v must increase. Such a process will, of course, require an energy source. It will be safe to assume that the primary supply of angular momentum comes from the initial reservoir associated with the earth's rotation, that there are no internal sources or sinks, and that the only significant boundary flux is at the lower sea surface boundary.

The secondary circulation is, therefore, essential for intensification. Inflow in the lower layers leads to cyclonic spin up and outflow aloft leads to spindown. This

¹⁵For physicists, angular momentum is a vector and is defined with respect to a *point* of origin. In the absence of torques, it is conserved componentwise. Concern here will be only with the component normal to the surface of the earth, i.e. vertical, which considers only motions in planes parallel to the surface, i.e. horizontal; and vertical parcel displacements will be much smaller than horizontal ones. This allows us to refer to a scalar angular momentum with respect to a central *axis* (rather than point) of a cyclone. Included in the angular momentum of a parcel is a term from the rotation of the earth when the parcel is at rest with respect to the earth. The resulting expression for angular momentum is then $M = \hat{z} \cdot (\mathbf{r} \times \mathbf{v}) + \frac{f}{2} r^2$, where \hat{z} is a vertical unit vector, \mathbf{r} is the position vector, r is the magnitude of \mathbf{r} , and f is the Coriolis parameter for the specified latitude [$f = 2 \sin(\text{latitude}) \cdot \text{earth's angular rotation rate}$], which is twice the projection of the earth's rotation on the central axis of the storm. If we further restrict the situation so that the horizontal motion is dominated by the primary azimuthal circulation, then $\hat{z} \cdot \mathbf{r} \times \mathbf{v} \approx rv$, where v is the azimuthal velocity, positive counterclockwise.

¹⁶That is $\mathbf{r} \times \mathbf{F} = 0$, where \mathbf{F} is a force.

process was first correctly described by Ferrel (1856), who realized that the air motions were essentially spiral and that convection provided the energy source for the inflowing motion. If a parcel flows out to a radius beyond its initial position, it will develop anticyclonic flow with respect to the earth. Further, if a parcel loses angular momentum to the earth at low levels by friction, it will become part of an anticyclonic circulation at even a smaller radius than where it started, when it reaches the upper levels.

At 15° latitude quasihorizontal motions feel only about one quarter ($\sin 15^\circ$) of the rotation of the earth. Vertical motions feel nearly the full rotation rate ($\cos 15^\circ \approx 0.97$), or about four times greater. Nevertheless, it is the projection of the earth's rotation on motions nearly parallel to the surface that is more important. This is because motions in the vertical have a range of only about 10 km, while horizontal transport of a parcel during spinup is hundreds of kilometers. So, the exchange between relative angular momentum and planetary angular momentum for lateral motions is much greater on the relevant time scale of a few days. Angular momentum budgets are discussed in virtually all of the previously noted references that examine energy budgets (see p. 60). For discussions emphasizing angular momentum budgets also see Holland 1982, Pfeffer 1958, and Challa and Pfeffer 1984.

Closely related to angular momentum, through a spatial derivative, is vorticity. We will not often rely on vorticity dynamics in the analysis of later chapters. When vorticity conservation is derived, using angular momentum conservation and the continuity relation for conservation of fluid, it can be seen that the notion of spinup from vortex tube stretching is tightly linked to spinup from fluid laterally converging on the central axis

2.5 Precursors

Though it was noted at the start of this chapter that one needed the right type of initial disturbance to generate a tropical cyclone, it is still not known what

the necessary characteristics for those initial disturbances are. The most well studied precursors are the easterly waves of the North Atlantic (see Riehl 1954). Many storms come from other types of weak systems, but these have not been well characterized. Some seedlings seem first to appear in the Caribbean or Gulf of Mexico (Scofield 1938, N. Frank and Clark 1979) and some appear first over mid-ocean (N. Frank and Clark 1979). Ramage (1959, see also the references cited therein) puts in a word for cyclones that seem to develop strictly from the effect of upper level divergent circulations. Many cyclones near Australia begin along the shear line of the nearby monsoon (McBride and Keenan 1982). In addition to Riehl's (e.g. 1948a) reliance on the interaction of independent upper and lower level disturbances, Sadler (1976, 1978) has pushed the importance of variations in the large scale tropical upper tropospheric trough (TUTT) for tropical cyclone intensification.

One of the earliest suggestions that Atlantic hurricanes could be traced to westward propagating waves originating over Africa, was made by Piersig (1944) in 1936; others soon followed (Brooks 1940 and the references cited therein). Dunn (1940) traced many tropical storms back to waves that began over or near Africa. These low latitude waves are now called "easterly waves".¹⁷ Riehl provided the first structural description of the North Atlantic easterly waves from which the storms often originate (1954, ch. 9), as well as a description of full blown tropical storms (1954, ch. 11). In the North Atlantic, they occur only during the summer and autumn (Piersig 1944, Burpee and Reed 1982). Pacific easterly waves have been described by Reed and Recker (1971). A detailed review of observations from the GARP Atlantic Tropical Experiment (GATE), as well as a good summary of earlier work, was provided by Burpee and Reed (1982).

The best descriptions that we have for these waves while they are over the oceans are by Thompson et alii (1979) for the Atlantic, who provide energy balance as well as structural information, and Reed and Recker (1971) for the Pacific. Atlantic easterly waves have wavelengths of about 2500 km, and travel at about

¹⁷This is because they form in a current that goes west.

7–9 m/sec. Pacific waves are slightly longer and faster. In the North Atlantic trade wind region, one passes by every three to four days from May to November. For the Atlantic, it has been conjectured that they are the result of a barotropic instability of the easterly jet south of the Saharan desert at about 70 kPa (3 km above ground) (Burpee 1972). In a study of easterly waves at very low latitudes, Liebmann and Hendon (1989) noted that “[t]he anomalies appear to originate at upper levels and then propagate downward.” The strongest precipitation and surface convergence were observed slightly ahead of the surface trough. A theoretical analysis was made by Stevens et alii (1977) based on wave-CISK. Mass (1979) used a linear numerical model to produce modes that in some ways resemble easterly waves, but as yet the problems of easterly wave genesis and propagation are not fully solved.

Though not all of the following is well established, I will take the following as needed for intensification of these weak disturbances. Further development requires that the initial disturbance tap the energy sources of the CAPE for parcels in the boundary layer with respect to the air column above and the additional heat in the upper ocean. First, there must be sufficient CAPE, which can be provided by high temperature and humidity in the boundary layer and/or low temperatures in the upper troposphere. Minimal stability for the lower troposphere (above the boundary layer), which will comprise most of the inflow layer, with respect to the upper troposphere may also be needed. Finally, there must be sufficient convergence in the boundary layer near the disturbance trough to force convection and build a warm core intensifying the low pressure.

Chapter 3

Previous Work

But to return from this digression, in *August* the weather at *Tonquin* is more moderate, as to heat or wet, yet not without some showers, and *September* and *October* are more moderate still: yet the worst weather in all the year for Seamen, is in one of the 3 months last mentioned: for then the violent Storms, called *Tuffoons*, (*Typhones*) are expected. These winds are so fierce, that for fear of them the *Chinese* that Trade thither, will not stir out of the Harbour, till the end of *October*: after which month there is no more danger of violent Storms, till the next year.

Tuffoons are a particular kind of violent storms, blowing on the Coast of *Tonquin*, and the neighboring coasts in the months of *July*, *August*, and *September*. They commonly happen near the full change of the Moon, and are usually preceded by very fair weather, small winds and a clear Sky. Those small winds veer from the common Trades of that time of the year, which is here at S.W. and shuffles about to the N. and N.E. Before the Storm comes there appears a boding Cloud in the N.E. which is very black near the Horizon, but towards the upper edge, it looks of a dark copper colour, and the higher still it is brighter, and afterwards it fades to a whitish glaring colour, at the very edge of the Cloud. The Cloud appears very amazing and ghastly, and is sometimes seen 12 hours before the Storm comes. When that Cloud begins to move apace, you may expect the wind presently. It comes on fierce, and blows very violent at N.E. 12 hours more or less. It is also commonly accompanied with terrible claps of Thunder, large and frequent flashes of Lightning, and excessive hard rain. When the wind begins to abate it dies away suddenly, and falling flat calm, it continues so an hour, more or less: then the wind comes about to the S.W. and it blows and rains as fierce from thence, as it did before at N.E. and as long. (Dampier 1699, Part I, p. 35.)

Tropical cyclones have been known to the Europeans for several centuries. Ludlam (1963) traces hurricane descriptions for the north Atlantic back to the late voyages of Christopher Columbus. The basic “whirlwind” flow was recognized at least by the late seventeenth century (Bohun 1671),¹ though Redfield (1831) is often credited with first clearly describing the surface cyclone. The distinguishing feature of the the warm core was not always considered a distinguishing feature. In the latter part of the nineteenth century a “thermal theory of cyclones” was developed, which suggested that all cyclones had warm cores. This theory is discussed in depth by Kutzbach (1979). It was generally (though not unanimously) held that the latent heat of vaporization from the condensation of water vapor in the ascent of warm, moist air, and the resulting relative buoyancy, provided the energy for cyclone formation. This was put forward clearly by Espy in 1841 (also see Kutzbach, ch. 2.2ff). Some of the impetus for this theory was data from tropical cyclones.

The work of Reye in 1872 on storm formation was primarily on tropical cyclones, yet Reye thought that similar processes drove all cyclones (see Kutzbach ch. 4.4). Since there was no great amount of data to the contrary, this was a reasonable application of Okham’s razor² — with incorrect result. Redfield, who is given great credit for his observations of tropical storms, also did not make a clear distinction between tropical and midlatitude cyclones (see Kutzbach, ch. 1.2). Margules in 1906 was probably the first to note that very different mechanisms and structures might be associated with storms in different locations (see Kutzbach, p. 193). He claimed that horizontal temperature gradients drove cyclones in the middle and upper latitudes while convection of warm saturated air provided the energy for tropical ones.

¹Bohun (1671) also provided an early description of metal corrosion and building degradation from atmospheric pollution in an urban area (London).

²*Pluralitas non est ponenda sine necessitate* (Plurality is not be be posited without necessity); or *Frustra fit per plura quod potest fieri per pauciora* (What can be explained by the assumption of fewer things is vainly explained by the assumption of more things). Ockham was not the first to state such a principle. See the discussion in Boehner 1957.

3.1 Observations

Despite observations such as those by Dampier that led this chapter and analysis by Bohun (1671), until the nineteenth century, tropical cyclones were known more for their violence than for any structural regularity. There was extended battle between Redfield and Espy, with Espy claiming that the surface flow was primarily toward the center of the cyclone while Redfield correctly noted that the winds were primarily cyclonic with a small amount of inflow (the dispute is discussed by Ludlam 1969). Though the surface wind structure was finally well established by the second half of the nineteenth century, no upper air data were available until well into the twentieth. Comparison of disturbances that intensified with those that remained innocuous did not begin in earnest until the 1970s, and is still far from definitive.

Compared to the voluminous data available on midlatitude cyclones (which still frequently proves inadequate for some purposes), measurements on tropical cyclones are quite sparse. Several issues compound the problem. The primary difficulties for obtaining data are that the phenomena of interest occur over the oceans, where human presence is limited, and further that the storm creates conditions in which most creatures would rather not be. Most of the important spatial scales of the disturbances are of order 100 km or less. These are smaller than even the densest of the regularly operating land based synoptic grids. Finally, though there is great damage and some loss of life from the occasional tropical storm making landfall on one of the industrialized nations, the greatest effects and the largest number of occurrences are over poorer nations without well established programs of atmospheric research.

Of the data that have been collected, far greater emphasis has been placed on determining storm tracks than anything else. Next in importance have been measurements of the wind field. Data on the internal thermodynamic structure are limited. Since a large motivation for the study of tropical storms is related to track prediction, this remains the largest item on the research agenda. Forecasts of intensity changes and development have been far less sophisticated. Though

the observational record is poor for mature, intense tropical cyclones, the available record on developing disturbances is even more meager. And still less information has been collected on tropical disturbances that failed to intensify. Hence, there are few papers comparing growing and nongrowing systems. Elsberry (1987) described in detail the current observing program.

The observations discussed here will be restricted to those that describe or analyze growing disturbances or weak disturbances that failed to intensify. Full strength hurricanes will not be covered. Several books provide basic descriptions of the genesis, development, and intensification. W. Frank (1987) provided a good recent review of our knowledge of tropical cyclone formation. He divided the formation process into three stages:

- (i) Genesis — transition from a disturbance to a depression, the initial formation of a rotational circulation with a scale of a few hundred km;
- (ii) Development — transition from tropical depression to tropical storm; and
- (iii) Intensification — the evolution from the tropical storm stage to a hurricane (mature cyclone).

I will usually lump both of the last two categories under *intensification* and include the creation of the initial disturbance under *genesis*. So here, genesis will refer to processes that occur frequently, such as those that lead to cloud clusters, and intensification will refer to the less frequent processes that transform a weak disturbance, such as a cloud cluster, into a tropical cyclone. The review by Anthes (1982) was more limited in its analysis of the development process than that of W. Frank, but is much easier to locate. R. Simpson and Riehl (1981, p. 71ff) presented several scenarios of cyclones developing from synoptic scale tropical disturbances.

Satellite photographs and other remote observations have greatly improved tracking and forecasting but give few clues to the internal dynamics, except for providing cloud patterns. In the formative days of a cyclone, the disturbance is over open ocean where few data are regularly collected. Frequently, by the time

data collection has begun, if it is to be done at all, intensification has already begun in earnest. Observational studies come in three basic groups: case studies, composite studies, and climatological studies.

3.1.1 **Climatology and Composite Studies**

The climatological works that examine large numbers of storms have avoided detailed discussions of the initial disturbance. Providing a small improvement on Dampier's note of seasonality, Tannehill (1935) showed a strong correlation of tropical cyclone occurrence with sea surface temperature (SST) in several locations around the world, even matching the occasional local temporal double maximum that occurs in some locations. Several criteria have been empirically determined as necessary for hurricane formation. The first of these, as proposed by Palmén in 1948, were the requirements that the SST be at least 26–27°C in the formation region and that formation occur outside a narrow region of the equator. In 1956, he added the additional criterion of weak vertical wind shear. These criteria have stood the test of time well. The SST requirement was obtained strictly by observation. Palmén realized that lack of storms at the equator was tied to the need for a source of planetary vorticity (or angular momentum). Using monthly mean soundings, he found that during the hurricane season it appeared that surface parcels were unstable up to about 10 km (referred to as the “level of neutral buoyancy”). Tropical cyclones occur virtually everywhere that these conditions are met, though infrequently in some of these regions.

Cyclones are most likely to intensify over very warm water and will weaken if they move over cooler water (Fisher 1958; Pelroth 1962, 1967). Pelroth (1969) determined that not just the SST needed to be high, but that the warmth must extend down some depth, say 200 feet, for tropical cyclone initiation. Wendland (1977) found an approximately exponential increase in tropical cyclone and hurricane frequencies with increasing ocean area of SST greater than 80°F (26.8°C), for the North Atlantic. Bansal and Datta (1972) provided some climatology of

the vertical atmospheric stratification for the Indian Ocean basin. For pseudoadiabatic ascent of surface parcels, they found monthly mean buoyancies of 4–8 K in the upper troposphere (c. 30 kPa) during the months with frequent storms, but considerably less than this during the remainder of the year. The drop in storm frequency for the Arabian Sea during the summer monsoon is matched by a drop in CAPE. A weak correlation between hurricane frequency and the quasi-biennial oscillation and climatological variables, such as SST and sea level pressure, was found by Shapiro (1982a, b). Even large scale cross-equatorial influences have been implicated in tropical cyclone formation (Love 1985) and Carpenter et alii (1972) found a statistical correlation between storm formation and lunar tides, but provided no mechanistic discussion.

Several other formation criteria have been added. Recent lists can be found in Gray 1968, 1979, and the decision ladder shown by Hebert (1978). Gray's (1979) parameters were used to create an overall index based on the product of six indices which in turn were based on (1) low level relative vorticity, (2) Coriolis parameter, (3) inverse of vertical shear between upper and lower troposphere, (4) ocean thermal energy—sea temperature excess above 26°C to a depth of 60 m, (5) vertical gradient of θ_e between surface and 500 mb, and (6) middle troposphere relative humidity. Gray's list is basically climatological. It ignores the problem of the initial disturbance.

The results of McBride and Zehr (1981) were based on the analysis of many developing and nondeveloping systems. They state their findings so succinctly that it is best to quote most of their abstract here directly:

- (i) Both non-developing and developing systems are warm core in the upper levels. The temperature (and height) gradients are more pronounced in the developing system, but the magnitudes are so small that the differences would be difficult to measure for individual systems.
- (ii) The developing or pre-typhoon cloud cluster exists in a warmer atmosphere over a large horizontal scale, for example, out to 8° latitude radius in all directions.
- (iii) There is no obvious difference in vertical stability for moist convection between the systems.
- (iv) There is no obvious difference in moisture content or moisture gradient.
- (v) Pre-typhoon and pre-hurricane systems are located in large

areas of high values of low-level vorticity. The low-level vorticity in the vicinity of a developing cloud cluster is approximately twice as large as that observed with non-developing cloud clusters. (vi) Mean divergence and vertical motion for the typical western Atlantic weather system are well below the magnitudes found in pre-tropical storm systems. (vii) Once a system has sufficient divergence to maintain 100 mb or more per day upward vertical motion over a 4° radius area, there appears to be no relationship between the amount of upward vertical velocity and the potential of the system for development. (viii) Cyclogenesis takes place under conditions of zero vertical wind shear near the system center. (ix) There is a requirement for large positive zonal shear to the north and negative zonal shear close to the south of a developing system. There is also a requirement for southerly shear to the west and northerly shear to the east. The scale of this shear pattern is over a 10° latitude radius circle with maximum amplitude at 6° radius.

Under the assumption of a symmetric disturbance, these findings can be synthesized into one parameter for the potential of a system for development into a hurricane or typhoon: Daily Genesis Potential (DGP) = $\zeta_{900\text{mb}} - \zeta_{200\text{mb}}$, when applied over $0-6^\circ$ radius. [The symbol ζ refers to relative vorticity.]

The presence of large scale positive vorticity ensures that the converging flow imports even more vorticity into the cyclone than just the planetary vorticity. The result of McBride and Zehr that both developing and nondeveloping storms can have large vertical velocities is interesting. I surmise that for the nondeveloping cases the horizontal inflow is not sufficiently concentrated near the surface. Inflow near the surface is a response to friction while middle level inflow is an adjustment response to the heating in cumulus convection. The high entropy inflow from the boundary layer, though smaller, is energetically more important for further intensification. Middle Level inflow during spin-up is still important for providing angular momentum convergence.

The tropical cyclone's aversion to vertical shear has been confirmed by several workers (see Merrill 1988a). Using aircraft obtained winds at 500 m, Middlebrooke and Gray (1987) found that the low level radial winds within 150 km of the disturbance center, were about twice as large in developing as opposed to nondeveloping disturbances. Tangential winds and central pressure provided no distinguishing

signal. These results are only compatible if the gradients of pressure and tangential wind are greater for developing disturbances even though the minimum pressure and maximum winds are similar.

A follow up on the work of McBride and Zehr was made by Lee. He noted (1989b) that enhanced surface energy fluxes for intensifying over nonintensifying cases "is found only after the formation of a tropical cyclone with a well-defined center." (Though this is supportive of a CISK type theory that relies on preëxisting CAPE, I find the result difficult to believe.) The cloud clusters destined to intensify had much stronger inflow below 80 kPa on a large scale, and overall had a larger scale circulation (1989a), hence the inward flux of angular momentum was much greater in the prehurricane disturbances. For all clusters in their early stages, precipitation was about three times evaporation in the inner 444 km, and about double from 444 km to 888 km (1989b). Lee also found that convergence prior to the presence of the prominent cloud cluster "appear[ed] to cause the region to be initially populated with shallow cumulus convection", which moistened the middle troposphere; this is consistent with the recent hypothesis of Emanuel (1989b) on the finite amplitude nature of tropical cyclongenesis.

All of these works suffer from the defect of insufficient definition of a control group. *Something* must be constant between the two groups for the comparison to be meaningful. It is conspicuous in the work of Lee (1989a) that even the weakest of the case groups that later intensify have stronger tangential winds and lower minimum surface pressure than either of the nonintensifying classes. This makes it impossible to determine what is different between intensifying and nonintensifying clusters when they have similar surface strengths (unless by some magical transformation disturbances destined to become tropical cyclones have their pressures drop and their winds increase discontinuously in time).

McBride and Keenan (1982) examined several seasons of storms near the northern coast of Australia. Cyclones crossed over land more than once per year, weakening but maintaining their integrity, then quickly reintensifying upon returning to a marine environment (they also review earlier works noting this process). Most disturbances for tropical cyclones near Australia began on the monsoon

shear line. McBride and Keenan also looked for correlations of intensification with nearby upper level troughs, but found that the most rapidly intensifying storms were accompanied by rather slowly evolving upper level patterns. This is in direct contradiction to the scenarios presented by Riehl (1948a, etc.) and those that have followed in his path.

3.1.2 Case Studies

The best case studies of tropical cyclone development are of the disturbance that became Hurricane Alma (1962), by Yanai (1968); of the beginnings of Hurricane Hilda (1964), by Hawkins and Rubsam (1968a); and of Typhoon Doris (1958), by Yanai (1961a). Yanai (1961a) first recognized the change in forcing from barotropic, with an indirect circulation, to a direct convection dominated development phase. In the earliest stages that preceded Hurricane Alma, Yanai (1968) again found that the circulation was indirect. Intensification into a tropical depression began after the precipitation area moved close to the center of circulation forming a direct circulation, with the upper tropospheric warm core located over it, and the anticyclone became vertically aligned with the low level cyclone. The most detailed case study of the complete life cycle of a hurricane was by Hawkins and Rubsam (1968a, b, c), which described the development of a warm core, and the inhibition of development and degradation while the center was over land. They saw the anticyclone as a consequence not a cause. The clouds and the warm mass were together, but both were to the east of the surface low, as in Yanai 1968. This does not match the easterly wave climatology of Reed and Recker (1971) or Thomson et alii (1979) which show the convergence, convection, and heating leading the trough, though not by much. These differences may be due to the vertical shear (F. Sanders, personal communication). The longest case study ran over three weeks using satellite photos to follow Hurricane Carmen from its days as an African overland disturbance (Thompson and Miller 1976). Vincent and Waterman (1979) provided a large scale synoptic analysis during the intensification phase of that storm. These papers contain the most detailed sequences of

events for development that have been published; it is difficult, however, to separate the elements that are general from those that are peculiar, with so few cases for comparison. Deppermann (1938; 1939a, b) provided many brief descriptions of typhoon formation, but almost all are couched in the language of frontal theory.

Two distinct sequences of typhoon formation were presented by Riehl (1948a), one for disturbances in the trade easterlies and one for disturbances in the equatorial westerlies. He described an upper level high passing over a lower level trough as an instigator of tropical cyclones in the trades, or a low level disturbance passing under an upper one; but in any case the requirement was still "*superposition in consequence of relative motion*" [emphasis in original]. This meeting is possible because of the difference in the propagation speeds of the upper and lower disturbances. A case study was presented fitting this progression. In the regions of intensification Riehl noted that the lower troposphere humidity is high and no trade inversion is present. Based on the intensity of rainfall associated with a nonintensifying travelling depression, Riehl concluded that "condensation energy alone cannot create intense tropical storms." His additional requirement was an upper level ridge. He later noted (1954, p. 327) "many of the heaviest tropical rainfalls occur without a closed cyclonic circulation. Even closed depressions with torrential precipitation often fail to deepen, traveling in a relatively steady state for 1,000–1,500 miles and more." More recently, Riehl (1975) has presented evidence that baroclinic energy sources are important in development.

Fett (1968a) described formation of a trough from the convergence of two anticyclones impinging on the intertropical convergence zone. Rapid intensification occurred after the disturbance moved north and interacted with a polar front. In particular Fett claimed that there was no evidence of an easterly wave. The description was similar to the formation mechanism for cyclones originating from equatorial westerlies mentioned in Riehl 1948a but not elaborated upon there. Fett (1968b) also noted from observations during aircraft reconnaissance that a significant descent was occurring in the eye and that some of the circulation warming the core was from that descent.

Anthes (1982) provided a fairly detailed scenario of the rather complicated machinations that the atmosphere might go through to produce a hurricane. His description included an easterly wave interacting with an upper level anticyclone, following Riehl. Emphasis was placed on the middle level convergence driven by cumulus convection providing vorticity for spin-up. Yanai (1968) provided a list of several early studies of tropical cyclone formation that used only visible or infrared satellite data, but as he noted these lack dynamically useful data. Case studies of several Indian Ocean cyclones were presented by Lee et alii (1989), with emphasis on asymmetric features of the wind field, but the discussion of the formation process was weak. Willoughby et alii (1984) described the development of concentric eyewalls in two strong storms. These outer convective bands can contract, as the initial eyewall does, until they choke off and replace the initial eyewall. It is not known if this process is similar to the initial eyewall formation. Two disturbances close in space and time, one which developed into a hurricane and one which did not, were examined by Foster and Lyons (1984). They found that the nondeveloper was subject to more environmental vertical shear and that the developer was imbedded in large scale cyclonic shear.

There have been attempts to correlate intensification with convective bursts observed in satellite infrared images (Steranka et alii 1986) and also with cloud top equivalent blackbody temperature (Gentry et alii 1980). Lags of 6 to 24 hours between convective activity and intensified surface winds were suggested. These efforts were only partially successful. Possibly, more consistent results would have been obtained by examining temperature gradient changes rather than looking for locations with infrared temperatures below some fixed temperature cutoff.

A case study based on budgets of mass, energy, and angular momentum was prepared by Riehl and J. Malkus (1961) from two separate days while a cyclone was intensifying. The separation between inflow and outflow was at about 50 kPa. They also noted that the internal dissipation was of the same order or greater than the surface friction, and determined that most of the momentum mixing was from vertical exchange. The secondary circulation was shown to increase as the storm intensified, even as the intensification rate approached zero. Also, the

fraction of the inflow associated with the surface layer increased over time. This is because the net cumulus heating is decreasing with decreasing CAPE,³ while the surface friction continues to increase with increasing surface winds. Merceret (1976) also found the kinetic energy dissipation in the bulk equal to about 1.5 times the boundary dissipation, for a mature storm.

There are some case studies of disturbances that failed to intensify, but these are mostly of no great utility since the data are so meager. A September tropical storm described as “relatively small and immature” was studied by R. Simpson (1954). He noted the lack of strong circular symmetry, that the eye was not as warm as a more intense storm, nor was the level of maximum temperature gradient as high as in a more intense storm. J. Simpson et alii (1967) examined a disturbance during late summer that failed to develop despite heavy rainfall. It had almost no surface signal and was imbedded in westerly shear. A disturbance that developed a warm core, but failed to intensify to tropical storm strength, was studied by Leary and Thompson (1976). However, they provided no discussion on the reasons for the failure of this system to develop further. A satellite photo comparison of a tropical storm with a weak tropical depression was made by Wright (1976), with little of use in the way of conclusion. Stossmeister and Barnes (1989) are analyzing a tropical storm that weakened while still over the ocean, from which we await further results.

Several case studies within the past decade have emphasized the importance of “momentum surges” in tropical cyclone formation. These are asymmetric structures and are viewed by all of the workers discussing them as external influences not induced by the cyclone itself. The first of these was by Molinari and Skubis (1985), which looked at low level features. More recently Molinari and Vollaro (1989) examined upper level features. Several works from Colorado State University have emphasized such processes: e.g. Love 1985, Lee 1986, Lunney 1988, Lee

³According to the point of view of Emanuel 1986, this is because the disequilibrium between the sea surface and the air column above is decreasing, since most CAPE is assumed to be eliminated by convection almost immediately upon its creation.

1989a, Lee et alii 1989. Little in the way of dynamical reasoning for the sources of these surges has been provided. I hazard a guess that such surges will eventually be shown to be a gravity wave induced response to convection in a cloud cluster, rather than a cause of it.

3.2 Theory and Numerical Modelling

Six basic groups of theories have been applied to the hurricane problem. These groups are not mutually exclusive. Convective theories are the oldest and date back to before the realization that the energy sources of tropical and midlatitude storms might be different. Brief attempts were made to apply the frontal theories of the Norwegian school. The next group called on inertial instability, or the related symmetric instability, to initiate explosive growth of the large scale storm.⁴ An hypothesis was then suggested that the superposition of upper and lower level disturbances was necessary for development. Later CISK was introduced and combined conditional convective instability with a frictional boundary layer. The most recent addition was air-sea interaction theory. Each of these will be discussed in more detail below.

⁴Inertial instability occurs if there is an unstable balance between the centrifugal force (including the Coriolis force) and the pressure gradient. If a parcel is displaced outward, conserving its angular momentum, the pressure gradient of its new surroundings will let the parcel continue outwards rather than returning it towards its initial position. The requirement for inertial instability, first stated by Rayleigh, is that the radial derivative of the square of the absolute angular momentum is negative. This stability problem is discussed in some detail by Chandrasekhar (1961, ch. 7).

For a baroclinic flow, i.e. pressure surfaces and density surfaces do not coincide, parcel displacements are not usually horizontal. The related instability for parcels perturbed along isentropic surfaces is called "symmetric instability". For a discussion of this, including the effects of moisture, see Emanuel 1983a.

3.2.1 Early Theoretical Work

An early review of the status of hurricane formation theories was provided by Riehl in 1950. At that time, none of the available theories was convincing. Important data on the development of the boundary layer were already available and are described by Riehl. In particular he referred to the great rise in the moisture content of the boundary layer and that the boundary layer remains nearly laterally isothermal despite the drop in pressure moving toward the center, as noted by Byers (1944, p. 432).⁵ This appears to provide a rather large source of energy, as Riehl noted while comparing soundings on a tephigram. The recognition of the energy source was crucial, but this did not provide a mechanism for release of that energy or provide any clue as to why that energy was not released more often. Riehl reviewed three classes of hypotheses before proposing one of his own. These were the convectonal hypothesis, the frontal hypothesis, and the hypothesis of “dynamical instability”.

As noted, the convectonal hypothesis is the oldest and is basically the thermal theory of cyclones mentioned in the introduction and reviewed in depth by Kutzbach (1979). Riehl noted that it provides no explanation for organized mass removal aloft nor any reason for the organization of the convection. He noted that most heavy tropical rainfalls occur without any strong organized disturbance. The frontal hypothesis (Scofield 1938, and the references therein [many from the German language meteorology literature]) was the Norwegian school’s explanation for midlatitude cyclogenesis, i.e. baroclinic instability. It results in a cold core aloft, or at least large temperature perturbations at the upper and lower boundaries, which is clearly not applicable to tropical cyclones. An attempt to rescue frontal theory in this context was made by Bergeron (1954). Dynamical instability referred to works such as those by Sawyer (1947) and Solberg (1936) which appealed to inertial instability of the anticyclone aloft. Riehl objected to this with arguments

⁵It is now thought that most of the dry entropy increase is from a *downward* flux of heat rather than a large sensible heat flux from the sea surface (W. Frank 1984).

involving the evolution of the mass field and continuity which are simply incorrect. (These theories actually fail on energetic grounds. The energy source for the inertial instability is the convection and the already existing spatial pattern of the disturbance convection. Any inertial instability is the result of convective updrafts being more vertical than angular momentum surfaces. The inertial instability drives parcels towards a surface of the same absolute angular momentum.) Riehl's own hypothesis noted that upper level cyclones and anticyclones propagate faster than the surface cyclone. The initial disturbance was claimed to rapidly intensify when an upper level cyclone is colocated with a low level trough. Farrell (personal communication) finds this consistent with his initial value problem approach to midlatitude cyclogenesis (e.g. 1988, and other works by Farrell cited therein).

The early theoretical conjectures tried to explain tropical cyclones with instability mechanisms applicable to the dry atmosphere alone. Sawyer (1947) proposed that inertial instability was responsible for driving mass from the vortex center. Kleinschmidt (1951) appears to have been the first to correctly realize that the sea surface was the primary energy source for a tropical cyclone. The bottom of the troposphere was recognized to be moist unstable, providing energy for the storm. Above the moist unstable layer, moist neutrality was assumed. Above the friction dominated boundary layer, parcels were assumed to move radially outward with increasing height conserving their absolute angular momentum. (Emanuel 1986 makes similar assumptions.) The conditions for what was then called "dynamic instability" (and what is now called moist symmetric instability) were declared the conditions for tropical cyclone creation.

The work of Yanai (1961b) was a logical continuation of that of Kleinschmidt. However, Yanai was quite conscious of the problem that simple moist convective theories lead to the smallest lateral scales providing the fastest growing instabilities. He viewed the formation process as having three distinct stages: forced vertical motions in easterly waves, excitation of cumulus convection and warming at the center, which then induced a large radial temperature gradient. This would

then supposedly lead to a large violent free convection from baroclinic instability. After demonstrating that horizontal inertial instability was not nearly energetic enough to drive the storms, Yanai (1961b) proposed a baroclinic instability. What he called “baroclinic instability” would now be called symmetric instability, though it does rely on a baroclinic energy source. Symmetric instability is essentially an inertial instability along isentropes, dry or moist as is appropriate, when the isentropes are not coincident with pressure surfaces, i.e. the flow is baroclinic. However this mechanism also comes up energetically short.

The early numerical models of hurricane instabilities that included moist processes (e.g. Kasahara 1961) were often representing instabilities on the cumulus convective scale forced into an axisymmetric context (see Lilly 1960). Problems of this kind must be watched for closely and still occasionally plague numerical models. There are several works that purport to provide theories for tropical cyclone initiation, but are instead more relevant to single cumulus clouds with an imposed cylindrical symmetry and a vertically unstable air mass. The first of these was by Haque (1952). This contained the useful innovation of using different physics for updrafts and downdrafts with matching conditions at the internal boundary. Lilly (1960) showed that on the scale of a tropical cyclone, convection could be unstable, especially if a frictional boundary layer with Ekman pumping was added. However, his solutions still had the property that smaller cells grew faster. Syōno (1953) put forward a linear instability theory that would now be referred to as moist symmetric instability. The energy source was still a vertical moist convective instability, but an attempt was made to combine notions that relied on vertical instability with those calling on inertial instability. A definitive review of work up through the early 1960s can be found in Yanai 1964.

The peak in theorizing on tropical cyclone formation was probably the Third Technical Conference on Hurricanes and Tropical Meteorology held in Mexico during June of 1963. Spar (1964) presented a review of the theoretical work up to that time. His comments on scale selection in instability theory and his critique of existing theory still remain relevant. Two of the papers, Ooyama (1964) and Charney and Eliassen (1964a), concerned an instability based on cooperation

between the larger scale flow and cumulus convection. These will be discussed in the following section (3.2.2). The problem of concern at this time was explaining the observed horizontal spatial scale, for it was well known that the preferred scale for an instability resulting from small random perturbations in a vertically conditionally unstable atmosphere was that of cumulus clouds.

Both Árnason (1964) and Kuo (1964) suggested instability mechanisms that combined baroclinic and convective processes. However, their approaches were quite different. Árnason proposed that the baroclinicity of the basic flow forced the most rapidly growing mode to be in the range of a few hundred kilometers to a couple of thousand kilometers. He linearly examined a system that was both baroclinically and statically unstable. The analysis of Kuo was closely tied to a gradient wind balanced vortex. Here the relevant baroclinicity was that of the vortex rather than that of the global zonal circulation. Heating was tied to the upward branch of the secondary circulation and the interior of the fluid was assumed conditionally unstable; the descending branch was not discussed. Alaka (1964) concentrated on the anticyclone aloft for determination of the horizontal length scale and suggested that inertial instability served as a “triggering mechanism” to explain the great increase in intensification rate that occurs early on, though still relying on conditional instability as the primary energy source.

3.2.2 Conditional Instability of the Second Kind — CISK⁶

Theories for tropical cyclone development that relied on conditional instability needed to explain the large spatial scale of the storm, the organized structure of the convective cells, and the long lifetime of the system. CISK was the answer provided, though a not completely adequate one. Friction at the bottom boundary leads to flow down the pressure gradient towards the center of a cyclone. Convergence or divergence of this flow leads to Ekman pumping or suction, respectively, out of or into the boundary layer. *The basic assumption of CISK, as the term will be used in this work, is that the deep convective cells are forced where there is Ekman pumping lifting moist parcels to their level of free convection.*

The best known of the existing body of work on possible instabilities leading to a hurricane, is that of Charney and Eliassen (1964b). Their conditional instability of the second kind (CISK) is based on positive feedback between the low level frictional moisture convergence of a synoptic scale disturbance and cumulus convection. A similar theory was developed contemporaneously by Ooyama (1964),⁷ that avoided some of the shortcomings of Charney and Eliassen, especially with respect to the parameterization of cumulus heating.

There had been some earlier work along this path, such as Syōno et alii (1951)

⁶Several things that are not CISK occasionally steal its name. Sometimes reference is made to a “CISK parameterization” as a scheme for specifying heating due to cumulus convection. Though both of the primary 1964 papers assume that the heating is mostly proportional to the positive vertical velocity out of the boundary layer and a simple constant, there is nothing inherent in the concept of CISK that requires this parameterization. There is also a concept known as “wave-CISK” (e.g. Lindzen 1974) which also ties heating to forced vertical motions, but in this case to some particular types of wave motions. To distinguish CISK with organization provided by boundary layer frictional convergence from some other induced convergence, say by waves, it has sometimes been called “Ekman-CISK” (e.g. Davies and de Guzman 1979), but this will not be used here.

⁷Issues regarding the priority of these contributions and their independence remain, and probably will remain, unsettled. See the Acknowledgments at the end of Charney and Eliassen 1964b, footnote 2 in Ooyama 1969, and the comments in Ooyama 1982.

claiming that rainfall was proportional to positive low level vorticity. CISK was presaged by Lilly (1960) when he put a frictional boundary layer under a model of moist convection and showed that this led to an increase in the lateral dimension of the largest unstable mode, though the smallest scales were still the fastest growing. All of these workers were aware of the result of Bjerknes (1938) that showed that conditional instability preferred “*a system with appreciable upward velocity in narrow cloud towers and slow downward motion in the wide cloudless spaces* [emphasis in original]”, and suggested that the actual width would be limited by turbulence. In the opening of their abstract, Charney and Eliassen (1964b) clearly state part of the problem and their solution:

Why do cyclones form in a conditionally unstable atmosphere whose vertical thermal structure is apparently more favorable to small-scale cumulus convection than to convective circulations of tropical cyclone scale? It is proposed that the cyclone develops by a kind of secondary instability in which existing cumulus convection is augmented in regions of low-level horizontal convergence and quenched in regions of low-level divergence. The cumulus- and cyclone-scale motions are thus to be regarded as cooperating rather than competing—the clouds supplying latent heat to the cyclone, and the cyclone supplying the fuel, in the form of moisture, to the clouds.

They assumed an axisymmetric disturbance in quasi-geostrophic balance and a frictionally induced vertical velocity at the top of the boundary layer proportional to the geostrophic vorticity (as they had derived in a paper from 1949). Since the large scale secondary circulation was taken to be forced, rather than a free buoyancy driven convection, the hydrostatic approximation was made.

One of the initial conditions was that the atmosphere was not saturated with water vapor in the mean, but rather in a large scale equilibrium with scattered cumulus convection. In the region of low level convergence, middle level heating was assumed proportional to the moisture convergence and also, less strongly, to middle level ascent; in the region of low level divergence the heating was assumed to vanish. Additionally, Charney and Eliassen relied on the cross isobar Ekman flow to provide a continual source of warm moist air in the boundary layer by

importing it from a distance away from the updraft region making up the eyewall of the hurricane. The model had two levels; and also two regions, an interior with positive vorticity and an exterior with negative vorticity. The radius separating these two regions was found as an eigenvalue solution to a transcendental equation resulting from the matching condition requiring continuity of the secondary circulation at the discontinuity. This was taken as the length scale of the solution, rather than the normal mode lengths of either region separately.

The results had two conspicuous defects. For high values of the relative humidity (greater than 0.91) the growth rate became unbounded at a finite disturbance size. (This problem has been addressed by Mak 1981 and Wang 1987.) More disappointingly, the solutions had increasing growth rates with decreasing scale length as does regular conditional instability. The only encouraging sign was that the growth rate was nearly independent of disturbance size up to 100 km, so scale selection might just be highly dependent on the initial disturbance (rather than scale selection by fastest growing mode). Ogura (1964) modelled this system numerically, though unbridled growth results.

The cumulus parameterization of Ooyama (1964, 1969) was markedly different from the choice made by Charney and Eliassen (1964b) and most of the workers who have followed in their (Charney and Eliassen's) path. Convective activity was still assumed proportional to mass forced out of the boundary, but there was the additional requirement that boundary layer air had a greater moist entropy than the air aloft, rather than simply requiring "moisture convergence" for net heating (which is insufficient). Charney and Eliassen included some heating from middle level moisture convergence, while Ooyama relied strictly on the boundary layer for providing buoyant air. Ooyama also relied more on local fluxes of moisture from the sea surface to sustain the moist boundary layer, though this is not apparent at lowest order in the linearized analysis where the entropies are fixed.

There have been many attempts to cure the fast growing small mode problem. Ooyama (1964) and Syōno and Yamasaki (1966) included an eddy viscosity so that the smallest disturbances no longer had positive growth rates. Charney (1973b) imbedded the problem in a constant current, which changed the surface stress

pattern and yielded a short length cutoff. Chang and Williams (1974) noted that the damping of adiabatic cooling from Ekman pumping, as in the standard Ekman spin-down problem, would provide strong damping at small scales if one allowed temperature fluctuations at the lower boundary. Some further technical quibbles can be found in Holton 1974 and a reply by Charney (1974). Chang (1971) found a fastest growing mode of about 4000 km for a particular vertical heating distribution. Other calculations with varying vertical distributions of heating are presented in Koss 1976, Davies and de Guzman 1979, Emanuel 1983b, Pederson and Rasmussen 1985, and in Bratseth 1985. These workers were all able to produce a short length scale cutoff for growing disturbances.

Fraedrich and McBride (1989) examined CISK in the short length scale limit, with a Charney and Eliassen type of cumulus parameterization. As already noted (Charney and Eliassen 1964b), the growth rate becomes independent of length in this limit. They reach this limit in a mathematically sloppy way.⁸ The assumption in the thermodynamic equation is that condensational heating from lifting a parcel matches the given stratification. They call this approximation the “free-ride balance”. This changes the thermodynamic equation from prognostic to diagnostic. There is still a need for cumulus heating. This work makes clear, however, that in the small scale limit the primary spinup mechanism for CISK is through driving the middle tropospheric secondary circulation which imports angular momentum. This “free-ride balance” is quite similar to Ooyama’s parameterization which also has no prognostic thermodynamic equation.

The length and time scale selection is different in works such as Ooyama 1964, 1969; Chang 1971; and Yamasaki 1969; that assume negative heating (i.e. cooling) in regions with Ekman suction, than in works such as Charney and Eliassen 1964b and this work, which correctly recognize that the thermodynamics of the convergent and divergent regions are not symmetrical. Syōno and Yamasaki (1966) made

⁸The analysis in Fraedrich and McBride 1989 creates a singular system without any remaining differential system for the interior region. However, the result can be rescued with a rigorous limit procedure. Since they later analyze the system properly and show that their result can be obtained as a limit, the sloppiness is surprising and unnecessary.

a direct comparison of the two approaches and showed that the updraft scales were similar, but smaller scale disturbances develop if there is both heating and cooling. Further, growth occurred at about half the rate when the heating was conditional upon upwards motion.

The first attempt to explain why so few disturbances develop, in the context of CISK, was made by Rodenhuis (1971). He showed that dry stable stratification could stabilize the system in the presence of moisture convergence and suggested that environmental stratification of the middle troposphere “control[led] the instability mechanism [emphasis in original].” (I note that this process was already included in the full model of Ooyama 1969.) After examining the sensitivity of various CISK type modes with differing moisture and heating profiles, Koss (1976) also concluded that the tropics are not often very unstable to CISK type processes.

The “generalization of the CISK theory” by Bates (1973), might better be called a muddying of the waters. His “Type A CISK” was essentially the CISK of Charney and Eliassen with the inclusion of increased pumping out of the boundary layer due to the time rate of change of the boundary layer pressure (the allobaric wind [see footnote 2 of Bates]). “Type B CISK” was due to convergence only above the boundary layer. This development provided the seed for “wave-CISK” and other corruptions of the acronym. Charney also (1973a)⁹ expanded slightly on CISK and suggested the CISK mechanism might also be responsible for the InterTropical Convergence Zone (ITCZ).

3.2.3 Hurricane Air-Sea Interaction Theory — HASIT

The air-sea interaction theory was first put forward by Emanuel in 1986. Using analytic techniques, the theory has only been applied to a steady state, mature tropical cyclone. Though originally just called “air-sea interaction theory”, I will

⁹This work also contains a clear, useful summary and historical review of almost all of the known instabilities relevant to the atmosphere.

refer to it as the Hurricane Air-Sea Interaction Theory (HASIT), since a similar approach has been brought to bear on other problems such as the Madden-Julian oscillation (e.g. Emanuel 1987, Neelin et alii 1987).

The primary assumptions of HASIT are fairly simple. It is assumed that the thermodynamic structure of the entire vortex is determined mostly by the radial thermodynamic structure of the boundary layer, with soundings along a momentum surface essentially following a (reversible) moist adiabat. The time scale of cumulus convection is taken to be sufficiently shorter than the time scale of the vortex evolution that changes in the boundary layer can be assumed to be immediately communicated aloft. Increases in the moist entropy of the boundary layer are brought about by increased surface moisture fluxes caused by the surface winds of the vortex. The reliance on this process provided the motivation for the name.

This alone will not lead to a growing disturbance. If the radius of maximum heating, or maximum boundary layer entropy, is coincident with the radius of maximum winds, the vortex will decay (see p. 60). In its early formulation (Emanuel 19886), HASIT relied on the radial advection of entropy by the frictionally forced cross isobar flow to shift the entropy maximum toward the center of the disturbance. The more recent work (Emanuel 1989b) suggested that differences in the moisture content of downdrafts into the boundary layer add to the boundary layer entropy gradient.

The steady model of Emanuel 1986 cannot be easily extended to very weak disturbances. Congruence of the equivalent potential temperature (θ_e^*) surfaces (allowing the approximation that θ_e^* is a proxy for calculating buoyancy) and the absolute angular momentum (M) surfaces does not apply to weak perturbations where the θ_e^* surfaces are nearly horizontal and the M surfaces are nearly vertical, unless one believes, as does Emanuel, that the entire troposphere above the boundary layer is essentially convectively neutral. The entire secondary circulation is treated implicitly. In the regions of descent, where radiative cooling is likely to be important, the dynamical structure cannot be sufficient, but in the

energetically important parts of the interior with updraft and outflow, the model does quite well for what might be called a maximal hurricane.

Emanuel (1989b) has recently extended these notions in an attempt to explain the intensification threshold. Since this is the only other theoretical discussion of the need for a finite amplitude disturbance preceding intensification, I quote at length:

Ekman pumping first induces upward motion and adiabatic cooling. The initial response of the model to this convective destabilization is to produce LPE [low precipitation efficiency] clouds. These are ineffective in opposing the adiabatic cooling but maintain convective neutrality by drying out the subcloud layer. The vortex thus cools and θ_e decreases... in the subcloud layer. Only when the lower-to-middle troposphere becomes nearly saturated can anomalous surface fluxes counter the drying effect of convective downdrafts to the extent that subcloud-layer θ_e actually increases. This increase is associated with an increase in temperature aloft and thus with an amplification of the cyclone.

.... The cyclone can only spin up if there is inflow *above* the boundary layer in this model. But the inflowing air is, in the model and in nature, potentially cold (i.e., it has low θ_e). If this air were to simply flow inward and upward, the vortex core would cool. What happens instead is that the lower-tropospheric air follows an indirect route to the tropopause. Before ascending, air above the subcloud layer first descends in convective downdrafts, is moistened by surface evaporation, and finally ascends in deep, HPE [high precipitation efficiency] convective clouds. Only if fluxes from the ocean succeed in raising the entropy above that of the ambient subcloud layer can the vortex core warm and the cyclone amplify.... The important limitation on initial growth is the low θ_e of the middle troposphere. Even if the initial ascent is due to processes other than Ekman pumping (e.g., ascent associated with a large-scale disturbance) the initial convection will be low precipitation efficiency and the argument presented here pertains.

The LPE clouds are also crucial to the maintenance of an intense vortex. By keeping the subcloud layer relatively dry outside the core, conditional instability to deep convection is reduced and the new upward convective mass flux remains concentrated in the core.

In its present form, HASIT has not yet fully solved the threshold problem. The analysis does not yet provide a way to determine the sufficient amplitude

for development, though the threshold is tied to the disturbances ability to saturate the middle troposphere. Observational tests that might distinguish between HASIT and CISK will be discussed in section 8.2.

3.2.4 Other Theoretical Work

Several theoretical works contain analysis relevant to tropical cyclone development, but cannot rightly be called full theories of hurricane development in and of themselves. Some arbitrarily constrain the system in some ad hoc manner. Many works entirely specify the thermal forcing and have no damping. The intensification is then not the result of any type of instability, but can still provide some information on vortex development.

A body of work, some analytic and some numerical, is based on equations developed by Eliassen (1951). Eliassen considered a gradient wind balanced circular vortex of arbitrary velocity profile, stratification, and baroclinicity to examine induced meridional circulations from thermal or frictional forcing. After much manipulation, a diagnostic equation for the secondary circulation stream function obtains, which depends only on the instantaneous structure of the vortex and the sources of heat and angular momentum (including friction). The equation is elliptical and solvable for all vortices that are inertially and baroclinically stable. Thermally driven meridional circulation is resisted, though not prevented, by inertial stability, and static stability fights vertical motion. Baroclinic effects tilt the elliptical streamlines. Though Eliassen used his model with zonal flows on a globe, the equations can be used for axisymmetric flows that are not pole centered. Though all of the dynamical fields are allowed to vary, the forcing, i.e. the momentum and buoyancy sources, is imposed with no feedback. Still some important lessons can be learned from these works.

Shapiro and Willoughby (1982) provided a fairly careful scaling analysis of the Eliassen equation for the case of a tropical cyclone. Using the basic Eliassen balance, but with a slightly different vertical coordinate, Schubert and Hack (1982) examined cyclone development with an imposed internal heat source. They found

that increased inertial stability decreases the forced secondary circulation for given heating. An encouraging but expected result was that when most of the heating is inward of the radius of maximum wind, the radius of maximum wind shifts inward. They also examined the induced inflow and the feedback between inertial stability and heating effects, possibly leading to eyewall formation. Hack and Schubert (1986) ran a similar model with invariantly imposed heating, and showed that the conversion of total potential energy to balanced rotational flow (the energy needed for both kinetic energy and added potential energy needed to maintain the thermal wind balance) becomes more efficient as the vortex intensifies. They also found that a vortex develops far more slowly as the heat source moves away from the center. This is part of the reason for the slow development of axisymmetric models that have only a quadratic drag law.

Ooyama (1969) and Sundqvist (1970) used continual evolution of this basic balance in their fairly successful numerical models. If the cyclone is inertially stable, Ooyama noted that the cyclone scale disturbance may still decay even if convection is unstable. Based on their extension of Sundqvist's (1970) model, Pfeffer and Challa (1981) comment that the secondary flow transport of moisture is required for hurricane growth. However the secondary flow in their model is strongly dependent on a realistic but imposed eddy momentum flux. Challa and Pfeffer (1984, 1990) have continued to argue through their modelling work for the importance of eddy momentum fluxes aloft as a driving force in tropical cyclone development. However, it is not clear if they view these as exogenous forcing, as do Molinari and Skubis 1985 and Molinari and Vollaro 1989, or as something intrinsic to the storm. Handel (1990) has provided energy based reasons to believe that the asymmetries and enhanced momentum fluxes may be intrinsic to the dynamics of a tropical cyclone.

Some models are even more restricted than just requiring gradient wind balance. If no momentum diffusion is allowed in the equations for the secondary circulation, a transformation can be made that is the cylindrical equivalent of semigeostrophy (Shutts and Thorpe 1978, Schubert and Hack 1983). In the new coordinates, the regions of strong positive vorticity are expanded, which greatly

improves numerical accuracy in computation. Additional integrations of such a system have been made by Thorpe (1985) and Emanuel (1989b) used this as a jumping off point for a more general numerical model which included dissipative processes. A closely related work by Shutts et alii (1988) closely traced parcels that are allowed to engage in a sort of penetrative convection. Without dissipation these models, of course, have no stationary states in the presence of *any* secondary circulation (including frictional boundary layer inflow).

Several other works are related to the intensification problem, but are more tangential, or proved to be dead ends. A heuristic model of hurricane intensification was developed by Carrier (1971b). It assumed, ad hoc, a hurricane-like structure in some detail and provided a rate for later stages of the cyclone development. The primary time scale was based on the removal of dense air from the central region replacing it with warm moist air that has been transported inward, while the inflow rate was based on earlier solutions by Carrier (1971a) on the behavior of a time dependent frictional boundary layer. Another exercise was by Gill (1982). Here the convergence was from the ageostrophic, heating induced, isallobaric wind (proportional to the time rate of change of the pressure). However, as in Carrier's model and the simplest CISK models, the requirement for an unlimited source of saturated boundary layer air remained. Contributions to boundary layer convergence from the isallobaric wind were also studied by Syōno and Yamasaki (1966). Shapiro (1977) derived a criterion for development based on the relative importance of nonlinearity, which emphasized that the nonlinear momentum advection terms enhance development of a hurricane, unlike many other disturbance types where these nonlinear terms are stabilizing. Confirmation of this mechanism is provided in this thesis. Relevant to precyclone disturbances, Dobrysham (1982) reviewed wave propagation and formation for modes that can exit in the tropics and in the 5°–15° latitude belt. He emphasized nonlinear and nonconstant coefficient effects that may be more important in the tropics than in the middle and upper latitudes.

3.2.5 Other Numerical Modelling Work

Numerical modelling efforts have been of two fairly distinct types. There have been simplified models, using idealized initial conditions, to elucidate the underlying dynamics of tropical cyclone development, some of which have already been discussed. The other modelling work is more in the tradition of numerical weather prediction, comparing model development from observed initial and boundary conditions with observed development, using full three dimensional models. Much of the work using actual storm data has concentrated on track prediction, rather than development, but there are some useful exceptions. Some of the earliest work was simply to show that it was possible to numerically model a tropical cyclone. One of the surprises is how many different models, with quite different internal physics, have all been able to generate hurricane-like vortices.

Variations in development from variations in vertical heating were examined by Yamasaki (1968a, b). He including changes in the heating distribution changes as the modelled cyclone matured and the vertical soundings approached moist neutral. Anthes (1971) noted that a vertical distribution of heating that provided more heating at higher levels than would be implied by changes from one pseudoadiabat to another, resulted in a more realistic simulation. This is consistent with the many processes that transport heat upwards.

Kurihara and Tuleya (1981) analyzed the genesis of a tropical storm from a shallow easterly wave, using a three dimensional primitive equation model with a moist convective adjustment scheme (that did not totally eliminate convective instability for unsaturated air). The development, except in the earliest stages, showed maxima in low level vorticity, vertical velocity, and precipitation, all near the vortex center; the simulation was not extended long enough to develop an eye. This is markedly different from axisymmetric two dimensional models with quadratic surface friction. In these models the vortex center has a relative minimum in convergence and vertical velocity (e.g. Kurihara 1975, Rotunno and Emanuel 1987). They also examined the vorticity and heat budgets in some detail. The effects of environmental shear have been investigated by Tuleya and

Kurihara (1981). They showed that easterly vertical shear was more conducive to intensification than westerly shear, and that strong westerly shear could inhibit development. Low level cyclonic shear and upper level anticyclonic shear were found to assist growth. The resolution of a model greatly affects the simulated development. Even without improving the resolution of the initial conditions, improving the model resolution greatly increases the intensification modelled to more realistic values (Krishnamurti and Oosterhof 1989).

In a high resolution axisymmetric model, Yamasaki (1977) found that convection was preferentially located in regions of frictional convergence. In another axisymmetric model by Willoughby et alii (1984a), convective processes were spatially resolved with resolution of 1 km in the vertical and 2 km in the horizontal near the center and ice related processes were included, though the cloud microphysics was parameterized. The major success of the model was generating multiple convective rings which propagate inward to become eyewalls. This behavior in an actual hurricane is described in Willoughby et alii 1982 and the many references listed therein. In a work than impinges on both CISK and HASIT, Nuss (1989) emphasized the importance of both the location of elevated sea surface fluxes and the boundary layer convergence of high entropy air in his analysis of numerical simulations of midlatitude marine cyclones.

An early attempt to model both intensifying and nonintensifying disturbances using the same model but with different initial conditions was made by Miller et alii (1972). The model correctly failed to develop an initial trough that failed to develop, and developed two hurricanes from data-derived initial conditions, albeit too slowly and with insufficient strength. A similar exercise, was performed by Ceselski (1974) with with a similar lack of strong response for the hurricane case. A recent modelling effort by Tuleya (1988) has proven more successful. The mechanistic analyses in all of these papers were insufficiently detailed to provide this reader with an understanding of the intensification process.

In an axisymmetric model, Rotunno and Emanuel (1987) demonstrated threshold behavior, with weak disturbances decaying or failing to intensify. This work has been used as a justification for HASIT. However, though they engaged in

the exercise of neutralizing the vertical structure of the initial conditions, the simulated vortex first decays while the boundary layer remoistens restoring vertical instability, before intensification begins. They also showed that “the horizontal size of the mature tropical cyclone is determined by that of the initial disturbance.” DeMaria and Pickle (1988) have generalized the equations of Ooyama 1969 by relaxing the assumptions of incompressibility and allowing the boundary layer to have the full dynamics of the upper layers. Using this simple model (not far removed from the one used here), they were able to capture the strong sensitivity of development to SST, model the observed variation of increasing size with increasing latitude (Merrill 1984), and tenuously examine the intensification threshold.

“I thought you were the Weather Man,” said Milo, very confused.
“Oh no,” said the little man, “I’m the Whether Man, not the Weather
Man, for after all it’s more important to know whether there will be weather
than what the weather will be.” And with that he released a dozen balloons
that sailed off into the sky. “Must see which way the wind is blowing,” he said
...

Norton Juster
The Phantom Tollbooth

Chapter 4

De Gustibus Non Est Disputandum

There are many issues important for the study of tropical cyclone development that remain unsettled. Different modellers and theoreticians have made differing assumptions when confronting these problems. The following sections discuss the rationale of some of the assumptions made in this work.

4.1 A Weak Disturbance is Not a Hurricane

The structure of both mature tropical cyclones and the particular tropical disturbances that precede them were discussed in sections 2.1 and 2.5, respectively. There is no single eigenfunction providing the spatial dependence of the disturbance simply changing in amplitude with time. For example, not only does a weak disturbance not have an eye with dry descent, but the center of the disturbance is a region of ascent and possibly the area of most intense ascent. Approximation schemes useful for one are not necessarily applicable to the other. Assumptions that the dominant processes are similar may lead to more confusion than enlightenment, for a weak tropical disturbance is not a hurricane.

The intensities are, of course, the first conspicuous difference. In an easterly wave the relative vorticity of the organized disturbance is less than half the planetary vorticity (Burpee 1972 gives velocities of order 2 m/sec at 70 kPa) throughout

the disturbance (i.e. the Rossby number is less than 0.5). For this case, the simplifying assumption of geostrophy is not great, but neither is it absurd. In the eyewall of a strong hurricane, the Rossby number can exceed 50. Here the flow is cyclostrophic and in much of the storm at greater radius all three terms of the gradient wind balance are of the same order. To examine the threshold, only weak disturbances will be considered and geostrophy will be assumed at lowest order.

One way of coping with large Rossby number problems has been to use what are usually called angular momentum coordinates or potential radius coordinates. These have been used in Schubert and Hack 1983; and Emanuel 1986, 1989b. The advective nonlinearities of the momentum equations are fully included and convective parameterizations almost automatically become slantwise convection schemes. Angular momentum coordinates were not used here because none of these equation sets have been generalized for viscous problems. In the simple numerical model of Emanuel (1989b), the problem is formulated with a potential radius coordinate and dissipation is included, however, the viscous terms are still in physical radius coordinates and that model is integrated numerically.

The symmetries of weak and strong systems are different. The most intense tropical cyclones are the ones closest to cylindrical symmetry (Willoughby et alii 1984b). Easterly waves are just that, wave-like. However, even while a system is still fairly weak a warm core can develop with closed isobars, closed isotherms, and a partially closed circulation, but a still largely asymmetric convective structure. This is possible because the meridional pressure and temperature gradients of the tropics are weak. Analytic techniques are fairly adept at dealing with circular symmetry using Bessel functions, or wave-like and decaying structures represented by trigonometric and exponential functions. The transition from waves to vortices remains the province of numerical techniques. Since even disturbances that have developed closed circulations still often fail to develop, I have chosen to perform my analysis with cylindrical symmetry, but neither choice is wholly satisfactory. Some of the mathematical consequences of this choice are discussed in section 4.4.

We might also expect that the inner radius limit of anticyclonic motion in the upper troposphere is smaller for an immature disturbance than for a fully

developed storm. In figure 2.3(b), one can see that within the outflow layer of mature typhoons, the inner radius of the anticyclone ranges from about 800 km to about 100 km decreasing with height. However, in the early stages of development, the initial radius of most of the outflow air is quite small, so the angular momentum of the parcels in the outflow is also small. This implies that such parcels will quickly acquire negative relative vorticity as their radius increases. Later in a storm's lifetime, the air flowing out from the eyewall will have originated at greater radius and will not develop negative relative vorticity until approaching that radius (depending on how much angular momentum it lost to the surface and other mixing processes). I am aware of no observational studies discussing this change in radius of the anticyclone during development.

Convective intensity does not vary monotonically with overall disturbance intensity. Cumulus convection is most intense during the most rapid cyclogenesis, while it is weaker both before and after. While a disturbance is weak, angular momentum surfaces are nearly vertical, so distinctions between vertical and slantwise convection are probably not important. The convective scheme employed here will assume vertical convection. In a mature storm cells are tilted so dramatically that it is quite noticeable when flying through, but this extreme regime is also not relevant for this study. Since we will be concerned here with the stability of weak tropical disturbances, the physical model used will be appropriate to that regime rather than that of an intense storm.

4.2 Objections to CISK

Emanuel (1986) has objected to CISK on several grounds. First he noted that CISK is a linear theory and if such linear instability actually existed "weak tropical cyclones should be ubiquitous and not confined to maritime environments." Linear theory can not capture the knowledge that tropical cyclones arise out of rather strong preexisting disturbances, such as easterly waves. He also argued that the assumed CAPE does not exist. Even assuming that some CAPE does

exist, Emanuel (1986), and Emanuel and Rotunno (1986) noted that the boundary layer in its undisturbed state is incapable of powering sufficient pressure drop for a tropical cyclone. (They quote J. Malkus and Riehl 1960.) CISK, as stated by Charney and Eliassen, makes no allowance for increasing the entropy of the boundary layer. Emanuel (1989a, b) has recently gone further to state that Ekman pumping¹ has a *negative* effect on development, which will be explained below. An additional objection, noted by the original proposers of CISK, is that without internal friction CISK suffers from one of the defects that it sought to surmount, namely that moist convective theory leads to fastest growth for the smallest spatial scales for updrafts for many vertical heating profiles. Each of these objections will now be examined separately.

There is nothing inherently linear in the basic ideas of CISK (see discussion in Ooyama 1982). Most of the mathematical parts of this thesis are devoted to presenting a finite amplitude version of CISK that exhibits instability only to finite amplitude perturbations. At the time of the original CISK papers, no weakly finite amplitude stability theory had yet been published in the fluid dynamics literature.² It is therefore not surprising that such techniques were not used. (As of yet, no analytic finite amplitude version of HASIT has been presented either. The finite amplitude threshold for further intensification within this theory has only been demonstrated in the context of numerical models.) This is now being remedied here. The theory in this work will show that one can have a CISK type theory with states that are linearly stable, but yet unstable to finite perturbations.

The nonexistence of CAPE has not been established to my satisfaction, nor to the satisfaction of many other atmospheric scientists. There is, in fact, evidence

¹If there is friction between the atmosphere and the surface below, flow is forced down the pressure gradient. If the stress is not spatially constant there can be a local net convergence or divergence of this frictionally induced flow, which results in vertical motions out of or into the surface boundary layer. This vertical motion is the Ekman pumping (or suction).

²W. Malkus and Veronis (1958) looked at the equilibration of a finite amplitude state, not the stability of that finite amplitude state.

for the existence of significant amounts of CAPE. These issues will be discussed in the following section (4.3). Emanuel is correct that the undisturbed boundary layer has insufficient entropy to cause a pressure drop as great as is observed in a mature tropical cyclone. This only demonstrates that CISK theory is insufficient to explain the full development of a storm. To be incomplete is not to be wrong. It is inescapable that the boundary layer entropy must be increased for a tropical storm to reach hurricane intensity. It does not necessarily follow that the boundary layer entropy must be significantly increased for the intensification process to begin.

Emanuel has also claimed (personal communication) that CISK theories do not allow for any surface fluxes at all. This is simply incorrect. Applying the same logic one would similarly conclude that the linear instability problem of Bénard convection had no boundary fluxes. In Charney and Eliassen (1964b), the boundary layer is assumed to be nearly saturated, though there is no explicit moisture equation for the boundary layer. This implies a moisture flux into the boundary layer to keep it saturated in the presence of the outer region return flow, regardless of the rhetoric of the original paper. The assumption is quite similar to the imposition of constant temperature at the boundaries in the Bénard problem. The entire treatment of the boundary layer is just a complicated determination of a boundary condition on what is really a two layer system with a bottom entropy flux that grows exponentially with the rest of the solution. In Ooyama's (1969) linear model the similar logic applies. In his numerical model, which still relies on Ekman pumping to determine the location for deep convection, the moisture flux into the boundary layer is treated explicitly. Here, however, the entropy of the boundary layer and the upper layer are no longer fixed and develop relies on their difference, which decreases with time. Emanuel (personal communication) argues that if one allows the boundary to change this is no longer CISK, in the manner of Charney and Eliassen. However, as long as a theory relies on the presence of CAPE and requires frictionally forced pumping out of the boundary layer to release it, I will consider it to be in the realm of CISK theories.

Emanuel has also properly attacked the simplistic, and incorrect notion, that

“moisture convergence”, as proposed by Charney and Eliassen is sufficient to guarantee an energy source for intensification. As already noted in section 2.3, condensation and precipitation can be forced in a stable environment with moisture convergence. If the environment is moist stable such a process releases no additional energy supply and will have energetic cost to drive the motion and warm the atmosphere. The work of Ooyama does not suffer from this defect since the cumulus parameterization is quite different.³

The most recent addition to Emanuel’s objections is based on a simplified numerical model (1989a, b). He claims:

The Ekman-induced vertical velocity peaks near the top of the boundary layer and decays upward. The resulting adiabatic cooling leads to primarily shallow clouds of low precipitation efficiency, which are ineffective at countering the adiabatic cooling but which do dry out the subcloud layer. Thus the vortex core cools and its subcloud layer dries out, leading to decay. *The effect of Ekman pumping is therefore negative.* [Emphasis in original (1989a).]

The process would only occur as outlined if convection initiated from Ekman pumping was primarily shallow and the lifted parcels did not become positively buoyant. However, observational evidence shows deep, heavily precipitating, convection in the regions of positive Ekman pumping (Cho and Ogura 1974).

4.3 Existence of CAPE

Any CISK type theory is predicated on the existence of some conditional instability. The existence of such vertical instability has recently been questioned. Arguments from both sides of the controversy will be presented, though I will come down on the side supporting the existence of synoptic scale convective available potential energy (CAPE). We turn now to observations of the vertical structure of the summertime tropical atmosphere.

³This renders the term “CISK parameterization” absolutely confusing.

Palmén (1948) showed that a surface parcel (85% relative humidity) for September climatology in the North Atlantic tropics lifted pseudoadiabatically had a large amount of CAPE (though he did not use that term) and a relative buoyancy of order 6 K in the hurricane region. A similar parcel in February had little CAPE and a relative buoyancy of order 1 K. Kasahara (1954) obtained similar results with climatological soundings for Guam. Palmén later (1969) repeated the exercise using better data, from Jordan 1958, with the same conclusion. The same pattern was observed for the Indian Ocean (Bansal and Datta 1972). The acquisition of more recent data has not altered these results, though the analysis of Gray and Shea (1973) gives the erroneous impression that there exists enormous amounts of CAPE.⁴

This simple notion was challenged by Betts (1982). He showed that for some soundings from GATE and a composite hurricane sounding for a mature storm at about 50 km from the center (from W. Frank 1977a), that the soundings were very close to a reversible moist adiabat (condensed liquid water was retained in calculating parcel buoyancies). (He refers to such paths as θ_{vc} isopleths.) This analysis was performed only for the lower third of the troposphere. It is worth noting, however, that tropical systems that do intensify rarely do so if passing through the GATE region and that one would expect the sounding of a mature hurricane to indicate the exhaustion of CAPE. Figure 4.1 shows an extreme case for the difference between reversible and pseudoadiabatic ascent (ice formation is not included in the reversible process, which would decrease the difference somewhat).

Xu and Emanuel (1989) examined this question more carefully for three tropical small island stations during the summer cyclone season: Truk (8°N, 152°E), Koror (8°N, 134°E), and Majuro (8°N, 175°E). Note that Truk is in an area of moderate tropical cyclone activity, Koror is in an area of frequent tropical cyclone

⁴To obtain the relative buoyancy of a lifted parcel (ignoring liquid water and ice effects), the parcel's θ_e must be compared with the ambient upper *saturation* equivalent potential temperature, θ_e^* , not the smaller upper level θ_e . This is why θ_e^* is used for the upper layer in the cumulus parameterization in both Ooyama 1969 and here.

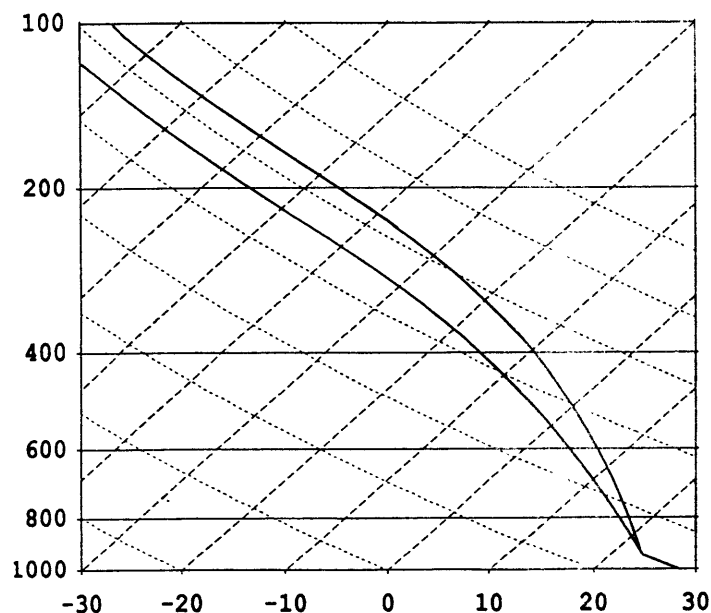


Figure 4.1: Temperature sounding for pseudoadiabatic ascent (right line) compared with virtual temperature (including water loading, but no ice formation) for reversible ascent (left line). The parcel saturates at about 95 kPa. The left axis is pressure in mb, the bottom axis and the long dashes are for temperature in $^{\circ}\text{C}$ with a 10°C interval, and the short dashes are for potential temperature with a 20 K interval.

activity, and there are few storms in the vicinity of Majuro (Gray 1979). For Truk they found a shallow stable layer, with buoyancies of about 1 K for parcels lifted reversibly and about 5 K for pseudoadiabats, in the middle troposphere. The errors were estimated at about 1 K, so the reversible path was considered to be neutral.⁵ When only soundings unstable for reversible ascent were included, the buoyancies were found to be about 2 K, or double the standard deviation. Buoyancies were found to be largest at Koror and smallest at Majuro (see also Xu 1987), which is consistent with the tropical cyclone climatology. For boundary layer parcels at Koror, the buoyancy for parcels lifted reversibly exceeded 2 K from 90 kPa on up and even reached 3 K. (Xu would probably argue that these numbers should be reduced by the standard deviation, which increased monotonically from

⁵Their analysis has the peculiar property, that the greater the variance of the data and the greater the assumed instrumental error, the stronger the support for their thesis of nearly neutral soundings.

1 K at 90 kPa to 2 K at 30 kPa, because of the sampling decision to examine only unstable parcels.)

In addition to the large buoyancies implied by the pseudoadiabats, there is much evidence for quite intense convection. For a mature storm, Burpee et alii (1989) found vertical velocities in the eyewall, at an altitude of about 14 km, of more than 13 m/sec. Despite seventeenth century reports of lightning in typhoons (Dampier 1699, Part I, p. 36; quoted here on p. 65), it has been recently thought that lightning is not very common in hurricanes (Black et alii 1986). Lyons et alii (1989) have observed large lightning bursts just before rapid cyclone intensification, but little lightning in the core region is observed from mature hurricanes. A burst of lightning lasting five hours accompanied the intensification of Tropical Storm Florence into a hurricane on 9 September 1988 (Venne et alii 1989). The count exceeded 1000 cloud to ground strokes for an hour (personal communication Walter Lyons [1989] to Earle Williams) during the period of intensification. Venne et alii estimate the updrafts for these electrically active cells “are in the 15 m sec^{-1} range, with large amounts of graupel, hail, and supercooled water. . . . This is decidedly atypical for mature hurricanes. . . .” Such behavior during intensification is similar to thunderstorms over land where the presence of large amounts of CAPE is not questioned. Even in a weak hurricane, Moss and Merceret (1976) found a slightly stable layer at the top of the boundary layer, which would allow the buildup of potential instability.

This matter cuts to the heart of what it means for a system to be marginally stable. If the only possible instabilities are simple linear ones, the marginal states are unambiguous. In the presence of finite amplitude instabilities, the states that are marginal to very small perturbations may still be unstable with respect to larger disturbances. Reversible moist adiabats, above the top of the surface boundary layer, may well be the marginal state for the undisturbed summer tropics. Forcing convection with boundary layer convergence may lead to less mixing and more precipitation. For precipitating convection, the reversible paths provide an underestimate of the CAPE, though it remains the case that the large buoyancies of pseudoadiabats are almost surely an overestimate. The energy release from

perturbations can vary in still other ways. For example, the tilting angle of the clouds determines how much of the rain falls back down through the updraft (see discussion in Cheng 1989); clouds that are close to vertical can choke themselves off with large amounts of water loading in the lower layers.

W. Frank and Cohen (1989) performed numerical experiments with and without forced low level vertical velocities using their own (1987) cumulus parameterization. In the absence of forcing the resulting soundings closely followed the suggestion of Betts by stabilizing nearly on a reversible moist adiabat. With forcing the final profiles were considerably more stable. That is, *convection initiated by large scale weak low level forcing is able to extract far more potential energy from the base state*. Hence, the reversible moist adiabat with full water loading may not be a relevant reference state in the presence of low level convergence, as claimed by Emanuel. The formation of a cloud cluster also leads to additional heating gradient at upper levels, by changes in the radiative transfer processes and the location and size of the downdrafts (Houze 1982, Cheng and Yanai 1989).

Cho and Ogura (1974) found a strong correlation between low level convergence and deep cumulus convection in easterly waves. There were many other areas with cumulus convection, but these tended to be shallow in the absence of large scale low convergence. This large scale upwelling was of the order of 0.01 m/sec, though at cloud base the vertical velocities were of order 1 m/sec, so it was unlikely that the vertical cloud velocities were forced by large scale dynamical processes, though the location of the deep convection appears to have been determined this way. Similar conclusions were reached by Reeves et alii (1979).

When convergence is forced by large scale motions, the level of any convergence is crucial for the existence of CAPE with respect to the lifted parcels. The boundary layer is not well mixed with respect to moisture, and θ_e often drops several Kelvin in the lowest 5 kPa. Hence, the system is quite sensitive to small changes. As an example, a parcel rising 15 km with an additional 1 K of relative buoyancy for the entire depth of the troposphere provides about 500 J/kg of additional energy (sufficient to accelerate a parcel to more than 20 m/sec from rest).

Disturbances such as easterly waves that are strongest at about 70 kPa force convergence over some depth, however convergence above the boundary layer provides moisture and may lead to much precipitation but still provides little or no release of CAPE. Heavy precipitation may even occur in a region of negative CAPE.

The formation of ice also provides additional buoyancy that is not included in many calculations. The heat is again extracted within the atmosphere at the melting level,⁶ though this is well below the freezing region. This process transfers heat from the lower to upper troposphere. The greatest effect of freezing appears to be the increase of intensity in both updrafts and downdrafts (see Lord et alii 1984, and Wada 1989).

Emanuel (1989b) is correct “that the *direct* effect of convective overturning of less than 100% precipitation efficiency is always to lower the subcloud-layer entropy”. Nevertheless, if the precipitation efficiency is greater than zero the result is still a warming of the atmosphere, *ceteris paribus*. The warming, of course, need not result in the generation of kinetic or usable potential energy. A net warming of the core, at the expense of a decrease in boundary layer entropy, through the loss of water vapor by condensation and precipitation, can provide energy to drive the cyclone. However, unless the boundary layer entropy is restored and then enhanced, this process cannot continue.

Entrainment, mixing, and dilution also reduce the the relative buoyancy of ascending parcels. This, however, is not problematic. We will later assume that the entrainment is so great as to provide all of the middle level momentum convergence. All parcels eventually reach a level of neutral buoyancy. The amount of entrainment and the degree of stability between the middle and upper troposphere will make that level of neutral buoyancy lower than it would be for a nondilute parcel. The cumulus parameterization scheme will assume that mixed parcels are neutral upon reaching the upper layer. It is still necessary for parcels to be unsta-

⁶Rarely do frozen hydrometeors reach the surface in the tropics, though I have been pelted by hail while along the Gulf of Mexico.

ble with respect to the air aloft when they begin their ascent; sufficient instability does appear to exist to justify this assumption.

4.4 Circular Disturbances

The calculations in this work are cast in cylindrical symmetry and represented using cylindrical coordinates. Implied in this choice is the belief that the finite amplitude disturbance states that divide intensifying and decaying perturbations are closer to cyclone-like than wave-like. This is based on the observation that tropical depressions that already have closed isobars and closed circulations still frequently fail to intensify. Though these measures are not Galilean invariant, the weakness of the meridional shear in the tropics leaves them useful. Since the forcing usually has strong asymmetries, the robustness of nearly circular vortices is surprising. Though this is not totally understood recent progress has been made. Vortices develop spontaneously out of turbulent flow fields even in numerical models (McWilliams 1984). Elliptical vortices decay into circular ones by shedding filaments near the ends of the major axis (Melander et alii 1987). Carr and Williams (1989) have shown that a large class of axisymmetric perturbations to a barotropic vortex decay under a wide range of conditions. As was noted in section 3.1.2, there are some workers who believe that asymmetric forcing is important for tropical cyclone development. However, Willoughby (1990) has found that symmetric disturbances intensify most rapidly and that asymmetric convection disrupts intensification.

The choice of the symmetry of the hypothetical disturbance, however, is not crucial. Some workers have chosen to use cylindrical symmetry (e.g. Haque 1952, Charney and Eliassen 1964b), others have ignored the curvature and used slab symmetry (e.g. Ooyama 1969, Wang 1987), and Lilly (1960) worked the same examples using both symmetries for comparison. In Cartesian coordinates one obtains equations that resemble the form $\left(\frac{\partial^2}{\partial x^2} + \frac{\partial^2}{\partial y^2}\right)v + m^2v = 0$. Slab symmetric solutions assume that there is no variation in one of the Cartesian directions.

(There are, of course, other options for the behavior in the two orthogonal directions.) For positive m^2 the solutions are the common trigonometric functions *sine* and *cosine*; for negative m^2 the solutions are spatially growing and decaying exponentials. Cylindrically symmetric problems of the type under consideration lead to equations that resemble $\frac{\partial}{\partial r} \left(\frac{\partial r v}{r \partial r} \right) + m^2 v = 0$. For positive m^2 the solutions are first order Bessel functions and for negative m^2 the solutions are modified first order Bessel functions. The m will be referred to as Bessel function wave numbers, or just simply wave numbers. The most significant differences concern the relation of the Ekman pumping to the velocity structure, which will be discussed in the next section. Another major difference is that for a given ratio of ascent region length scale to descent region length scale, the ratio of the area of the descent region to the area of the ascent region is much larger for the cylindrically symmetric case.

If one were to examine a spatially oscillatory phenomenon, there would be a large *qualitative* difference between using plane waves, which continue undiminished to infinity, and first order Bessel functions, which resemble decaying oscillations. For an isolated disturbance the differences are not as dramatic. Less than one full “wave” is used of the Bessel function in the core region, so the decay is not evident. In the downdraft region, there is not much qualitative difference between a decaying modified Bessel function and a decaying exponential. The actual asymptotics can be found in Abromowitz and Stegun (1964). Figure 4 in Lilly 1960 provided a direct comparison for an inviscid moist convection problem. Another comparison, made by Syōno and Yamasaki (1966), showed that growth occurs more rapidly with a cylindrical disturbance. This is probably due to the area relation just noted and the greater Ekman pumping of cylindrical disturbances, discussed below.

4.5 Ekman Layers

The momentum loss from the boundary layer to the planet below is very important for the CISK mechanism. (It is also necessary for development by HASIT.) We

will not be interested here in the full structure of the Ekman spiral, which is acutely dependent on the vertical profile of the lateral stress and the depth of the boundary layer. The mechanically forced vertical velocity out of the boundary layer is, however, crucial. This depends only on the total lateral stress at the surface. Charney and Eliassen (1949) appear to have derived the first explicit expression for this, which had the vertical velocity strictly proportional to relative vorticity, and they did not refer to the process as Ekman pumping. We will also be concerned with the cross isobar flow within the boundary layer, which also depends only on the total stress.

In eq. 5.8 we will set the surface stress, τ_s , equal to $\rho(k_s v_1 + C_D |v_1| v_1)$, where ρ is the fluid density, k_s is a linear drag coefficient with velocity units, C_D is a dimensionless quadratic drag coefficient, and v_1 is the low level tangential velocity of the primary circulation. For the lowest order solutions, which will be linear, the stress is then linearly proportional to the tangential velocity. Whether or not one includes a linear stress term leads to radically different radial profiles of the forced vertical velocity. *The linear term alone produces a maximum in the top of the boundary layer vertical velocity, at the center of the vortex. For stress proportional to the square of the velocity, the Ekman pumping vanishes at the center.* Ekman's (1905) original paper on a frictional boundary layer included analyses of both linear and quadratic stress laws, but did not examine flow into or out of the boundary layer.

Even for a stress law that is essentially quadratic, things are not as simple as just presented. Where we have just written $|v_1|$, should really have been $(u_1^2 + v_1^2)^{\frac{1}{2}}$, where u_1 is the low level radial velocity. For a flow that has absolute rotational symmetry, u vanishes at the central axis as does the Ekman pumping. Similarly, if the assumption is made that $v_1 \gg u_1$, the first stress form presented with just the quadratic term is again obtained. If in the early stages of development there are turbulent horizontal velocities in the boundary layer greater than, or of order of, the organized vortical flow, this will have the same effect as having a linear term in the stress. This essentially assumes that there is some isotropic turbulence

with $(u_1^2 + v_1^2)$ approximately constant. The linear stress term is a return to simple eddy viscosity theory.

Several examinations have been made of the frictional boundary layer under a circular vortex, including time dependence, variations in boundary layer depth, and vertical stratification (e.g. Rosenthal 1961, 1962; Greenspan and Howard 1963; Carrier 1971a; McWilliams 1971). A comparison of the vertical velocity using different stress laws was performed by Eliassen (1971), and a further examination of the Ekman layer under a circular vortex with quadratic drag was made by Eliassen and Lystad (1977) (see Eliassen 1971 and the works cited therein for more theoretical discussion). Eliassen suggested that the vertical velocities from quadratic drag were somewhat responsible for the hurricane eye, though there is no discussion of why this structure only existed once the storm was fairly intense.

I conjecture that this difference may be partially responsible for the formation of an eye as the storm intensifies. In the early stages of a tropical disturbance, the convection is concentrated near the center. This is as if a linear stress term were dominating. As the flow intensifies, $C_D v$ can become much greater than any effective k_s . Hence, the maximum in w will become a ring displaced out from the center. In the context of the weakly nonlinear theory, both of these terms are important. At second order the Ekman pumping and cross isobar flow increase faster than linearly. This is important for the threshold behavior of intensification.

There are several differences in the horizontal structure of the Ekman pumping between slab symmetry and circular symmetry. Considering a linear drag law first, the central updraft strength is greater for the cylindrical case than the slab case (about double). For the slab case the Ekman pumping vanishes at the position of the maximum winds, while for the cylindrical case Ekman pumping is still positive at the radius of maximum winds and does not vanish until farther from the center. In the model used here, this will force some convection in locations that serve to weaken the vortex, but this effect is dominated by the stronger convection at smaller radius. At second order, it is still the case that the forced updraft is stronger for cylindrical symmetry and extends to a greater distance from the center.

4.6 Sensitivity

There has been great traditional resistance to any theory which is very sensitive to initial conditions for the choice of spatial scale. It is usually declared that such results are not robust, which is true. However, the leap that because a result is not robust it is wrong, is unfounded. Similar objection is made to any theory which is quite sensitive to the form of the dissipative processes. The immediate dismissal of results under this condition is also premature. Further, though our knowledge of a process may be poor, that does not imply that the process itself is not robust.

There are certain processes to which a tropical cyclone model should be quite sensitive and others to which it should be quite insensitive. For example, any theory which was quite sensitive to the value of the planetary vorticity would be suspect, since cyclones can form over a wide range of latitudes. Based on the observation that the storms do not occur within a few degrees of latitude of the equator, a theory should require some amount of planetary vorticity, but not depend on large gradients of the planetary vorticity. The translation speed of the initial disturbance seems unimportant, as does whether the energy source of the initial disturbance is barotropic or baroclinic, or if it begins over land or over water.

On the other hand, if a theory robustly gave strong size selection we should consider it inappropriate, since the storms can vary over almost an order of magnitude under much smaller variations in the large scale conditions. The initial disturbance scale may be the most important determinant of the size of a mature storm. For intensification, strong sensitivity appears to exist with respect to both the SST and the vertical stability. Most importantly for this work, the differences between disturbances that intensify and those that do not, appear to be small and subtle.

As already discussed, some disturbances can propagate across the ocean for several days either slowly weakening, remaining nearly constant, or slowly intensifying. During the entire time, there are large amounts of rain, therefore large

amounts of net heating aloft, and large amounts of angular momentum convergence. Since the rain, and hence heating, are near the low pressure center, this only seems possible if the dissipative processes and radiative cooling are significant at this weak stage. During the periods of most rapid intensification, the aforementioned nonconservative processes are dominated by conservative ones. Nevertheless, certain parts of the development, and certain forms of solutions, are not possible without dissipation and radiation, such as the closing of the secondary circulation.

The horizontal length scales of CISK type theories are quite sensitive to the vertical distribution of heating. If large amounts of low level heating are specified the results are unrealistic (e.g. Charney and Eliassen 1964b). Since net heating from cumulus convection consistently appears greater at upper levels and with a robust distribution, the great sensitivity of any theory to the heating distribution is not problematic as long as the results are reasonable for the observed heating distribution.

Quantitative information on the radiative and heating mechanisms for warming up the tropical atmosphere is still quite lacking. Yet, we know that the vertical profile of temperature closely matches that of a virtual moist adiabat for conservative ascent by a saturated parcel. As the state of the atmosphere changes, moving between such isopleths, one can calculate the heating distribution needed to accomplish the change. It is quite different from the heating distribution from the latent heat release of an ascending saturated parcel. (This is strongly tied to tropical cyclone observations which show a large moisture sink in the lower half of the troposphere and a large heat source in the upper half [e.g. Yanai et alii 1976].) The actual temperature profile is unavoidably quite sensitive to the very large amounts of heating and cooling that occur but remain closely balanced. This in fact provides a strong constraint on believable theories, but the sensitivity can not be avoided. As the accuracy of our knowledge of momentum transport improves, we may find similar strong constraints on the form of dissipative theories.

"I often find," [the Mathemagician] casually explained to his dazed visitors, "that the best way to get from one place to another is to erase everything and begin again. Please make yourself at home."

"Do you always travel that way?" asked Milo...

"No indeed," replied the Mathemagician, and this time he raised the sharpened end of his staff, drew a straight line in the air, and walked gracefully across it from one side of the room to the other. "Most of the time I take the shortest distance between two points. And, of course, when I should be in several places at once," he remarked, writing $7 \times 1 = 7$ carefully on the notepad, "I simply multiply."

"How did you do that?" gasped Milo.

"There's nothing to it," they all said in chorus, "if you have a magic staff." Then six of them canceled themselves out and simply disappeared.

"But it's only a big pencil," the Humbug objected, tapping at it with his cane.

"True enough," agreed the Mathemagician; "but once you learn to use it, there's no end to what you can do."

Norton Juster
The Phantom Tollbooth

Chapter 5

Physics of the Model

The physics of the model used here is closely based on that presented in Ooyama 1969. The model used is set in cylindrical coordinates (r, z) , where r and z are, as usual, the radius and height. The disturbance is centered on the origin of the coordinate system and will remain so fixed. All fields are assumed to be axisymmetric, so no azimuthal coordinate is used. The coordinate system is rotating and the Coriolis parameter is constant, i.e. the f -plane approximation is made. Essentially, the model has two layers. A third layer at the lower boundary is treated separately, but is of fixed height. The layers are designated 0 for the boundary layer, 1 for the lower layer, and 2 for the upper layer. Azimuthal (or tangential) motion; i.e. the velocities v_0 , v_1 , and v_2 ; will be referred to as the primary circulation. Motion in the (r, z) -plane, is the secondary circulation.

5.1 Basic Equations

We will follow Ooyama 1969 closely in setting up the basic equations, though not at all in solving them. The three layers have only two different densities, with the lower layer and the boundary layer having the same density, defined as

$$\begin{aligned}\rho_0 &= \rho_1 \equiv \rho \\ \rho_2 &= \epsilon \rho, \quad \epsilon < 1.\end{aligned}$$

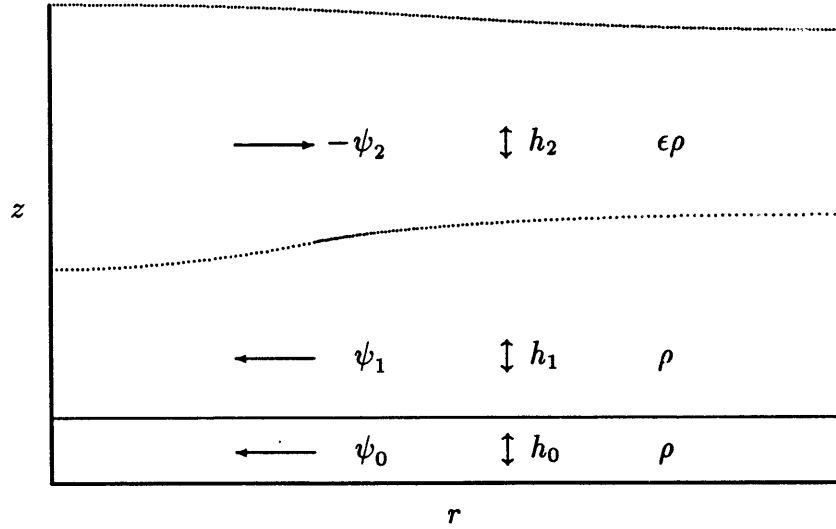


Figure 5.1: Coordinates and layers.

Hence, there is no energetic cost associated with moving parcels between the boundary layer and the lower layer. The equating of the boundary and lower layer densities makes this essentially a *two* layer problem. We will later see that this forces the tangential velocities in these two layers to also be equal. This assumption is made strictly to keep the problem as simple as possible. The *inward* radial mass flux, ψ_j , is defined by:

$$\rho\psi_j \equiv -\rho_j h_j u_j r \quad (5.1)$$

where h_j is the layer thickness and u_j is the (positive outward) radial velocity. This practice arbitrarily follows Ooyama's usage. The layout is illustrated in figure 5.1. In general, subscripts will always designate the layer to which the variable applies, with a generic subscript of j indicating that the expression applies to all layers.

Conservation of mass is maintained in each layer. The boundary layer is assumed to have constant thickness with respect to both space and time, so $\frac{\partial h_0}{\partial r} \equiv 0$ and $\frac{\partial h_0}{\partial t} \equiv 0$. The resulting continuity equations are:

$$0 = \frac{\partial \psi_0}{r \partial r} - w \quad (5.2)$$

$$\frac{\partial h_1}{\partial t} = \frac{\partial \psi_1}{r \partial r} - Q + w \quad (5.3)$$

$$\epsilon \frac{\partial h_2}{\partial t} = \frac{\partial \psi_2}{r \partial r} + Q \quad (5.4)$$

$w \equiv w^+ - w^- \equiv$ vertical velocity out of boundary layer
 $[w^+ \text{ (upward)} \geq 0, w^- \text{ (downward)} \geq 0]$

$Q \equiv Q^+ - Q^- \equiv$ interlayer mass flux (velocity units)
 between layers 1 and 2
 $[Q^+ \text{ (upward)} \geq 0, Q^- \text{ (downward)} \geq 0]$.

The vertical velocity out of the boundary layer, and the interlayer mass flux from latent heat release and diabatic processes, are separated into upward and downward motions, both of which are defined to be nonnegative. There can be both upward and downward interlayer mass fluxes at the same radius, simultaneously. These cancel in their contributions to the continuity equations, but have different effects in the equations for conservation of angular momentum. This simply indicates that there are physical processes on scales smaller than those resolved by the model solutions. This could apply to both Q and w , but in the course of this analysis, only one of w^+ and w^- will be allowed to be nonzero at any given radius.

Conservation of angular momentum, M_j , can be expressed as follows:

$$\frac{\partial}{\partial t}(h_0 M_0) = \frac{\partial}{r \partial r}(\psi_0 M_0) - Z_{01} + Z_s \quad (5.5)$$

$$\frac{\partial}{\partial t}(h_1 M_1) = \frac{\partial}{r \partial r}(\psi_1 M_1 + \Lambda_1) - Z_{12} + Z_{01} \quad (5.6)$$

$$\epsilon \frac{\partial}{\partial t}(h_2 M_2) = \frac{\partial}{r \partial r}(\psi_2 M_2 + \Lambda_2) + Z_{12} \quad (5.7)$$

$$M_j \equiv v_j r + \frac{f}{2} r^2$$

$\Lambda_j \equiv$ lateral eddy fluxes of angular momentum

$Z_s, Z_{ij} \equiv$ vertical fluxes of angular momentum .

There is no azimuthal pressure gradient because of the assumption of axisymmetry. In the boundary layer, lateral diffusion has been assumed to be much less than the surface stress and is ignored, i.e. $\Lambda_0 = 0$. Vertical fluxes of angular momentum will be included from two processes. Interlayer friction is included with the linear coefficients μ and ν . Vertical flow will also transport angular momentum. The vertical fluxes are

$$Z_s = -\tau_s r / \rho, \quad \tau_s = \rho(k_s v_1 + C_D |v_1| v_1) \quad (5.8)$$

$$Z_{01} = M_0 w^+ - M_1 w^- + \nu(M_0 - M_1) \quad (5.9)$$

$$Z_{12} = M_1 Q^+ - M_2 Q^- + \mu(M_1 - M_2), \quad (5.10)$$

where Z_s is the flux at the surface, with τ_s the surface stress; Z_{01} is the flux between the boundary layer and the lower layer; and Z_{12} is the flux between the lower and upper layers. Note that the drag law in eq. (5.8) has a linear term included. The term proportional to ν will soon be shown to vanish. The lateral eddy flux of angular momentum is assumed to follow a simple Fickian diffusion law with respect to solid body rotation (where the v_j are proportional to r). This is one of the simplest possible models. The flux is

$$\Lambda_j = \epsilon_j \lambda_j h_j r^3 \frac{\partial}{\partial r} \left(\frac{v_j}{r} \right) = k_j r^3 \frac{\partial}{\partial r} \left(\frac{v_j}{r} \right), \quad (5.11)$$

where λ_j is an eddy diffusivity, $k_j \equiv \epsilon_j \lambda_j h_j$ is a layer integrated diffusion coefficient, and $\epsilon_1 = 1$, $\epsilon_2 = \epsilon$.

The pressure field will be assumed to be hydrostatic, so

$$\begin{aligned} p_0(r, z) &= g\rho(h_0 + h_1 + \epsilon h_2 - z), & 0 \leq z < h_0 \\ p_1(r, z) &= g\rho(h_0 + h_1 + \epsilon h_2 - z), & h_0 < z \leq h_0 + h_1 \\ p_2(r, z) &= \epsilon g\rho(h_0 + h_1 + h_2 - z), & h_0 + h_1 \leq z \leq h_0 + h_1 + h_2, \end{aligned} \quad (5.12)$$

where g is the acceleration due to gravity. If cumulus convection were to be resolved explicitly, this approximation would fail. However, the parameterized convection of this model allows this simplification. Since homogeneous layers are being used,

after removing the pressure of the rest state (no motion), the geopotential perturbations are $\phi_j(r) \equiv [p_j - p_j^{(0)}(z)] / \rho_j$, where the superscript (0) refers to the variable values for the state of no motion. These perturbations obey

$$\begin{aligned}\phi_0 &= \phi_1 = g [(h_1 - h_1^{(0)}) + \epsilon(h_2 - h_2^{(0)})] \\ \phi_2 &= g [(h_1 - h_1^{(0)}) + (h_2 - h_2^{(0)})]\end{aligned}\tag{5.13}$$

or, equivalently,

$$\begin{aligned}h_1 &= h_1^{(0)} + \frac{\phi_1 - \epsilon\phi_2}{g(1 - \epsilon)} \\ h_2 &= h_2^{(0)} + \frac{\phi_2 - \phi_1}{g(1 - \epsilon)}.\end{aligned}\tag{5.14}$$

The gradient wind relation can be expressed in terms of the ϕ_j as

$$\left(f + \frac{v_j}{r}\right) v_j = \frac{\partial \phi_j}{\partial r}.\tag{5.15}$$

From eqs. (5.13) and (5.15) it is then clear that

$$v_0 = v_1 \quad \text{and} \quad M_0 = M_1.\tag{5.16}$$

The lowest order balance in a tropical cyclone is the gradient wind balance of the pressure field with the primary circulation. This constraint is only diagnostic and is highly degenerate. It provides the link between development of the pressure field and development of the tangential velocity field. The changes in these fields, however, are controlled more by the secondary circulation. A change in one of them then must be accompanied by a corresponding change in the other.

Substituting the expressions for the vertical flux of angular momentum, eqs. (5.8)–(5.10), into the equations for conservation of angular momentum (5.5)–(5.7), and using eq. (5.16), yields

$$h_0 \frac{\partial v_1 r}{\partial t} = \zeta_1 \psi_0 - \frac{\tau_s r}{\rho} \quad (5.17)$$

$$h_1 \frac{\partial v_1 r}{\partial t} = \zeta_1 \psi_1 + (Q^- + \mu)(v_2 - v_1)r + \frac{\partial \Lambda_1}{r \partial r} \quad (5.18)$$

$$\epsilon h_2 \frac{\partial v_2 r}{\partial t} = \zeta_2 \psi_2 + (Q^+ + \mu)(v_1 - v_2)r + \frac{\partial \Lambda_2}{r \partial r} \quad (5.19)$$

$$\zeta_j \equiv f + \frac{\partial r v_j}{r \partial r}.$$

The ζ_j are the total vorticity and from eq. (5.16), $\zeta_0 = \zeta_1$. The assumption made by Ooyama that h_0 is small enough to allow the neglect of the time derivative in eq. (5.17) has not been made here. It is kept so that the energy equations appear more consistent, but does not change the physics in any large way. Combining the equation for continuity in the boundary layer (5.2), with a radial derivative of the equation for conservation of angular momentum (5.17), and the parameterization of the surface momentum sink (5.8) yields an expression for the vertical pumping out of the boundary layer,

$$\begin{aligned} w &= \frac{\partial}{r \partial r} \left(\frac{\tau_s r}{\rho \zeta_1} + \frac{h_0}{\zeta_1} \frac{\partial r v_1}{\partial t} \right) \\ &= \frac{\partial}{r \partial r} \left[\frac{k_s r v_1 + C_D r |v_1| v_1 + h_0 \frac{\partial r v_1}{\partial t}}{\left(f + \frac{\partial r v_1}{r \partial r} \right)} \right]. \end{aligned} \quad (5.20)$$

The terms due to friction (those proportional to k_s or C_D) are the Ekman pumping, though I may occasionally refer to the whole of the mechanically forced vertical velocity under this rubric. In a similar manner ψ_1 and ψ_2 could be eliminated from the system, but this will be much simpler after setting up the perturbation expansion.

Parameterization of the vertical mass flux in response to heating and cooling is one of the more crucial, yet regrettably ad hoc, parts of this model. There exist far more sophisticated schemes for parameterizing cumulus convection than the one used here, but on the whole they are not yet amenable to analytic treatment by most mortals. Treatments of the cumulus heating and the radiative cooling will be provided separately below.

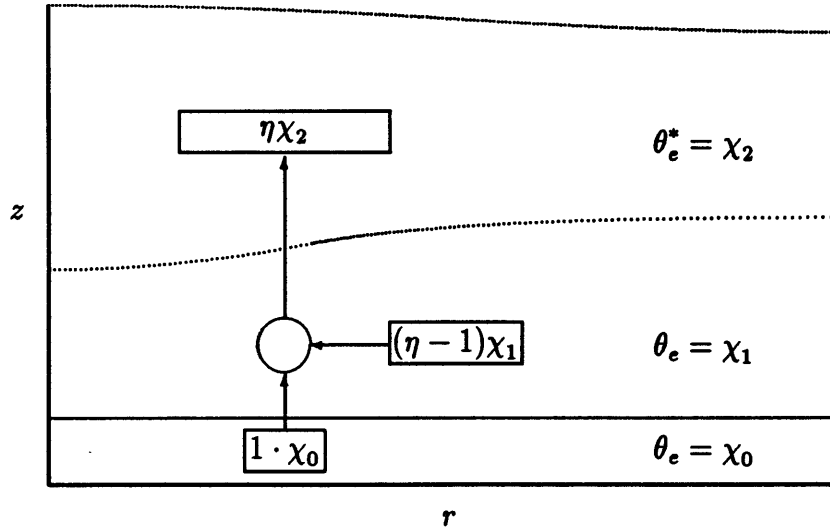


Figure 5.2: Cumulus parameterization scheme. For every unit mass of air with equivalent potential temperature equal to χ_0 forced out of the boundary layer, $\eta - 1$ units of air with equivalent potential temperature equal to χ_1 are entrained. When the combined η units of mass reach the upper layer they are assumed to be neutrally buoyant with saturated equivalent potential temperature equal to χ_2 , which is the same as is the environment.

The positive vertical interlayer mass flux is taken such that $Q^+ = \eta w^+$, where η is a nonnegative entrainment parameter. It is assumed that cumulus heating and entrainment will only occur where there is Ekman pumping out of the boundary layer. As already noted, this is the central assumption of CISK. In a mature hurricane there are often convective bands outside of this region. However, in weak disturbances there is much less convection outside of the central region and what convection there is tends to be scattered. Scattered convection will not have any great effect on the organized lateral mass flow of the cyclone. Since we will not allow both w^+ and w^- to be nonzero simultaneously, it will be easier to hide the requirement that Q^+ vanish when $w^+ = 0$ in the definition of η rather than the definition of Q^+ . So, we set

$$Q^+ = \eta w, \quad (5.21)$$

with

$$\eta = \begin{cases} 1 + \frac{\chi_0 - \chi_2}{\chi_2 - \chi_1}, & w > 0 \quad (w^+ > 0) \\ 0, & w \leq 0 \quad (w^+ = 0) \end{cases} \quad (5.22)$$

$\chi_0 \equiv \theta_e$ in boundary layer

$\chi_1 \equiv \theta_e$ in lower layer

$\chi_2 \equiv \theta_e^*$ in upper layer ,

where θ_e is the equivalent potential temperature for a layer, and θ_e^* is the saturation equivalent potential temperature.¹ A schematic of the parameterization is shown in figure 5.2. For every unit mass of air forced from the boundary layer, $\eta - 1$ units are entrained in the lower layer and η units enter the upper layer. It is assumed that saturated cloud air has nearly the same potential temperature (θ not θ_e) as its environment when it reaches the upper layer, and that the χ_j mix linearly. The amount of lower layer air entrained is the amount that neutralizes the boundary layer air with respect to the upper layer. The buoyancies, or potential temperatures, of two parcels are approximately equal when their saturation equivalent potential temperatures are equal, which ignores the effects of water in all of its phases. For a saturated parcel, of course, $\theta_e = \theta_e^*$. Cloud air is then neutral with respect to the upper layer when its θ_e (equal to $[\chi_0 + (\eta - 1)\chi_1]/\eta$ by the mixing assumptions just given) matches θ_e^* of the upper layer (equal to χ_2). This assumes that most entrainment is lateral rather than at cloud top.² A fuller

¹The *saturation equivalent potential temperature* is the equivalent potential temperature a parcel would have if its moisture level were increased to the saturation value, but the temperature and pressure remained unchanged.

²Entrainment and mixing are not equivalent, though the distinction is avoided here. There can be large amounts of entrainment and still have undilute parcels reaching cloud top. Further, it can be the case that though most of the entrainment is lateral, parcels reaching the cloud top mix mostly with other parcels at the upper reaches of the cloud. The parcel mixing argument used to determine the source of most of the entraining air (e.g. Paluch 1979) may be misleading.

A simple gedanken experiment may clarify this. Imagine a moist buoyant parcel near the surface in an infinitely extensible (with no work), insulating balloon. Once released, this parcel will rise, release heat through condensation, and accelerate upwards. The acceleration and heat release will induce an accompanying solenoidal circulation. Fluid

derivation of this scheme can be found in Ooyama 1969.

Equation (5.22) can be rewritten as $\chi_0 = \eta(\chi_2 - \chi_1) + \chi_1$. We require that $\chi_2 > \chi_1$, ensuring that the two main layers are stably stratified (though for an unsaturated atmosphere $\chi_1 > \chi_2$ does not imply instability). It is assumed that the boundary layer is not saturated and that it is only conditionally unstable rather than absolutely unstable. Convection will only occur where forced. It is clear from this equation that $\eta < 0$ implies that $\chi_0 < \chi_1$ and there is no available potential energy. For $0 < \eta < 1$ then $\chi_1 < \chi_0 < \chi_2$. This would not allow deep convection, but would still require that some mass be shifted from layer 1 to layer 2 to account for the heating in layer 1. The only case we will be concerned with is where $\eta > 1$ and $\chi_0 > \chi_2 > \chi_1$.

To spin up a tropical cyclone, angular momentum must be transported inward throughout a fairly thick layer (about 5 km). The magnitude of $\chi_0 - \chi_2$, found in the numerator of eq. (5.22), is a measure of the convective potential energy available to drive the system. To advect, entrain, and then vertically stretch a parcel from the lower layer, the static stability between the layers must be overcome. Hence, decreasing $\chi_2 - \chi_1$, found in the denominator of eq. (5.22), increases the forcing parameter. Increasing χ_0 in the boundary layer only increases the numerator in η . However decreasing χ_2 by cooling the upper layer does double duty.

It is worth noting that the cumulus heating is continuous with respect to radius and that its radial derivative has a simple jump discontinuity. Let us look at the term involving the derivative of that function. If we apply the two inverse

that flows inward toward the path of the contained parcel and follows it upward should be considered as entrained, though no mixing has occurred. The entrainment process decreases the kinetic energy of the rising parcel.

If the balloon is then popped at the level of neutral buoyancy, the parcel will then mix with its surroundings aloft. The resulting mixed parcels provide no information on the amount of fluid entrained as the parcel rose. In the absence of a containing balloon, the process should be similar for some fraction of the ascending air. We might expect some parcel to reach cloud top nearly undilute and mix with parcels there, and some parcels to mix with entrained air during ascent and never reach cloud top.

operators $\frac{\partial}{\partial r}$ and \int , then we can remove one odd problem. We will assume that η has only jump discontinuities from some positive value η_H to 0, when crossing r_0 from below, while w is continuous crossing 0 at r_0 , so that $Q = 0$ when $w \leq 0$. If the lower layer is taken to be inviscid, w need not be continuous and the following result does not hold. The forcing parameter can be expressed as

$$\eta = \eta_H H(r_0 - r) + \eta_s, \quad (5.23)$$

where H is the Heaviside function, equal to zero for arguments less than zero and equal to one otherwise, η_H is a constant, and η_s is a continuous function of r equal to 0 at r_0 . The derivative of the Heaviside function is the Kronecker delta function, and so the radial derivative of ηw is

$$\begin{aligned} \frac{\partial}{\partial r} \int \frac{\partial}{\partial r} (\eta w) &= \frac{\partial}{\partial r} \int \left(\eta \frac{\partial w}{\partial r} + \frac{\partial \eta}{\partial r} w \right) r dr \\ &= \frac{\partial}{\partial r} \int \left[\eta \frac{\partial w}{\partial r} - \eta_H \delta(r_0 - r) w + \frac{\partial \eta_s}{\partial r} w \right] r dr \\ &= \eta \frac{\partial w}{\partial r} + \frac{\partial \eta_s}{\partial r} w \end{aligned} \quad (5.24)$$

because $w = 0$ at $r = r_0$ by definition. This term has only a jump discontinuity, though all of the factors, except w , in the last expression could be discontinuous. The procedure is only useful for taking one radial derivative of ηw since it requires that the cofactor of η vanish at the discontinuities of η .

In a hydrostatic model it is impossible to close the secondary circulation of a steady solution without some diabatic cooling process. The simplest parameterization of such a process is Newtonian radiative cooling. Cooling is set proportional to the difference between the mean potential temperature with no motion and the mean potential temperature of the two layers, θ_m :

$$Q^- = \beta(\theta_m - \theta_m^{(0)}), \quad (5.25)$$

where β is a cooling constant in units of $\text{msec}^{-1}\text{K}^{-1}$ and $\theta_m^{(0)}$ is θ_m for the rest state. Between two given pressure surfaces, the mean temperature is proportional

to the thickness between the surfaces (see a standard meteorology text such as Holton 1979, pp. 19, 70; or Ooyama 1969):

$$\theta_m - \theta_m^{(0)} = \frac{\phi_2 - \phi_1}{c_p(\pi_1 - \pi_2)} \quad (5.26)$$

$$\pi_j \equiv (p_{0j}/p_{00})^{2/7},$$

where c_p is the specific heat of dry air at constant pressure, and p_{0j} is an average pressure for the layer j . Making use of the gradient wind relation, eq. (5.15),

$$\frac{\partial \theta_m}{\partial r} = \frac{\left(f + \frac{v_2}{r}\right) v_2 - \left(f + \frac{v_1}{r}\right) v_1}{c_p(\pi_1 - \pi_2)}. \quad (5.27)$$

(The only other use of the gradient wind relation has been to show that $M_0 = M_1$, for the simplification that the boundary layer and the lower layer have the same density.) This assumes that $\frac{\partial \pi}{\partial r} \ll \frac{\partial \phi}{\partial r}$. Since $\frac{d\pi}{\pi} = \frac{2}{7} \frac{dp}{p}$, this requirement is $\frac{2}{7} \frac{\partial p}{p \partial r} \ll \frac{\partial \phi}{\partial r}$, or after using the definition of ϕ , that $\frac{2}{7} \frac{p - p^{(0)}}{p} \ll 1$, which holds. This also assumes that $\theta_m = \theta_m^{(0)}$ where $\phi_2 = \phi_1$. We then obtain an expression for the radial derivative of the cooling, though not the cooling directly:

$$\frac{\partial Q^-}{\partial r} = b \left[\left(f + \frac{v_2}{r}\right) v_2 - \left(f + \frac{v_1}{r}\right) v_1 \right] \quad (5.28)$$

where $b \equiv \beta/[c_p(\pi_1 - \pi_2)]$. Radiative cooling is allowed everywhere in the domain. A great shortcoming of this scheme is that there is no difference in cooling rates between cloudy and cloud free regions (see W. Frank 1977c for observational evidence of the importance of this difference). In real tropical cyclones the decreased radiative cooling in cloudy regions may provide a source of destabilization encouraging intensification, though in the scheme used here the cooling is strictly dissipative.

We will also need to determine the variations of the χ_j that affect both Q^+ and Q^- . In the boundary layer

$$\frac{\partial \chi_0}{\partial t} + u \frac{\partial \chi_0}{\partial r} + \frac{w^-}{h_0} (\chi_0 - \chi_1) = \quad (5.29)$$

$$\frac{C_E}{h_0} |v_1| (\chi_s - \chi_0) + \frac{\partial}{\partial r} \left(k \chi r \frac{\partial \chi_0}{\partial r} \right),$$

where C_E is a bulk exchange coefficient and k_χ is a Fickian diffusion coefficient. The equivalent potential temperature of a parcel saturated at the sea surface temperature is designated χ_s , which provides an upper limit for χ_0 as the system evolves. This value was kept fixed in the weakly nonlinear calculations, though for strong disturbances it must be taken as a function of surface pressure. Allowing χ_s to vary would provide an additional boost for intensification.

There are also changes aloft. At lowest order, χ_2 is fixed. The first order pressure changes are the result of changes in the thickness of the layers, not changes of the potential temperature or density within each layer. At next order the atmosphere must be warming up due to the latent heat release, which is expressed in the change of layer thickness. In the upper layer the perturbations will be crudely approximated as

$$\chi_2 = \chi_2^{(0)} + \Xi(\theta_m - \theta_m^{(0)}) . \quad (5.30)$$

This assumes that changes in the saturation equivalent potential temperature are Ξ times the perturbations of the potential temperature in the upper troposphere. We will set $\Xi = 1.2$, which is roughly the case. This ratio is also approximately equal to ratio of the dry adiabatic lapse rate to the moist adiabatic lapse rate in the upper troposphere. The mean temperature perturbation is as determined by eq. (5.26). The assumption that most of the mean column temperature perturbation is in the upper layer is supported by observations such as those shown in figure 2.1.

The value of χ_1 will be assumed constant and there is no turbulent entropy exchange between the boundary and lower layers in eq. (5.29). This was done mostly for simplicity and in retrospect may have been less than wise. As will be seen in chapter seven, a consequence of this is unrealistic growth of χ_0 for realistic values of the bulk transfer coefficient C_E . Since at lowest order the vertical thermodynamic structure must be in equilibrium, there can be no linear exchange term proportional to $\chi_1 - \chi_0$. A turbulent transfer proportional to $v_1(\chi_1 - \chi_0)$ might be sensible, but this was not done. Any process that served to increase the

lower layer moist entropy, χ_1 , would assist development of a disturbance (unless it created a situation with $\chi_1 > \chi_2$, in which case the model would break down) by increasing the forcing parameter through the reduced vertical stability of the two upper layers.

This completes the specification of the full nonlinear problem in this highly simplified model.

5.2 Expansions

The fields will be expressed with an amplitude expansion similar in purpose to that used by W. Malkus and Veronis (1958) or by Krishnamurti (1969), in their weakly nonlinear analyses. The azimuthal velocity in each of the layers is expanded as

$$v_j = av_j^{(1)} + a^2v_j^{(2)} + \dots \quad (5.31)$$

for $j = 0, 1, 2$. The amplitude, a , is a Rossby number measured as $a = \frac{V}{fL}$, where V is the magnitude of the velocity perturbation and L is the length scale (as yet to be determined). In other words, V is the dimensional amplitude of the solution and a is the nondimensional amplitude. We will only be examining solutions that are cyclonic in the lower layer near the axis, so both a and V are nonnegative. The nondimensional amplitude will be assumed to be much less than one, while the radial structure functions v_j are for the time being dimensional and will be normalized to have maxima of order fL . The amplitude of stationary solutions will have the symbol \bar{a} , while the amplitude of infinitesimal time dependent perturbations will be designated \tilde{a} . All of the fields of motion will be expanded in similar fashion. In practice the values of \bar{a} will push the small Rossby number approximation; \tilde{a} is strictly an infinitesimal test perturbation and hence arbitrarily small. Superscripts in parentheses will indicate the expansion order of a variable or parameter. Some parameters have constant values in the absence of motion; these will be designated with a superscript (0).

It will also be necessary to expand the critical forcing parameter, η , and the growth rate, γ , which are both scalars. Time dependent perturbations will only be considered to be growing off of stationary states and will have an assumed time dependence of $e^{\gamma t}$. Hence the growth rate may only depend on the basic rest state and an added steady state of stationary amplitude \bar{a} . The growth rate is expanded as

$$\gamma = \gamma^{(0)} + \bar{a}\gamma^{(1)} + \bar{a}^2\gamma^{(2)} + \dots \quad (5.32)$$

For solutions that are stationary at first order, $\gamma^{(0)} = 0$. A solution for which $\gamma^{(0)} = 0$, but $\gamma^{(1)} \neq 0$ will be referred to as *slowly varying*.

The parameter η serves as the forcing parameter of the system. Unlike in most stability problems, η can be modified by the *first* order solutions through changes in the χ_j . The part of η that may vary is designated, η_r . It is a function of the motion and may depend on r . There is still a need to expand the constant part of η , as is done in most weakly finite amplitude problems. The required expansion part, η_c , has no spatial dependence and is determined with a solvability condition, as will be explained below. To second order then,

$$\eta = \eta^{(0)} + \bar{a}\eta_c^{(1)} + (\bar{a} + \tilde{a})\eta_r^{(1)}(r) + \bar{a}^2\eta^{(2)} + \dots \quad (5.33)$$

Expansion of $\eta^{(2)}$ is not performed since this term will not be needed. The solvability condition, to be derived in chapter seven, will relate the steady state amplitude to the forcing. Since \bar{a} is positive, if $\eta_c^{(1)} < 0$ then a subcritical instability may be possible.³ By itself, $\eta_c^{(1)} < 0$ only indicates the possibility of a subcritical sta-

³In the problem of Rayleigh-Benard convection, the forcing parameter is the Rayleigh number. Increases in steady state amplitude correspond to increases in the Rayleigh number, for weakly supercritical forcing. In that problem the first nontrivial solvability condition leads to $R = R^{(0)} + \bar{a}^2 R^{(2)}$ and $R^{(2)} > 0$ (note that $R^{(1)} = 0$). This implies that the amplitude increases as the square root of the degree of supercriticality.

Usually if the stability of a system is altered at second order, any resulting bifurcation is referred to as *transcritical*. This can be a subset of supercritical or subcritical instabilities (see Bergé et alii 1986, p. 272ff).

tionary solution; it is still necessary to determine the stability of that solution. The expansion for $\eta_r^{(1)}$ is based on a Taylor series expansion of eq. (5.22) after performing an amplitude expansion of the χ_j :

$$\begin{aligned}\eta_r^{(1)} &= \frac{(\chi_2^{(0)} - \chi_1^{(0)})(\chi_0^{(1)} - \chi_2^{(1)}) - (\chi_0^{(0)} - \chi_2^{(0)})\chi_2^{(1)}}{(\chi_2^{(0)} - \chi_1^{(0)})^2} \\ &= \frac{\chi_0^{(1)} - \eta_r^{(0)}\chi_2^{(1)}}{\chi_2^{(0)} - \chi_1^{(0)}} .\end{aligned}\quad (5.34)$$

Boundary layer increases in temperature or moisture causing increases in $\chi_0^{(1)}$ help drive intensification. Warming aloft that increases $\chi_2^{(1)}$ stabilizes the system.

The expansion of η_r requires the expansion of the χ_j . The first order expansion of eq. (5.29) for χ_0 , for stationary ($\gamma = 0$) or slowly varying ($\gamma^{(0)} = 0$, $\gamma^{(1)} \neq 0$) solutions, results in an inhomogenous equation for $\chi_0^{(1)}$:

$$\begin{aligned}\frac{\partial}{\partial r} \left(k\chi r \frac{\partial \chi_0^{(1)}}{\partial r} \right) = \\ - \frac{C_E |v_1^{(1)}|}{h_0} (\chi_s^{(0)} - \chi_0^{(0)})r + \frac{w^{-(1)}}{h_0} (\chi_0^{(0)} - \chi_1^{(0)})r .\end{aligned}\quad (5.35)$$

This can be integrated after $v_1^{(1)}$ and $w^{-(1)}$ are determined. At lowest order, $\chi_2^{(0)}$ is also fixed. The first order expansion from eq. (5.30) is

$$\chi_2^{(1)} = \Xi\theta_m^{(1)} . \quad (5.36)$$

The value of χ_1 will be assumed constant at all orders. All of the $\chi_j^{(1)}$ are determined diagnostically after the $v_j^{(1)}$ have been calculated.

Several other terms will now be expanded for later use. The momentum flux divergence at first order is

$$\frac{\partial \Lambda_j^{(1)}}{r^2 \partial r} = k_j^{(0)} \frac{\partial}{\partial r} \left(\frac{\partial r v_j}{r \partial r} \right) = k_j^{(0)} \square^2 v_j . \quad (5.37)$$

The box operator is defined as

$$\square^2 v \equiv \frac{\partial}{\partial r} \left(\frac{\partial r v}{r \partial r} \right) = \frac{\partial}{r^2 \partial r} \left[r^3 \frac{\partial}{\partial r} \left(\frac{v}{r} \right) \right] = \frac{\partial^2 v}{\partial r^2} + \frac{\partial v}{r \partial r} - \frac{v}{r^2}$$

and will be used frequently. It is similar to, but not the same as, the Laplacian operator in cylindrical coordinates. (The first two terms of the expanded form are the radial part of the Laplacian.) This operator is only defined when raised to even powers. It is not self-adjoint, but the operators $r\Box^{2n}$, for positive integers n , are self-adjoint. This property will prove convenient when deriving the solvability conditions that hold at second order. Though the operator has been defined in terms of partial derivatives, the same notation will be used when full derivatives with respect to r are intended. The already ad hoc diffusion will not be complicated further. For second order terms only v_j will be expanded with $k_j = k_j^{(0)}$ and $k_j^{(1)} = 0$, which ignores the dependence of k_j on h_j .

The expansion of the total vorticity ζ_j has

$$\zeta_j^{(0)} = f \quad (5.38)$$

and

$$\zeta_j^{(1)} = \frac{\partial r v_j^{(1)}}{r \partial r} . \quad (5.39)$$

These are useful in determining the expansion for w . At first order for slowly varying solutions, the vertical velocity expands to

$$w^{(1)} = \frac{k_s}{f} \frac{\partial r v_1^{(1)}}{r \partial r} , \quad (5.40)$$

which applies whether the amplitude is \bar{a} or \tilde{a} . At second order there are differences between the stationary and the slowly varying time dependent expansions with

$$\bar{w}^{(2)} = \frac{\bar{a}^2 \partial}{r \partial r} r \left[\frac{k_s}{f} v_1^{(2)} + \frac{C_D}{f} |v_1^{(1)}| v_1^{(1)} - \frac{k_s}{f^2} v_1^{(1)} \frac{\partial r v_1^{(1)}}{r \partial r} \right] \quad (5.41)$$

applying to stationary solutions and

$$\begin{aligned} \tilde{w}^{(2)} = & \frac{2\tilde{a}\bar{a}k_s}{f} \frac{\partial r v_1^{(2)}}{r \partial r} + \frac{\tilde{a}\bar{a}\gamma^{(1)}h_0}{f} \frac{\partial r v_1^{(1)}}{r \partial r} \\ & + \frac{2\tilde{a}\bar{a}\partial}{r \partial r} r \left[\frac{C_D}{f} |v_1^{(1)}| v_1^{(1)} - \frac{k_s}{f^2} v_1^{(1)} \frac{\partial r v_1^{(1)}}{r \partial r} \right] \end{aligned} \quad (5.42)$$

applying to slowly varying solutions. The time dependent expansion is an infinitesimal linear perturbation, with amplitude \tilde{a} , about a small amplitude stationary state, with amplitude \bar{a} to be determined, such that $a = \bar{a} + \tilde{a}$. In particular, the expansions require that the spatial functions $\bar{v}_1^{(1)}$ of the steady first order solutions and the infinitesimal time dependent perturbations $\tilde{v}_1^{(1)}$, are identical, since at first order stationary and slowly varying solutions are both solutions to the identical linear system. So, $\bar{v}_1^{(1)} = \bar{a}v_1^{(1)}$ and $\tilde{v}_1^{(1)} = \tilde{a}v_1^{(1)}$, where $v_1^{(1)}$ is a solution to the linear stationary problem of normalized amplitude. The spatial form of $v_1^{(2)}$ and $\bar{v}_1^{(2)}$ are not the same, hence the use of the diacritical marks above the (2) to distinguish them. Note that $\bar{v}_j^{(2)} = \bar{a}^2 v_j^{(2)}$, but $\tilde{v}_j^{(2)} = 2\tilde{a}\bar{a}v_j^{(2)}$. Similar expansions will be performed below without additional comment. For later convenience when the linear and nonlinear terms will be included in separate integrals in creating the solvability conditions at second order, $w^{(2*)}$ is defined as $w^{(2)}$, but without the terms linear in the v_j :

$$\bar{w}^{(2*)} = \bar{a}^2 \frac{\partial}{r \partial r} \left[\frac{C_D}{f} |v_1^{(1)}| v_1^{(1)} r - \frac{k_s}{f^2} r v_1^{(1)} \frac{\partial r v_1^{(1)}}{r \partial r} \right] = \bar{a}^2 w^{(2*)} \quad (5.43)$$

$$\tilde{w}^{(2*)} = 2\tilde{a}\bar{a} \frac{\partial}{r \partial r} \left[\frac{C_D}{f} |v_1^{(1)}| v_1^{(1)} r - \frac{k_s}{f^2} r v_1^{(1)} \frac{\partial r v_1^{(1)}}{r \partial r} \right] = 2\tilde{a}\bar{a} w^{(2*)} \quad (5.44)$$

Up through second order, the cumulus heating expands as

$$Q^{+(1)} = \eta^{(0)} \frac{k_s}{f} \frac{\partial r v_1^{(1)}}{r \partial r} \quad (5.45)$$

$$\bar{Q}^{+(2)} = \eta^{(0)} \bar{w}^{(2)} + \bar{a}^2 \eta^{(1)} w^{(1)} \quad (5.46)$$

$$\tilde{Q}^{+(2)} = \eta^{(0)} \tilde{w}^{(2)} + \bar{a} \eta_c^{(1)} \tilde{a} w^{(1)} + 2\tilde{a}\bar{a} \eta_r^{(1)} w^{(1)}, \quad (5.47)$$

where for the first order expression, the amplitude, a , can be steady or time dependent as needed by the context. We also define $Q^{+(2*)}$, which is similar to $Q^{+(2)}$ except that $w^{(2)}$ is replaced by $w^{(2*)}$ and $\eta^{(1)}$ is replaced by $\eta_r^{(1)}$:

$$\bar{Q}^{+(2*)} = \eta^{(0)} \bar{w}^{(2*)} + \bar{\eta}_r^{(1)} \bar{w}^{(1)} \quad (5.48)$$

$$\tilde{Q}^{+(2*)} = \eta^{(0)} \tilde{w}^{(2*)} + 2\tilde{a}\bar{a} \eta_r^{(1)} w^{(1)}. \quad (5.49)$$

Similarly for the radiative cooling

$$\frac{\partial Q^{-(1)}}{\partial r} = bf(v_2^{(1)} - v_1^{(1)}) \quad (5.50)$$

$$\frac{\partial \bar{Q}^{-(2)}}{\partial r} = bf(\bar{v}_2^{(2)} - \bar{v}_1^{(2)}) + \frac{b}{r}\bar{a}^2(v_2^{(1)}v_2^{(1)} - v_1^{(1)}v_1^{(1)}) \quad (5.51)$$

$$\frac{\partial \tilde{Q}^{-(2)}}{\partial r} = bf(\tilde{v}_2^{(2)} - \tilde{v}_1^{(2)}) + 2\frac{b}{r}\tilde{a}\bar{a}(v_2^{(1)}v_2^{(1)} - v_1^{(1)}v_1^{(1)}) \quad (5.52)$$

$$\frac{\partial \bar{Q}^{-(2*)}}{\partial r} = \frac{b}{r}\bar{a}^2(v_2^{(1)}v_2^{(1)} - v_1^{(1)}v_1^{(1)}) = \bar{a}^2\frac{\partial Q^{-(2*)}}{\partial r} \quad (5.53)$$

$$\frac{\partial \tilde{Q}^{-(2*)}}{\partial r} = 2\frac{b}{r}\tilde{a}\bar{a}(v_2^{(1)}v_2^{(1)} - v_1^{(1)}v_1^{(1)}) = 2\tilde{a}\bar{a}\frac{\partial Q^{-(2*)}}{\partial r} . \quad (5.54)$$

5.3 Stationary Solutions

Stationary solutions are subject to certain relations not applicable to time varying solutions. The determination of stationary solutions and their stability properties are central to this work. We will now examine some of those special relations. At the origin, radial flow must vanish in all layers, so $\psi_j|_{r=0} = 0$. Then adding eqs. (5.2)–(5.4) and integrating once, for stationary solutions

$$\bar{\psi}_0 + \bar{\psi}_1 + \bar{\psi}_2 = 0 . \quad (5.55)$$

This is only stating that for time independent solutions, inflow balances outflow at all radii. The overbars indicate stationary solutions. Equation (5.55) also holds at first order for solutions varying slowly, i.e. at second order.

If there were no diffusive terms, it would be difficult to have solutions with any secondary circulation. The equations for conservation of angular momentum (5.17)–(5.19), with all of the frictional terms eliminated, except those from surface friction, are

$$\begin{aligned} 0 &= \zeta_{1i}\psi_{0i} - \frac{\tau_{si}r}{\rho} \\ 0 &= \zeta_{1i}\psi_{1i} + Q_i^-(v_{2i} - v_{1i})r \\ 0 &= \zeta_{2i}\psi_{2i} + Q_i^+(v_{1i} - v_{2i})r , \end{aligned}$$

where the subscript i indicates inviscid solutions. We are only concerned with solutions having positive ζ_{ji} , positive v_{1i} , and $v_{1i} > v_{2i}$. This is all consistent with $\psi_{0i} > 0$ and $\psi_{1i} > 0$, representing inflow in the boundary and lower layers. However, it is then impossible to have any balancing outflow as required by eq. (5.55) in regions without cumulus heating. The impossibility of a stationary solution at first order is simple and obvious, where

$$0 = f\psi_{1i}^{(1)}$$

$$0 = f\psi_{2i}^{(1)}$$

disallowing any secondary circulation aloft, but still requiring a frictionally driven inflow in the boundary layer that cannot be balanced with outflow. More useful results can be obtained with the inclusion of diffusive processes.

This argument alone provides no clue for choosing between the necessity of vertical or horizontal mixing. In some studies of the Hadley circulation, such as Held and Hou (1980), only vertical diffusion is included. It will be shown below that lateral diffusion is necessary in the context of this model.⁴ If we add the linearized stationary equations derived from eqs. (5.18) and (5.19),

$$f(\bar{\psi}_1^{(1)} + \bar{\psi}_2^{(1)}) + \frac{\partial}{\partial r}(\bar{\Lambda}_1^{(1)} + \bar{\Lambda}_2^{(1)}) = 0, \quad (5.56)$$

where the overbar indicates a stationary solution. For the case with no lateral momentum diffusion, this requires $\bar{\psi}_1^{(1)} + \bar{\psi}_2^{(1)} = 0$. From the sum of the continuity equations for stationary solutions, eq. (5.55), the sum of the radial transports must vanish. This implies that in the absence of horizontal diffusion, at first order, $\bar{\psi}_0^{(1)} = 0$, and hence $\bar{w}^{(1)} = 0$, a rather uninteresting case. Adding all of eqs. (5.17)–(5.19), for the first order stationary system:

⁴Though some are uncomfortable with models that rely on dissipation because the formulation seems ad hoc, others have occasionally worried about its omission from geophysical fluid dynamics problems. In response to Henry Stommel's inviscid ocean models, it has been reported that Willem Malkus once labeled the fresh-water and salt-water taps in Stommel's lab $\nu \neq 0$ (viscous) and $\nu = 0$ (inviscid), respectively (Veronis 1981).

$$-\frac{\bar{\tau}_s r}{\rho} + \frac{\partial}{r \partial r}(\bar{\Lambda}_1^{(1)} + \bar{\Lambda}_2^{(1)}) = 0 . \quad (5.57)$$

So, lateral mixing is needed to balance the effects of momentum transport from the boundary layer into the upper layers for stationary solutions to exist other than the trivial one of no motion in the lower layer. One could partially solve this problem by having an Ekman layer at the top of the fluid as well, but that is more artificial than what is being used here and still does not allow a steady interior secondary circulation. As long as there is frictionally forced inflow, by continuity there must be an outflow aloft, and for steady solutions there must be some way of balancing the advection of planetary angular momentum. We will return to some of these issues when examining Ooyama's linear analysis in section 6.1.

5.4 Energy Equations

It is easy to build an energy equation from the equations for conservation of angular momentum. Multiplying eqs. (5.17)–(5.19) by their respective v_j we get

$$\begin{aligned} \frac{h_0 r}{2} \frac{\partial v_1^2}{\partial t} &= v_1 \zeta_1 \psi_0 - \frac{\tau_s r}{\rho} v_1 \\ \frac{h_1 r}{2} \frac{\partial v_1^2}{\partial t} &= v_1 \zeta_1 \psi_1 + (Q^- + \mu)(v_2 - v_1)v_1 r + v_1 \frac{\partial \Lambda_1}{r \partial r} \\ \frac{\epsilon h_2 r}{2} \frac{\partial v_2^2}{\partial t} &= v_2 \zeta_2 \psi_2 + (Q^+ + \mu)(v_1 - v_2)v_2 r + v_2 \frac{\partial \Lambda_2}{r \partial r} . \end{aligned} \quad (5.58)$$

Adding these up,

$$\begin{aligned} \frac{\partial \mathcal{U}}{\partial t} &= v_1 \zeta_1 (\psi_0 + \psi_1) + v_2 \zeta_2 \psi_2 + (v_1 - v_2)(v_2 Q^+ - v_1 Q^-) \\ &\quad - \frac{\tau_s r}{\rho} v_1 - \mu(v_1 - v_2)^2 r + v_1 \frac{\partial \Lambda_1}{r \partial r} + v_2 \frac{\partial \Lambda_2}{r \partial r} \\ \mathcal{U} &\equiv \frac{r}{2} \left[(h_0 + h_1)v_1^2 + \epsilon h_2 v_2^2 \right] . \end{aligned} \quad (5.59)$$

This is an equation for the vertically integrated kinetic energy density per unit mass. The surface stress, τ_s , and the boundary layer velocity are of the same sign, making the first term of the second line dissipative. The interlayer friction term,

proportional to μ , is clearly negative. It is easy to show that the last two terms are also energy sinks. Using eq. (5.37) and integrating over the domain,

$$\begin{aligned} \int v_j \frac{\partial \Lambda_j}{r \partial r} &= \int \frac{v_j}{r} \frac{\partial}{\partial r} \left[k_j r^3 \frac{\partial}{\partial r} \left(\frac{v_j}{r} \right) \right] dr \\ &= \left[k_j r^2 v_j \frac{\partial}{\partial r} \left(\frac{v_j}{r} \right) \right] - \int k_j r^3 \left[\frac{\partial}{\partial r} \left(\frac{v_j}{r} \right) \right]^2 dr . \end{aligned}$$

At the outer boundary v_j will vanish by fiat, so all that remains is the negative integral of a positive quantity. The term in the first line proportional to the vertical shear will also be dissipative for the solutions found here, but that cannot yet be rigorously shown.

The primary source of kinetic energy comes from forcing ψ through the continuity equations, i.e. flow down the pressure gradient. We can assume that the total vorticity in both layers is positive. However the relative vorticity, especially in the upper layer may be negative. The first term is the primary kinetic energy source. The sign of the second term will depend mostly on the sign of v_2 .

For linearized solutions evolving slowly (i.e. $\gamma^{(0)} = 0$),

$$\begin{aligned} \frac{\partial \mathcal{U}}{\partial t} &= f v_1^{(1)} (\psi_0^{(1)} + \psi_1^{(1)}) + f v_2^{(1)} \psi_2^{(1)} \\ &\quad - \left[\frac{\tau_s^{(1)} r}{\rho} v_1^{(1)} + \mu (v_1^{(1)} - v_2^{(1)})^2 - k_1^{(0)} v_1^{(1)} \square^2 v_1^{(1)} - k_2^{(0)} v_2^{(1)} \square^2 v_2^{(1)} \right] \end{aligned} \quad (5.60)$$

All of the terms in square brackets are dissipative. Only the terms in the first line can provide an energy source. Making use of eqs. (5.55), (5.2), and (5.8)

$$\begin{aligned} f v_1^{(1)} (\psi_0^{(1)} + \psi_1^{(1)}) + f v_2^{(1)} \psi_2^{(1)} &= \\ &= f (v_1^{(1)} - v_2^{(1)}) \left[\frac{\eta^{(0)} \tau_s^{(1)} r}{f \rho} - \int_0^r r' Q^{-(1)}(r') dr' \right] . \end{aligned} \quad (5.61)$$

By comparing this with eq. 5.60, it is clear that if η is not at least one there are not even stationary solutions, no less growing ones, except for the trivial solution. If η is less than one there is not sufficient energy from heating to overcome the energy loss due to surface friction.

The terms for the upper layer have somewhat counterintuitive properties. Typical tropical cyclone builders are not particularly interested in spinning up a

strong anticyclone aloft . Increases in the last term of \mathcal{U} are therefore viewed as a drain on the system. Emanuel (1988) noted that increasing the size (and hence strength for parcels conserving angular momentum) of the anticyclone weakens the storm providing an absolute limit on the anticyclone extent. Emanuel and Rotunno (1989) concluded that any energy used to provide kinetic energy at upper levels was a loss since it could not contribute to enhancing sea surface fluxes. Dissipative terms aloft, though causing a net loss of kinetic energy may provide a positive influence in increasing the kinetic energy of the lower layer (Willoughby, personal communication). This will be discussed further in the analysis of the solvability conditions of chapter seven.

"... for one of the nicest things about mathematics, or anything else you might care to learn, is that many of the things which can never be, often are. You see," he went on, "it's very much like your trying to reach Infinity. You know that it's there, but you just don't know where— but just because you can never reach it doesn't mean that it's not worth looking for."

*The Mathemagician in
Norton Juster
The Phantom Tollbooth*

Chapter 6

Linear Theory

There are several linear problems that could be based on the system of equations presented in the previous chapter. These are mostly distinguished by the inclusion or exclusion of time dependence, various frictional terms, and various thermodynamic processes. We will first examine the linear model presented by Ooyama and show why this is an inappropriate starting point for the weakly nonlinear analysis. The stationary system with friction, presented in section 6.2, is the only one that will be fully solved and it is the basis of the finite amplitude expansions in chapter seven. At the end of the chapter are examinations of the dispersion relations with subsets of the frictional terms included and finally the growth rate equation for the full viscous linear system.

6.1 Ooyama's Linear Model

In Ooyama's first published paper on tropical cyclone instability (1964), a linear analysis was presented for an instability based on cooperation between the cyclone and cumulus scales. This was repeated in the lengthier paper of 1969. As already noted, the work here is an extension of that done by Ooyama. We will look briefly at the linear model that he presented.

The equations already provided above were linearized and neither internal dissipation nor radiative cooling was included. This is equivalent to setting $\mu = 0$,

$\lambda_j = 0$, and $b = 0$. The linear solutions are assumed to have time dependence of the form $e^{\gamma^{(0)}t}$. The equations for conservation of angular momentum, (5.18) and (5.19), then reduce to

$$h_1^{(0)}\gamma^{(0)}\tilde{v}_1^{(1)}r = f\tilde{\psi}_1^{(1)} \quad (6.1)$$

$$\epsilon h_2^{(0)}\gamma^{(0)}\tilde{v}_2^{(1)}r = f\tilde{\psi}_2^{(1)} . \quad (6.2)$$

The change in the relative angular momentum depends only on the advection of planetary angular momentum and it is clear that in the absence of time dependence, i.e. $\gamma^{(0)} = 0$, no secondary circulation is allowed. The tilde is used to indicate infinitesimal perturbations, which here represent perturbations about the rest state (i.e. the $\bar{v}_j = 0$). Momentum loss from the boundary layer to the surface was kept, so

$$\tilde{w}^{(1)} = \frac{\partial}{f r \partial r} [(k_s + h_0\gamma^{(0)})r\tilde{v}_1^{(1)}] .$$

Though the term proportional to the boundary layer thickness was dropped by Ooyama, it is kept here. This time dependent term increases the strength of the vertical velocity out of the boundary layer. Keeping terms proportional to h_0 does not change the order or coupling of any equation. After substitution of the heating parameterization eq. (5.21), the continuity equations (5.3) and (5.4) become

$$\begin{aligned} \gamma^{(0)}\tilde{h}_1^{(1)} &= \frac{d\tilde{\psi}_1^{(1)}}{r dr} - (\eta^{(0)} - 1)\tilde{w}^{(1)} \\ \gamma^{(0)}\epsilon\tilde{h}_2^{(1)} &= \frac{d\tilde{\psi}_2^{(1)}}{r dr} + \eta^{(0)}\tilde{w}^{(1)} . \end{aligned}$$

Note that the left hand side of these contain the first order variations of the layer thickness. Taking a radial derivative of these equations, substituting in the gradient wind relation, eq. (5.15), with the relations between the layer thickness perturbations and the pressure perturbations, eqs. (5.13) and (5.14), yields the two coupled equations

$$\begin{aligned}
\frac{\gamma^{(0)} f}{g(1-\epsilon)}(\tilde{v}_1^{(1)} - \epsilon \tilde{v}_2^{(1)}) = \\
\Box^2 \left(\frac{h_1^{(0)} \gamma^{(0)}}{f} \tilde{v}_1^{(1)} \right) - \frac{\partial}{\partial r} \left\{ (\eta^{(0)} - 1) \frac{\partial}{f r \partial r} [(k_s + h_0 \gamma^{(0)}) r \tilde{v}_1^{(1)}] \right\} \\
\frac{\epsilon \gamma^{(0)} f}{g(1-\epsilon)}(\tilde{v}_2^{(1)} - \tilde{v}_1^{(1)}) = \\
\Box^2 \left(\frac{\epsilon h_2^{(0)} \gamma^{(0)}}{f} \tilde{v}_2^{(1)} \right) + \frac{\partial}{\partial r} \left\{ \eta^{(0)} \frac{\partial}{f r \partial r} [(k_s + h_0 \gamma^{(0)}) r \tilde{v}_1^{(1)}] \right\}.
\end{aligned}$$

If we now assume that the solutions are first order Bessel functions, so $\Box^2 v = -m^2 v$ where m^2 is a constant similar to a wavenumber but for Bessel functions (if this is not obvious see the footnote on p. 144), and note that $\eta^{(0)}$ is constant except at a finite number of discontinuities, a relation between the horizontal length scale and the growth rate is obtained:

$$\begin{aligned}
\gamma^{(0)} \left\{ \frac{f^2}{g^2(1-\epsilon)} + \frac{m^2(h_0 + h_1^{(0)} + h_2^{(0)})}{g(1-\epsilon)} + \frac{m^4 h_2^{(0)} [h_1^{(0)} - (\eta^{(0)} - 1)h_0]}{f^2} \right\} \\
= \left\{ \frac{m^4 k_s h_2^{(0)} (\eta^{(0)} - 1)}{f^2} - \frac{m^2 k_s}{g(1-\epsilon)} \right\}.
\end{aligned}$$

The m are dimensional Bessel function wave numbers. This equation applies except at the discontinuities in $\eta^{(0)}$.

Since $h_1^{(0)}$ is surely greater than $(\eta^{(0)} - 1)h_0$, for positive growth rates the right hand side must be greater than zero. Hence, $\eta^{(0)} > 1$ in ascent regions for growing disturbances.

With the further simplifying assumptions made by Ooyama that $h_0 \ll h_1^{(0)}$ and $h_1^{(0)} = h_2^{(0)}$, the growth rate is then

$$\gamma^{(0)} = \frac{k_s}{h_2^{(0)}} \frac{(\eta^{(0)} - 1 - \xi^2)}{[1 + 2\xi^2 + (1-\epsilon)\xi^4]},$$

where ξ is a nondimensional length scale defined by $\xi^2 \equiv \frac{f^2}{g(1-\epsilon)h_2^{(0)}m^2}$. Ooyama ignored the effects of curvature by using $\frac{d^2}{dr^2}$ rather than \Box^2 , though the only difference is that the solutions are first order Bessel functions of the first kind

rather than sine functions, which is little in the way of additional simplification.

The previous two relations apply in the ascent region. In the descent region where $Q = 0$, the same expressions can be used by setting $\eta^{(0)} = 0$. For a matched modal solution, $\gamma^{(0)}$ must be the same throughout the domain. The dispersion relation then no longer has solutions with positive m^2 . The solutions then are Bessel functions with only imaginary arguments, or equivalently one can replace m^2 with $-m^2$ and use modified Bessel functions.

Ooyama's determination of the dependence of growth rate on length scale simply made use of the just derived expression. Technically, this is not sufficient. For any given value of $\gamma^{(0)}$, there are two values of m^2 for each of the ascent and descent regions, and hence four linearly independent solutions in each region. Some of the solutions can be immediately eliminated for regions including the origin or extending out to infinity. At this point boundary and matching conditions should be applied and the point(s) separating ascent and descent regions should be calculated (not imposed). Since we will not be using these solutions, these further calculations will not be carried out, though we will engage in a similar process later. It is worth noting that Charney and Eliassen (1964b) did determine the length scale in their CISK problem by matching solutions from ascent and descent regions and obtained a similar dependence of growth rate on length scale as was obtained with the more naïve approach used by Ooyama.

In the limit as $\eta^{(0)} \rightarrow 1$, the critical value of $\eta^{(0)}$ for positive growth rate, the solution collapses to a zero width ascent region. It is impossible to expand about this neutral solution, since the solution is trivial. It also appears that there exists a neutral solution for $\xi^2 = \eta^{(0)} - 1$. However, this limit is singular and only applies when faster growing modes are allowed. A search for modes with slow second order growth is of limited value if modes growing more rapidly at first order exist.

As noted in section 5.3, the total elimination of internal dissipation means that steady solutions can have no secondary circulation. The only steady solutions allowed by Ooyama's linearized model are those with no motion in the lower layer

and arbitrary velocity structure for v_2 in the upper layer. These solutions are essentially trivial for our purposes.

6.2 Linear Stationary Problem

6.2.1 Dissipative Linear Stationary System

To develop a problem with time dependence controlled at second order (or beyond), we must first solve a linear stationary problem about which we will later expand. We turn now to a linearization of the equations of chapter five, keeping the viscous and radiative cooling terms. One could directly reduce the resulting linear problem to an eighth order equation in one variable, though it then becomes very difficult to follow the physics. This also requires taking several derivatives of the discontinuous parameter η , which is very problematic when it becomes time to impose matching conditions at the boundaries between ascent and descent regions. There is a clearer way to proceed using a vector equation. Two new variables are now introduced:

$$v_3 \equiv \frac{f}{k_s} \frac{\psi_1}{r}, \quad v_4 \equiv \frac{f}{k_s} \frac{\psi_2}{r}. \quad (6.3)$$

These are proportional to $-u_1$ and $-u_2$ as well, respectively, with $v_{j+2} = -\epsilon_j h_j \frac{f}{k_s} u_j$. (Use of u_1 and u_2 directly would require carrying several constants throughout the calculation. Also, at second order where the h_j are not constant, v_{j+2} are no longer directly proportional to ψ_j/r .) The constants k_s and f are included in the definitions simply to make v_3 and v_4 have the same units (velocity) as v_1 and v_2 . Neither of those constants will ever be set to zero, since that would eliminate the basic driving physics of the problem.

The linear stationary versions of the momentum equations (5.18) and (5.19) at lowest order are

$$0 = k_1^{(0)} r \square^2 \bar{v}_1^{(1)} + \mu(\bar{v}_2^{(1)} - \bar{v}_1^{(1)})r + k_s \bar{v}_3^{(1)} r \quad (6.4)$$

$$0 = k_2^{(0)} r \square^2 \bar{v}_2^{(1)} + \mu(\bar{v}_1^{(1)} - \bar{v}_2^{(1)})r + k_s \bar{v}_4^{(1)} r. \quad (6.5)$$

The first term in each of these represents lateral diffusion of angular momentum, the second term is the vertical diffusion, and the last term is the lateral advection of planetary vorticity by the secondary circulation (though the factor f is hidden in the variable definitions). The overbars indicate stationary solutions.

The radial derivative of the first order stationary version of the continuity equations (5.3); with the first order expansion of w , eq. (5.40); the substitution of the heating parameterization at first order, eq. (5.45); and the cooling parameterization, eq. (5.50); is

$$0 = \frac{k_s}{f} \square^2 \bar{v}_3^{(1)} - \frac{d}{dr} \left[(\eta^{(0)} - 1) \frac{k_s}{f} \frac{dr \bar{v}_1^{(1)}}{r dr} \right] + b f (\bar{v}_2^{(1)} - \bar{v}_1^{(1)}) . \quad (6.6)$$

The \square^2 operator now refers to total derivatives with respect to r , rather than partial derivatives, but this should cause no confusion. The first term here is the derivative of the lateral flow divergence, the next terms are the derivatives of the vertical transport to the upper layer and the vertical transport from the lower layer, and the last term is the derivative of the descent into the lower layer from radiative cooling.

Rather than using the upper level continuity equation (5.4), we use the sum of the continuity equations. Integrating once, with the boundary condition of no flow at the origin, yields

$$\bar{v}_1^{(1)} + \bar{v}_3^{(1)} + \bar{v}_4^{(1)} = 0 . \quad (6.7)$$

Since we will be dealing with two separate domains, the application of the boundary condition at the origin does not constrain the integral of the summed continuity equations in the outer region. The boundary condition that there is no net lateral flow at the outer boundary of the domain leads to the same result. (Also see the comment on p. 169). The three terms are proportional to the inward horizontal transport in the boundary layer, lower layer, and upper layer, respectively.

The last four equations can be reduced to three, eliminating $\bar{v}_4^{(1)}$, and recast as a single vector equation:

$$\frac{d}{dr} \left(B' \frac{dr \bar{\mathbf{v}}^{(1)}}{r dr} \right) + A' \bar{\mathbf{v}}^{(1)} = 0 \quad (6.8)$$

$$B' = \begin{pmatrix} k_1^{(0)} & 0 & 0 \\ 0 & k_2^{(0)} & 0 \\ -(\eta^{(0)} - 1)k_2^{(0)} & 0 & k_2^{(0)} \end{pmatrix}$$

$$A' = \begin{pmatrix} -\mu & \mu & k_s \\ \mu - k_s & -\mu & -k_s \\ -\frac{bf^2 k_2^{(0)}}{k_s} & \frac{bf^2 k_2^{(0)}}{k_s} & 0 \end{pmatrix},$$

where $\mathbf{v} = (v_1, v_2, v_3)$. Use has been made of the fact that all of the coefficients not involving η are constant. Multiplication of the third equation by $k_2^{(0)}$ was performed only to keep the matrix entries dimensionally similar. The matrices are primed for notational uniqueness since they will later be transformed. This vector form will be useful when dealing with the inhomogeneous systems of chapter seven. Further, the equation holds even at discontinuities in $\eta^{(0)}$, though one of the coefficients in B' is discontinuous.

The boundary conditions we will impose are the simplest homogeneous ones and easy to express in vector form. At the center (origin), the tangential velocities and the radial transports must vanish. The same conditions will be used at the outer boundary of the domain, $r = r_1$, so

$$\mathbf{v}|_{r=0} = 0 \quad (6.9)$$

$$\mathbf{v}|_{r=r_1} = 0. \quad (6.10)$$

Note that there are three conditions contained in each of eqs. (6.9) and (6.10).

One of the major complications in this problem is the discontinuity in the coefficients of the linear equations at the boundaries between updraft and downdraft

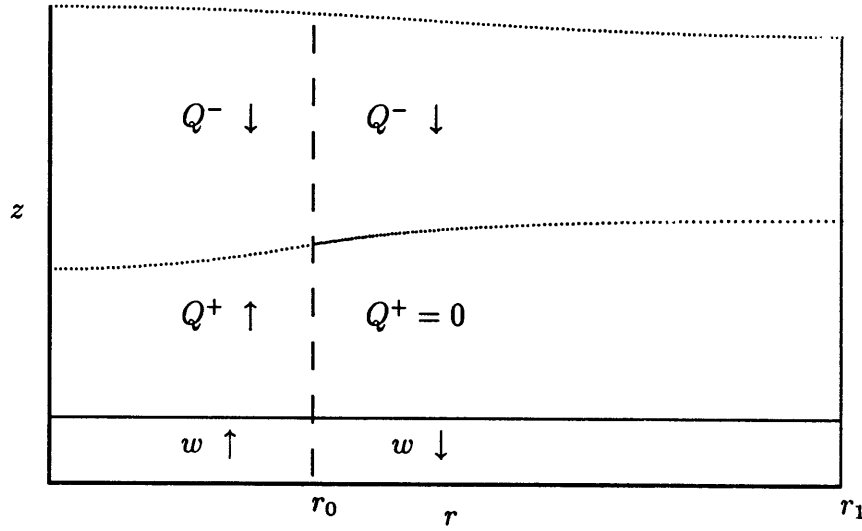


Figure 6.1: Schematic of regions and forcing.

regions. There are two distinct general solutions, each applying to a different region. We will assume that the interior region, closest to the origin, has positive w and that there is only a single region outside of that, with Ekman suction throughout that outer region. By solving this system, we will show that it is consistent.¹ For the existence of a solution degenerate only with respect to a single amplitude coefficient, there must be as many matching conditions at the boundary between these two regions as the order of the system, which is the same as the number of boundary conditions imposed at the two endpoints. The internal boundary where $w = 0$ is labeled r_0 , and there, at first order,

$$\left. \frac{drv_1^{(1)}}{r dr} \right|_{r=r_0} = 0. \quad (6.11)$$

This is required through eqs. (5.22) and (5.40). It will be necessary to find r_0 as an eigenvalue of the problem. The required matching conditions are that all of the

¹The solution is not necessarily unique. There may exist solutions with multiple updrafts, but I have not attempted to find them (though I suspect they do exist), nor have I tried to prove their nonexistence.

variables, v_j and their first derivatives (or equivalently $\frac{dr v_j}{r dr}$) are continuous. These conditions can be derived rigorously by integrating eq. (6.8) across r_0 assuming only that \mathbf{v} is finite in a small neighborhood of r_0 . For matching conditions we require that the vectors

$$\mathbf{v}^{(1)} \quad \text{and} \quad \frac{dr \mathbf{v}^{(1)}}{r dr} \quad \text{are continuous at } r_0. \quad (6.12)$$

The continuity requirements represent six equations. The requirement that $\frac{dr \mathbf{V}^{(1)}}{r dr}$ be continuous, is equivalent to a continuity requirement on $\frac{d\mathbf{V}^{(1)}}{dr}$, as long as $\mathbf{v}^{(1)}$ is also required to be continuous. If instead of using the vector form, the system had been reduced to a sixth order equation in a single variable, it would have been necessary to derive complicated jump conditions on the derivatives of that single variable and cope with a very high order singularity.

6.2.2 Basis Functions and Nondimensionalization

Since $\frac{d}{dr} \left(\eta^{(0)} \frac{dr v_1^{(1)}}{r dr} \right) = \eta^{(0)} \square^2 v_1^{(1)}$ [see eq. (5.24)], we can replace eq. (6.8) with

$$\mathbf{B}' \square^2 \bar{\mathbf{v}}^{(1)} + \mathbf{A}' \bar{\mathbf{v}}^{(1)} = 0. \quad (6.13)$$

Since both \mathbf{B}' and \mathbf{A}' are piecewise constant matrices, we can deal separately with each region as a standard linear problem. In the ascent region we will assume that the solutions are sums of first order Bessel functions² so that $\square^2 v = -m^2 v$. The

²The first and zeroeth order Bessel functions and their derivatives satisfy:

$$\begin{aligned} \frac{d}{dr} r J_1(mr) &= m J_0(mr) & \frac{d}{dr} J_0(mr) &= -m J_1(mr) \\ \frac{d}{dr} r Y_1(mr) &= m Y_0(mr) & \frac{d}{dr} Y_0(mr) &= -m Y_1(mr) \\ \frac{d}{dr} r K_1(mr) &= -m K_0(mr) & \frac{d}{dr} K_0(mr) &= -m K_1(mr) \\ \frac{d}{dr} r I_1(mr) &= m I_0(mr) & \frac{d}{dr} I_0(mr) &= m I_1(mr), \end{aligned} \quad (6.14)$$

where J_1 and Y_1 are the first order Bessel functions of the first and second kind, respectively; K_1 and I_1 are modified Bessel functions of the first and second kind, respectively; and the functions with subscript 0 are the corresponding zeroeth order Bessel and modi-

m^2 then satisfy

$$\det (A' - m^2 B') = 0 . \quad (6.16)$$

This expands to

$$\begin{aligned} k_1^{(0)} k_2^{(0)} m^6 - [(\eta^{(0)} - 1) k_s k_2^{(0)} - \mu(k_1^{(0)} + k_2^{(0)})] m^4 \\ + [\mu k_s + b f^2 (k_1^{(0)} + k_2^{(0)})] m^2 + b f^2 k_s = 0 . \end{aligned} \quad (6.17)$$

The degree of this expression implies that there are six linearly independent solutions to eq. (6.13) in the ascent region.

There are six independent parameters (the forcing parameter, four frictional parameters, and one cooling parameter) in eq. (6.17). These can be reduced to four by nondimensionalizing, which eliminates two frictional parameters. The simplest nondimensionalization uses a length scale of $L = \sqrt{k_2^{(0)}/k_s}$. For any limits that still allow stationary hurricane-like solutions, both of the parameters used are kept finite (see section 6.4). The square of the nondimensional wavenumbers (in roman type) are transformed as

$$m^2 = \frac{k_s}{k_2^{(0)}} m^2 . \quad (6.18)$$

fied Bessel functions. (For a discussion of the behavior of these function see Abramowitz and Stegun 1964). Graphs of these functions are shown in figures (6.2).

The following equations have the accompanying general solutions:

Equation	General Solutions	
$\square^2 v + m^2 v = 0$	$v = c_1 J_1(mr) + c_2 Y_1(mr)$	(6.15)
$\square^2 v - m^2 v = 0$	$v = c_3 K_1(mr) + c_4 I_1(mr)$	
$\square^2 v = 0$	$v = c_5 r + c_6 / r ,$	

where the c_i are arbitrary constants. Though the operator \square^2 is not constant coefficient, operators of the form $D_l = \square^2 + m_l^2$ are commutative. Hence, an equation of the form $[a_0 + \sum_{j=1}^n a_j \square^{2j}] v = 0$ can be easily solved after factoring it into the form $[a_n \prod_{l=1}^n (\square^2 + m_l^2)] v = 0$, where the m_l are a function of the a_j and n is a positive integer.

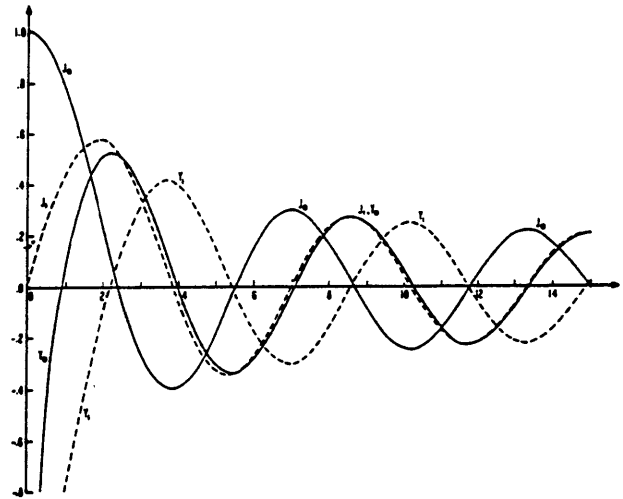
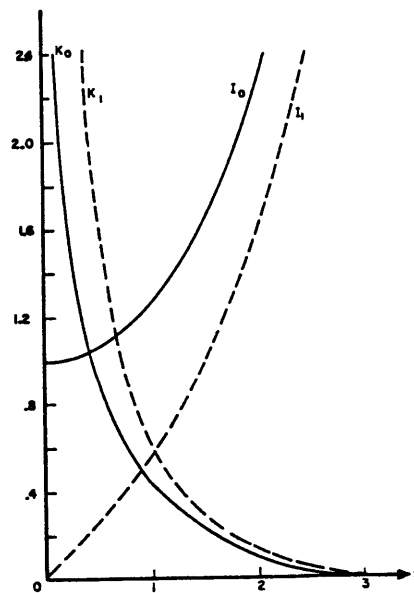
FIGURE 9.1. $J_0(x)$, $Y_0(x)$, $J_1(x)$, $Y_1(x)$.FIGURE 9.7. $I_0(x)$, $K_0(x)$, $I_1(x)$ and $K_1(x)$.

Figure 6.2: (a) Bessel functions J_1 , J_0 , K_1 , K_0 ; and (b) Modified Bessel functions I_1 , I_0 , Y_1 , Y_0 [from Abramowitz and Stegun 1964].

The nondimensional wavenumbers satisfy

$$\begin{aligned} Km^6 - [\eta^{(0)} - 1 - M(1 + K)]m^4 \\ + [M + B(1 + K)]m^2 + B = 0, \end{aligned} \quad (6.19)$$

where the nondimensional parameters are as defined

$$\begin{aligned} M &\equiv \frac{\mu}{k_s} \\ K &\equiv \frac{k_1^{(0)}}{k_2^{(0)}} \\ B &\equiv \frac{bf^2 k_2^{(0)}}{k_s^2}. \end{aligned}$$

The frictional dependence of the form of the linear solutions has now been greatly simplified. Rather than needing the not-well-known magnitudes of the frictional parameters, we need only their ratios.

If all of the roots m^2 were negative, i.e. there were no Bessel function solutions but only modified Bessel function solutions, or any of the roots are complex, it would be impossible to satisfy the homogeneous boundary conditions at the origin and the matching conditions, except with the trivial solution. These conditions provide requirements for a critical value of $\eta^{(0)}$ which will be designated $\eta_{crit}^{(0)}$. This in fact is the same critical value for the existence of linearly unstable modes in the ascent region (see section 6.3). (This is not necessarily the critical value for linearly unstable solutions meeting the boundary conditions and the matching conditions [see discussion on p. 163].) The full requirement for real roots (derived from a result in Abramowitz and Stegun 1964, p. 17) is that

$$0 > \left(\frac{a_1}{3}\right)^3 + \left(\frac{a_0}{2}\right)^2 - \frac{a_0 a_1 a_2}{2 \cdot 3} + a_0 \left(\frac{a_2}{3}\right)^3 - \frac{a_1^2 a_2^2}{2^2 \cdot 3^3} \quad (6.20)$$

$$a_2 = -[\eta_{crit}^{(0)} - 1 - M(1 + K)]/K$$

$$a_1 = [M + B(1 + K)]/K$$

$$a_0 = B/K,$$

which is a cubic for $\eta_{crit}^{(0)}$ and more easily evaluated numerically. The requirements of the eigenvalue problem may enforce additional restrictions on $\eta^{(0)}$.

Some limits and approximations can be found analytically. Let us assume $\eta^{(0)} > \eta_{crit}^{(0)}$ so that there are only real roots. Since the last coefficient of eq. (6.17) (the constant term) is positive, then either only one root is negative or all three are negative.³ For the case that only one root is negative, the second coefficient of eq. (6.17) (for the term proportional to m^4) must be negative.⁴ This requires that at least

$$\eta_{crit}^{(0)} > 1 + M(1 + K) . \quad (6.21)$$

The requirement that all the roots must be real may necessitate that $\eta^{(0)}$ be still greater than this bound for the existence of nontrivial solutions. Cubic equations can be treated analytically by the formulae above, though the results are often more messy than illustrative. Some limiting cases are helpful. In the limit of small radiative cooling (small B)

$$\eta_{crit}^{(0)} \approx 1 + M(1 + K) + 2\sqrt{MK} + B(1 + K)\sqrt{\frac{K}{M}} + B\frac{K^2}{M} .$$

This was determined by performing an expansion of eq. (6.20) for small B. It is worth noting that for believable values of the frictional coefficient ratios, the critical value of $\eta^{(0)}$ can be significantly greater than 1 ($\eta_{crit}^{(0)}$ for the inviscid case). The

³This result is obvious if one creates a generic cubic in x of the factored form $(x - a)(x - b)(x - c) = 0$, where a , b , and c are the three roots. Expanded this is $x^3 - (a + b + c)x^2 + (ab + bc + ca)x - abc = 0$. The term corresponding to $-abc$ in eq. 6.17 is clearly positive.

⁴Assume that $a > 0$, $b > 0$, and $c < 0$; i.e. two positive roots and one negative root. Let $q = a + b + c$, which is the coefficient of $-x^2$ in our generic cubic. Since the coefficient of m^2 in eq. (6.17) is clearly positive, then the corresponding term here, i.e. the x term, provides the slightly rearranged inequality $ab + c(a + b) > 0$. Multiplying q by $(a + b)$ we get $q(a + b) = (a + b)^2 + c(a + b)$. Adding the last two relations and performing some additive cancelling yields $q(a + b) > a^2 + ab + b^2$. The right hand side is clearly greater than zero. Since $(a + b)$ is a positive factor, then $q > 0$ for the case with all three roots real with only one negative.

vertical diffusion ratio, M , is less than one as long as the bulk vertical momentum diffusion is less than the frictional momentum losses from the boundary layer to the ocean surface. In many models this is taken to be zero. In a mature hurricane, with large vertical convective transports the diffusive momentum transports are of the same order. For the linear case, where the explicit inclusion of cumulus momentum transports does not yet appear, the parameterized turbulent transport serves as a proxy. The values chosen for M will fall mostly in the range from 0.1 to 0.5. Expansion of the lateral diffusion ratio has $K = \frac{h_1^{(0)}\lambda_1}{\epsilon h_2^{(0)}\lambda_2}$. If the lateral eddy diffusivities, λ_j , were taken to be equal, since $\epsilon < 1$ and $h_2^{(0)} \leq h_1^{(0)}$, then K would be greater than one. However, in a symmetric model it is more sensible to have $\lambda_2 > \lambda_1$. This is justified by the presence of the unresolved asymmetries and jet-like structures of the upper layer, along with inertial instabilities on short time scales. The enormous deviations from cylindrical symmetry create much greater internal velocity gradients than appear in the azimuthally averaged quantities. So, the values chosen for K will also fall mostly in the range from 0.1 to 0.5.

Plots of $\eta_{crit}^{(0)}$ are provided in figures 6.3. Note that in the singular limit of $K \rightarrow 0$, then $\eta_{crit}^{(0)} = 1 + M$ is the requirement for at least one positive value for m^2 . The critical value increases rapidly with M though slowly with K . This difference becomes less pronounced as one increases B . The graph does not extend to larger values of the parameters because these lead to values of $\eta_{crit}^{(0)}$ so large as to be irrelevant.

[This paragraph provides a clue to nonlinear things yet to come.] Later in this chapter, we will find an $\eta^{(0)} > \eta_{crit}^{(0)}$ as an eigenvalue. Since it has already been stated that this condition is the same as that for the existence of linearly unstable modes, it is important to note that no assumption will be made that the ambient atmosphere is linearly unstable to hurricane-like disturbances. In the next chapter we will calculate $\eta_c^{(1)}$ for a given disturbance. The effective value of η for a given finite amplitude disturbance is defined so that

$$\eta_e \equiv \eta^{(0)} + \bar{a}\eta_c^{(1)}$$

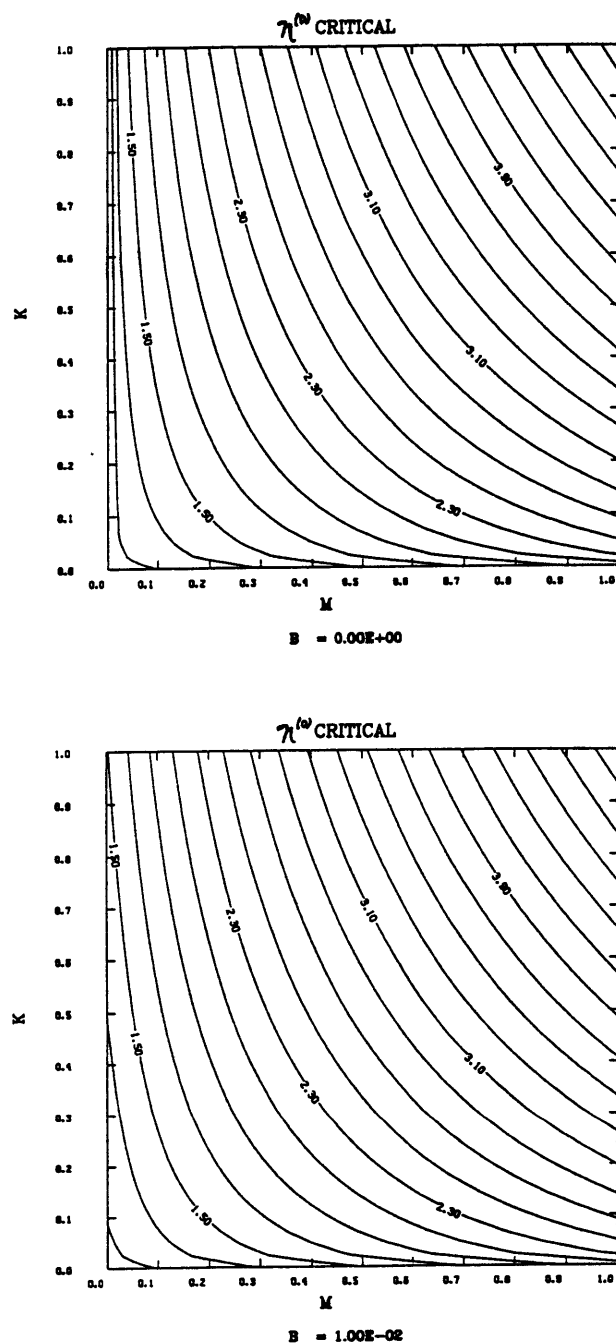


Figure 6.3: Plots of the critical value of the forcing parameter, $\eta^{(0)}$, as a function of the vertical and lateral diffusion ratios, M and K , for two values of the cooling parameter (a) $B = 0$ and (b) $B = 0.01$. This is the requirement for all m^2 to be real and at least one of them positive.

(n.b. only the constant part of $\eta^{(1)}$ is included). We will later find that $\eta_c^{(1)} < 0$ for cyclonic disturbances ($a > 0$). For that case, *the forcing parameter needed to maintain a finite amplitude disturbance is less than that needed for an infinitesimal one*. If $\eta^{(0)}$ is less than $\eta_{crit}^{(0)}$, then there are no solutions to this system except that of no motion. However it is possible that

$$\eta^{(0)} > \eta_{crit}^{(0)} > \eta_a > \eta_e = \eta^{(0)} + \bar{a}\eta_c^{(1)}, \quad (6.22)$$

depending on the amplitude \bar{a} and the value of $\eta_c^{(1)}$, where η_a is the value of the forcing parameter for the ambient atmosphere.

For every value of m^2 there are two values for m of opposite sign. It is possible to express two linearly independent solutions in terms of just the positive root; i.e. $J_1(mr)$, $Y_1(mr)$. In the interior ascent region, where eq. (6.17) holds, there is one solution with $m^2 < 0$ so that it is a modified Bessel function, contrary to the *ansatz* with which we started. The positive roots of the positive m^2 will be designated m_1 and m_2 , and the positive imaginary root of the the one negative m^2 will be designated m_3 (so m_3/i is real). In the interior region, the general solution is a sum of the basis functions $J_1(m_1r)$, $J_1(m_2r)$, $I_1(m_3r/i)$, $Y_1(m_1r)$, $Y_1(m_2r)$, $K_1(m_3r/i)$; each multiplied by an arbitrary coefficient. The boundary conditions at the origin require that the coefficients of the last three of these functions be zero, since those functions are unbounded at $r = 0$.

Graphs of the nondimensional m^2 as functions of the parameters are plotted in figures 6.4–6.7. We note, in figure 6.4, the collapse to degeneracy and vanishing of the roots representing Bessel functions as $\eta^{(0)}$ goes to $\eta_{crit}^{(0)}$ and the relative insensitivity of the modified Bessel solution due mostly to radiative cooling. The behavior in figure 6.5 leads us to expect that the length scales will increase with increasing K . Figures 6.6 and 6.7 lead us to expect decreasing length scales with increasing M or increasing B . The dependencies will be discussed with more detail in terms of the full solutions in section 6.2.5.

In the descent region where $\eta = 0$, modified Bessel functions are assumed with $\square^2 v = m^2 v$. The operator \square^2 is the nondimensional version of \square^2 . For the

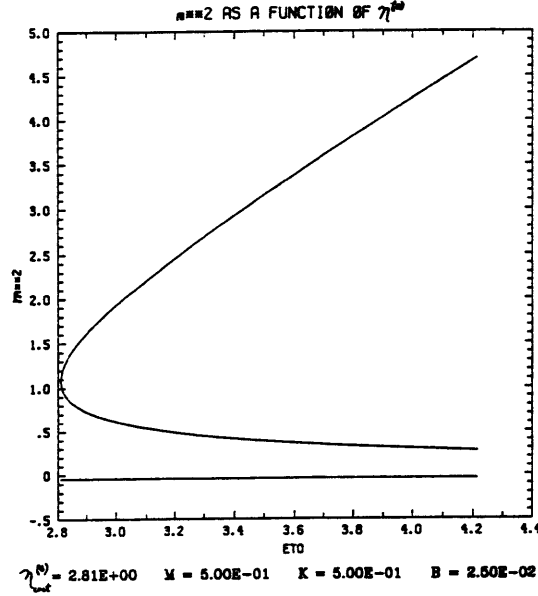


Figure 6.4: The squares of the nondimensional wavenumbers as a function of the forcing parameter, $\eta^{(0)}$. Values are plotted such that Bessel function solutions are associated with positive m^2 while modified Bessel functions are associated with negative m^2 .

outer region, the nondimensional equation for the m^2 is

$$Km^6 - [1 + M(1 + K)]m^4 + [M + B(1 + K)]m^2 - B = 0. \quad (6.23)$$

There do exist values of the parameters for which not all of the roots are real. If there are any complex roots, then there are four of them in complex conjugate pairs. From these one can find linear combinations that are real and satisfy the boundary conditions. The basis functions of complex argument exhibit oscillatory behavior, but if r_1 is finite and not too large one might be able to find solutions to the homogeneous problem without oscillations. We will strenuously avoid the complication of parameter ranges with complex m^2 by keeping B sufficiently small. From the signs of the coefficients in eq. (6.23), it is clear that any real values of m^2 must be positive. The roots with positive real part of this equation will be designated m_4 , m_5 , and m_6 . In the exterior region, the general solution is a sum over the basis functions $I_1(m_4r)$, $I_1(m_5r)$, $I_1(m_6r)$, $K_1(m_4r)$, $K_1(m_5r)$, $K_1(m_6r)$. If the domain were to extend to infinity then all of the first three functions of

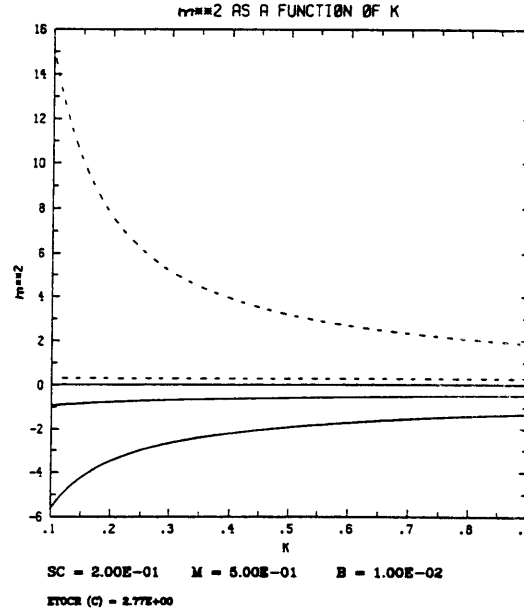


Figure 6.5: The squares of the nondimensional wavenumbers as a function of the lateral diffusion ratio, K . The solid lines show the values of m^2 for the ascent region with the value of $\eta^{(0)}$ set to $\eta_{crit}^{(0)} + 0.2$ for each value of K ; the supercriticality of $\eta^{(0)}$ designated in the label as “SC”. The critical value of $\eta^{(0)}$ for $K = 0.5$ is provided at the bottom labeled “ET0CR (C)”. Dashed lines are used for the descent region where $\eta^{(0)} = 0$. Unlike the previous figure, positive values of m^2 are associated with modified Bessel functions and negative values of m^2 are associated with Bessel functions. Note that there are two nearly indistinguishable lines — one solid, one dashed — just above zero.

this list must have vanishing coefficients. For a finite domain all of these basis functions must be kept.

6.2.3 Transformation to Self-Adjoint System

Since we will later be determining solvability conditions on inhomogeneous versions of the linear system, it is necessary to construct the adjoint system. It would be preferable, however, to transform the linear system into one that is self-adjoint. This avoids the need to solve a second linear problem (though the eigenvalues are identical). Further, the solvability conditions can be interpreted as energy equations when the solution to the adjoint homogenous problem is the same as that of the original linear problem. These issues are discussed at greater length in section 7.1.1.

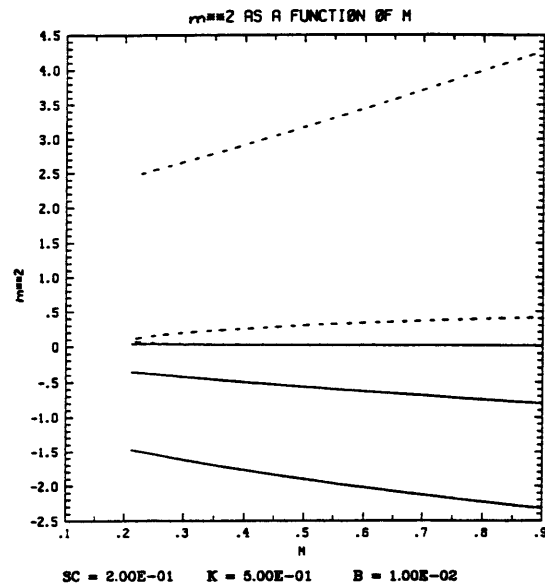


Figure 6.6: The squares of the nondimensional wavenumbers as a function of the vertical diffusion ratio, M , plotted similarly to figure 6.5. No values are plotted for parameter ranges that result in complex values of m^2 in the descent region.

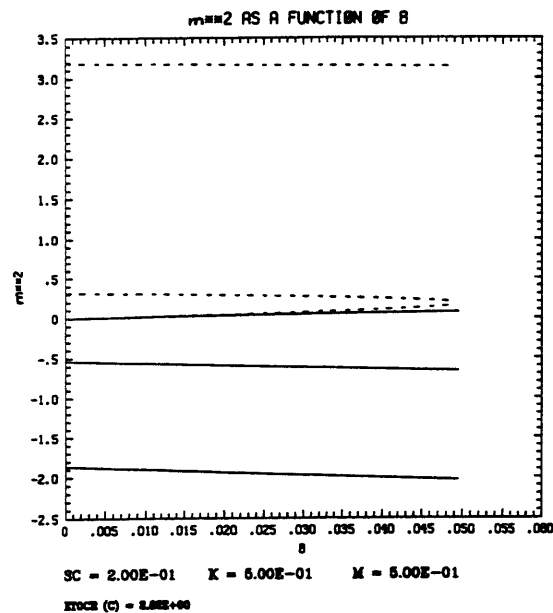


Figure 6.7: The squares of the nondimensional wavenumbers as a function of the cooling parameter, B , plotted similarly to figure 6.6.

The vector equation (6.8) can be transformed to the self-adjoint form

$$r \frac{d}{dr} \left(B \frac{dr \bar{\mathbf{v}}^{(1)}}{r dr} \right) + A r \bar{\mathbf{v}}^{(1)} = 0 \quad (6.24)$$

where

$$B = k_2^{(0)} \begin{pmatrix} KM - M - BK^2 + 1 - \eta^{(0)} & M - BK & 1 \\ M - BK & -B & 0 \\ 1 & 0 & 0 \end{pmatrix}$$

$$A = k_s \begin{pmatrix} \frac{M^2}{K} - M + BK - B & -\frac{M^2}{K} + B & -\frac{M}{K} \\ -\frac{M^2}{K} + B & \frac{M^2}{K} & \frac{M}{K} \\ -\frac{M}{K} & \frac{M}{K} & \frac{1}{K} \end{pmatrix}.$$

The transformation matrix that accomplishes this feat is

$$T = \begin{pmatrix} M - \frac{M}{K} - BK & M - BK & 1 \\ \frac{M}{K} - B & -B & 0 \\ \frac{1}{K} & 0 & 0 \end{pmatrix}. \quad (6.25)$$

Note the multiplication by r in eq. (6.24) and also that T is a constant matrix even across r_0 . This form is unique up to multiplication throughout by a constant.

The determination of this transformation was not trivial. Note that the only discontinuity in B is in the first entry of the first column. If discontinuous terms multiplied any element of $\frac{dr \mathbf{v}^{(1)}}{r dr}$ other than $\frac{dr v_j^{(1)}}{r dr}$, one would not be able to transform without creating additional terms that were not self-adjoint. This is because only for $j = 1$ does $\frac{d}{dr} \left(\eta^{(0)} \frac{dr v_j^{(0)}}{r dr} \right) = \eta^{(0)} \square^2 v_j^{(0)}$. Since a real matrix B must be symmetric for the differential equation to be self-adjoint, discontinuous terms are further restricted to the first entry of the first column. There was no restriction on the presence of discontinuous terms in matrix A , though none appears. Oddly, if the system was made eighth order by using a derivative of the second continuity

equation (5.4), rather than an integral of the sum of the continuity equations, it is then impossible to transform the system into one that is self-adjoint, subject to the constraint on discontinuous terms in B (this can be proven and in the course of this work proved enormously distressing).

The solutions to eq. (6.24) are identical to the solutions to eq. (6.8). The transformation is only important when we deal with the inhomogeneous problems at second order. Then the same transformation that was used to generate the self-adjoint linear system must be applied to the inhomogeneous terms.

6.2.4 Calculation of the Linear Solution

[The mathematically unadventurous may skip to section 6.2.5, p. 160.]

For each of the regions there is a set of six linearly independent solutions, each with an accompanying coefficient. Hence, there are fifteen coefficients to be determined leaving only an undetermined overall amplitude. Also to be determined is the radius, r_0 , where w crosses 0. An additional parameter constrained to eigenvalues, as required in most homogeneous two point boundary value problems, must also be found. The general solutions of eq. (6.8) are all of the types given in eqs. (6.15) (see footnote on p. 143). They are all either Bessel functions or modified Bessel functions, depending on the sign of m^2 . The linear problem will be solved using nondimensional variables, with $r = r\sqrt{k_s/k_2^{(0)}}$.

Of the twelve functions that make up the general solutions of the two regions, three have already been eliminated as incompatible with the boundary conditions at the origin. Let the remaining nine make up the vector of elements X_l given as $(J_1(m_1r), J_1(m_2r), I_1(m_3r/i), I_1(m_4r), I_1(m_5r), I_1(m_6r), K_1(m_7r), K_1(m_8r), K_1(m_9r))$, where for convenience during summations $m_7 = m_4$, $m_8 = m_5$, and $m_9 = m_6$. The general solutions for $\bar{v}_1^{(1)}$ can then be expressed as

$$\bar{v}_1^{+(1)}(r) = \bar{a} \sum_{l=1}^3 \alpha_l X_l(r) \quad (6.26)$$

$$\bar{v}_1^{-(1)}(r) = \bar{a} \sum_{l=4}^9 \alpha_l X_l(r) , \quad (6.27)$$

where the superscript + indicates that the solution applies in the interior or up-draft region, and the superscript - indicates that the solution applies in the outer or descent region. The coefficients α_l need to be determined by application of the boundary and matching conditions, yielding the particular solution to the problem.

By applying the linear system of eq. (6.8), $v_2^{(1)}$ and $v_3^{(1)}$ can be found as functions of $v_1^{(1)}$. The relations apply for each of the X_l separately, as well as any linear combinations of them. The vector $\mathbf{v}^{(1)}$ can be expressed as

$$\bar{v}_j^{+(1)}(\mathbf{r}) = \bar{a} \sum_{l=1}^3 s_{jl} \alpha_l X_l(\mathbf{r}), \quad j = 1, 2, 3 \quad (6.28)$$

$$\bar{v}_j^{-(1)}(\mathbf{r}) = \bar{a} \sum_{l=4}^9 s_{jl} \alpha_l X_l(\mathbf{r}), \quad j = 1, 2, 3 \quad (6.29)$$

(n.b. the index limits above and below). The complications are hidden in the s_{jl} defined as

$$\begin{aligned} s_{1l} &= 1, \quad l = 1, 2, \dots, 9 \\ s_{2l} &= \begin{cases} -\left(\frac{1 + K m_l^2}{m_l^2}\right), & l = 1, 2, 3 \\ \left(\frac{1 - K m_l^2}{m_l^2}\right), & l = 4, 5, \dots, 9 \end{cases} \\ s_{3l} &= \begin{cases} \left[\frac{K m_l^4 + M(1 + K) m_l^2 + M}{m_l^2}\right], & l = 1, 2, 3 \\ -\left[\frac{K m_l^4 - M(1 + K) m_l^2 + M}{m_l^2}\right], & l = 4, 5, \dots, 9 \end{cases} \end{aligned}$$

The formulae for the coefficients of the Bessel basis functions in the two regions are interchangeable by changing the sign of m^2 . This corresponds to choosing the sign in $\square^2 v = \pm m^2 v$. Note that $m_3^2 < 0$.

The matching and boundary conditions can now be expressed as a homogeneous linear system:

$$\sum_{l=1}^3 \alpha_l s_{jl} X_l(r_0) - \sum_{l=4}^9 \alpha_l s_{jl} X_l(r_0) = 0, \quad j = 1, 2, 3 \quad (6.30)$$

$$\sum_{l=1}^3 \alpha_l s_{jl} W_l(r_0) - \sum_{l=4}^9 \alpha_l s_{jl} W_l(r_0) = 0, \quad j = 1, 2, 3 \quad (6.31)$$

$$\sum_{l=4}^9 \alpha_l s_{jl} X_l(r_1) = 0, \quad j = 1, 2, 3 \quad (6.32)$$

where $W_l \equiv \frac{drX_l}{rdr}$ defines the derivative vector $(m_1 J_0(m_1 r), m_2 J_0(m_2 r), m_3 I_0(m_3 r/i)/i, m_4 I_0(m_4 r), m_5 I_0(m_5 r), m_6 I_0(m_6 r), -m_7 K_0(m_7 r), -m_8 K_0(m_8 r), -m_9 K_0(m_9 r))$ and m_3/i is a positive real number. This can also be directly written in matrix form as

$$S\alpha = 0, \quad (6.33)$$

where α is the vector of the α_l and the 9×9 matrix S will not comfortably fit on a single page. The three equations from eq. (6.30), making up the first three rows of S , are the equations for continuity of v_1 , v_2 , and v_3 ; respectively; at r_0 . The next three state the continuity of the $\frac{drv_j}{rdr}$ at r_0 . The last three are the boundary conditions for the v_j to vanish at r_1 . The system only has a solution if the determinant of the matrix S vanishes. Since all nine equations are linearly independent, this requirement defines an eigenvalue problem as is standard in two point boundary value problems.

As an additional condition it is necessary that eq. (6.11) hold, i.e. $\frac{drv_1^{(1)}}{rdr} \Big|_{r=r_0} = 0$, so

$$\sum_{l=1}^3 \alpha_l W_l(r_0) = 0. \quad (6.34)$$

Since $\frac{drv_1^{(1)}}{rdr}$ is continuous, it is also the case that $\sum_{l=4}^9 \alpha_l W_l(r_0) = 0$, but this condition is redundant. We now have a double eigenvalue problem. Only the smallest value of r_0 for which eq. (6.34) holds will be used, otherwise a downdraft would have been allowed with the physics that applies only to updraft regions.

In the time dependent tropical cyclone related problems of say Haque (1952) and Charney and Eliassen (1964b), there was no additional constraint correspond-

ing to eq. (6.34) and a problem with only a single eigenvalue was generated, corresponding to the requirement that the matching condition matrix be singular. This allowed a continuous relation between the growth rate and the horizontal length scale of the updraft, with the downdraft extending out to infinity. The works of Bretherton (1987) and Emanuel et alii (1987) are more closely related mathematically to the problem presented here, i.e. they have different physics in two different regions *and* an additional condition leading to a double eigenvalue problem, though they are not on tropical cyclones. In these works the two parameters that were varied as eigenvalues were the divider between the regions of different physics, i.e. r_0 in our notation, and the growth rate. Instead of a continuous relationship, the solution set is a countable (though infinite) set of points in the parameter space of length scale and growth rate, with interest primarily in the point with smallest r_0 , i.e. the solution with only a single updraft region.

What separates the problems with two eigenconditions from those with only one is the requirement that w actually vanish at r_0 , rather than just change sign with a jump discontinuity. This requirement is imposed because the problem is viscous, as is the case here, or for other reasons, such as in Emanuel et alii 1987. In the inviscid problem there can be a jump discontinuity in the vertical velocity. If a jump is allowed, there is no condition that really “defines” r_0 ; it can vary over a range. For our viscous stationary problem, the eigenvalue determination fully sets the disturbance size, unlike in the linear time dependent problems where the additional eigencondition provides a relation between the growth rate and the horizontal size. The problem is singular with respect to viscosity and internal boundary layers would develop in the limit of the viscosity vanishing. Since there is more than one viscosity coefficient, different types of behavior can result depending on how these limits are taken.

Here, only stationary solutions are being considered, which fixes the growth rate at zero. Therefore an additional parameter is still needed to be determined as an eigenvalue of the system. I first attempted to use the outer limit of the disturbance, r_1 , as an eigenvalue; this failed for reasons that will be discussed below. The problem was solved by varying $\eta^{(0)}$ with a fixed outer boundary.

Another possibility would be to vary the ratio of the inflow to outflow layer depths, which changes the value of K . The determination of the eigenvalues r_0 and $\eta^{(0)}$ that make S singular, subject to the constraint of eq. (6.34), is exceedingly nonlinear. The pencil-based technology that we have mostly employed so far is swamped and refuge is taken in electronic computers.

Bretherton solved the double eigenvalue problem by first doing a coarse search in the space of length and growth rate by evaluating the determinant of the matrix and then evaluating the remaining condition by fixing one of the values of the solution vector (corresponding to α in our notation) and using all of the rows of the matrix but the last. Emanuel et alii created two square matrices with partially redundant rows. Since their system was of lower order, yielding only 2×2 matrices, this was a reasonable choice. The matrices were treated on equal footing and the eigenvalues were sought numerically as the points where both determinants vanished.

In an iterative numerical scheme, it is not possible to treat the making of the matrix S singular and the additional constraint that w vanish at r_0 on an equal footing, unless one creates two square matrices as was done by Emanuel et alii. Further, it is necessary to find the smallest positive r_0 that satisfies the system or w would have changed sign within the interior, in violation of our assumptions. It is therefore easier to make sure that the constraint that the first vanishing of w is at r_0 , is in the innermost loop of any iterative calculation. In practice, the system was not solved as posed by eqs. (6.33) and (6.34). The requirement that w vanish at r_0 was incorporated into the matrix, while the equation for continuity of $\frac{dr_0}{dr}$ was made the additional constraint (changing row 6 of S). This new matrix will be designated S' .

The procedure used had both an inner and an outer iteration. The inner iteration varied r_0 , while the outer one varied $\eta^{(0)}$. For the inner scheme a nonlinear root finding routine from the IMSL⁵ package was used with r_0 taken as the

⁵IMSL is a commercially available package of mathematical subroutines obtainable

independent variable. The nonlinear function used was the determinant of the matrix S' . If a poor initial guess was made for r_0 , the algorithm could converge to a solution with oscillations. This unwanted solution then provided a clue to a better starting value for the iterative scheme with its first zero crossing of $\frac{drv_1^{(1)}}{r dr}$. When the determinant of S' was approximately zero, then there was also an eigenvalue of the matrix approximately equal to zero. The eigenvector of S' associated with the zero eigenvalue provides the relative coefficients of the basis functions for the solution that satisfies all but one of the boundary and matching conditions. The solution for α was then used to evaluate the remaining condition for the continuity of $\frac{\partial rv_3^{(1)}}{r \partial r}$. The forcing parameter $\eta^{(0)}$ was then varied iteratively until the additional condition was satisfied, with the inner scheme again performed at every outer iteration. This outer iteration was performed manually. Automated procedures failed because the inner iterations would often converge to oscillatory solutions and round-off errors for the inner procedure would cause instabilities of the chosen outer procedures. Human intervention was tedious, but effective.

6.2.5 Linear Solutions

An example of a solution to the linear stationary problem is shown in figure 6.8. Note that in the end, only the values of B , K , M , and r_1 are relevant to the linear calculation. The parameter values that go into these ratios are discussed in the next chapter. The solutions have been normalized so that the maximum of $v_1^{(1)}$ is one. Velocities in the lower and upper levels are directly comparable. The vertical velocity can be obtained from the curve for $\frac{drv_1^{(1)}}{r dr}$ after scaling by $\frac{k_s}{fL} = \frac{k_s^{3/2}}{fk_2^{(0)1/2}} \sim 3 \cdot 10^{-4}$ for comparison. The lower level horizontal velocity, indirectly given by v_3 , must be scaled by $-(\epsilon_j h_j f / k_s)^{-1} \sim -10^{-2}$ for comparison.

from IMSL, Inc., Houston, TX. Several routines from this package were used, including polynomial root finders for evaluating m^2 , matrix handling routines for determining eigenvalues and eigenvectors, and approximation routines for all of the Bessel and modified Bessel functions.

All of the parameters will be kept fairly small. Large values of M , K , and B , would lead to excessively large requirements for $\eta^{(0)}$. We will later make use of solutions with $\eta^{(0)}$ of order 2. In this section solutions will be shown with $\eta^{(0)}$ even greater than 4, but these are included just to illustrate the dependence of the linear solutions on the various parameters. Even an $\eta^{(0)}$ of order 2 seems to imply a much greater amount of CAPE than even the believers would claim exists. However, when the linear solutions are used in the nonlinear calculations of chapter 7, it will be seen that solutions with an $\eta^{(0)}$ of say 2.5 are relevant to finite amplitude disturbances in an environment with an ambient η_a of say 1.2, which does not require a large amount of positive buoyancy for lifted parcels.

The assumption that M is small is equivalent to assuming that the strong surface friction exceeds internal vertical momentum mixing. In the presence of strong convection this is less likely to be the case and such processes show up explicitly at second order. For K to be small, $\epsilon h_2^{(0)} \lambda_2$ must be greater than $h_1^{(0)} \lambda_1$. Since the upper layer is less dense than the lower (i.e. $\epsilon < 1$), and the inflow layer is usually more shallow than the outflow layer (i.e. $h_2^{(0)} < h_1^{(0)}$), this is only possible if λ_2 is significantly greater than λ_1 . We will assume that this is the case. Justification is provided by the much greater asymmetry of the outflow layer. Our axisymmetric model can compensate for the lack of asymmetries through a greater eddy viscosity. Observational and modelling (e.g. Challa and Pfeffer 1990 and the references cited therein) works have also shown that momentum mixing is stronger and more important aloft. Small scale inertial instability probably contributes to this mixing. Radiative cooling is a very weak process compared to the others in this system, though still necessary to close the circulation of steady solutions. In the downdraft region, if B is made too large, oscillatory solutions would develop. We arbitrarily restrict B to prevent this, but choose it to be nearly as large as this limit.

Several basic things should be noted about the linear stationary solution. The lower layer has cyclonic circulation throughout the domain, $v_1^{(1)} \geq 0$. In the upper layer the flow is everywhere anticyclonic, $v_2^{(1)} \leq 0$. It is appropriate for a solution applying to a young disturbance to not be cyclonic at small radius since

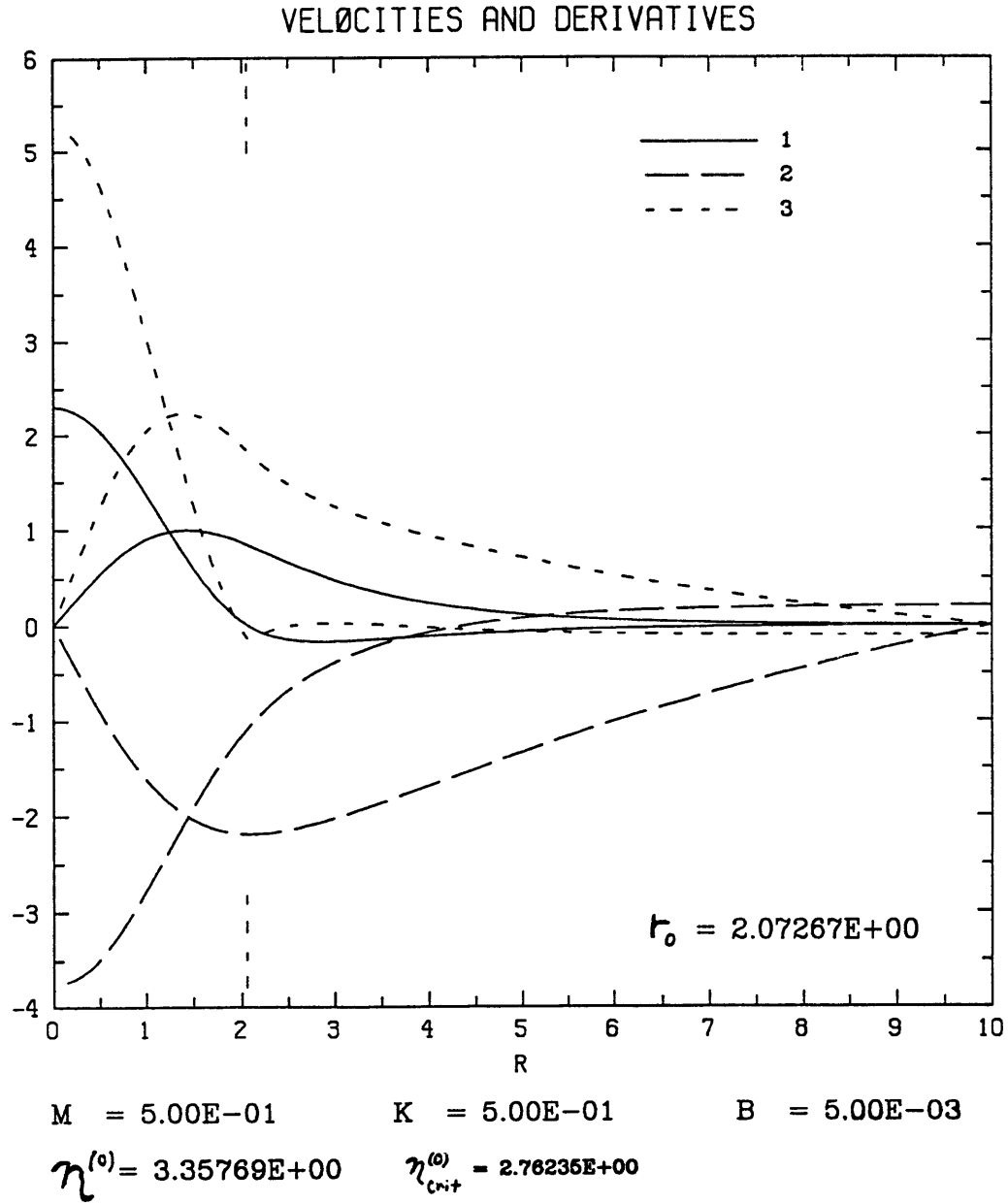


Figure 6.8: A solution to the linear stationary problem with $M = 0.5$, $K = 0.5$, $B = 0.005$, $r_1 = 10.0$. The velocities $v_1^{(1)}$ and $v_2^{(1)}$ are the upper and lower layer tangential velocities, respectively, and $v_3^{(1)}$ is proportional to the lower layer inflow velocity. The $v_j^{(1)}$ are all equal to zero at the origin and can be distinguished according to the key in the upper right corner. The lines for $\frac{drv_j^{(1)}}{rdr}$ all have nonzero values at the origin and follow the same pattern as the corresponding v_j . The Ekman pumping is proportional to $\frac{drv_j^{(1)}}{rdr}$. There are dashed lines near the upper and lower borders noting the location of r_0 .

the air flowing outward did not begin with large amounts of angular momentum (see discussion on p. 96). This is also consistent with the observations of Black and Anthes (1974) that weak cyclones and ones still in early development do not have a cyclonic regime in the outflow. There is inflow throughout the entire lower layer, $v_3^{(1)} \geq 0$. The maximum strength of the anticyclone aloft is at a greater radius (about double) than that of the maximum wind of the low level cyclone.

The vertical velocity is greatest in the center, at the origin. (Linear and nonlinear drag laws lead to very different spatial distributions for the Ekman pumping, and it is a linear drag law which controls the lowest order solutions here. For quadratic drag w vanishes at the origin.) The radius of maximum cyclonic winds is smaller than the radius where w crosses zero. It is also of order one nondimensionally and hence of order $L \sim 100$ km dimensionally.

Figures 6.9 along with figure 6.8 show that there is little variation in the form of the solutions as r_1 varies, nor is there much variation in the eigenvalue for $\eta^{(0)}$, except as r_1 approaches r_0 . Additional examples are provided in table 6.1 items (7)–(9) and (14)–(18). As r_1 increases evaluation of the growing Bessel and modified Bessel functions becomes less accurate. The very weak nonmonotonic variations of $\eta^{(0)}$ and r_0 with increasing r_1 should be viewed with caution. The lack of sensitivity of $\eta^{(0)}$ to variation of r_1 is why it is not possible to vary r_1 in search of eigenvalues. Given a parameter set $\{M, K, B\}$, there is only a very small range of $\eta^{(0)}$ for which solutions exist. The eigenvalue for $\eta^{(0)}$ increases as r_1 decreases. At its minimum, $\eta^{(0)}$ is still significantly greater than $\eta_{crit}^{(0)}$. *This indicates that the actual critical value of $\eta^{(0)}$ for solutions consistent with the boundary conditions is greater than that which simply ensures positive real values of m^2 .* Rigorous confirmation of this requires solution of the linear, viscous, time dependent problem, which has not been done.

As can be seen by comparing figure 6.10 with figure 6.8, decreases in M lead to increases in the anticyclone relative to the cyclone. This is consistent with the simple view that the greater the amount of vertical diffusion the lesser the amount of the vertical shear. Additional comparisons can be made from table 6.1 using item sets $\{(1), (4), (20)\}$; $\{(2), (5), (8)\}$; and $\{(6), (15), (21)\}$,

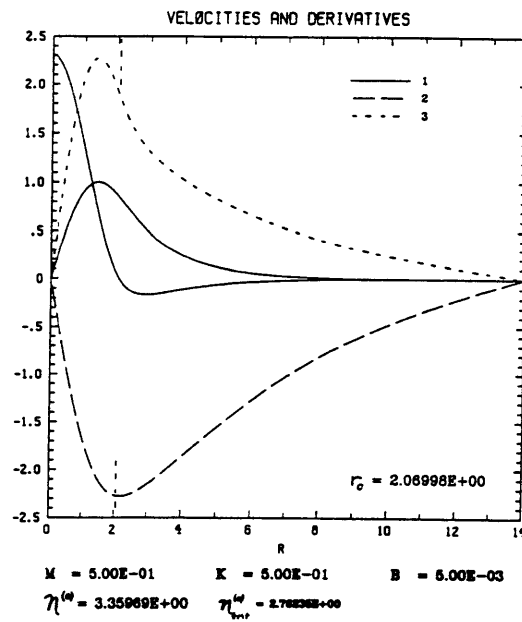
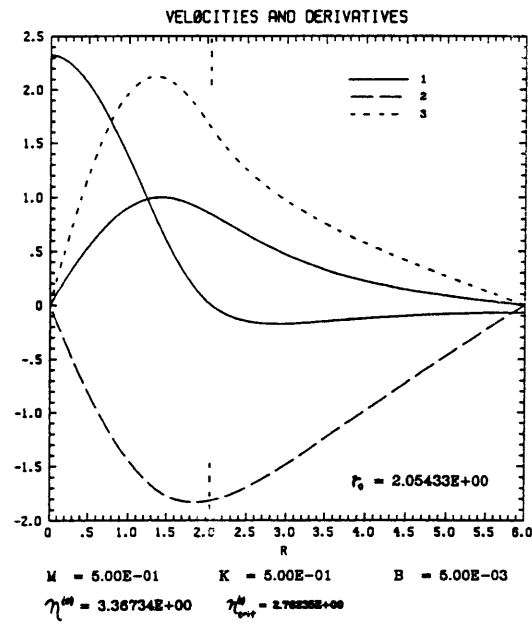


Figure 6.9: Solutions to the linear problem with the same parameter values as in figure 6.8, but varying the outer radius, $r_1 = 6.0, 14.0$.

Properties of Linear Stationary Solutions								
	Parameters				Eigenvalues		Ratio of Maxima	
	M	K	B	r_1	$\eta^{(0)}$	r_0	R_2	R_3
1)	0.1	0.1	0.002	10.0	1.474	1.969	2.0	0.4
2)	0.1	0.2	0.002	8.0	1.627	2.328	2.2	0.5
3)	0.1	1.0	0.002	10.0	2.284	3.520	4.9	1.1
4)	0.2	0.1	0.005	8.0	1.720	1.675	1.4	0.7
5)	0.2	0.2	0.005	10.0	1.932	2.002	1.9	0.8
6)	0.2	0.5	0.005	10.0	2.370	2.526	2.9	1.3
7)	0.5	0.2	0.005	6.0	2.644	1.633	1.2	1.5
8)	0.5	0.2	0.005	10.0	2.641	1.638	1.4	1.6
9)	0.5	0.2	0.005	12.0	2.642	1.637	1.4	1.6
10)	0.5	0.2	0.020	6.0	2.680	1.599	1.2	1.5
11)	0.5	0.2	0.050	6.0	2.745	1.542	1.1	1.5
12)	0.5	0.2	0.050	8.0	2.753	1.533	1.2	1.6
13)	0.5	0.2	0.050	10.0	2.756	1.529	1.2	1.6
14)	0.5	0.5	0.005	6.0	3.367	2.054	1.9	2.1
15)	0.5	0.5	0.005	8.0	3.357	2.074	2.1	2.2
16)	0.5	0.5	0.005	10.0	3.358	2.073	2.3	2.3
17)	0.5	0.5	0.005	12.0	3.359	2.071	2.3	2.3
18)	0.5	0.5	0.005	14.0	3.360	2.070	2.3	2.3
19)	0.5	1.0	0.005	8.0	4.252	2.468	3.0	3.0
20)	1.0	0.1	0.005	6.0	3.156	1.157	0.8	2.1
21)	1.0	0.5	0.005	8.0	4.749	1.757	1.7	3.6

Table 6.1: Properties of stationary solutions. Eigenvalues of $\eta^{(0)}$ and r_0 for various sets of parameter values. Also included are the ratios $R_j \equiv |\max(v_j) / \max(v_1)|$.

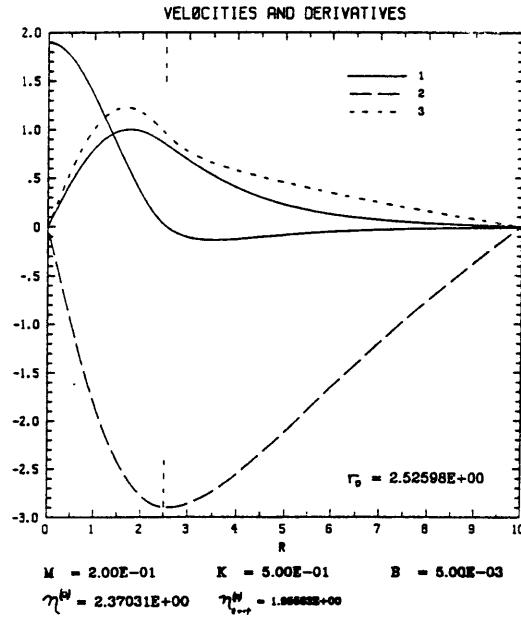


Figure 6.10: Solution to the linear problem with $M = 0.2$, $K = 0.5$, $B = 0.005$, $r_1 = 10.0$.

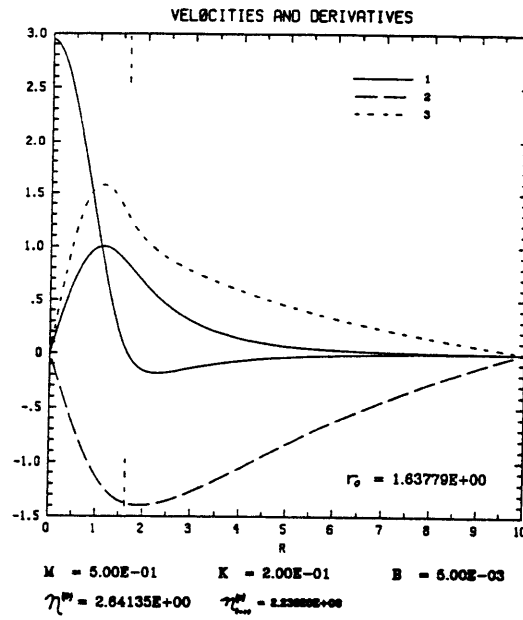


Figure 6.11: Solution to the linear problem with $M = 0.5$, $K = 0.2$, $B = 0.005$, $r_1 = 10.0$.

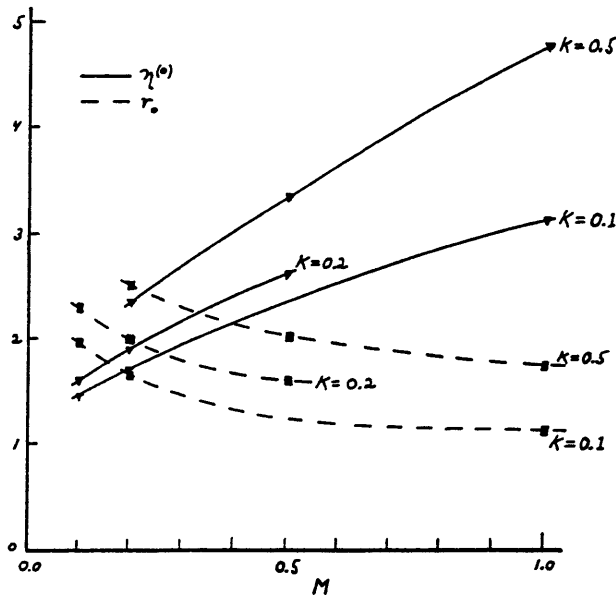


Figure 6.12: Variations in the neutral forcing parameter, $\eta^{(0)}$, and the updraft extent, r_0 , for linear stationary solutions as a function of vertical diffusion ratio, M . Curves are presented for various values of the lateral diffusion ratio, K .

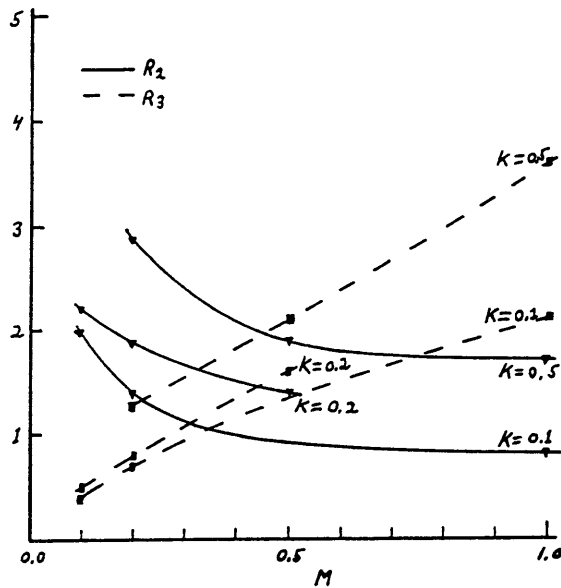


Figure 6.13: Variations in relative anticyclone strength, R_2 , and relative inflow strength, R_3 , for linear stationary solutions as a function of vertical diffusion ratio, M . Curves are presented for various values of the lateral diffusion ratio, K .

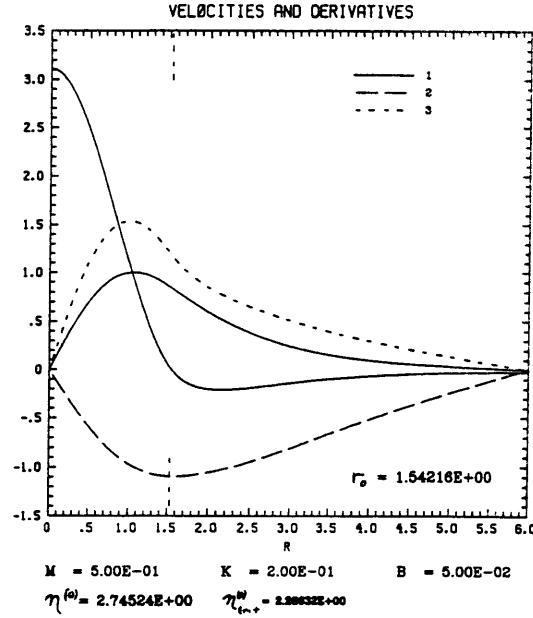


Figure 6.14: Solution to the linear problem with $M = 0.5$, $K = 0.2$, $B = 0.050$, $r_1 = 6.0$.

which are presented as curves in figures 6.12 and 6.13. Increases in M lead to increases in the required forcing parameter $\eta^{(0)}$, decreases in the relative anticyclone strength ($R_2 \equiv |\max(v_2)/\max(v_1)|$), increases in the lower layer inflow ($R_3 \equiv |\max(v_3)/\max(v_1)|$), and decrease in the relative size of the updraft region r_0 .

Variations in K may be examined with figures 6.8 and 6.11 or with items sets from table 6.1 of $\{(1), (2), (3)\}$; $\{(4), (5), (6)\}$; $\{(8), (15), (19)\}$; and $\{(20), (21)\}$. These comparisons can also be seen comparing across curves at constant M in figures 6.12 and 6.13. Increases in K , which correspond to increases in the eddy viscosity of the lower layer, lead to increases in all of the required forcing, the upper level anticyclone (or weakens the lower cyclone), lower level inflow (to compensate the diffusion), and relative size of the updraft region. Since K is also proportional to the ratio of the layer depths, increasing K is a proxy for increasing the depth of the cyclone layer or decreasing the depth of the anticyclone layer. Hence it is detrimental to cyclone development to have a thin outflow layer.

The effect of variation in radiative cooling can be seen by comparing figures 6.11 and 6.14 (the difference in the outer radii is not particularly significant) or the set of items $\{(7), (10), (11)\}$ in table 6.1. The primary effects of increases in the radiative cooling are to require increased forcing and to decrease the strength of the anticyclone. As also can be seen from figure 6.14, if vertical diffusion is fairly strong and lateral diffusion in the lower layer fairly weak, the cyclone and anticyclone of the weak stationary solutions are approximately equal.

The procedure of integrating one of the equations of a system separately, as was done to obtain eq. (6.7) is unusual. As a check, the linear system was also solved using the derivative of the upper layer continuity equation instead of the integrated sum of the three continuity equations. This leads to an eighth order differential system in each region. The additional linearly independent solutions are r and $1/r$, rather than Bessel functions. For this problem, v_4 remains in the system. The additional boundary conditions are that v_4 vanish at 0 and r_1 . The additional matching conditions are that v_4 and $\frac{drv_4}{rdr}$ be continuous at r_0 . Identical results were obtained for this system. As the outer iteration converged to its eigenvalues, the coefficients of the basis functions r and $1/r$ became very small. This confirmed the correctness of the procedure used. Failure of this would have been quite unfortunate. Though there are no additional difficulties in solving the higher order system, it is impossible to transform the higher order system into one that is self-adjoint.

6.3 Time Dependent Linear Problem

[This section may be skipped without loss of continuity.]

For completeness and to show the significance of $\eta_{crit}^{(0)}$ in the time dependent problem, we now derive the dispersion relation for the linear, viscous, time dependent problem.

The linear time dependent equations for conservation of angular momentum,

in dimensional form, are

$$\begin{aligned} h_1^{(0)} \gamma^{(0)} \tilde{v}_1^{(1)} r &= k_s \tilde{v}_3^{(1)} r + \mu(\tilde{v}_2^{(1)} - \tilde{v}_1^{(1)}) r + k_1^{(0)} r \square^2 \tilde{v}_1^{(1)} \\ \epsilon h_2^{(0)} \gamma^{(0)} \tilde{v}_2^{(1)} r &= k_s \tilde{v}_4^{(1)} r + \mu(\tilde{v}_1^{(1)} - \tilde{v}_2^{(1)}) r + k_2^{(0)} r \square^2 \tilde{v}_2^{(1)} . \end{aligned}$$

These are obtained from eqs. (5.18) and (5.19). The linear time dependent continuity equations; after taking one radial derivative of eqs. (5.3) and (5.4), using the continuity of $\eta \frac{\partial r v_1^{(1)}}{r \partial r}$, and inserting the parameterizations for heating and cooling; are

$$\begin{aligned} \frac{\gamma^{(0)} f}{g(1-\epsilon)} (\tilde{v}_1^{(1)} - \epsilon \tilde{v}_2^{(1)}) &= \\ \frac{k_s}{f} \square^2 \tilde{v}_3^{(1)} - (\eta^{(0)} - 1) \left(\frac{k_s}{f} + \frac{\gamma^{(0)} h_0}{f} \right) \square^2 \tilde{v}_1^{(1)} + b f (\tilde{v}_2^{(1)} - \tilde{v}_1^{(1)}) \\ \frac{\gamma^{(0)} f \epsilon}{g(1-\epsilon)} (\tilde{v}_2^{(1)} - \tilde{v}_2^{(1)}) &= \\ \frac{k_s}{f} \square^2 \tilde{v}_4^{(1)} + \eta^{(0)} \left(\frac{k_s}{f} + \frac{\gamma^{(0)} h_0}{f} \right) \square^2 \tilde{v}_1^{(1)} - b f (\tilde{v}_2^{(1)} - \tilde{v}_1^{(1)}) . \end{aligned}$$

For the time dependent case it is not possible to use the trick of integrating the sum of the continuity equations, so the system cannot be reduced below eighth order. The two additional solutions are now in the Bessel function family rather than being algebraic functions. With the assumption that $\square^2 v = -m^2 v$ (appropriate to the ascent region), these lead to the nondimensional dispersion relation

$$\begin{aligned} \Upsilon^2 \left\{ H_2 [H_1 - (\eta^{(0)} - 1)H_0] m^4 + \frac{\epsilon(H_0 + H_1) + H_2}{G} m^2 + \frac{\epsilon(1-\epsilon)}{G^2} \right\} \\ + \Upsilon \left\{ [H_1 - (\eta^{(0)} - 1)H_0 + K H_2] m^6 \right. \\ \quad + \left[\frac{(1+\epsilon K)}{G} + M(H_0 + H_1 + H_2) - (\eta^{(0)} - 1)H_2 \right] m^4 \\ \quad + \left[\frac{\epsilon}{G} + \frac{M(1-\epsilon)}{G} + B(H_0 + H_1 + H_2) \right] m^2 + \frac{B}{G} \left. \right\} \\ + \left\{ K m^8 - [\eta^{(0)} - 1 - M(1+K)] m^6 \right. \\ \quad \left. + [M + B(1+K)] m^4 + B m^2 \right\} = 0 , \end{aligned}$$

where $\Upsilon \equiv \gamma^{(0)}/f$ is the nondimensional growth rate (we lack a non-italic version of γ). The additional nondimensional parameters are

$$\begin{aligned} H_0 &\equiv \frac{fh_0}{k_s} \sim 10 \\ H_1 &\equiv \frac{fh_1}{k_s} \sim 50 \\ H_2 &\equiv \frac{f\epsilon h_2}{k_s} \sim 20 \\ G &\equiv \frac{g(1-\epsilon)k_s^2}{f^3k_2^{(0)}} \sim 50 . \end{aligned}$$

This can be solved for Υ as a function of m^2 , or *vice versa*.

Since H_0 is small compared to H_1 and H_2 , the coefficient of Υ^2 is positive. The signs of the coefficient of Υ and the constant term are both dependent on the magnitude of $\eta^{(0)}$. For simple connection to the linear stationary problem, we will assume that the coefficient of Υ is positive. Positive growth rate with real m^2 requires that the constant term be negative. This is only possible if $\eta^{(0)} > \eta_{crit}^{(0)}$, where $\eta_{crit}^{(0)}$ is the same as determined by eq. (6.20). Figure 6.15 shows Υ as a function of m^2 for several values of $\eta^{(0)}$. The lowest line is for $\eta_{crit}^{(0)}$, which is tangent to 0 from below as expected. As noted by Ooyama (1969) when presenting a similar figure, a short length scale cutoff (on the right side in wavenumber space) does appear if friction is included. There is a sharper long wave cutoff that would exist even in the inviscid case.

Though we have plotted growth rate as a function of m^2 , for every value of the growth rate there are four values of m^2 . To construct the linear growing solutions all of these are needed. The resulting disturbance length scale is a function of all of the m^2 and generates an eigenvalue problem for r_0 and $\eta^{(0)}$ as a function of Υ . Solution of the eigenvalue problem with an energy draining descent region will probably require that $\eta^{(0)}$ be greater than $\eta_{crit}^{(0)}$. Since the limit of $\gamma^{(0)} \rightarrow 0$ is not spatially singular, I expect that the critical value for $\eta^{(0)}$, *consistent with the boundary conditions and the need for a descent region*, is the value of $\eta^{(0)}$ found as an eigenvalue of the stationary problem, despite the existence of growing solutions to the linear equation alone with smaller forcing parameter.

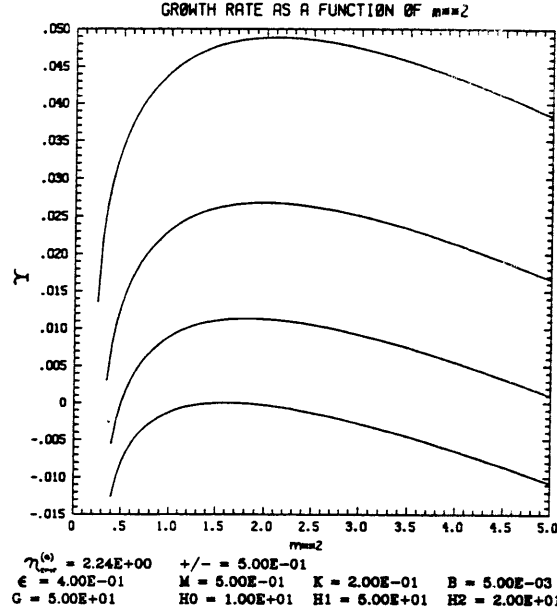


Figure 6.15: Growth rate as a function of the square of the nondimensional cylindrical wavenumber. The lowest line is for $\eta^{(0)} = \eta_{crit}^{(0)}$; the lines above are at increments of 0.5 in $\eta^{(0)}$. The values of the other nondimensional parameters are as given.

6.4 Only a Little Friction

[This section may be skipped without loss of continuity.]

We will examine briefly whether it is possible, and if so advantageous, to eliminate any of the frictional terms. The example of Ooyama's linear solution in section 6.1 showed that the elimination of all of the frictional terms prevents non-trivial stationary solutions. It is also easy to see that the lack of cooling terms, or some process that allows descent, would prevent a stationary solution without flow through the boundaries. We now turn to each of the less radical possibilities.

The simplest change involves dropping the linear vertical momentum diffusion. Momentum transport from vertical flow (e.g. what is often called cumulus friction [e.g. Stevens et alii 1977]) does not appear at the lowest (linear) order. The limit of $\mu \rightarrow 0$ is well behaved and nonsingular, so one can just set $\mu = 0$ in eq. (6.17) yielding

$$\begin{aligned}
& k_1^{(0)} k_2^{(0)} m^6 - (\eta^{(0)} - 1) k_s k_2^{(0)} m^4 \\
& + b f^2 (k_1^{(0)} + k_2^{(0)}) m^2 + b f^2 k_s = 0 .
\end{aligned} \tag{6.35}$$

The linear friction between the layers could be omitted without a breakdown of the model, but its presence does not increase the order of the system so there is not much overhead in keeping it. Further, it is counter to the observational evidence that dissipation from vertical momentum fluxes throughout the depth of the troposphere are similar in magnitude to the surface boundary layer losses, though much of this mixing is probably due to convection. Solutions to this system also have a very strong anticyclone aloft, which makes them unsuitable for comparison with real disturbances. For small values of B , eliminating vertical diffusion sends the critical value of $\eta^{(0)}$ close to one. This leaves little room to prevent linear instability yet still allow finite amplitude instability.

From the discussion of eq. (5.57) it was shown that for steady solutions there must be some internal lateral dissipation. It now appears that lateral friction may only be needed in the upper layer ($k_2^{(0)} \neq 0$), while an inviscid lower layer ($k_1^{(0)} = 0$) still allows nontrivial solutions. Eliminating lateral dissipation in the lower layer results in the fourth order relation

$$\left[-(\eta^{(0)} - 1) k_s k_2^{(0)} + \mu k_2^{(0)} \right] m^4 - \left[\mu k_s + b f^2 k_2^{(0)} \right] m^2 + b f^2 k_s = 0 .$$

Though there is observational evidence that momentum mixing is greater in the upper outflow layer than the lower layer, it seemed unreasonable to treat the two main layers in a qualitatively different way with respect to their momentum budgets. Hence, this system was not solved.

Letting lateral dissipation in the upper layer vanish prevents any steady solutions. The momentum equations then reduce to

$$\begin{aligned}
& k_s v_3^{(1)} + \mu (v_2^{(1)} - v_1^{(1)}) + k_2^{(0)} \square^2 v_1^{(1)} = 0 \\
& k_s v_4^{(1)} + \mu (v_1^{(1)} - v_2^{(1)}) = 0 .
\end{aligned}$$

The continuity equations remain unchanged as

$$\square^2 v_3^{(1)} - (\eta^{(0)} - 1) \square^2 v_1^{(1)} - k_1^{(0)} \square^2 v_1^{(1)} = 0$$

$$v_1^{(1)} + v_3^{(1)} + v_4^{(1)} = 0 .$$

From these one can derive

$$k_1^{(0)} \square^2 v_1^{(1)} - k_s v_1^{(1)} = 0 ,$$

which only allows modified Bessel functions as solutions. Therefore, upper layer diffusion is necessary for stationary solutions. This confirms the safety of our choice of nondimensionalization using $k_2^{(0)}$ in the scaling.

THE ROCK:

*The lot of man is ceaseless labour,
Or ceaseless idleness, which is still harder,
Or irregular labour, which is not pleasant.
I have trodden the winepress alone, and I know
That it is hard to be really useful, resigning
The things that men count for happiness, seeking
The good deeds that lead to obscurity, accepting
With equal face those that bring ignominy,
The applause of all or the love of none.
All men are ready to invest their money
But most expect dividend.
I say to you: Make perfect your will.
I say: take no thought of the harvest,
But only of proper sowing.*

*T.S. Eliot
from "The Rock"*

Chapter 7

Finite Amplitude Disturbances

7.1 Weakly Finite Amplitude Theory

Before continuing, we will present a brief symbolic review of the mathematics. The whole nonlinear, time dependent system with linear and nonlinear terms separated can be represented as

$$\tilde{\mathcal{L}}_{\boldsymbol{\eta}}[\mathbf{v}(r, t)] = \mathcal{R}_{\boldsymbol{\eta}}[\mathbf{v}(r, t)] . \quad (7.1)$$

Here $\tilde{\mathcal{L}}_{\boldsymbol{\eta}}$ is a linear operator which may include derivatives with respect to both space and time, and may have nonconstant (in space) coefficients. All of the remaining terms are represented by $\mathcal{R}_{\boldsymbol{\eta}}$. Both operators are dependent on the parameter set $\boldsymbol{\eta}$ (which includes a forcing parameter η , amongst others). There is no prohibition on linear terms in \mathcal{R} , but $\tilde{\mathcal{L}}$ must be linear. Section 5.1 presented this much of the problem, though without always clearly separating the linear and nonlinear parts.

Most stability analyses are based on systems that are linearized and time dependent. These problems usually assume that the temporal and spatial variability are separable and that the time dependence is of the form $e^{\gamma^{(0)}t}$. Such systems will be symbolically expressed as

$$\tilde{\mathcal{L}}_{\boldsymbol{\eta}^{(0)}}[\tilde{\mathbf{v}}(r, t)] = 0 . \quad (7.2)$$

For this linear case, \tilde{v} is the proverbial infinitesimal perturbation and $\boldsymbol{\eta}^{(0)}$ is the set of parameters applying to the linearized problem. The standard result of this type of analysis is a relationship between the growth rate, $\gamma^{(0)}$, and the wave number, m , for given values of the parameter set, $\boldsymbol{\eta}^{(0)}$. One parameter will be referred to as the *forcing parameter* and given the symbol $\eta^{(0)}$. There is some arbitrariness in deciding which parameter is so designated. In the context of the problem presented in the previous chapters, it is worth noting that for sufficiently large values of $\eta^{(0)}$, linearly unstable modes exist that are consistent with the boundary conditions. However, such large values of the forcing parameter are not expected to occur in nature. The earlier CISK models are solutions to this type of system. This problem was presented briefly in section 6.3, but not pursued.

To perform the weakly nonlinear analysis, we will first need to solve the linearized and stationary problem

$$\mathcal{L}_{\boldsymbol{\eta}^{(0)}}[\tilde{v}^{(1)}(r)] = 0. \quad (7.3)$$

There is no time dependence, nor are there time derivatives in the linear operator \mathcal{L} , though it may still be a function of r . The linear stationary solution is represented by $\tilde{v}^{(1)}$. The linear equation, along with the boundary conditions, determines the form of the solutions that will be used in the weakly nonlinear analysis. The boundary conditions that will be imposed are all to be homogeneous and will number the same as the order of the system. They will be imposed at two points, one the origin and the other at an outer boundary designated r_1 .

Usually this type of problem is a simple eigenvalue problem. (The conditions that determine the eigenvalues are solvability conditions.) However, the “nonlinearity” brought about by the discontinuous change in the heating, where w changes sign, is a severe complication in the problem treated here. This leads to an operator \mathcal{L} that rather than being simply linear, is piecewise linear with a finite number of jump discontinuities in the coefficients. At each discontinuity, the same number of matching conditions is needed as the order of the system. Solutions may exist only for restricted values of the parameters $\boldsymbol{\eta}$ and the outer boundary r_1 . Still,

after imposing the matching conditions, there will be a single solution (or countable number of solutions) of undetermined amplitude for a given set of parameter values, as is usual for homogeneous problems. Section 6.2 presented and solved a problem of this type.

The next step is to expand the variables and equations in an amplitude expansion as outlined in section 5.2, i.e. $\mathbf{v}(r) = a\mathbf{v}^{(1)}(r) + a^2\mathbf{v}^{(2)}(r) + \dots$, with the $\mathbf{v}^{(j)}$ being spatial structure functions of r with maxima of order 1 and the amplitude $a \ll 1$. For the lowest order solution $\bar{\mathbf{v}}^{(1)}$, eq. (7.3) is assumed to hold. At second order, the weakly nonlinear and stationary problem leads to an equation of the form

$$\mathcal{L}_{\boldsymbol{\eta}^{(0)}}[\bar{\mathbf{v}}^{(2)}(r)] = \mathcal{M}_{\eta_c^{(1)}}^{(2)}[\bar{\mathbf{v}}^{(1)}(r)] . \quad (7.4)$$

On the left side are linear terms corresponding exactly to the linear terms of the first order equation but with the second order terms of $\bar{\mathbf{v}}$. The form of \mathcal{L} remains unchanged throughout. Since the inhomogeneous terms are all functions of $\bar{\mathbf{v}}^{(1)}$, only the functional forms but not the amplitude of the inhomogeneous terms are specified. The functional $\mathcal{M}^{(2)}$ may depend on the parameter set used in the linear operator $\boldsymbol{\eta}^{(0)}$ and some additional parameters $\boldsymbol{\eta}^{(1)}$. There is at least one such additional parameter, designated $\eta_c^{(1)}$, from the expansion of the forcing parameter (see pp. 126 and 150). The term proportional to $\eta_c^{(1)}$ must be linear in $\bar{\mathbf{v}}^{(1)}$ to end up as a second order term. With the imposition of the same homogeneous boundary conditions applied to eq. (7.3), the system under consideration is an inhomogeneous two point boundary value problem. The general solutions to the corresponding homogeneous equation for $\bar{\mathbf{v}}^{(2)}$ are the same as those for $\bar{\mathbf{v}}^{(1)}$. However, there is no guarantee that this inhomogeneous problem has a solution; many inhomogeneous boundary value problems do not. The inhomogeneous problem only has a solution if a certain integral condition on the inhomogeneous term holds.

Associated with the linear inhomogeneous problem is an adjoint homogeneous problem designated as

$$\mathcal{L}_{\boldsymbol{\eta}^{(0)}}^\dagger[\mathbf{y}(r)] = 0 . \quad (7.5)$$

If eq. (7.3) is self-adjoint it is not necessary to solve a separate adjoint problem. The solvability condition for eq. (7.4), in the domain $[0, r_1]$, is

$$\int_0^{r_1} \mathbf{y}'^T \mathcal{M}_{\eta_c^{(1)}}^{(2)}[\bar{\mathbf{v}}^{(1)}(r)] dr = 0, \quad (7.6)$$

for all solutions \mathbf{y}' to eq. (7.5) with its accompanying boundary conditions. The superscript T designates a transpose. For our problems there is only one such solution, though of arbitrary amplitude a' . Derivations of such conditions can be found in some standard texts on ordinary differential equations, such as Ince 1926 or Coddington and Levinson 1955. A derivation, in the limited context of this problem, follows in section 7.1.1. If the boundary conditions are not homogeneous, or the number of boundary conditions does not lead to a single linearly independent solution, the solvability condition is more complicated. None of these additional difficulties will confront us.

If there is a free parameter that first appears at second order, the solvability condition of eq. (7.6) can be viewed as an equation for that parameter. Here, the solvability condition will be used to provide a relationship between the amplitude of the solutions and the forcing parameter, i.e. a relationship between $\bar{a}\mathbf{v}^{(1)}$ and $\bar{a}\eta_c^{(1)}$. The expansion of η allows us to calculate this balance. Section 7.2 applies eq. (7.6) to determine this relation. The solvability condition can also be viewed as requiring the balance of the inhomogeneous terms when projected on, or weighted by, the solution to the adjoint homogeneous system. When the problem is self-adjoint, as is the case here, \mathbf{y}' is proportional to $\mathbf{v}^{(1)}$, so the resulting equation resembles an integrated energy balance for the second order terms over the specified domain. (I am not aware of any simple physical interpretation for problems that are not self-adjoint.)

In many weakly finite amplitude problems the solvability condition at this order ends up trivially satisfied, providing no relationship between the forcing and the amplitude of the first order solutions. In those cases it is necessary to go to higher order. The problem under consideration here will, however, be settled at this order. This is, in fact, unusual and is due to the asymmetry in the forcing of vertical motions between cyclonic and anticyclonic vorticities in the lower layer.

Having found the linear solutions, and determined their amplitudes through use of the solvability condition at second order, we will next examine the stability of those solutions. The steady solutions are perturbed with infinitesimal time dependent disturbances. At first order the slowly varying infinitesimal disturbances are assumed to satisfy the linear stationary equation (7.3), i.e. $\mathcal{L}_{\eta^{(0)}}[\tilde{\mathbf{v}}^{(1)}(r, t)] = 0$. At second order

$$\mathcal{L}_{\eta^{(0)}}[\tilde{\mathbf{v}}^{(2)}(r, t)] = \mathcal{N}_{\eta_c^{(1)}, \gamma^{(1)}}^{(2)}[\bar{\mathbf{v}}^{(1)}(r), \tilde{\mathbf{v}}^{(1)}(r, t)] . \quad (7.7)$$

The time and spatial dependencies of the perturbations are assumed to be separable with the time dependence proportional to $e^{\bar{\alpha}\gamma^{(1)}t}$. There is no first order rapid time dependence proportional to $e^{\gamma^{(0)}t}$, which would be inconsistent with the expansion. The second order terms contained in $\mathcal{N}_{\eta_c^{(1)}, \gamma^{(1)}}^{(2)}$ include nonlinear terms, linear terms proportional to $\eta_c^{(1)}$, and linear terms proportional to $\gamma^{(1)}$.

Equation (7.7) also has a solvability condition associated with it:

$$\int_0^{r_1} \mathbf{y}'^T \mathcal{N}_{\eta_c^{(1)}, \gamma^{(1)}}^{(2)}[\bar{\mathbf{v}}^{(1)}(r), \tilde{\mathbf{v}}^{(1)}(r)] dr = 0 . \quad (7.8)$$

This provides a relation between the forcing parameter, the amplitude of the stationary solution, and the growth rate for perturbations to that stationary solution. Again, when the linear homogeneous problem is self adjoint, this equation can be interpreted as an energy equation. Section 7.3 applies this condition to the problem at hand. If the growth rate is positive then the finite amplitude stationary states found using eqs. (7.4) and (7.6) are unstable. This does not imply that the resting state is unstable.

7.1.1 Adjoins and Solvability Conditions¹

[This section may be skipped by the mathematically unadventurous and the mathematically sophisticated (for whom it is superfluous).]

We will now derive the solvability condition and show that eq. (6.24) is self-adjoint (and show why self-adjointness is useful). For the moment, assume that \mathbf{v} and \mathbf{y} are arbitrary real n -vectors, and functions of the independent variable r . The real matrices \mathbf{A} and \mathbf{B} are arbitrary $n \times n$ functions of r . Under the rules of matrix multiplication these satisfy the relation $\mathbf{y}^T \mathbf{B} \mathbf{v} = \mathbf{v}^T \mathbf{B}^T \mathbf{y}$, where the superscript T indicates a transpose. (Complex operators need be treated slightly differently and are not considered here.)

Without any additional conditions, except that the differentiated quantities are differentiable, after two integrations by parts

$$\int_a^b \mathbf{y}^T r \left[\frac{d}{dr} \left(\mathbf{B} \frac{d\mathbf{v}}{r dr} \right) + \mathbf{A} \mathbf{v} \right] dr = \int_a^b \mathbf{v}^T r \left[\frac{d}{dr} \left(\mathbf{B}^T \frac{d\mathbf{y}}{r dr} \right) + \mathbf{A}^T \mathbf{y} \right] dr - \left[\mathbf{y}^T \mathbf{B} \frac{d\mathbf{v}}{r dr} - \mathbf{v}^T \mathbf{B}^T \frac{d\mathbf{y}}{r dr} \right]_a^b.$$

The left hand side of side of this relation is an inner product of an arbitrary vector with our linear operator, \mathcal{L} , operating on another arbitrary vector. We will designate the similar operator on the right hand side \mathcal{L}^\dagger , where $\mathcal{L}^\dagger \mathbf{y} = r \left[\frac{d}{dr} \left(\mathbf{B}^T \frac{d\mathbf{y}}{r dr} \right) + \mathbf{A}^T \mathbf{y} \right]$, and call it the *adjoint* of \mathcal{L} . If both \mathbf{A} and \mathbf{B} are symmetric, then $\mathcal{L} = \mathcal{L}^\dagger$ and we will say that \mathcal{L} is *self-adjoint*. According to this definition, the differential operator in eq. (6.24) is self-adjoint. Note that it would not be possible to do this simply for nonconstant \mathbf{B} , if that matrix were not imbedded in the operator as it is.

Let us now restrict the vectors \mathbf{v} and \mathbf{y} such that

¹This section has been included because the only published discussions of solvability conditions I have been able to find cover either arbitrary order equations of a scalar function or systems of coupled first order equations. It was more useful for this problem to deal with a system of coupled higher order equations.

$$\mathcal{L}\mathbf{v} = \mathcal{M}(r)$$

$$\mathcal{L}^\dagger \mathbf{y} = 0 .$$

Directly from these relations

$$\int_a^b \mathbf{y}^T \mathcal{L}\mathbf{v} \, dr = \int_a^b \mathbf{y}^T \mathcal{M}(r) \, dr$$

$$\int_a^b \mathbf{v}^T \mathcal{L}^\dagger \mathbf{y} \, dr = 0 .$$

If we now further assume that the vectors satisfy the homogeneous boundary conditions

$$\mathbf{v}(a) = \mathbf{v}(b) = \mathbf{y}(a) = \mathbf{y}(b) = 0$$

using the integral relation derived above, we obtain

$$\int_a^b \mathbf{y}^T \mathcal{M}(r) \, dr = 0 .$$

This is the solvability condition. It must hold for *all* \mathbf{y} that satisfy the adjoint equation with its accompanying boundary conditions. For the system under examination here, there are sufficient linearly independent boundary conditions such that there is only one linearly independent \mathbf{y} . Further if the system is self-adjoint, \mathbf{y} is identical to the homogenous solution to the initial problem, i.e. $\mathbf{y} = \mathbf{v}_h$ where $\mathcal{L}\mathbf{v}_h = 0$, with $\mathbf{v}_h(a) = \mathbf{v}_h(b) = 0$. It is for this reason that we went to the trouble to derive the transformation of section 6.2.3.

7.2 Amplitude of the Stationary Solutions

In the previous chapter, the solution of the linear stationary system was found. That solution has, as yet, no determined amplitude. The stationary system can be expanded to second order. The solvability condition on the resulting inhomogeneous system will provide a relationship between the forcing parameter and

the stationary solution amplitude. It is already assumed from eq. (6.8) that $\frac{d}{dr} \left(\mathbf{B}' \frac{dr \bar{\mathbf{v}}^{(1)}}{r dr} \right) + \mathbf{A}' \bar{\mathbf{v}}^{(1)} = 0$, where $\bar{\mathbf{v}}^{(1)} = \bar{a} \mathbf{v}^{(1)}$.

The vector $\bar{\mathbf{v}}$ at second order will be expanded as

$$\bar{\mathbf{v}}^{(2)} = \bar{a}^2 \left[\mathbf{v}^{(2h)} + \mathbf{v}^{(2)} \right],$$

where $\mathbf{v}^{(2h)}$ is the solution to the associated homogeneous equation at second order and $\mathbf{v}^{(2)}$ is a particular solution to the inhomogeneous problem that is orthogonal to the solutions to the homogeneous problem. The trick of W. Malkus and Veronis (1958) was to realize that since the spatial structure of $\mathbf{v}^{(2h)}$ is identical to $\bar{\mathbf{v}}^{(1)}$, it should be absorbed into the coefficient \bar{a} of $\bar{\mathbf{v}}^{(1)}$ and then $\mathbf{v}^{(2h)}$ taken to be zero everywhere.

Expansion of the stationary conservation equations at second order leads to

$$0 = k_1^{(0)} \square^2 \bar{v}_1^{(2)} + \mu(\bar{v}_2^{(2)} - \bar{v}_1^{(2)}) + k_s \bar{v}_3^{(2)} + \bar{\zeta}_1^{(1)} \frac{k_s}{f} \bar{v}_3^{(1)} + \bar{Q}^{- (1)} (\bar{v}_2^{(1)} - \bar{v}_1^{(1)}) \quad (7.9)$$

$$0 = k_2^{(0)} \square^2 \bar{v}_2^{(2)} + \mu(\bar{v}_1^{(2)} - \bar{v}_2^{(2)}) + k_s \bar{v}_4^{(2)} + \bar{\zeta}_2^{(1)} \frac{k_s}{f} \bar{v}_4^{(1)} + \bar{Q}^{+ (1)} (\bar{v}_1^{(1)} - \bar{v}_2^{(1)}) \quad (7.10)$$

$$0 = \frac{k_s}{f} \square^2 \bar{v}_3^{(2)} - (\eta^{(0)} - 1) \frac{k_s}{f} \square^2 \bar{v}_1^{(2)} + b f (\bar{v}_2^{(2)} - \bar{v}_1^{(2)}) - \frac{d}{dr} (\bar{a} \eta_c^{(1)} \bar{w}^{(1)}) - \frac{d}{dr} (\bar{Q}^{(2*)} - \bar{w}^{(2*)}) \quad (7.11)$$

$$0 = \frac{k_s}{f} (\bar{v}_1^{(2)} + \bar{v}_3^{(2)} + \bar{v}_4^{(2)}) + \frac{C_D}{f} |\bar{v}_1^{(1)}| \bar{v}_1^{(1)} - \frac{k_s}{f^2} \bar{v}_1^{(1)} \frac{dr \bar{v}_1^{(1)}}{r dr}. \quad (7.12)$$

Equations (7.9) and (7.10) are expansions of eqs. (5.18) and (5.19), respectively, and enforce conservation of angular momentum. The first order cooling, $\bar{Q}^{- (1)}$, is determined by integrating eq. (5.50) after solving the first order problem. Equation (7.11), which is the continuity equation for the lower layer, is an expansion of a radial derivative of eq. (5.3) for stationary solutions. Equation (7.12) is an

integral of the sum of the continuity equations and also makes use of eqs. (5.17) and (5.8). The terms with the superscript (2*) are the nonlinear contributions at second order as defined earlier in eqs. (5.48), (5.53), and (5.43). In each of these equations the terms similar to the terms in the first order linear problem are in the first line and terms that first appear at second order are in the second line. The only linear term in the second lines is the one proportional to $\eta_c^{(1)}$ in eq. (7.11).

The four coupled equations can be put in a three-vector form as was done for the linear problem. The resulting inhomogeneous equation is

$$\frac{d}{dr} \left(B' \frac{dr \bar{\mathbf{v}}^{(2)}}{r dr} \right) + A' \bar{\mathbf{v}}^{(2)} = \mathcal{M}'^{(2)} \quad (7.13)$$

where

$$\mathcal{M}'^{(2)} = \begin{pmatrix} \bar{Q}^{-(1)}(\bar{v}_1^{(1)} - \bar{v}_2^{(1)}) - \frac{k_s}{f} \bar{\zeta}_1^{(1)} \bar{v}_3^{(1)} \\ \bar{Q}^{+(1)}(\bar{v}_2^{(1)} - \bar{v}_1^{(1)}) + \frac{k_s}{f} \bar{\zeta}_2^{(1)}(\bar{v}_1^{(1)} + \bar{v}_3^{(1)}) + C_D |\bar{v}_1^{(1)}| \bar{v}_1^{(1)} - \frac{k_s}{f} \bar{v}_1^{(1)} \frac{dr \bar{v}_1^{(1)}}{r dr} \\ \bar{a} \eta_c^{(1)} \frac{f k_2^{(0)}}{k_s} \frac{d \bar{w}^{(1)}}{dr} + \frac{f k_2^{(0)}}{k_s} \frac{d}{dr} (\bar{Q}^{(2*)} - \bar{w}^{(2*)}) \end{pmatrix}$$

is the three-vector of inhomogeneous terms. The only term involving $\eta_c^{(1)}$ can be found at the beginning of the last entry. For convenience we define

$$\mathcal{M}'^{(2*)} \equiv \mathcal{M}'^{(2)} - \begin{pmatrix} 0 \\ 0 \\ \bar{a} \eta_c^{(1)} \frac{f k_2^{(0)}}{k_s} \frac{d \bar{w}^{(1)}}{dr} \end{pmatrix}$$

so as to easily separate the linear and nonlinear inhomogeneous terms at second order.

Multiplication of eq. (7.13) by rT puts the system into self-adjoint form, so there is no need to solve a separate adjoint problem. The solvability condition for the domain $[0, r_1]$ is then

$$\int_0^{r_1} r \mathbf{v}^{(1)T} T \mathcal{M}'^{(2)} dr = 0.$$

where $\mathbf{v}^{(1) \prime}$ is a solution to the homogeneous problem with amplitude a' . The solvability condition can be expanded as

$$a' \bar{a} \bar{\alpha} \Sigma + \bar{a} \eta_c^{(1)} a' \bar{a} \Omega = 0 \quad (7.14)$$

where Σ and Ω are definite integrals defined below. As noted earlier, this is essentially an integrated energy equation. This is easily solved for the perturbation to the forcing parameter that allows a steady solution:

$$\eta_c^{(1)} = \frac{-\Sigma}{\Omega} . \quad (7.15)$$

After evaluating $\frac{d\bar{\psi}^{(1)}}{dr}$, one of the integrals is

$$\begin{aligned} \Omega &= \int_0^{r_0} k_2^{(0)} v_1^{(1)} \square^2 v_1^{(1)} r \, dr \\ &= - \int_0^{r_0} k_2^{(0)} \left(\frac{dr v_1^{(1)}}{r \, dr} \right)^2 r \, dr < 0 . \end{aligned} \quad (7.16)$$

The expression for Ω is integrated only over the interval $[0, r_0]$ because η vanishes outside of that subdomain. It is clear that Ω is negative. The integral that comprises Σ is much more complicated:

$$\begin{aligned} \Sigma &= \int_0^{r_1} r \mathbf{v}^{(1)T} T \mathcal{M}'^{(2*)} dr \\ &= \int_0^{r_1} \left\{ \left[v_1^{(1)} \left(M - \frac{M}{K} - BK \right) + v_2^{(1)} \left(\frac{M}{K} - B \right) + \frac{v_3^{(1)}}{K} \right] \mathcal{M}_1'^{(2*)} \right. \\ &\quad \left. + \left[v_1^{(1)} (M - BK) - v_2^{(1)} B \right] \mathcal{M}_2'^{(2*)} + \left[v_1^{(1)} \right] \mathcal{M}_3'^{(2*)} \right\} r \, dr , \end{aligned} \quad (7.17)$$

where the $\mathcal{M}_j'^{(2*)}$ are the elements of the vector functional $\mathcal{M}'^{(2*)}$. In examining this integral, it is first helpful to show that all of the factors in square brackets are positive. This is obvious for the coefficient of $\mathcal{M}_3'^{(2*)}$, consisting just of $v_1^{(1)}$. The only negative term in the coefficient of $\mathcal{M}_2'^{(2*)}$ is $-BKv_1^{(1)}$, which is relatively small since B is small. Through use of the transformed linear system, eq. (6.24),

one can show that the coefficient of $\mathcal{M}'_1^{(2*)}$ satisfies

$$v_1^{(1)} \left(M - \frac{M}{K} - BK \right) + v_2^{(1)} \left(\frac{M}{K} - B \right) + \frac{v_3^{(1)}}{K} = \\ v_1^{(1)}(M - BK) - v_2^{(1)}B - \frac{k_s}{k_2^{(0)}} \square^2 v_3^{(1)} .$$

Examination of the linear solution in figure 6.8 illustrates that $\frac{d}{dr} \frac{dr v_3^{(1)}}{r dr} = \square^2 v_3^{(1)} < 0$, except in a tiny region just outside of r_0 . Since, as above, $-BKv_1^{(1)}$ is small, the entire coefficient is positive. To determine the signs of the terms in Σ , we now need only determine the signs of the various terms of the $\mathcal{M}'_j^{(2*)}$.

Since we have already shown that Ω is negative, for subcritical finite amplitude stationary states to exit Σ must also be negative. The first term of $\mathcal{M}'_1^{(2*)}$ represents vertical momentum mixing from radiative cooling and weakens the lower level vortex. Advection of positive disturbance vorticity, the second term, helps maintain the vortex, though it is weakly negative outside of r_0 . The first two terms of $\mathcal{M}'_2^{(2*)}$ may seem counterintuitive to some. Though spin-up of the lower level cyclone also drives the energy pump, spin-up of the upper level anticyclone is only an energy drain on the system. Hence, the cumulus mixing term is a positive influence. The outward advection of negative relative vorticity aloft also weakens the anticyclone, though at large radius ζ_2 changes sign to positive. The last two terms of $\mathcal{M}'_2^{(2*)}$ are the nonlinear second order terms of w . They lead to additional outflow in the upper layer and are a negative influence since they contribute to spin-up of the anticyclone.

The most important second order driving terms are those of $\mathcal{M}'_3^{(2*)}$. They represent the radial derivative of the net forcing from diabatic and latent heat releasing processes. If the heating is concentrated at small radius this is a positive influence on the cyclone. The radiative cooling provides additional damping since it is strongest in the central warm core, possibly contrary to the actual effect of radiative perturbations. These last terms are somewhat easier to follow after integration by parts and some expansion:

$$\begin{aligned}
\int_0^{r_1} r v_1^{(1)} \frac{d}{dr} (Q^{(2*)} - w^{(2*)}) dr &= - \int_0^{r_1} \frac{dr v_1^{(1)}}{r dr} (Q^{(2*)} - w^{(2*)}) r dr \\
&= - \int_0^{r_0} \frac{dr v_1^{(1)}}{r dr} (\eta^{(0)} w^{(2*)} + \eta_r^{(1)} w^{(1)}) r dr + \int_0^{r_1} \frac{dr v_1^{(1)}}{r dr} (Q^{-(2*)} + w^{(2*)}) r dr .
\end{aligned}$$

From 0 to r_0 , $\frac{dr v_1^{(1)}}{r dr}$ is positive and outside of that radius it is negative. Since the net of the second order terms of w is to enhance the Ekman pumping, $\eta^{(0)} \bar{w}^{(2*)}$ provides additional forcing and represents the probably most important second order terms. Another positive contribution is made by $\eta_r^{(1)} w^{(1)}$ term as long as $\eta_r^{(1)}$ is positive inside of r_0 . This term includes increases in the boundary layer entropy from enhanced sea surface heat and moisture fluxes as in HASIT. The second integral is a net damping term. At this order there is no need to correct r_0 for changes in the zero crossing of w . Further, as will later be seen in figure 7.4, the radius of zero crossing for $w^{(2)}$ is almost identical to r_0 .

For Σ and Ω both negative, $\eta_c^{(1)}$ is also negative. This allows subcritical stationary states for $\bar{a} > 0$. Most of what has preceded this only applies for positive \bar{a} . One could examine this system with anticyclonic circulations in the lower layer, but the assumptions on the location of the heating would no longer apply. For a given ambient η_a and disturbance requiring a forcing parameter $\eta^{(0)}$, there is a critical amplitude, a_{crit} , where $\eta_e = \eta_a$ such that

$$a_{crit} = (\eta^{(0)} - \eta_a) \frac{\Omega}{\Sigma} = \frac{\eta_a - \eta^{(0)}}{\eta_c^{(1)}} . \quad (7.18)$$

It is essential that this result and the statement in eq. (6.22) be grasped to understand this work. The numerical evaluation of the integrals is performed in section 7.4.

7.3 Stability of the Stationary Solutions

Having found a stationary solution, it is now possible to look at time dependent perturbations to that solution. It is simple, though tedious, to derive an equation for infinitesimal perturbations to the stationary equations found in the previous

subsection. The system is separable for the independent variables r and t . With respect to t the equations are linear and constant coefficient, so we may assume solutions proportional to $e^{\gamma t} = e^{\bar{\alpha}\gamma^{(1)}t}$. At first order we again have

$$\frac{d}{dr} \left(\mathbf{B}' \frac{dr \tilde{\mathbf{v}}^{(1)}}{r dr} \right) + \mathbf{A}' \tilde{\mathbf{v}}^{(1)} = 0. \quad (7.19)$$

The vector $\tilde{\mathbf{v}}$ at second order will be expanded as

$$\tilde{\mathbf{v}}^{(2)} = 2\tilde{a}\bar{a} \left[\mathbf{v}^{(2h)} + \mathbf{v}^{(2)} \right],$$

where $\mathbf{v}^{(2h)}$ is the solution to the associated homogeneous equation at second order and $\mathbf{v}^{(2)}$ is a particular solution to the inhomogeneous problem which is orthogonal to the solutions of the homogeneous problem. As with the stationary case, the spatial structure of $\mathbf{v}^{(2h)}$ is identical to $\tilde{\mathbf{v}}^{(1)}$. By a renormalization similar to that of the last section, $\mathbf{v}^{(2h)}$ is set equal to zero everywhere.

For the stationary solution being perturbed, eq. (7.13) still holds, so only time dependent terms remain. The coupled time dependent inhomogeneous equations at second order are

$$\begin{aligned} \tilde{a}\bar{a}\gamma^{(1)}h_1^{(0)}v_1^{(1)}r &= 2\tilde{a}\bar{a}[k_1^{(0)}r\Box^2v_1^{(2)} + \mu(v_2^{(2)} - v_1^{(2)})r + k_s v_3^{(2)}r] \\ &+ (\tilde{a}\bar{a} + \bar{a}\tilde{a}) \left[\zeta_1^{(1)} \frac{k_s}{f} v_3^{(1)}r + Q^{-(1)}(v_2^{(1)} - v_1^{(1)})r \right] \end{aligned} \quad (7.20)$$

$$\begin{aligned} \tilde{a}\bar{a}\gamma^{(1)}\epsilon h_2^{(0)}v_2^{(1)}r &= 2\tilde{a}\bar{a}[k_2^{(0)}r\Box^2v_2^{(2)} + \mu(v_1^{(2)} - v_2^{(2)})r + k_s v_4^{(2)}r] \\ &+ (\tilde{a}\bar{a} + \bar{a}\tilde{a}) \left[\zeta_2^{(1)} \frac{k_s}{f} v_4^{(1)}r + Q^{+(1)}(v_1^{(1)} - v_2^{(1)})r \right] \end{aligned} \quad (7.21)$$

$$\begin{aligned} \frac{\tilde{a}\bar{a}\gamma^{(1)}f}{g(1-\epsilon)} (v_1^{(1)} - \epsilon v_2^{(1)}) &= \\ 2\tilde{a}\bar{a} \left[\frac{k_s}{f} \Box^2 v_3^{(2)} - (\eta^{(0)} - 1) \frac{k_s}{f} \Box^2 v_1^{(2)} + b f (v_2^{(2)} - v_1^{(2)}) \right] & \\ - \tilde{a}\bar{a} \frac{d\eta_c^{(1)}w^{(1)}}{dr} - \tilde{a}\bar{a}(\eta^{(0)} - 1) \frac{\gamma^{(1)}h_0}{f} \Box^2 v_1^{(1)} & \\ - (\tilde{a}\bar{a} + \bar{a}\tilde{a}) \frac{d}{dr} (Q^{(2*)} - w^{(2*)}) & \end{aligned} \quad (7.22)$$

$$\begin{aligned}
\int_r^{r_1} \left(\frac{\partial h_1^{(1)}}{\partial t} + \epsilon \frac{\partial h_2^{(1)}}{\partial t} \right) r' dr' = \\
2\tilde{a}\bar{a} \frac{k_s}{f} (v_1^{(2)} + v_3^{(2)} + v_4^{(2)}) r \\
\frac{h_0}{f} \bar{a} \gamma^{(1)} \tilde{a} v_1^{(1)} r + 2\tilde{a}\bar{a} \frac{C_D}{f} |v_1^{(1)}| v_1^{(1)} r - 2\tilde{a}\bar{a} \frac{k_s}{f^2} \frac{\partial r v_1^{(1)}}{r \partial r} v_1^{(1)} r .
\end{aligned} \tag{7.23}$$

As in the previous section, the first line of each of these four equations after the equals sign corresponds to the terms of the first order stationary equation. The remaining terms, including those on the left hand side are inhomogeneous. Equations (7.20)–(7.23) are derived in a nearly identical fashion to eqs. (7.9)–(7.12).

Before proceeding we will examine the integral on the left hand side of eq. (7.23). From eq. (5.13) it is clear that $g \left(\frac{\partial h_1}{\partial t} + \epsilon \frac{\partial h_2}{\partial t} \right) = \frac{\partial \phi}{\partial t}$. We also have $\frac{\partial \tilde{\phi}_1^{(1)}}{\partial t} = \bar{a} \gamma^{(1)} \tilde{\phi}_1^{(1)}$. From the expansion of eq. (5.15), $\frac{\partial \phi_1^{(1)}}{\partial r} = f v_1^{(1)}$. Integrating once yields

$$\phi_1^{(1)}(r) = \int_0^r f v_1^{(1)}(r') dr' + C' ,$$

where C' is an as yet undetermined constant. Multiplying by r and again integrating leads to

$$\begin{aligned}
\Phi_1^{(1)}(r) &\equiv \int_0^r \phi_1^{(1)}(r') r' dr' \\
&= \int_0^r \left[\int_0^{r'} f v_1^{(1)}(r'') dr'' \right] r' dr' - \frac{r^2}{r_1^2} \int_0^{r_1} \left[\int_0^{r'} f v_1^{(1)}(r'') dr'' \right] r' dr' .
\end{aligned} \tag{7.24}$$

The integration constants have been determined by requiring that $\Phi_1^{(1)}(0) = \Phi_1^{(1)}(r_1) = 0$. These are the only conditions consistent with eqs. (7.20)–(7.23). Figure 7.1 shows $\Phi_1^{(1)}(r)$ for the solution of figure 6.8. The integration procedures are discussed in section 7.4.

We now rework eqs. (7.20)–(7.23) into the same vector form used above, with

$$r \frac{d}{dr} \left(B \frac{dr \tilde{\mathbf{v}}^{(2)}}{r dr} \right) + r \mathbf{A} \tilde{\mathbf{v}}^{(2)} = r \mathbf{T} \mathcal{N}^{(2)} ,$$

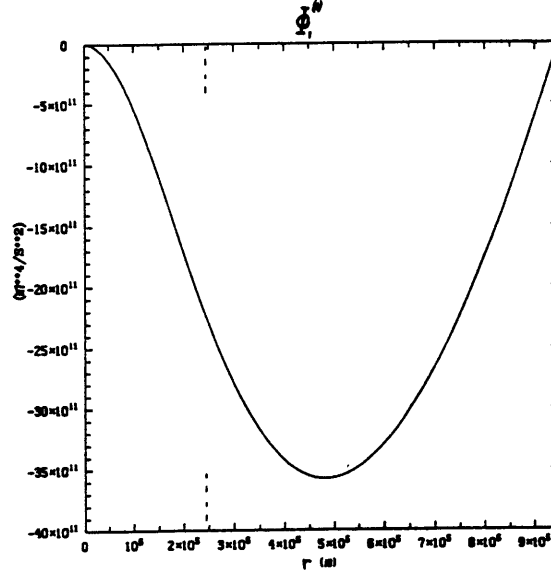


Figure 7.1: The function $\Phi_1^{(1)}(r)$ for the solution in figure 6.14. The parameter values are as given in table 7.2.

where

$$\begin{aligned}
 \mathcal{N}^{(2)} = & \tilde{a}\bar{a}\eta_c^{(1)} \begin{pmatrix} 0 \\ 0 \\ \frac{fk_2^{(0)}}{k_s} \frac{dw^{(1)}}{dr} \end{pmatrix} \\
 & + \tilde{a}\bar{a}\gamma^{(1)} \begin{pmatrix} h_1^{(0)}v_1^{(1)} \\ \epsilon h_2^{(0)}v_2^{(1)} - \frac{f}{gr}\Phi_1^{(1)} + h_0v_1^{(1)} \\ \frac{f^2k_2^{(0)}}{g(1-\epsilon)k_s}(v_1^{(1)} - \epsilon v_2^{(1)}) + (\eta^{(0)} - 1)\frac{h_0k_2^{(0)}}{k_s}\square^2v_1^{(1)} \end{pmatrix} \\
 & + 2\tilde{a}\bar{a} \begin{pmatrix} Q^{-(1)}(v_1^{(1)} - v_2^{(1)}) - \frac{k_s}{f}\zeta_1^{(1)}v_3^{(1)} \\ Q^{+(1)}(v_2^{(1)} - v_1^{(1)}) + \frac{k_s}{f}\zeta_2^{(1)}(v_1^{(1)} + v_3^{(1)}) + c_D|v_1^{(1)}|v_1^{(1)} - \frac{k_s}{f}v_1^{(1)}\frac{drv_1^{(1)}}{rdr} \\ \frac{fk_2^{(0)}}{k_s}\frac{d}{dr}(Q^{(2*)} - w^{(2*)}) \end{pmatrix}.
 \end{aligned} \tag{7.25}$$

Note that the linear operator is the same as that which appeared in all the earlier stationary parts of the problem. A large number of the inhomogeneous terms are similar to those that appeared in eq. (7.13).

The solvability condition is

$$\int_0^{r_1} r \mathbf{v}^{(1)'} \mathbf{T} \mathcal{N}^{(2)} dr = 0, \quad (7.26)$$

which expanded is

$$a'(\tilde{a}\bar{a} + \bar{a}\tilde{a})\Sigma + \bar{a}\gamma^{(1)}a'\tilde{a}\Gamma + \bar{a}\eta_c^{(1)}a'\tilde{a}\Omega = 0. \quad (7.27)$$

The integrals for Ω and Σ are identical to those derived in the previous section. The only term left to expand is Γ , which is

$$\begin{aligned} \Gamma = \int_0^{r_1} \left\{ \left[v_1^{(1)} \left(M - \frac{M}{K} - BK \right) + v_2^{(1)} \left(\frac{M}{K} - B \right) + \frac{v_3^{(1)}}{K} \right] h_1^{(0)} v_1^{(1)} \right. \\ + \left[v_1^{(1)} (M - BK) - v_2^{(1)} B \right] \left[\epsilon h_2^{(0)} v_2^{(1)} - \frac{f}{gr} \Phi_1^{(1)} + h_0 v_1^{(1)} \right] \\ \left. + v_1^{(1)} \left[\frac{f^2 k_2^{(0)}}{g(1-\epsilon)k_s} (v_1^{(1)} - \epsilon v_2^{(1)}) + (\eta^{(0)} - 1) \frac{h_0 k_2^{(0)}}{k_s} \square^2 v_1^{(1)} \right] \right\} r dr. \end{aligned} \quad (7.28)$$

As in the expansion of Σ , the first coefficient in square brackets for Γ is positive except in a very small region where it is negative by only a small amount. The term proportional to $h_1^{(0)} v_1^{(1)}$ is large and positive, while the one proportional to $\epsilon h_2^{(0)} v_2^{(1)}$ is large and negative. Some complicated arguments can be made to show that $-\Phi_1^{(1)} > 0$, but it is simpler to just refer to the example in figure 7.1. Of the remaining terms all, except for one proportional to $(\eta^{(0)} - 1)h_0$ that is small, are positive. Since mostly this integral is dominated by expressions for the kinetic energy and the vortex potential energy, we might expect that Γ is positive. Numerical evaluation will later show this.

From eqs. (7.27) and (7.15),

$$\gamma^{(1)} = \frac{-\Sigma}{\Gamma}. \quad (7.29)$$

So if subcritical stationary states exist and $\Gamma > 0$, they are unstable. Since the theory really only applies at stationary states

$$\gamma = a_{crit} \gamma^{(1)}, \quad (7.30)$$

where a_{crit} is determined by eq. (7.18). If one were to stretch the result past this, superexponential growth would be indicated. Such a process could not last long, but it may ease our minds somewhat when the numerically determined values for $\gamma^{(1)}$ appear a bit small.

7.4 Thresholds and Growth Rates

Evaluation of the integrals Ω , Σ , and Γ , is performed in this section along with the determination of functions of the first order terms on which those integrals depend. All integrations were performed using a simple trapezoidal rule on a fixed mesh. The mesh consisted of 100 equal intervals from 0 to r_0 and 100 equal intervals from r_0 to r_1 . This is about the least sophisticated quadrature scheme imaginable. Given the accuracy with which the parameter values going into the calculation are known, order of magnitude results are all that are meaningful. For this, the technique chosen is more than sufficient. It is also sufficient to determine the sensitivity of the results to any of the parameters. In fact, the scheme is good to one part in 10^3 when comparing the integrals $\frac{1}{r'} \int_0^{r'} \frac{dr v_i}{r} r dr$ with $v_j(r')$ as a test.

The integrations were all performed with dimensional variables. When using the nondimensional solutions obtained in chapter six, the independent variable r needs to be rescaled by $L = \sqrt{k_2^{(0)}/k_s}$, the v_j are scaled by fL and the $\frac{dr v_j}{r dr}$ are scaled by f . Terms of the form $v_i \square^2 v_j$ were integrated once by parts. Several of the parameters were kept fixed throughout the following calculations, either because they do not vary much on our planet or insufficient researcher energy. These are listed in table 7.1.

Values of Fixed Parameters

$h_0 = 1 \cdot 10^3 \text{ m}$	$c_p = 1005 \text{ J/(kg}\cdot\text{K)}$
$h_1^{(0)} = 5 \cdot 10^3 \text{ m}$	$g = 9.8 \text{ m/sec}^2$
$h_2^{(0)} = 5 \cdot 10^3 \text{ m}$	$\pi_1 = (.8)^{2/7} \approx 0.94$
$\epsilon_2 = 0.4$	$\pi_2 = (.3)^{2/7} \approx 0.71$
$\Xi = 1.2$	

Table 7.1: Values of parameters kept fixed in the following calculations.

The analysis of Xu (1987, figure 3.1) was used as a rough guide for determining suitable values of the χ_j . Choosing very optimistically to maximize η_a , one could take a boundary layer equivalent potential temperature of $\chi_0^{(0)} \approx 355 \text{ K}$, a lower troposphere equivalent potential temperature of $\chi_1^{(0)} \approx 340 \text{ K}$, and an upper troposphere saturation equivalent potential temperature of $\chi_2^{(0)} \approx 345 \text{ K}$, yielding $\eta_a \approx 3$. In practice we will assume that η_a is usually much smaller than this due to water loading effects and less favorable values of the moist entropies. It is probably even less than 1.5 in most regions of development, though it must still be greater than 1. A shift of $\chi_2^{(0)}$, to which η_a is most sensitive, to 350 K drops η_a to about 1.5. For a given value of $\eta^{(0)}$ only two of the three $\chi_j^{(0)}$ can be chosen. In choosing $\chi_1^{(0)}$ and $\chi_2^{(0)}$ representative values for the inflow and outflow are desired, rather than the minimum in θ_e for the inflow and the value of θ_e^* at the tropopause for the outflow.

The bulk aerodynamic transfer coefficients, C_D and C_E , were both assigned somewhat standard values of order 10^{-3} . The linear surface drag was then chosen to be about $k_s \sim C_D \cdot 5 \text{ m/sec} \sim 5 \cdot 10^{-3} \text{ m/sec}$. For a given value of vertical diffusion ratio M , this then fixes the bulk vertical diffusion coefficient μ . Multiplication by the vertical length scale indicates that the values of μ for $M < 1$ imply vertical eddy diffusivities of less than $10 \text{ m}^2/\text{sec}$, which are quite small compared to the values chosen in some numerical models (e.g. Anthes 1971 used a vertical diffusivity of $5 \cdot 10^2 \text{ m}^2/\text{sec}$). Once given k_s , the value of $k_2^{(0)}$ was chosen to keep r_0 of order a couple of hundred kilometers and r_1 a couple of thousand kilometers or less.

This implied an upper level eddy viscosity $\lambda_2 \sim 10^4 \text{ m}^2/\text{sec}$. For the values of K chosen, λ_1 was smaller still. These values are smaller than those chosen for many axisymmetric numerical models (e.g. Anthes 1971 used a lateral eddy diffusivity of $5 \cdot 10^4 \text{ m}^2/\text{sec}$). With B set; f , $k_2^{(0)}$, and k_s already chosen; b is also determined and ends up of order 10^{-6} sec/m , β is of order $2 \cdot 10^{-4} \text{ m}/(\text{sec K})$, or after multiplication by the lapse rate and taking the reciprocal this implies a radiative relaxation time of one to two weeks. This cooling rate seems slightly smaller than realistic, but as already noted larger values of B require the use of Bessel functions of complex argument, which we wish to avoid. The eddy diffusivity in the boundary layer is the one parameter given unbelievable values; this is explained below in the discussion of the evaluation of $\chi_0^{(1)}$.

Two of the needed functions that are obtained as integrals, are the first order entropy perturbations in the boundary and upper layers, $\chi_0^{(1)}$ and $\chi_2^{(1)}$, respectively. The boundary layer perturbation is obtained after integrating eq. (5.35) twice. As additional conditions we require that $\left. \frac{\partial \chi_0^{(1)}}{\partial r} \right|_{r=0} = 0$ and $\chi_0^{(1)}(r_1) = 0$. This fixes the integration constants yielding

$$\chi_0^{(1)} = \int_r^{r_1} \frac{1}{k_\chi r'} \int_0^{r'} \left[-\frac{C_E v_1^{(1)}}{h_0} (\chi_s^{(0)} - \chi_0^{(0)}) + \frac{w_1^{(1)}}{h_0} (\chi_0^{(0)} - \chi_1^{(0)}) \right] r'' dr'' dr'. \quad (7.31)$$

The parameters k_χ , C_E , $\chi_s^{(0)}$, and $\chi_1^{(0)}$, appear in this integral and no others. Since there are only two terms in this equation, this set of parameters is effectively reduced to two. Further, the first term (proportional to $\chi_s^{(0)} - \chi_0^{(0)}$) dominates this formulation since in this model there are no strong downdrafts into the boundary layer. Because this linear (in factors involving v_j) expression has no feedback for reducing the entropy difference between the sea surface and the boundary layer, nor is there any boundary layer drying from downdrafts, $\chi_0^{(1)}$ can get so large that $\alpha \chi_0^{(1)}$ can exceed $\chi_s^{(0)} - \chi_0^{(0)}$, which is physically absurd. The lack of any turbulent fluxes of moist entropy from the boundary to lower layer also contributes to the excessive response in the boundary layer. To yield more reasonable values, k_χ was made unrealistically large. This is the only parameter that has been kludged to an unrealistic value. Another possible fix might have been to allow for variation in χ_1 , setting $\chi_0^{(1)} = \chi_1^{(1)}$, and replacing h_0 with $h_0 + h_1^{(0)}$ in eq. (7.31).

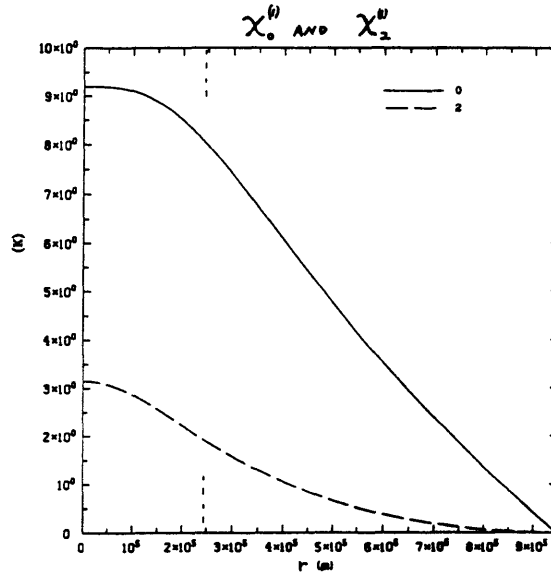


Figure 7.2: First order variations of the boundary layer and upper layer entropy, $\chi_0^{(1)}$ and $\chi_2^{(1)}$, respectively, for the linear solution in figure 6.14 and the parameters in table 7.2.

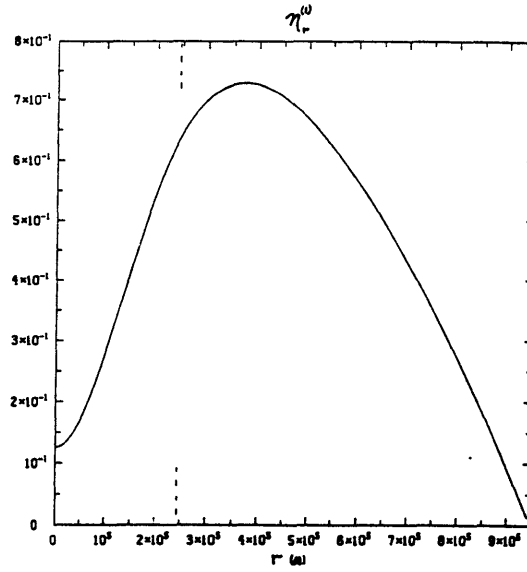


Figure 7.3: First order variation of the forcing parameter due to entropy changes, i.e. $\eta_r^{(1)}$, based on the $\chi_j^{(0)}$ of figure 7.2.

To find $\chi_2^{(1)}$ only a single integration is necessary. Equation (5.36) and the linearization of eq. (5.27), with the boundary condition $\chi_2^{(1)}(r_1) = 0$ leads to

$$\chi_2^{(1)} = \int_r^{r_1} \frac{\Xi f}{c_p(\pi_1 - \pi_2)} (v_2^{(1)} - v_1^{(1)}) dr' . \quad (7.32)$$

The radiative cooling at lowest order, $Q^{-(1)}$, is proportional to $\chi_2^{(1)}$ and is obtained directly from this expression. The parameters c_p , π_1 , π_2 , appear only in this integral, so this integral can be tuned through them. However, c_p is fixed, the π_j vary only slowly with the mean pressure of the layers, f is fixed for a given location, and the ad hoc factor $\Xi = 1.2$ can only be varied slightly. So, this integral cannot be easily tuned. Since it represents the thermal perturbation needed to maintain gradient wind balance, this is not surprising. Perturbations that are spatially large, intense, or at high latitude, require large temperature anomalies. A similar strong dependence on length scale and intensity is found in the integral for $\chi_0^{(1)}$. Plots of both of $\chi_0^{(1)}$ and $\chi_2^{(1)}$ are in figure 7.2. From these functions and eq. (5.34), one can determine the perturbation to the forcing parameter $\eta_r^{(1)}$, which is plotted in figure 7.3. To obtain a positive $\eta_r^{(1)}$, it must be that $\chi_0^{(1)} > \eta^{(0)} \chi_2^{(1)}$. One can always tune $\chi_0^{(1)}$ to meet this condition throughout the domain, though for large vortices or at high latitudes this might require unrealistic increases in the boundary layer entropy. The only other needed first order integral function is $\Phi_1^{(1)}$, for which the expression is given in eq. (7.24) and the plot has already been provided in figure 7.1.

Also provided is a plot of the second order terms of the Ekman pumping, $w^{(2*)}$, given in figure 7.4. At large amplitude, where the terms that make up this function dominate the Ekman pumping, it is easy to see that such a radial distribution of forced vertical velocity could lead to a well defined eyewall, as observed. Though $w^{(1)}$ must be nonnegative in the interval $[0, r_0]$ there is no such requirement on $w^{(2)}$. It must only be the case that $w = aw^{(1)} + a^2w^{(2)} \geq 0$. This appears to be violated in a very small region in the vicinity of the origin, but the area under the curve is so small that it has been ignored. Similarly, there is no requirement on the sign of $Q^{-(2)}$ (not shown), which is negative throughout.

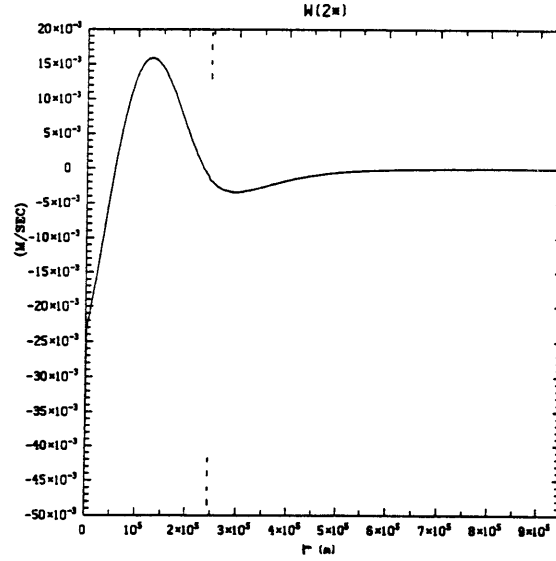


Figure 7.4: Second order correction to Ekman pumping, $w^{(2*)}$, for the linear solution in figure 6.14 and the parameters in table 7.2.

A negative value of either of these second order functions serves mostly to reduce the size, though not the sign, of the total quantities.

An evaluation of the integrals for the linear solution of figure 6.14, is shown in table 7.2. Values of all of the parameters are given in SI units. The evaluation of Σ has been broken into nine parts. Listing only the integrands (i.e. we need to operate on each of these with $\int_0^{r_1} \cdot r dr$, though terms involving η are only integrated on the interval $[0, r_0]$) they are:

1. $\left[v_1^{(1)} \left(M - \frac{M}{K} - BK \right) + v_2^{(1)} \left(\frac{M}{K} - B \right) + \frac{v_3^{(1)}}{K} \right] Q^{-(1)}(v_1^{(1)} - v_2^{(1)})$
2. $-\left[v_1^{(1)} \left(M - \frac{M}{K} - BK \right) + v_2^{(1)} \left(\frac{M}{K} - B \right) + \frac{v_3^{(1)}}{K} \right] \frac{k_A}{f} \zeta_1^{(1)} v_3^{(1)}$
3. $\left[v_1^{(1)} (M - BK) - v_2^{(1)} B \right] Q^{+(1)}(v_2^{(1)} - v_1^{(1)})$
4. $\left[v_1^{(1)} (M - BK) - v_2^{(1)} B \right] \frac{k_A}{f} \zeta_2^{(1)} (v_1^{(1)} + v_3^{(1)})$
5. $-\left[v_1^{(1)} (M - BK) - v_2^{(1)} B \right] \left[C_D |v_1^{(1)}| v_1^{(1)} - \frac{k_A}{f} v_1^{(1)} \frac{dr v_1^{(1)}}{r dr} \right]$

Evaluation of Integrals
Parameter Values and Eigenvalues

$M = \mu/k_s = 0.5$	$\eta^{(0)} = 2.75$
$K = k_1^{(0)}/k_2^{(0)} = 0.2$	$\mu = 2.5 \cdot 10^{-3} \text{ m/sec}$
$B = bf^2k_2^{(0)}/k_s^2 = 5.0 \cdot 10^{-2}$	$b = 4.0 \cdot 10^{-6} \text{ sec/m}$
$\lambda_1 = 5.0 \cdot 10^3 \text{ m}^2/\text{sec}$	$k_1^{(0)} = 2.5 \cdot 10^7 \text{ m}^3/\text{sec}$
$\lambda_2 = 1.2 \cdot 10^4 \text{ m}^2/\text{sec}$	$k_2^{(0)} = 1.2 \cdot 10^8 \text{ m}^3/\text{sec}$
$C_D = 2.0 \cdot 10^{-3}$	$C_E = 2.0 \cdot 10^{-3}$
$\chi_s = 365 \text{ K}$	$\chi_2^{(0)} = 344. \text{ K}$
$\chi_0^{(0)} = 352 \text{ K}$	$\chi_1^{(0)} = 340 \text{ K}$
$f = 5.0 \cdot 10^{-5} \text{ sec}^{-1}$	
$k_s = 5.0 \cdot 10^{-3} \text{ m/sec}$	$L = (k_2^{(0)}/k_s)^{1/2} = 1.6 \cdot 10^5 \text{ m}$
$k_\chi = 4.0 \cdot 10^6 \text{ m}^2/\text{sec}$	$V = fL = 7.9 \text{ m/sec}$
$r_0 = 2.4 \cdot 10^5 \text{ m}$	$r_1 = 9.5 \cdot 10^5 \text{ m}$

Values of Integrals

	Σ_i m^5/sec^3	Γ_i m^5/sec^2
	1. $1.2 \cdot 10^{10}$	$2.8 \cdot 10^{16}$
	2. $-3.6 \cdot 10^{10}$	$-5.6 \cdot 10^{15}$
$\Omega = -1.8 \cdot 10^{10} \text{ m}^5/\text{sec}^3$	3. $-2.0 \cdot 10^{10}$	$1.6 \cdot 10^{13}$
$\Sigma = -9.0 \cdot 10^{10} \text{ m}^5/\text{sec}^3$	4. $-1.7 \cdot 10^{10}$	$8.3 \cdot 10^{14}$
$\Gamma = 2.0 \cdot 10^{16} \text{ m}^5/\text{sec}^2$	5. $1.6 \cdot 10^{10}$	$5.1 \cdot 10^{13}$
	6. $-1.8 \cdot 10^{10}$	$-3.1 \cdot 10^{15}$
	7. $-4.6 \cdot 10^{10}$	
	8. $1.9 \cdot 10^{10}$	
	9. $-2.4 \cdot 10^8$	

$\eta_c^{(1)} = -\frac{\Sigma}{\Omega} = -4.9$ $f\gamma^{(1)} = -\frac{\Sigma}{\Gamma} = 4.5 \cdot 10^{-6} \text{ sec}^{-1}$
--

Table 7.2: Evaluation of integrals. The linear solution is shown in figure 6.14. See text for explanation of Σ_i and Γ_i .

$$\begin{aligned}
6. \quad & v_1^{(1)} k_2^{(0)} \frac{d}{dr} \left(\eta_r^{(1)} \frac{dr v_1^{(1)}}{r dr} \right) = -k_2^{(0)} \eta_r^{(1)} \left(\frac{dr v_1^{(1)}}{r dr} \right)^2 \\
7. \quad & v_1^{(1)} \frac{f k_2^{(0)}}{k_s} \frac{d}{dr} (\eta^{(0)} w^{(2*)}) = -\frac{dr v_1^{(1)}}{r dr} \frac{f k_2^{(0)}}{k_s} \eta^{(0)} w^{(2*)} \\
8. \quad & -v_1^{(1)} \frac{f k_2^{(0)}}{k_s} \frac{d}{dr} (w^{(2*)}) = \frac{dr v_1^{(1)}}{r dr} \frac{f k_2^{(0)}}{k_s} w^{(2*)} \\
9. \quad & -v_1^{(1)} \frac{f k_2^{(0)}}{k_s} \frac{d}{dr} (Q^{-(2*)}) = \frac{dr v_1^{(1)}}{r dr} \frac{f k_2^{(0)}}{k_s} Q^{-(2*)} .
\end{aligned}$$

For discussion, the related integrals will be referred to as Σ_i , $i = 1, 2, \dots, 9$, respectively. Similarly with Γ , the six separated parts have integrands

$$\begin{aligned}
1. \quad & \left[v_1^{(1)} \left(M - \frac{M}{K} - BK \right) + v_2^{(1)} \left(\frac{M}{K} - B \right) + \frac{v_3^{(1)}}{K} \right] h_1^{(0)} v_1^{(1)} \\
2. \quad & \left[v_1^{(1)} (M - BK) - v_2^{(1)} B \right] \epsilon h_2^{(0)} v_2^{(1)} \\
3. \quad & - \left[v_1^{(1)} (M - BK) - v_2^{(1)} B \right] \frac{f}{gr} \Phi_1^{(1)} \\
4. \quad & \left[v_1^{(1)} (M - BK) - v_2^{(1)} B \right] h_0 v_1^{(1)} \\
5. \quad & v_1^{(1)} \frac{f^2 k_2^{(0)}}{g(1-\epsilon)k_s} (v_1^{(1)} - \epsilon v_2^{(1)}) \\
6. \quad & v_1^{(1)} (\eta^{(0)} - 1) \frac{h_0 k_2^{(0)}}{k_s} \square^2 v_1^{(1)} = -(\eta^{(0)} - 1) \frac{h_0 k_2^{(0)}}{k_s} \left(\frac{dr v_1^{(1)}}{r dr} \right)^2 .
\end{aligned}$$

These will be referred to as Γ_i , $i = 1, 2, \dots, 6$, respectively.

The expected signs of the Σ terms were discussed in section 7.2. Terms that tend to weaken the cyclone are Σ_1 , Σ_5 , and Σ_8 . The first of these represents transport of anticyclonic relative momentum into the cyclonic lower layer through radiative cooling. The two other terms are both tied to second order effects of the forced vertical velocity. One must recall that though in developing a tropical cyclone it is desirable to have lower level inflowing air, the accompanying outflow is a net cost. Ideally for development, inflowing air would just vanish, but alas the outflow is inevitable. Both Σ_5 and Σ_8 are from second order effects that lead to increased outflow aloft and hence increase the strength of the upper level anticyclone. In our first example, these terms are all of the same order of magnitude.

There are a surprisingly large number of second order terms that encourage tropical cyclone development. The largest of these in table 7.2 is Σ_7 . This is one of the two nonlinear CISK terms. It is from the increased convection based on the initial stratification and the faster than linear growth of the forced vertical velocity out of the boundary layer. The other nonlinear CISK term, Σ_6 , is from increases in the boundary layer entropy from wind enhanced sea surface fluxes (mostly of moisture), partially compensated by an increase in the stable stratification from warming aloft needed to maintain gradient wind balance. It is the only term dependent on the coefficient Ξ in eqs. (5.36) and (7.32) used to determine the magnitude of the saturation potential temperature perturbation in the upper level. This term is partially in the spirit of hurricane air-sea interaction theory, but not quite, since it still relies on frictionally forced vertical velocity to release any of this added potential energy. The competing processes of boundary layer moistening and upper tropospheric warming could be accounted separately, though we will not do so here. The relative magnitudes of these terms, both with respect to each other and with respect to the other second order terms, can be easily adjusted by tweaking the parameters and should not be viewed as a robust result of this analysis.

The nonlinear momentum advection terms in the lower and upper layers, Σ_2 and Σ_4 , both encourage development of the disturbance. In the lower layer it is easy to see that the advection of positive relative vorticity, in addition to the planetary vorticity, helps build the cyclonic flow. The situation aloft is more subtle. We have already argued that energy spent in developing the anticyclone hinders the development of the low level cyclone. Aloft, there is negative relative vorticity in the first order solutions, except at very large radius. Outward advection of negative relative vorticity reduces the anticyclone. Another way to view this, is to examine total vorticity advection and note that for overall disturbance development one wishes to minimize this advection aloft. The negative relative vorticity reduces the total vorticity that is being advected and so helps prevent the development of a stronger anticyclone. The last term to cover is Σ_3 , which is the cumulus momentum mixing term. In the presence of negative vertical shear,

this tends to reduce the strength of the anticyclone and so help overall disturbance growth.

In the presence of all of these positive influences from the second order terms, to maintain a steady state at finite amplitude, the forcing parameter need not be as large as it must be for a steady balance with an infinitesimal disturbance. The term $\eta_c^{(1)}\Omega$ in eq. (7.14) represents physics similar to that of Σ_6 , which is based on changes in the vertical thermodynamic structure due to the first order motion. By fiat, through the solvability condition, it is declared to balance the positive influences of the other second order terms. It therefore provides the quantitative measure of the amount by which the forcing parameter may be reduced to keep steady balance for a given amplitude.

If we do not have an exact balance, but instead have an evolving disturbance, the extra forcing (of either sign) goes into changing the energy of the system. Loosely, the forcing balances the time rate of change of the system energy, or for exponential growth it balances the growth rate times the energy. The integrals that make up Γ can be viewed in some sense as energies of the system. That large positive values of Γ lead to small growth rates, reflects the fact that the greater the energy of a system the more difficult it is to maintain exponential intensification. For rapid growth, small positive values of Γ are required. Again, the upper layer persists in its contrary role, by reducing overall Γ through Γ_2 . The integrals of Γ_4 and Γ_1 are closely related to the kinetic energies of the boundary and lower layers. The potential energy of tilted isotherms is represented by Γ_3 and Γ_5 . The term Γ_6 is related to the time dependent corrections to the forced vertical velocity at the top of the boundary layer.

If one assumes an ambient η_a of say 1.2, then the critical Rossby number is about 0.37. This corresponds to an organized tangential velocity maximum of 3.5 m/sec and a center surface vorticity of $5.7 \cdot 10^{-5} \text{ sec}^{-1}$ (n.b. nondimensionally $\frac{\partial r v_1^{(1)}}{r \partial r}$ is 3.1), which is slightly greater than f despite the not-large nondimensional amplitude. The e-folding time is $(3.75 \cdot 10^{-6} \text{ sec}^{-1})^{-1} \approx 3$ days, divided by the Rossby number. With $a_{crit} \approx 0.37$, this is too long at about 8 days. If one stretches the theory past the stationary point, at a Rossby number of 1, which for

these parameters requires a v_1 maximum of $fL \approx 8 \text{ m/sec}$, the e -folding time of about 3 days is quite reasonable. Even a disturbance requiring a large value of the forcing parameter, in an environment with only small amounts of CAPE, can be destabilized with sufficient amplitude. For solutions requiring a large value of $\eta^{(0)}$, unless the boundary layer entropy is allowed to become very large, the dominant terms at second order are the nonlinear advections of disturbance vorticity.

If we choose only to apply the theory *at* the stationary point, we are in the slightly odd position of finding that the closer a disturbance is to the linear instability criterion, the smaller its growth rate. This is absurd. If instead we continue to take the growth rate as $\gamma = a\gamma^{(1)}$, with a increasing in time, superexponential growth results. This will be discussed further in section 7.5.

We will now examine how the finite amplitude instability criteria vary with variations of many of the physical parameters. Unless specified otherwise, all of parameters are as specified in table 7.2. Results from variation of the quadratic bulk diffusion coefficient for the boundary layer, C_D , are shown in table 7.3. Increases in C_D lead to increases in the magnitude of $\eta_c^{(1)}$, hence decreases in the threshold amplitude for growth, and increases in the growth rate of the finite amplitude disturbances. So, increases in the loss of boundary layer momentum to the surface encourages tropical cyclone development. The only integrals affected by changes in C_D are Σ_5 , Σ_7 and Σ_8 . The magnitudes of all of these increase with increasing C_D . Though Σ_5 and Σ_8 are both dissipative, these are more than compensated by the additional cumulus heating driven by the additional Ekman pumping. Variations in the bulk entropy diffusion coefficient, C_E are even easier to understand since only Σ_6 is effected. Changes due to variations in this coefficient are shown in table 7.4. Increasing C_E also encourages development by increasing the perturbation to the forcing parameter, η . Variations in the sea surface entropy, χ_s , and the lateral entropy diffusion coefficient in the boundary layer, k_χ , can all be modelled through variations in C_E and will not be treated separately.

Examination of the variation of the finite amplitude instability criteria with variation of the remaining parameters is not simple. Varying one parameter can force variations in several other parameters. For example, varying the Coriolis

**Finite Amplitude Instability Criteria
With Varying C_D**

C_D	$\eta_c^{(1)}$	$f\gamma^{(1)}$ (sec ⁻¹)
0.001	-4.2	$3.8 \cdot 10^{-6}$
0.002	-4.9	$4.5 \cdot 10^{-6}$
0.003	-5.6	$5.1 \cdot 10^{-6}$

Table 7.3: Variations in finite amplitude instability criteria with variations in bulk momentum diffusion coefficient, C_D . All other parameters are as in table 7.2.

**Finite Amplitude Instability Criteria
With Varying C_E**

C_E	$\eta_c^{(1)}$	$f\gamma^{(1)}$ (sec ⁻¹)
0.001	-3.8	$3.5 \cdot 10^{-6}$
0.002	-4.9	$4.5 \cdot 10^{-6}$
0.003	-6.0	$5.5 \cdot 10^{-6}$

Table 7.4: Variations in finite amplitude instability criteria with variations in bulk entropy diffusion coefficient, C_E . All other parameters are as in table 7.2.

parameter with a constant nondimensional cooling constant, B , implies a variation of the dimensional cooling constant b . If one wished to vary f with constant b , one must also vary B and calculate a new linear stationary solution. Changes to the upper level lateral diffusion coefficient, $k_2^{(0)}$, are even more complicated, since they change the length scale, as well as requiring a proportional variation in $k_1^{(0)}$ for constant K . So as in the process of taking partial derivatives on a manifold (e.g. the determination of the Maxwell relations in classical thermodynamics), one must specify not only what is varied, but also what is held constant. For this reason graphs are not provided of the dependencies; they would be easy to digest, but might give a misleading impression of the solution behavior.

Results for variations in the Coriolis parameter are shown in table 7.5. The

**Finite Amplitude Instability Criteria
With Varying Coriolis Parameter**

f (sec ⁻¹)	$\eta_c^{(1)}$	$f\gamma^{(1)}$ (sec ⁻¹)	$-\frac{\eta_c^{(1)}}{fL}$ (sec/m)
$5.0 \cdot 10^{-6}$	-2.7	$2.5 \cdot 10^{-6}$	3.4
$1.0 \cdot 10^{-5}$	-3.0	$2.8 \cdot 10^{-6}$	1.9
$3.0 \cdot 10^{-5}$	-4.1	$3.8 \cdot 10^{-6}$	0.87
$5.0 \cdot 10^{-5}$	-4.9	$4.5 \cdot 10^{-6}$	0.62
$7.0 \cdot 10^{-5}$	-5.3	$4.8 \cdot 10^{-6}$	0.48
$1.0 \cdot 10^{-4}$	-5.3	$4.8 \cdot 10^{-6}$	0.34

Table 7.5: Variations in finite amplitude instability criteria with variations in Coriolis parameter. The dimensional cooling parameter, b , is allowed to vary, so that the nondimensional cooling parameter, B , can be held constant. All other parameters are as in table 7.2, with the exception of V .

dimensional vorticity and velocity scales, f and fL , increase linearly with increasing f . Hence the magnitude of the dimensional perturbation threshold continues to increase with latitude even though $-\eta_c^{(1)}$ is increasing, because the variation of the latter is weak. This can be seen in the last column of table 7.5. (If the dimensional magnitude of $-\eta_c^{(1)}/(fL)$ is made smaller, a stronger disturbance is needed to overcome the threshold.) At very low latitudes, where the threshold is quite small dimensionally, though it is easy for a disturbance to start growing, it is initially so weak and the growth rate so small that it would take weeks to become of notice (or hit land or be destroyed by shear). The magnitudes of Ω ; Γ_1 , Γ_2 , Γ_4 , Γ_6 ; and the terms Σ_1 , Σ_2 , Σ_3 , Σ_4 , Σ_9 ; are all proportional to f^2 . The terms Γ_3 , Γ_5 increase as f^4 . The various conflicting dependencies on the rotational parameter are still in need of additional analysis. However, it appears that it is more difficult to initiate development at higher latitude, but if the threshold is exceeded intensification is more rapid.

Proportional variations in the lateral diffusion coefficients $k_1^{(0)}$ and $k_2^{(0)}$ with constant K lead to a confounding change in the length scale of the system due to the choice of the nondimensionalization. Results of such variation are shown in

**Finite Amplitude Instability Criteria
With Varying Lateral Diffusion**

$k_1^{(0)}$ (m ³ /sec)	$\eta_c^{(1)}$	$f\gamma^{(1)}$ (sec ⁻¹)	$-\frac{\eta_c^{(1)}}{fL}$ (sec/m)
$1.0 \cdot 10^7$	-3.5	$3.2 \cdot 10^{-6}$	0.70
$2.0 \cdot 10^7$	-4.4	$4.0 \cdot 10^{-6}$	0.62
$2.5 \cdot 10^7$	-4.9	$4.5 \cdot 10^{-6}$	0.62
$3.0 \cdot 10^7$	-5.5	$5.0 \cdot 10^{-6}$	0.63
$4.0 \cdot 10^7$	-6.8	$6.2 \cdot 10^{-6}$	0.68

Table 7.6: Variations in finite amplitude instability criteria with proportional variations in the lateral diffusion coefficients, $k_1^{(0)}$ and $k_2^{(0)}$, keeping K constant. Other parameters are as in table 7.2, with the exceptions of L , V , r_0 , r_1 , b , and the λ_j .

**Finite Amplitude Instability Criteria
With Varying Vertical Diffusion**

k_s (m/sec)	$\eta_c^{(1)}$	$f\gamma^{(1)}$ (sec ⁻¹)	$-\frac{\eta_c^{(1)}}{fL}$ (sec/m)
0.003	-8.4	$4.6 \cdot 10^{-6}$	0.82
0.004	-6.1	$4.4 \cdot 10^{-6}$	0.69
0.005	-4.9	$4.5 \cdot 10^{-6}$	0.62
0.006	-4.2	$4.6 \cdot 10^{-6}$	0.58

Table 7.7: Variations in finite amplitude instability criteria with proportional variations in the linear boundary layer diffusion coefficient k_s and the vertical diffusion coefficient μ . The vertical diffusion ratio, M, is kept constant, so μ is also increasing as one moves down the table entries. Other parameters are as in table 7.2, with the exceptions of L , V , r_0 , r_1 , and b .

**Finite Amplitude Instability Criteria
With Varying r_1**

r_1	$\eta_c^{(1)}$	$f\gamma^{(1)}$ (sec^{-1})
6.0	-4.9	$4.5 \cdot 10^{-6}$
8.0	-5.1	$5.0 \cdot 10^{-6}$
10.0	-5.3	$5.2 \cdot 10^{-6}$

Table 7.8: Variations in finite amplitude instability criteria with variations in overall disturbance size, r_1 . All other parameters are as in table 7.2 except for the dimensional value of r_1 , though there is very slight variation in $\eta^{(0)}$ and r_0 (see table 6.1).

table 7.6. Increases in the diffusion coefficients imply an increase in both the length scale and the velocity scale, fL . Though $\eta_c^{(1)}$ is seen to increase monotonically with increases in $k_1^{(0)}$, seeming to imply a decrease in the threshold amplitude, the dimensional amplitude of the needed disturbance is fairly insensitive to these variations and does not vary monotonically, as can be seen in the last column of the table. Somewhat surprisingly (c.f. Emanuel 1986, Rotunno and Emanuel 1987), the larger disturbances grow faster (also see discussion of variations of r_1 , p. 205). It would have been possible to vary r_1 to compensate for changes in L so as to leave the disturbance size constant. However, this would have required variations of $\eta^{(0)}$ (albeit very small ones) and it still would not have been possible to provide compensatory change of the updraft radius, r_0 , which is probably much more important. Proportional variations in the linear vertical diffusion coefficients also change the length scale of the system through the nondimensionalization. These are shown in table 7.7. The growth rate is insensitive to this variation, but proportional increases in both vertical diffusion parameters require a stronger disturbance to exceed the intensification threshold.

Our remaining comparisons all require calculation of different linear solutions rather than simply varying the parameters needed to evaluate the integrals as second order. As can be seen in table 7.8, increases in the overall disturbance size lead to decreases in the threshold amplitude and increases in growth rate,

though the effect is not strong. This was surprising in view of the results of Emanuel (1986) and Rotunno and Emanuel (1987), which showed that the larger disturbances grew more slowly and very large ones barely intensified at all. One significant difference between the size variation here and in Emanuel and Rotunno, is that here the size of the inner core of the disturbance was basically unchanged as the outer extent was varied, while in Rotunno and Emanuel the entire structure of the disturbance was scaled proportionally. Here, the primary reason for this increase in development potential for large disturbances is that the boundary layer formulation leads to greater entropy perturbations in the disturbance core for overall larger disturbances. I am unaware of any observational evidence either supporting or contradicting this result. Evaluation of the integrals was not performed at still larger radius, to see if the variations changed sign, because of numerical difficulties solving the linear stationary problem with large r_1 , where some of the Bessel and modified Bessel functions become extremely large.

Tables 7.9 and 7.10 examine independent variations of the upper and lower layer lateral eddy diffusivities. These also require varying the lateral diffusion ratio, K , which in turn changes the threshold for the forcing parameter $\eta^{(0)}$. Variations of the upper level lateral diffusion, $k_2^{(0)}$, add the further complication of changes to the length scale. The most significant change with increases in $k_2^{(0)}$ is the accompanying decrease in $\eta^{(0)}$, which is a first order change. The magnitude of $\eta_c^{(1)}$ also increases and whether or not it is sufficient to compensate depends on the subcriticality of the rest state. For example, if $\eta_a = 2.0$ then the critical velocity maximum is 0.91 m/sec ($= [\eta_a - \eta^{(0)}]fL/\eta_c^{(1)}$) for the $K = 0.5$ case and 0.80 m/sec for the $K = 0.2$ case, so the linear effect of decreasing $\eta^{(0)}$ dominates. However, if η_a is more subcritical at say 1.5, then the critical velocities are 1.2 m/sec and 1.4 m/sec, respectively, and the relative thresholds are reversed. (The test values of η_a were chosen to be large only because the values of $\eta^{(0)}$ in the examples were quite large.) Similar arguments apply to variations of $k_1^{(0)}$ shown in table 7.10. However, since there is no additional help from variations in the length scale, unless the rest state is greatly subcritical increases in lower layer diffusion make it more difficult to create an intensifying disturbance.

**Finite Amplitude Instability Criteria
With Varying Upper Level Lateral Diffusion**

$k_2^{(0)}$ (m^3/sec)	K	$\eta^{(0)}$	$\eta_c^{(1)}$	$f\gamma^{(1)}$ (sec^{-1})	$-\frac{\eta_c^{(1)}}{fL}$ (sec/m)
$5.00 \cdot 10^7$	0.50	3.36	-7.5	$1.1 \cdot 10^{-5}$	1.49
$1.25 \cdot 10^8$	0.20	2.64	-6.4	$6.6 \cdot 10^{-6}$	0.80

Table 7.9: Variations in finite amplitude instability criteria with variations in the upper level lateral diffusion coefficient, $k_2^{(0)}$. The lateral diffusion ratio, K, is varied so as to keep $k_1^{(0)}$ constant. The cooling parameter is set at $B = 0.005$. Other parameters are as in table 7.2, with the exceptions of L , V , r_0 , r_1 , b , and λ_2 .

**Finite Amplitude Instability Criteria
With Varying Lower Level Lateral Diffusion**

$k_1^{(0)}$ (m^3/sec)	K	$\eta^{(0)}$	$\eta_c^{(1)}$	$f\gamma^{(1)}$ (sec^{-1})
$2.50 \cdot 10^7$	0.20	2.64	-6.4	$6.6 \cdot 10^{-6}$
$6.25 \cdot 10^7$	0.50	3.36	-9.8	$1.5 \cdot 10^{-5}$

Table 7.10: Variations in finite amplitude instability criteria with variations in the lower level lateral diffusion coefficient, $k_1^{(0)}$. The lateral diffusion ratio, K, is varied so as to keep $k_2^{(0)}$ constant. The cooling parameter is set at $B = 0.005$. Other parameters are as in table 7.2, with the exceptions of b and λ_1 .

Tables 7.11 and 7.12 apply to independent variations of the vertical diffusion coefficients μ and k_s , respectively. The effect of varying μ is similar to varying $k_1^{(0)}$, and the effect of varying k_s is similar to varying $k_2^{(0)}$. The only exception to this is that increases in k_s lead to decreases in the length scale, which is opposite to the effect of increases in $k_2^{(0)}$. Unless the rest state is very subcritical, larger values of boundary layer friction, k_s , require weaker disturbances for intensification and larger values of internal diffusion, μ , require stronger initial disturbances for intensification.

Each of the variations just examined has been treated one parameter at a

**Finite Amplitude Instability Criteria
With Varying Internal Vertical Diffusion**

μ (m/sec)	M	$\eta^{(0)}$	$\eta_c^{(1)}$	$f\gamma^{(1)}$ (sec ⁻¹)
0.0010	0.2	1.93	-3.9	$4.4 \cdot 10^{-6}$
0.0025	0.5	2.64	-6.4	$6.6 \cdot 10^{-6}$

Table 7.11: Variations in finite amplitude instability criteria with variations in the internal vertical diffusion coefficient, μ . The vertical diffusion ratio, M, is varied so as to keep k_s constant. The cooling parameter is set at $B = 0.005$. All other parameters are as in table 7.2, with the exception of b .

**Finite Amplitude Instability Criteria
With Varying Linear Drag Coefficient**

k_s (m/sec)	M	$\eta^{(0)}$	$\eta_c^{(1)}$	$f\gamma^{(1)}$ (sec ⁻¹)	$-\frac{\eta_c^{(1)}}{fL}$ (sec/m)
0.0050	0.5	2.64	-6.4	$6.6 \cdot 10^{-6}$	0.80
0.0125	0.2	1.93	-1.8	$4.9 \cdot 10^{-6}$	0.36

Table 7.12: Variations in finite amplitude instability criteria with variations in the linear drag coefficient, k_s . The vertical diffusion ratio, M, is varied so as to keep μ constant. The cooling parameter is set at $B = 0.005$. Other parameters are as in table 7.2, with the exceptions of L , V , r_0 , r_1 , and b .

time. Since the integral expressions are all nonlinear, there may be combinations of parameters that when varied together have a very strong effect. These possibilities have not yet been studied.

7.5 Amplitude Equations and Superexponential Growth

All of the complex machinations of this chapter can be reduced to a simple amplitude equation. We will now examine a heirarchy of such equations. These will also serve to provide justification for the claim that superexponential growth is an apporprate description for the intensification rate of disturbances that are of sufficient amplitude to grow.

The simplest amplitude equation we will consider is the linear homogeneous rate equation

$$\frac{da}{dt} = c_1 a , \quad (7.33)$$

where c_1 is a constant. Solutions to this equation have exponential growth for positive real c_1 , exponential decay for negative real c_1 , sinusoidal oscillations for pure imaginary c_1 , growing oscillations for complex c_1 with positive real part, and decaying oscillations for complex c_1 with negative real part. This list is exhaustive. The only stationary point is at $a = 0$. As noted earlier, such a linear equation is incapable of demonstrating threshold behavior.

The second equation in the heirarchy is the quadratic homogeneous rate equation

$$\frac{da}{dt} = c_1 a + c_2 a^2 , \quad (7.34)$$

where both c_j are constants. This equation is the one appropriate for comparison with the work already presented here. There are now two stationary points, again one at $a = 0$ and another at $a = -\frac{c_1}{c_2}$. Complex values of c_1 and c_2 allow various types of complicated oscillating behavior. No longer is there symmetry between positive and negative values of the amplitude. The full solution is

$$a = \frac{c_1 a_0}{(c_1 + c_2 a_0)e^{-c_1 t} - c_2 a_0} , \quad (7.35)$$

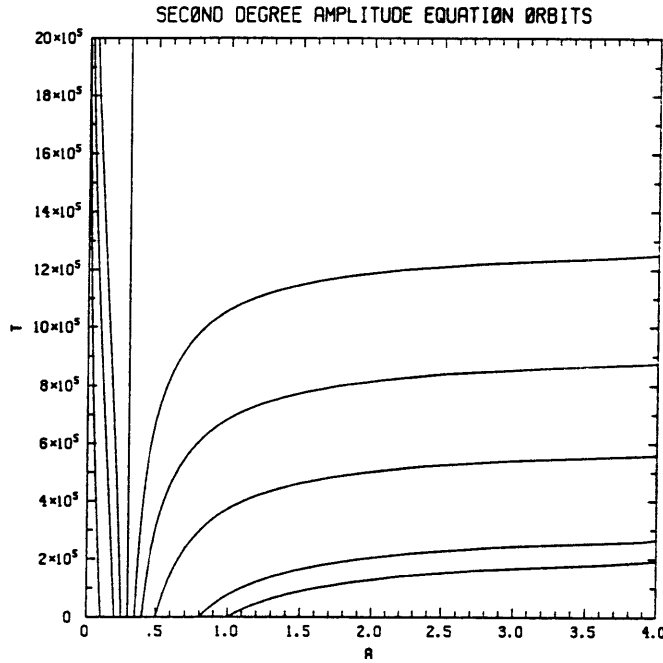


Figure 7.5: Orbits for the quadratic amplitude equation $\frac{da}{dt} = c_1 a + c_2 a^2$ with $c_1 = -1.5 \cdot 10^{-7}$, $c_2 = 5 \cdot 10^{-6}$.

where $a(t = 0) = a_0$ determines the one integration constant.² It is a simple matter for the curious to examine the behavior of this expression for a variety of conditions on c_1 , c_2 and a_0 . Further analysis will be restricted to the case of c_1 and c_2 real. For negative values of c_1 , $a = 0$ is a stable stationary point and for c_1 positive, $a = 0$ is an unstable stationary point; these correspond to similar results for the linear case. Figure 7.5 shows behavior for several initial conditions in the space of $a \times t$ for the case $c_1 < 0$ and $c_2 > 0$. If $a_0 < 0$ then $a(t)$ decays from below. If $0 < a_0 < -c_1/c_2$ then $a(t)$ decays to zero from above. If $a_0 > -c_1/c_2$ then $a(t)$ blows up in finite time and it makes no sense to press the solutions further. This is faster than exponential, or simply *superexponential* growth. We will return to this equation to show how the coefficients are chosen to correspond to our earlier analysis after examining the next equation in the sequence of amplitude equations.

²This solution is found using the standard indefinite integral $\int \frac{da}{a(c_1 + c_2 a)} = -\frac{1}{c_1} \ln \left(\frac{c_1 + c_2 a}{a} \right) + \text{constant}$.

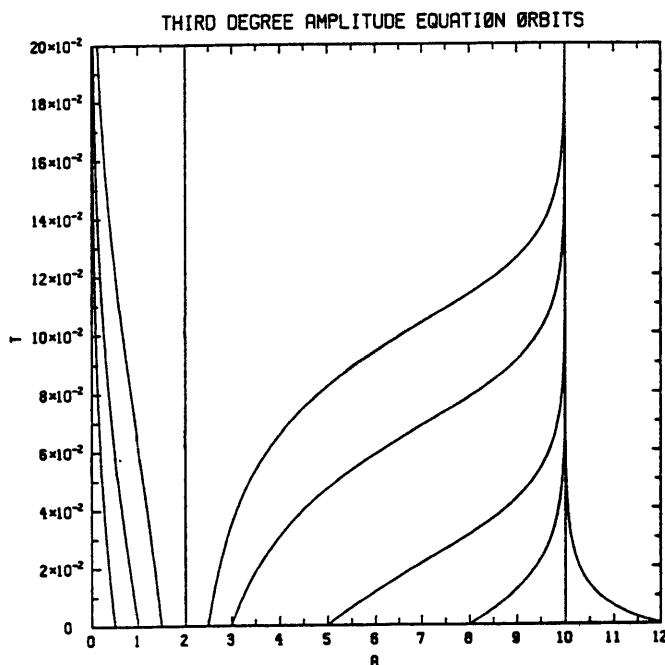


Figure 7.6: Orbits for the cubic amplitude equation $\frac{da}{dt} = c_1 a + c_2 a^2 + c_3 a^3$ with $c_1 = -20$, $c_2 = 12$, $c_3 = -1$.

The last equation in this hierarchy that we will examine is

$$\frac{da}{dt} = c_1 a + c_2 a^2 + c_3 a^3. \quad (7.36)$$

This equation has three stationary points: 0 , $[-c_2 \pm (c_2^2 - 4c_1c_3)^{1/2}]/(2c_3)$. The two nonzero stationary points will be designated a_+ and a_- depending on the choice of sign. In the limit of $c_3 \rightarrow 0$ this returns the single nonzero stationary point of the previous equation at $-c_1/c_2$. We will now assume that all of the c_i are real, that $c_1 < 0$, $c_2 > 0$, $c_3 < 0$, and that $c_2^2 > 4c_1c_3$. For these restrictions the stationary points are all real and ordered as $0 < a_+ < a_-$. The general solution can be found analytically, but requires different expressions depending on where one chooses the initial condition with respect to the stationary points. It is simpler to integrate numerically as was done to produce figure 7.6, which shows paths for several initial conditions. (The ratio of the amplitudes of the stable stationary point to the unstable stationary point is much too small to be

appropriate for a tropical cyclone, but an appropriate ratio would be of order 100 and would make it difficult to see the behaviors of the different types of orbits.) If $a_0 < a_+$ the amplitude decays to zero monotonically. If $a_0 > a_+$ the amplitude heads to a_- . In this context a_+ , which is an unstable stationary point, represents the threshold amplitude and a_- , which is stable, represents the amplitude of the mature disturbance. We might aspire to an analytic theory that exhibits the behavior of this amplitude equation.

We now return to the slightly simpler system with threshold behavior and runaway growth. At the critical amplitude the ambient and effective forcing parameters are equal. With eq. (7.18)

$$a_{crit} = \frac{\eta_a - \eta^{(0)}}{\eta_c^{(1)}} = -\frac{c_1}{c_2} > 0 . \quad (7.37)$$

Expansion of eq. (7.34) about a_{crit} with the perturbation amplitude \tilde{a} defined by $a = a_{crit} + \tilde{a}$ leads to the linear amplitude equation

$$\frac{d\tilde{a}}{dt} = c_1 a_{crit} + c_1 \tilde{a} + c_2 a_{crit}^2 + 2c_2 a_{crit} \tilde{a} = -c_1 \tilde{a} . \quad (7.38)$$

Comparing this with eq. (7.30) suggests equating $-c_1$ with $f\gamma^{(1)}a_{crit}$. With eq. (7.37) we then have

$$c_1 = \frac{f\gamma^{(1)}(\eta^{(0)} - \eta_a)}{\eta_c^{(1)}} < 0 \quad (7.39)$$

$$c_2 = f\gamma^{(1)} > 0 \quad (7.40)$$

and the amplitude equation

$$\frac{da}{f dt} = \frac{\gamma^{(1)}}{\eta_c^{(1)}}(\eta^{(0)} - \eta_a)a + \gamma^{(1)}a^2 . \quad (7.41)$$

Though this has the behavior we desire for $a < 0$, the coefficients are not at all correct in that regime since the physics used in the determination of the coefficients does not apply to a disturbance with a low level anticyclone near the origin.

The specific solution, at least for positive a_0 is

$$a(t) = \frac{a_0}{\frac{a_0}{a_{crit}} + (1 - \frac{a_0}{a_{crit}})e^{a_{crit}\gamma^{(1)}t}}, \quad \text{where} \quad (7.42)$$

$$0 < t < t_{max} = \frac{1}{\gamma^{(1)}a_{crit}} \ln \left(\frac{a_0}{a_0 - a_{crit}} \right).$$

The concept of a simple growth rate cannot be applied to this type of solution. Clearly if the initial amplitude equals the critical amplitude the singularity is never reached. However, if a_0 is only 20% greater than a_{crit} the singularity of infinite amplitude is reached in less than two weeks for the case examined in table 7.2 with $\eta_a \approx 1.2$. The mature amplitude would be reached a little more quickly. The paths of figure 7.5 roughly correspond to this case if t is measured in seconds and the velocity amplitude is nondimensionalized with a velocity scale of about 8 m/sec. As can be seen, the time required to reach maturation decreases rapidly with increases in the supercriticality of the initial disturbance.

"But how did we get here?" asked Milo, who was still a bit puzzled by being there at all.

"You jumped, of course," explained Canby. "That's the way most everyone gets here. It's really quite simple: every time you decide something without having a good reason, you jump to [the island of] Conclusions whether you like it or not. It's such an easy trip to make that I've been here hundreds of times."

"But this is such an unpleasant looking place," Milo remarked.

"Yes, that's true," admitted Canby; "it does look much better from a distance."

As he spoke, at least eight or nine more people sailed onto the island from every direction possible.

"Well, I'm going to jump right back," announced the Humbug, who took two or three practice bends, leaped as far as he could, and landed in a heap two feet away.

"That won't do at all," scolded Canby, helping him to his feet. "You can never jump away from Conclusions. Getting back is not so easy. That's why we're so terribly crowded here. . . . The only way back is to swim, and that's a very long and a very hard way."

"I don't like to get wet," moaned the unhappy bug, and shuddered at the thought.

"Neither do they," said Canby sadly. "That's what keeps them here. But I wouldn't worry too much about it, for you can swim all day in the Sea of Knowledge and still come out completely dry. Most people do. . . ."

Norton Juster
The Phantom Tollbooth

Chapter 8

Discussions and Conclusions

8.1 Discussions

8.1.1 Application to Real Disturbances

In section 7.3 it was shown that the finite amplitude stationary states found earlier in section 7.2 are unstable to perturbations with the same spatial structure. Such perturbations, rather than disrupting the structure, lead either to its intensification or decay. (This is in contrast to work such as Schlüter et alii 1965 where conditions were sought for the breakdown of otherwise stable stationary states.) It is straight forward conceptually that states with amplitudes below a certain value decay, while states with larger amplitudes grow. The relationship of the amplitude of the stationary states to the value of the forcing parameter is less intuitive.

To understand this work, it is crucial to understand how it is that though the lowest order value of the forcing parameter in the expansion, $\eta^{(0)}$, is greater than the value of the forcing parameter needed for the existence of linearly unstable solutions to the differential equations (though not compatible with the boundary conditions), there is no assumption that the rest state is linearly unstable. We defined earlier that the effective forcing parameter $\eta_e \equiv \eta^{(0)} + \bar{a}\eta_c^{(1)}$. One is stuck with whatever ambient value of η_a the atmosphere provides. This is determined mostly by the radiative-convective balance of the tropical atmosphere

for the underlying sea surface temperature (which is determined by the radiative-
evaporative balance and the ocean circulation) and the large scale atmospheric
circulation. For cyclonic disturbances, \bar{a} is positive and $\eta_c^{(1)}$ is negative. If the re-
sulting η_e is greater than η_a , then the disturbance will decay. Even if η_a is greater
than $\eta_{crit}^{(0)}$, it is still not necessarily greater than the value needed for the particular
disturbance being examined, since for any given disturbance $\eta^{(0)} > \eta_{crit}^{(0)}$. A value
of $\eta^{(0)}$ just barely greater than $\eta_{crit}^{(0)}$ allows the existence of real solutions to the
differential equations, but does not guarantee that any of these are consistent with
the boundary conditions. However, if we do have $\eta^{(0)} > \eta_{crit}^{(0)} > \eta_a > \eta_e$, as given
in eq. (6.22), there is subcritical instability from a transcritical bifurcation.

Figure 8.1 shows a schematic of the decaying and growing states as a function
of disturbance amplitude and the ambient value of the entrainment parameter,
 η_a . The theory presented here has determined the slope of the stability boundary
where it intersects the line of zero amplitude and the intercept (solid line), which
is the linear instability criterion. We also know that there are no hurricane-like
instabilities for $\eta < 1$, since that would lead to outflow rather than inflow in the
lower troposphere and would not spin-up a low level cyclone. Since a disturbance
can alter the boundary layer entropy, the local value of η can be greater than 1
even if the ambient value is less than 1. Therefore, one cannot declare that the
region with $\eta_a < 1$ is strictly stable. We might hope that the stability boundary
resembles the dense line of dots shown in the figure. The sparse dotted line
indicates what the stability boundary might look like if the curvature determined
at third order were positive and very large; the calculation of this next order
term would be an horrendous task. In that case the range of applicability of the
theory presented here would be so small that an amplitude threshold would not be
predicted. However, unless the nondimensional scaling was totally inappropriate
(or some important process totally omitted from the basic equations), I expect
that the stability boundary can be extended to near where a approaches 1 from
below or η_a approaches 1 from above, whichever is reached first.

Applying this theory does present difficulties. In any type of system, it is
difficult to deliberately arrange for motionless unstable stationary states. To find

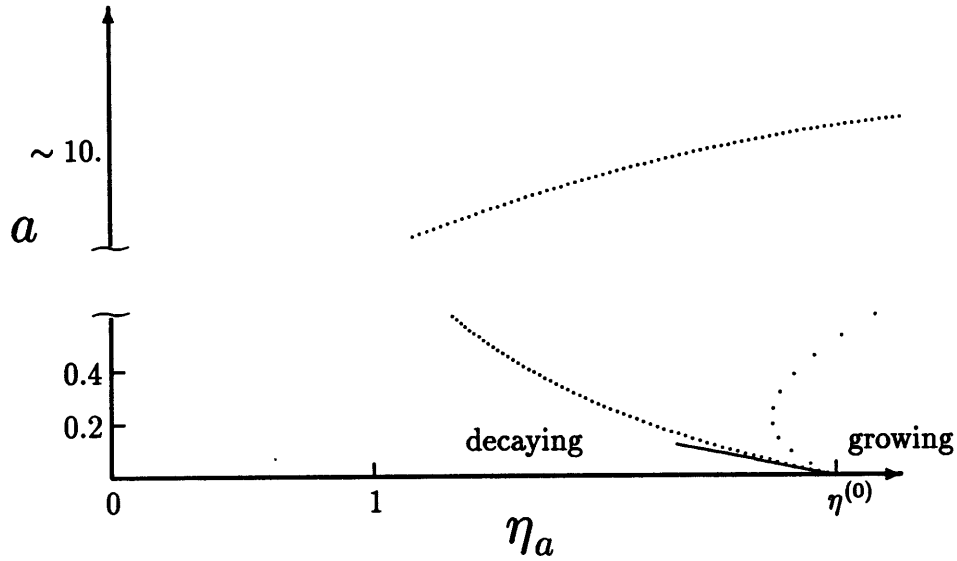


Figure 8.1: Schematic of the regions of decaying and growing states as a function of disturbance amplitude, a , and ambient forcing parameter, η_a . Points in the area labeled *decaying* evolve to the rest state, or if above the upper branch decay to a mature state. Points in the area labeled *growing* evolve towards the upper branch. The intercept on the horizontal axis gives the critical value of the forcing parameter for linear instability. The solid line shows the dependence of the threshold amplitude as a function of the ambient forcing parameter for small amplitude disturbances, as calculated in table 7.2. The dense dotted line shows a conjectured extension of that stability boundary, where the upper and lower branches are assumed to eventually connect at the left. (The conjectured upper branch would be determined by a different dominant balance than found in the solutions examined here.) The sparse dotted line indicates a possible behavior for a stability boundary that would greatly limit the usefulness of this type of theory. Note the break in the amplitude (vertical) scale.

by happenstance an unstable stationary state in a natural system, with motion just-so in three dimensions and several dependent variables, is absurd. The unstable solutions we have found are not expected to be observed; they serve as dividers between decaying and intensifying disturbances. However, the actual disturbances one observes do not have the exact spatial form of the linear eigenfunctions found in chapter six. In linear modes, the amplitudes of all measures of a disturbance evolve proportionately. When examining data from observed disturbances, which do not come in one eigenmode of only varying amplitude, different measures are not equivalent. Since the spatial structures of real disturbances are so variable

from case to case, and so different from the solutions dividing decaying from growing states presented here, it is not clear when a given disturbance exceeds the threshold for growth.

For our solutions separating growing from nongrowing disturbances, there are only two free parameters. These can be chosen as an amplitude and a length scale. Solutions for a range of lengths can be found by varying $\eta^{(0)}$. (The viscosity coefficients cannot be viewed as free, though they can be “tuned”.) To compare observed disturbances with this theory, I suggest using the magnitude of the near surface vorticity maximum (with derivatives determined appropriate to the scale of the cloud cluster) as an amplitude and the mean radius of the main region of positive relative vorticity as a length corresponding to r_0 . Strong surface winds with little vorticity on the cluster scale, do not force much convergence, and hence do not force much convection. Similarly, a strong surface pressure signal from a large diffuse system is not conducive to development.

In the context of this theory, relative vorticity is a good indicator of the organized forced vertical velocity out of the boundary layer. This choice is also consistent with the observations of McBride and Zehr (1981). A better measure might be the curl of the quotient of the near surface wind stress divided by the total vorticity, but the wind stress is not directly observable. The algebraic form of the surface drag dependence on wind and the magnitude of the Rossby number determine how similar these measures are. Distinction must be made between turbulent winds and large scale organized flow. Horizontally isotropic turbulent winds make a quadratic drag law behave like a linear one for the large scale flow. However, even if the drag law is quadratic in the horizontal velocity, the vorticity is at least a cofactor in the expression for the Ekman pumping, though it is not the only factor. Regretfully, there is no simple way to separate vertical velocities induced by surface stresses and those induced by internal heating, in observational data. If such a determination were possible, it would be much easier to test the basic ideas of CISK.

8.1.2 Disturbance Height and Vertical Instability

A crucial, and insufficiently studied requirement, is that whatever the form of the initial disturbance it must be felt at the surface. Both Conditional Instability of the Second Kind (CISK) and Hurricane Air-Sea Interaction Theory (HASIT) rely on the presence of an organized near surface flow provided by some other mechanism. For Atlantic hurricanes the source of these disturbances is primarily, though not exclusively, tropical easterly waves. These waves are thought to form as shear instabilities on the African easterly jet (Burpee 1972). This jet is, however, at about 70 kPa, which is quite far from the surface.

Conditions required for a disturbance to reach low levels have recently been examined by Miller (1990), who extended the results of a necessary condition for vertical propagation of planetary waves proposed by Charney and Drazin (1961). I originally thought that a condition for vertical propagation would be necessary for tropical cyclone development. However another possibility, raised by Miller (1990), is that even evanescent disturbances may have strong near surface signals. He concentrated on examining the forced vertical velocity from wave motions, not vertical motions induced by friction. However, since his model was linear, the same arguments apply to other measures of a disturbance, such as horizontal velocities and vorticity. He showed that trapped solutions may have a larger effect at low levels than propagating solutions, at least within one or two vertical e -folding scales of the disturbance source, i.e. the jet. This scale was estimated by Miller to be about 2 km for the observed shear in the GATE region. For evanescent modes, the surface signal is then sensitively dependent on the height of the forcing, since the e -folding scale is small. In practice, the determination of the vertical propagation characteristics of any given disturbance is still an unsolved problem. A great encouragement for use of conditions that determine the vertical extent and propagation of disturbances in forecasting is that they can be evaluated from synoptic scale, rather than mesoscale, measurements. It is presently considered a source of great confusion that tropical cyclones seem to develop from such a wide range of synoptic disturbances. We may eventually find that many of the details of the different initial conditions are irrelevant.

Analysis of the vertical structure of disturbances shows that at different periods in the lifetime of a disturbance, the effects of vertical shear can be quite different. As just noted, at early stages, low level shear affects the vertical propagation and decay lengths of disturbances. This may help determine whether or not a given wave generates sufficient near surface vorticity to drive mechanical convergence and intensification. However, upper level shear affects the ability of the warm core to remain vertically aligned with a strong low pressure signal at the surface. Strong vertical shear at middle and upper levels has been consistently shown to prevent intensification. Neither of these effects has been included in the theory presented here.

The presence of a visible cloud cluster on satellite photographs is not necessarily an indication that the circulation of a disturbance has penetrated to the surface. There is sufficient moisture in tropical air that forced upwards motion just above the boundary layer, which does not involve the boundary layer, will still lead to cloud formation. Such forced convection can even lead to precipitation. Even though I have argued that there is some CAPE for air in the lower boundary layer with respect to the air aloft, there is probably little if any energy to be had from forced convection of parcels starting above the boundary layer. Air from near the top of the boundary layer will provide less energy than air from closer to the surface. In a weak cloud cluster, it has been found that the deepest convection, reaching to the tropopause, had the lowest cloud bases (at 450–600 m) and occurred in areas of large scale confluence (and assumedly convergence), though this was also in an environment where lesser clouds had already contributed to the moistening of the area (Warner et alii 1980). Since there is a strong gradient of water mixing ratio in the boundary layer, lower cloud bases should be associated with lower parcel origination levels.

The notion of an atmosphere being stable or unstable with respect to “real” entraining convection with dissipative processes included, is subtle and not unambiguous. In the parameterization scheme used here, it is assumed that there is sufficient entrainment to neutralize boundary layer parcels with respect to the upper layer. However, it is nonsensical to refer to this as “neutral”. There is a

real vertical instability at work here. It is only that the vertical accelerations, *per se*, are irrelevant to the problem. Rather, it is the symmetric entrainment caused by the acceleration that is crucial. Hence, it is only sensible to refer to a vertical profile as stable if it is stable to *undilute* ascent in the presence of whatever dissipative (but not entraining) processes exist. Even this is quite complex. A profile that is neutral with respect to nonprecipitating convection is unstable to precipitating convection if the water content of a parcel becomes less than what would result from adiabatic cooling (e.g. by loss of liquid water due to precipitation). However, the presence of liquid water in excess of what can condense locally (e.g. by rainfall into parcels, such as those near cloud base) can create a stable layer choking off convection. We note that even if the tropics were neutral for boundary layer parcels rising while retaining their water content, they are quite unstable for the precipitating convection that actually occurs during most of the summer and early autumn.

8.1.3 Development at Second Order

The solvability conditions derived here are similar to integrated energy balance equations. The first order terms maintain their own energy balance regardless of their amplitude. For stationary solutions, the extent to which the second order terms are out of energy balance can be formally compensated by changes in the forcing parameter. For the time dependent case, this lack of balance drives the evolution of the fields. The more familiar case is that increases in disturbance amplitude are energetically expensive, so amplitude balances an amount of supercriticality. As a cyclone approaches its maximum intensity this would be the case.

However, in the low amplitude case examined here, increases in the amplitude of the motion increase the forcing of the system so a balance can be maintained subcritically. There are three major mechanisms for this. The surface stress increases faster than linearly, leading to a faster than linear increase of the mass flux of positively buoyant air out of the boundary layer. Surface velocity perturbations

increase the surface heat and moisture flux and so increase the available potential energy between the surface and the air aloft, or at least maintain the vertical available potential energy despite the warming of the air aloft. (Intensification ceases when the upper troposphere is so warm that this is no longer possible.) Lastly, vorticity advection increases in the lower layer by advecting perturbation vorticity at second order and decreases the buildup of the anticyclone aloft. The importance of self-advection of vorticity in the inflow layer confirms the suggestions of Shapiro (1977). Though at the weak stage examined here the vorticity advection aloft mostly assists development, during the later evolution of the storm this is more complicated. When the cyclone develops to the point where the vorticity of the outflow layer is positive at small radius, the nonlinear advection will change sign in some regions.

The dependence of growth on the magnitude of the Coriolis parameter has some conflicting effects. Smaller values of f lead to increases in the strength of the Ekman pumping out of the boundary layer. This cannot be pushed very far, since when the relative vorticity exceeds the planetary vorticity the planetary vorticity becomes irrelevant in determining the pumping. (Also when f gets small the expansion used here breaks down.) Another effect that makes development easier with small f is that a smaller thermal perturbation is needed for gradient wind balance, or conversely, a given thermal perturbation can support a stronger cyclone. The more important effect is that larger values f lead to greater imports of angular momentum for a given amount of middle level inflow. The consistency of the scaling of the growth rate in the finite amplitude analysis shows that this effect dominates. It is also suggested in the climatology of developing versus nondeveloping clusters found by Lee (1989a, fig. 4). However, these issues are still in need of further study.

To no surprise, the analysis has shown that boundary layer friction and large values of the bulk transfer coefficients support tropical cyclone intensification. Internal vertical diffusion discourages intensification. Though vertical momentum transports help weaken the anticyclone aloft, which is desirable for intensification, the cost to the lower level cyclone is too great. Proportional increase of all vertical

diffusive processes is still a net drain on development over the range of parameters examined, though in the limit of no vertical momentum transports (including at the surface) development would not occur.

The diffusion of angular momentum by the lower cyclonic vortex is more costly to the cyclone than any gain from increase in the secondary circulation or reduction in the upper anticyclone. Challa and Pfeffer (1984) explicitly examined this in their numerical model. However, increase in just the integrated upper level diffusion makes intensification easier. Though at first it might seem that upper and lower level diffusion processes must be similar, this is not so. The diffusion coefficients used here are products of the layer depth and a simple eddy diffusivity. The results here therefore indicate that a deep outflow layer assists the intensification process. A range of outflow depths have been observed, but this is probably more controlled by the vertical thermodynamic structure than by the large scale dynamics. More importantly, upper level momentum mixing is encouraged by the strong asymmetries that develop in the outflow. The only way to include this enhanced mixing in the context of an axisymmetric model is to increase the diffusion coefficient. I believe that the asymmetries of the outflow are necessary for the development of a tropical cyclone in the real atmosphere, given the rather weak vertical instability available as forcing.

The theory could be applied with less discomfort at higher Rossby number if transformed into potential radius or angular momentum coordinates. Since internal dissipation is needed, it will be necessary to use a system of equations in one of these transformed spaces that includes friction, such as in Emanuel 1989b.

8.1.4 Our Original Questions

By way of summary, we now return to the two question posed in the introduction. Some of this description is conjectural, but it forms a consistent picture of tropical cyclone formation and the barriers to that formation.

How Hurricanes Happen

Tropical cyclones need an energy source, an angular momentum source, and an initial disturbance. The primary source of angular momentum comes from parcels rotating with the earth. Though only a small fraction of this rotation is felt by parcels at low latitude moving horizontally, this planetary angular momentum leads to large relative angular velocities with respect to a cyclone center when fluid is transported large distances toward the cyclone center in the absence of torques with respect to that center. Forces strictly toward or away from the center exert no torque, though they do large amounts of work.

The forcing and power for this middle level convergence is organized deep cumulus convection. Initially, energy to drive this convergence comes from conditional instability of moist boundary layer parcels with respect to air aloft (convective available potential energy — CAPE). As the process continues, that reservoir is replenished and enhanced by evaporation at the sea surface and increasing boundary layer entropy due to the winds of the disturbance. This is eventually limited by the boundary layer becoming nearly saturated at the sea surface temperature below the updraft region. The lateral convergence driven by the deep convection is also encouraged by weak vertical stability throughout the troposphere above the boundary layer.

The convection performs two distinct tasks, in a compatible way — it drives inflow toward the convecting region and it warms the core region. Cumulus convection does not necessarily do either of these tasks well and isolated cumulus clouds do not greatly affect the lateral momentum fluxes of a region. The warming from convection does not only occur in the updraft but in the surrounding downdrafts at upper levels as well.¹ It is only because the core of a developing cyclone is a broad region encompassing both the updrafts and a large part of the accompanying upper level downdrafts of a very large number of convective cells

¹There are strong downdrafts at low levels as well. These are driven by different processes, such as evaporative cooling and precipitation loading, and have little to do with the largest part of the warming, which is a maximum at a level of about 30 kPa.

that one can engage in the fiction of considering warming to occur in the convective region due to convection. Even if the convective processes were not directly responsible for any net warming, the core region would warm through geostrophic adjustment to balance the winds induced by convective entrainment.

Though in an Eulerian sense² most of the warming occurs in the upper troposphere (maximum at about 40 kPa [Yanai et alii 1976]), most of the latent heat release is accomplished much lower in the troposphere (maximum at about 80 kPa, the location of the greatest apparent moisture sink [Yanai et alii 1976]). At the levels where most internal heating occurs, in a Lagrangian sense, and parcels are accelerating upwards, inflow is forced through the continuity equations. (To actually include the force that drives this motion, rather than including it diagnostically, requires the inclusion of sound pressure waves.) Cylindrically symmetric inflow requires the least energy. As already noted, it is the powering of this inflow that is one of convections two essential tasks.

The action of a single convective cell with a lifetime of about an hour would do little. It is the concentration of a large number of cells in close proximity, for an extended period of time, that is essential for inflow over a radius of several hundred kilometers. Ekman pumping serves to overcome the tendency of convective cells to keep their distance from each other. This concentration of convective cells is only possible if the convection is initiated or forced by larger scale processes. In tropical cyclones, we contend, that the convection is initiated by frictionally forced vertical velocities in the boundary layer. These mechanically forced motions lift unsaturated parcels to their level of free convection. This process, whereby frictional convergence in the boundary layer initiates cumulus convection, is called Conditional Instability of the Second Kind — CISK.

As the cyclone becomes more intense, the deep convective region becomes a ring, i.e. an eye forms. One reason for this change may be that as organized

²An *Eulerian* perspective looks at changes in fields for each point in space, i.e. *partial* derivatives with respect to time, $\frac{\partial}{\partial t}$. A *Lagrangian* perspective looks at changes following parcels of fluid, i.e. *total* derivatives, $\frac{d}{dt} = \frac{\partial}{\partial t} + \mathbf{u} \cdot \nabla$.

tangential flow exceeds the turbulent boundary layer velocities the surface drag becomes more closely quadratic in the mean tangential wind (rather than linear). Then the maximum forced vertical velocity is no longer at the center. The change in the vertical velocity structure from $w^{(1)}$ (see line proportional to $\frac{drv_1^{(1)}}{r dr}$ in fig. 6.8) to $w^{(2*)}$ (see fig. 7.4) as the cyclone intensifies, is strikingly similar to the observed development of a broad convective region to a sharply defined ring structure. Also, Kuo (1959) has shown that energy constraints limit how close a parcel can get to the center before rising as its tangential velocity increases. As a cyclone intensifies, angular momentum surfaces slant more outwards leading the convection to slant more outwards, so subsidence is forced in the center to maintain gradient wind balance. These processes, at work near the surface and aloft, create a nearly cloud free eye.

The phase relationship of the convection to the low pressure center contributes to the long lifetime of tropical cyclones. Unlike midlatitude disturbances, which are propagating disturbances, tropical cyclones mostly move with the flow in which they are imbedded (though there are systematic deviations of about 1 m/sec [Carr and Elsberry 1990]). They are essentially nondispersive. The secondary flow is primarily a simple direct circulation. Since the density perturbations, heating, and vertical velocity are to good approximation in phase, little in the way of wavelike behavior is possible. This phase relationship is maintained through the dynamics of the frictional boundary layer. For these reasons, one does not observe the rapid decay following intensification attributed to midlatitude baroclinic waves (Randel et alii 1987, Farrell 1988). Tropical cyclones continue until their power source is cutoff, or until they warm up the entire upper troposphere in their vicinity (which might be the cause of the decay of long-lived Pacific storms noted by Weatherford [1989]). Some propagating behavior does occur in the form of contracting concentric rings. This might still be viewed in the context of CISK, but would then require a fully nonlinear, time dependent approach to the boundary layer.

Why They Don't Occur More Often

Of the three necessary ingredients for a tropical cyclone, only one of them is continuously available—an angular momentum source, though it is insufficient within a narrow band of the equator. Supplies of energy and initial disturbances are more variable. The most fundamental potential energy limit is that in many regions of the globe, air saturated at the SST would still not allow for a cyclone of any great intensity (see Emanuel 1986). There is also a requirement for a potential energy supply within the atmosphere. The magnitude of this requirement is not absolute, but is based on a tradeoff between the ratio of conditional instability of the boundary layer to the midtropospheric stability, and the threshold amplitude of intensifying disturbances. It is conceivable that a very intense disturbance could develop further if it lasted long enough to sufficiently moisten and destabilize the boundary layer. Since disturbances come in many shapes and sizes, there is no simple concept of amplitude. The amplitude that matters is that of the boundary layer vorticity on spatial scales that include many cumulus clouds, say 100 km. This is a measure that directly ties to the amount of moist boundary layer air forced to its level of free convection.

The presence of internal friction all but eliminates the possibility of linear growth of a tropical cyclone type instability for a resting atmosphere, even with the most generous view of the amount of vertical instability. Even small amounts of internal momentum diffusion increase the required forcing parameter for linear instability to values greater than even strong believers in the existence of CAPE would claim exist. Conditions needed for linear growth from infinitesimal disturbances do not occur. Even in the presence of a trade inversion, the vertical structure never becomes sufficiently unstable. Further, without an imposed large scale disturbance, scattered cumulus convection would still be the preferred process for releasing this potential energy. Tropical cyclones are infrequent because the number of disturbances that meet the finite amplitude vorticity threshold near the surface, for the ambient vertical stratification, is small.

8.2 CISK vs. HASIT: Proposed Tests

It is time to test the CISK hypothesis rather than just waving it around as an unchallenged explanation, as has been done in many observational papers. In this thesis, I have tried to overcome some of the theoretical objections to the simple linear CISK theories presented by Charney and Eliassen, and by Ooyama, more than twenty-five years ago. The beginnings of a different theory, also based on control of development by the boundary layer, have been presented by Emanuel and his coworkers. That theory is not fully mature, but it presents testable issues that distinguish it from CISK. Though HASIT has not been worked out analytically for growing disturbances, comparisons can still be made between CISK and HASIT that are testable. However, as Emanuel (1989b) notes, there is great similarity between his results and the results of Ooyama 1969 (though he does not lump Ooyama's numerical work in with CISK of Charney and Eliassen). As he says, "This coincidence is at least partly accidental," and "... is due to the spatial near-coincidence of moisture convergence and HPE [high precipitation efficiency] convection." This makes some of the large conceptual differences between CISK and HASIT difficult to test observationally.

The existence of CAPE prior to the presence of a storm is crucial to CISK type theories. A stable capping layer would allow the buildup of CAPE. Mixing of small buoyant parcels from the boundary layer with the relatively low entropy air above it may also serve to quench convection. Sounding data need to be analyzed more carefully and without the broad temporal brush used by Xu and Emanuel (1989). In particular, a seasonal analysis is needed. If the summertime tropical atmosphere is as close to neutral as they claim, then based on the seasonal differences found by Palmén (1948, 1969), Kasahara (1954), and Bansal and Datta (1972), wintertime soundings would be quite stable. Soundings should be examined, where they can be found, for areas where a tropical cyclone intensified, but a few days before the storm arrived. More analysis is needed of the appropriate standard of neutrality, in particular regarding the inclusion of precipitation and ice related processes.

HASIT requires the development of a radial gradient in boundary layer entropy in concert with intensification and an advance increase in the middle troposphere entropy. Observations should be made on the moist entropy gradient of the boundary layer in nascent tropical storms. A crude analysis by Lunney (1988, table 6.7), using composites of flight data from below 1500 feet, shows virtually no gradient of equivalent potential temperature in the early stage of development. There was also no significant difference between developing and nondeveloping disturbances. Similar results can be inferred from the plots of θ_e based on sounding data made by Lee (1986) for developing precyclone cloud clusters. These results are consistent with CISK but not with HASIT. However, both of these analyses are spatially coarse. Examination of the moist entropy in the lower troposphere above the boundary layer should allow us to determine if significant moistening of this layer precedes large scale deep convection and the start of intensification, as posited by HASIT, or if intensification begins soon after the large scale vorticity of a disturbance reaches down to the boundary layer, consistent with CISK. A test should also be made of the assumption used in determining the linear CISK modes (and many other unrelated theoretical works) that there are sufficient turbulent motions in the boundary layer for the frictional forced convergence to be approximately proportional to the relative vorticity for weak disturbances.

We need to develop better budgets of energy, entropy, and angular momentum for weak disturbances while closely examining the dissipative processes. This has been done fairly well for mature tropical cyclones and with slightly less confidence for easterly waves and developing cyclones. Norquist et alii (1977) found that baroclinic and barotropic conversions in easterly waves would have led to a doubling of the wave intensity in 2–4 days in the absence of dissipation, and that latent heating was a noncontributor to development in the GATE region. Estimates are needed for internal dissipation in weak disturbances to see if they are indeed a major part of the energy budget as posited here. Lee (1989b) has shown that boundary layer drying by downdrafts plays an important role in the entropy budget (but his analysis is spatially quite coarse). It remains to be seen whether this plays any role in creating a threshold for intensification as suggested

by Emanuel (1989b).

Both CISK type theories and the air-sea interaction theory of Emanuel rely on dynamics of the surface boundary layer for controlling most of the intensification of a tropical cyclone (though neither speaks to the genesis of the initial disturbance). This is in contrast to those theories relying on fortuitous momentum surges for intensification, or older works emphasizing barotropic or baroclinic instability. So, if I have taken so much care to criticize HASIT, and have emphasized the differences between CISK and HASIT, it is because it is the only other theory I find at all credible. In the end we may find that several cooperating mechanisms contribute to tropical cyclone development.

8.3 Conclusions

*"Just the place for a Snark! I have said it thrice:
What I tell you three times is true."*

*The Bellman in
Lewis Carroll
The Hunting of the Snark*

This is the first analytic theory to include the need for a finite amplitude disturbance for tropical cyclone intensification. The need for sizeable disturbances has long been recognized from observations and some numerical models. Nonlinear mathematical techniques have been used because linear theory is incapable of describing a phenomenon with an amplitude threshold for development.

The analysis was based on the two layer hurricane model developed by Ooyama (1969), which includes a simple diagnostic cumulus parameterization. This convective scheme keeps most of the details of real cumulus convection out of sight. Convection is only initiated by boundary layer convergence and is assumed to release available potential energy. The primary effect of the convection is to drive middle level inflow, i.e. entrainment. The inflow is, in turn, responsible for convergence of angular momentum. The primacy of this task is reflected in the form of the forcing parameter, which depends on the ratio of the potential boundary layer buoyancy to the middle troposphere stability. This is a measure of the ease with which convection drives inflow, rather than an absolute measure of CAPE. Warming is an indirect consequence through geostrophic adjustment, with the parameterization chosen, though probably less so in nature.

The heart of CISK is that the location of deep convection is determined by the large scale flow, through frictional convergence, and that this convection serves to intensify the large scale flow. Linear stationary solutions were found for a system with CISK type forcing and dissipative processes, including internal friction and radiative cooling. The system was expanded to second order to determine the amplitudes of the stationary solutions for a given amount of vertical instability. It was found that a stationary balance was maintained by decreasing the forcing for increases of amplitude. (This is the opposite of the case where slightly unstable systems are stabilized by increases in the amplitude of linear modes.) Hence,

finite amplitude stationary solutions can exist in forcing regimes that are linearly stable. Further, these stationary states were found to be unstable. The amplitude of the stationary states therefore serves as a divider between growing and decaying disturbances for a given vertical stratification. The impediment to growth is primarily frictional, though radiative damping contributes as well.

It is clear that many of the objections to CISK have already been, or can be, defeated. The objection that CISK is a linear theory, and hence cannot show the need for a finite amplitude disturbance, has been quashed here (even if one was not satisfied by the numerical work in Ooyama 1969 that this was a spurious objection). CISK theories do require a reservoir of CAPE, but there is no need that the initial CAPE be sufficient to generate a mature storm, only that it be sufficient to overcome dissipative processes. The claim that CISK does not allow for entropy fluxes at the lower boundary has never been accurate, since maintaining a constant boundary layer entropy implies such a flux. In this thesis, as well as Ooyama's (1969) numerical integration, even an increase in the boundary layer entropy was incorporated into a CISK type theory. The naïve reliance on moisture convergence is not part of the formulation used here, nor was it used in any of Ooyama's work, so objections along those lines are irrelevant.

Objections to CISK based on length scale selection, or the lack thereof, are more subtle. For subcritical instabilities, the initial length scale is determined by the size of the initial disturbance. In the context of the viscous theory presented here, there is some disturbance size that has the smallest amplitude requirement for growth, and this size is determined by the various frictional parameters. For the somewhat believable values of these parameters we have examined, the radius of maximum winds for the disturbance requiring the smallest amplitude for excitation, is a couple of hundred kilometers. The length scale dependence on frictional parameters is also weak, going only as the square root. The eventual smaller scale to which tropical cyclones shrink, is not described by this work.

The instability found here is a finite amplitude version of CISK. There are several processes that contribute to the nonlinear balance at subcritical values of the forcing parameter.

1. Since the surface stress increases faster than linearly with tangential velocity, the Ekman pumping also increases faster than linearly. Therefore, there is an accompanying more rapid than linear increase in the cumulus heating.
2. The presence of a finite amplitude disturbance, cyclonic at low levels and anticyclonic aloft, leads to advection by the disturbance of disturbance angular momentum in addition to the planetary angular momentum. In the lower level cyclone this serves to help increase the cyclonic flow. In the upper level anticyclone this serves to weaken the resulting anticyclone, which decreases the energetic drain of the upper level flow on the overall system, and assists in cyclone development.
3. And in a vein similar to HASIT, the tangential velocities increase the surface entropy flux and can lead to an increase in the near surface entropy. The increased boundary layer entropy leads to more intense convection in the locations with positive Ekman pumping, which are also in phase with the positive temperature perturbations aloft.

The finite amplitude nature of the instability here is tied to the existence of dissipative processes. However, it is not as sensitive to the values of the frictional parameters as it is to their ratios. Inclusion of friction is a singular perturbation to the equations of motion that fundamentally changes the form of the threshold for *linear* instability. The linear instability criterion is strongly dependent on the ratio of the lateral friction coefficients and the ratio of the vertical friction coefficients, and only on their ratios. So the mere presence of friction quickly prevents linear hurricane-like instability.

"It has been a long trip," said Milo, climbing onto the couch where the princesses sat; "but we would have been here much sooner if I hadn't made so many mistakes. I'm afraid it's all my fault."

"You must never feel badly about making mistakes," explained Reason quietly, "as long as you take the trouble to learn from them. For often you learn more by being wrong for the right reasons than you do by being right for the wrong reasons."

"But there's so much to learn," he said with a thoughtful frown.

"Yes, that's true," admitted Rhyme; "but it's not just learning things that's important. It's learning what to do with what you learn and learning why you learn things at all that matters."

"That's just what I mean," explained Milo, as Tock and the exhausted bug drifted quietly off to sleep. "Many of the things I'm supposed to know seem so useless that I can't see the purpose in learning them at all."

"You may not see it now," said the Princess of Pure Reason, looking knowingly at Milo's puzzled face, "but whatever we learn has a purpose and whatever we do affects everything and everyone else, if even in the tiniest way. Why when a housefly flaps his wings, a breeze goes round the world; when a speck of dust falls to the ground, the entire planet weighs a bit more; and when you stamp your foot, the earth moves slightly off its course. Whenever you laugh, gladness spreads like the ripples in a pond; and whenever you're sad, no one anywhere can be really happy. And it's much the same thing with knowledge, for whenever you learn something new, the whole world becomes that much richer."

Norton Juster
The Phantom Tollbooth

Epilogue

Scientific Priorities

Routine airplane reconnaissance by the Air Force and Navy began in 1944 (R. Simpson 1954). Continuous satellite observations began in the 1960s (R. Simpson et alii 1969). However, there are very few data from storms that are just forming. Instrumented reconnaissance is performed primarily on mature storms, or ones that are already growing rapidly. The largest data set for comparing disturbances that intensified with those that did not, was created more by accident than design. Air Force reconnaissance from Guam was flown primarily to see if a closed circulation had already formed, to determine the strength of the circulation, and to obtain a positional fix on the storm center. Disturbances that were not expected to intensify were not investigated with aircraft. Only because forecasters were so poor in making this determination were so many flights made into nonintensifying disturbances. The data were collected manually and sparsely, as an adjunct to purely operational missions. Given the large cost of the flights compared to the additional cost of some minimal instrumentation, it is depressing how little good use was made of the air time. It is a tribute to the researchers at Colorado State University that they have gleaned as much as they have from these very sparse data (about one measurement every 15 min or 100 km).

Research flights in the Atlantic, made by various parts of the National Oceanographic and Atmospheric Administration, have been far more successful in avoiding weak disturbances. The most effective way to learn about tropical cyclone intensification is to fly a large number of aircraft missions in weak disturbances.

In situ measurements of tropical cyclones are *decreasing* (Elsberry 1987). The regular reconnaissance performed by the U. S. Air Force leaving from the Joint Typhoon Warning Center on Guam was recently ended in 1987 for budgetary reasons. Satellite data is increasing both in quantity and quality, but is becoming more a substitute for in situ observation than is wise. J. W. Nielsen (personal communication) has declared that research should be directed toward determining the dynamics of the appearance of hurricane intensification shown in satellite imagery; the actual intensification is becoming irrelevant or at least unknown. Though no one suggests that the landbased radiosonde network be shut down except when major atmospheric events are observed with satellites, this is essentially what is done over the oceans.

As the coastal population continues to grow, evacuation and preparation times will continue to lengthen. The economic incentive for accurate forecasts will also increase. For storms that develop in the warm basins of the world, such as the Gulf of Mexico and the Bay of Bengal, intensification predictions are operationally useful. If we are to understand how changes in the earth's climate will change the frequency, intensity, and size of tropical cyclones, we must develop a better understanding of how the current climate drives the current patterns; this is still in many ways unknown.

We must continually ask ourselves whether we are performing basic science or applied science in support of the engineering called forecasting. Neither of these tasks is morally suspect, but they lead to different questions and different research approaches. Though I have just presented some justifications for research on the cyclone intensification problem, a large part of my own interest is simply curiosity.

This thesis is somewhat unusual in the body of theoretical atmospheric dynamics in that it so strongly relies on dissipative and diabatic processes. One should remember that it is the nonconservative processes that are the *primum mobile* of the atmosphere, that which makes it go. Yet while it is going, essentially assuming that inertia guides the motions is quite accurate. A surprisingly large fraction of the theoretical atmospheric dynamics that is performed assumes that the atmosphere is inviscid and adiabatic. It is worth examining the surprising

degree to which these assumptions are quantitatively correct on short time scales and nevertheless logically absurd if extended. Every freshman physics student can analyze the trajectory of incoming cannon fire and show that after a shot leaves the cannon it closely follows a parabola. Eventually it becomes time to understand the physics of how the shot is fired and what happens when it strikes something. More theoretical work is needed throughout meteorology on forced dissipative dynamics.

Tropical Cyclone Modification

Modification of tropical cyclones by human activity may occur intentionally or unintentionally. Several attempts have been made to weaken, prevent the growth of, or redirect storms. On the whole, these have been unsuccessful. We may yet prove more effective in changing the frequency, strength, and range of tropical cyclones by altering the overall climate of the planet, though not in any intentional and constructive manner. We may also some day deliberately modify individual storms.

The scenarios for global warming from an increase in greenhouse gases lead to several conjectures relating to tropical cyclones. The area of the seas with surface temperatures in excess of 27°C , the somewhat ad hoc observed SST threshold for cyclone occurrence, is likely to increase. Further, the length of time that some areas that already reach this threshold remain so, will increase. This may increase the total number of tropical cyclones and increase the lifetime of some cyclones that would otherwise begin to decay because they reached unfavorable environments. However, should the entire planet surface warm, there are reasons to argue that this lower SST limit will also increase. As noted by Emanuel (1987), the maximum intensity of tropical cyclones may increase because of increases in the SST. Greenhouse theories predict a decreasing temperature above some altitude, but that level is not yet well determined. If it should prove to be below the hurricane outflow level, upper tropospheric cooling will also lead to an increase in

maximum intensity, based on Emanuel 1986. On the other hand, global warming from increases in greenhouse gases will most likely reduce the equator to pole temperature gradient and hence the overall baroclinicity of the atmosphere, with an accompanying decrease in the mean zonal currents. This may lead to a decrease in the synoptic scale disturbances that are the necessary precursors to tropical cyclones. As of yet, this is an unstudied area.

The relatively wealthy nations have an obligation to fund research to determine the degree to which anthropogenic greenhouse change will alter conditions in the tropics, since we in those nations will be the primary cause of any such change. Though there is no effective mechanism for adjudicating global torts, that does not obviate us of responsibility.

The great loss of life and large property losses from tropical cyclones have inspired attempts to interfere with the intensification process. The largest of these was project STORMFURY, which involved cloud seeding of North Atlantic storms. Reviews of this project have been provided by Anthes (1982, ch. 5) and Willoughby et alii (1985), the latter analysis took a more pessimistic view of the results. The basic idea was that by intensifying convection, and hence heating, outside of the radius of maximum wind (also the radius of maximum pressure gradient), the pressure gradient and maximum winds would decrease. Though some seeded storms did weaken, Willoughby et alii concluded that the variation was well within the realm of natural behavior and that the assumptions about the cloud microphysics were in error.

Several other schemes have been put forward for limiting the intensification of tropical cyclones. R. Simpson and Riehl (1981, ch. 15) discuss cloud seeding (as was done in STORMFURY), cooling of surface waters through Ocean Thermal-Energy Conversion (OTEC), cooling by the importation of icebergs, reduction of evaporation from the ocean by creating a thin film over the ocean (such as a monomolecular layer of hexadecanol), and the use of carbon black particulates to alter the radiation flux. My own view is that thin film approaches are most likely to be effective since they both reduce evaporation and may reduce surface friction which drives boundary layer convergence. However, it may be impossible

to develop a film over rough seas. Examination of oil slicks from accidental spills, many of which have occurred during disturbed conditions, may prove enlightening. Finding a substance that degrades innocuously may prove difficult.

As we learn more about the amplitude threshold for tropical cyclone development, the temptations that lead to project STORMFURY will return. Through preparedness and evacuation, the rate of injury and loss of life from these storms continues to decline despite increases of coastal population. However, property losses are still accelerating. Major storms making landfall in the United States regularly cause over \$1 billion of destruction (Sheets 1979).

However, tropical cyclones also have benefits. Usually a far greater area receives significant useful rainfall, without feeling the effects of damaging winds and flooding, than is damaged. (Sheets [1979] argued that modification by cloud seeding is not likely to disrupt large scale storm precipitation. This would not be true of schemes that reduce evaporation.) Large amounts of nutrient rich water are brought to the surface by wind stress driven Ekman pumping, though I am unaware of any calculations on the significance of this in the overall nutrient budgets in the affected regions. Tropical cyclones also play a significant role in poleward transport of heat and moisture. It may be that the number of cyclones that are a threat, and hence candidates for modification, is small enough that the averaged transports are not seriously affected. However, dissipating one storm might result in a strengthening of the next one to come through the same general region. Lastly, the "damage" caused by tropical cyclones is important for ecological cycling in some areas, performing a function similar to that of temperate zone forest fires.

Though there has been some discussion of the legal and ethical problems involved in tropical cyclone modification, such as that by Willheim (1979). These have concentrated on compensation for positive damage from, say, track changes. Loss of benefit has been mostly ignored. Almost any changes to the present pattern of tropical cyclones will create both winners and losers. It may well be that the costs of damage avoidable through modification far exceed the benefits from the storms plus the costs of modification. Quantitative estimates have so far

only been made of damage costs (e.g. Southern 1979). It is incumbent on those who modify tropical cyclones to provide compensatory benefits to those who lost benefits, if not also obtain their consent. Until there is sufficient international cooperation that there is compensation for any losers and negotiation in advance, I feel that any attempts to modify these powerful storms is unconscionable.

"It's only six o'clock," he observed with a yawn, and then, in a moment, he made an even more interesting discovery.

"And it's still today! I've been gone for only an hour!" he cried in amazement, for he'd certainly never realized how much he could do in so short a time.

Milo was much too tired to talk and almost too tired for dinner, so, without a murmur, he went off to bed as soon as he could. He pulled the covers around him, took a last look at his room—which somehow seemed very different than he'd remembered—and then drifted into a deep and welcome sleep.

*Norton Juster
The Phantom Tollbooth*

References

- Abramowitz, Milton and Irene Stegun, eds. 1964: *Handbook of Mathematical Functions*; corrected and reprinted in 1972 by Dover, New York, 1046pp.
- Alaka, M. A. 1962: On the occurrence of dynamic instability in incipient and developing hurricanes; *Mon. Weather Rev.* **90** (2), 49–58.
- Alaka, M. A. 1964: On the nature of the triggering mechanism in hurricane formation; *Geof. Int.* **4** (3), 231–240.
- Anthes, Richard A. 1971: A numerical model of the slowly varying tropical cyclone in isentropic coordinates; *Mon. Weather Rev.* **99** (8), 617–635.
- Anthes, Richard A. 1972: Non-developing experiments with a three-level asymmetric hurricane model; NOAA Tech. Mem. ERL NHRL-97, U. S. Dept. of Commerce, National Hurricane Research Laboratory, Coral Gables, Florida, Jan. 1972, 18pp.
- Anthes, Richard A. 1982: *Tropical Cyclones — Their Evolution, Structure and Effects*; *Meteorological Monographs* **19** (41), American Meteorological Society, 208pp.
- Anthes, Richard A. and Donald R. Johnson 1968: Generation of available potential energy in hurricane Hilda (1964); *Mon. Weather Rev.* **96** (5), 291–302.
- Árnason, Geirmundur 1964: The growth of incipient synoptic-scale disturbances in the tropics; *Geof. Int.* **4** (3), 111–116.
- Bansal, R. K. and R. K. Datta 1972: Certain aspects for intensification of tropical storms over Indian Ocean area; *Indian J. Meteor. Geophys.* **23** (4), 503–506.
- Bates, J. R. 1973: A generalization of the CISK theory; *J. Atmos. Sci.* **30**, 1509–1519.
- Bergé, Pierre, Yves Pomeau, Christian Vidal 1986: *Order Within Chaos*; Wiley, New York, 329pp. Trans. by Laurette Tuckerman from the French *L'ordre dans le chaos* (1984), Hermann, Paris.

- Bergeron, T. 1954: (Reviews of Modern Meteorology — 12) The problem of tropical hurricanes; *Quart. J. Roy. Met. Soc.* **80** (344), 131–164.
- Betts, Alan K. 1982: Saturation point analysis of moist convective overturning; *J. Atmos. Sci.* **39** (7), 1484–1505. Also appeared in an earlier shortened form as 1982: Convective overturning and the saturation point, in E. M. Agee and T. Asai, eds., *Cloud Dynamics*, Reidel.
- Bjerknes, J. 1938: Saturated-adiabatic ascent of air through dry-adiabatically descending environment; *Quart. J. Roy. Met. Soc.* **64**, 325–330.
- Black, Peter G. and Richard A. Anthes 1974: On the asymmetric structure of the tropical cyclone outflow layer; *J. Atmos. Sci.* **28** (8), 1348–1366.
- Black, Peter G., Robert A. Black, John Hallett, Walter A. Lyons 1986: Electrical activity of the hurricane; *Twenty-third Conf. on Radar Meteor. and Conf. on Cloud Phys. (preprints)*, American Meteorological Society, Boston, Massachusetts, J277–J280.
- Boehner, Philotheus 1957: Introduction; William of Ockham [c. 1280–1349] 1957, *Philosophical Writings: A Selection*, trans. by Philotheus Boehner, Edinburgh, ix–xxi.
- Bohun, R. 1671: *A Discourse Concerning the Origine and Properties of the Wind. With an Historicall Account of Hurricanes, and other Tempestuous Winds*; Oxford, 302pp.
- Bolton, David 1980: The computation of equivalent potential temperature; *Mon. Weather Rev.* **108**, 1046–1053.
- Bosart, Lance F. and Song C. Lin 1984: A diagnostic analysis of the President's day storm of February 1979; *Mon. Weather Rev.* **112** (11), 2148–2177.
- Bratseth, Arne M. 1985: A note on CISK in polar air masses; *Tellus* **37A** (Polar low special issue), 403–406.
- Bretherton, Christopher S. 1987: A theory for nonprecipitating moist convection between two parallel plates. Part I: Thermodynamics and “linear” solutions; *J. Atmos. Sci.* **44** (14), 1809–1827.
- Brooks, Charles F. 1940: Report on the African origin of the hurricane of September 1938; *Trans. Amer. Geophys. Un.* **21** (2), 251–253.
- Buchdahl, H. A. 1989: A definition of entropy; *Nature* **340** (17 August), 498.
- Burpee, Robert W. 1972: The origin and structure of easterly waves in the lower troposphere of North Africa; *J. Atmos. Sci.* **29** (1), 77–90.

- Burpee, Robert W., Michael L. Black and Frank D. Marks, Jr. 1989: Vertical motions measured by airborne doppler radar in the core of Hurricane Elena (1985); *Eighteenth Conference on Hurricanes and Tropical Meteorology, May 16-19, 1989 (extended abstracts)*, American Meteorological Society, Boston, Massachusetts, 69-70.
- Burpee, Robert W. and Richard J. Reed 1982: Synoptic scale motions; ch. 4 of *GARP* [Global Atmospheric Research Programme] *Atlantic Tropical Experiment (GATE) Monograph*, GARP Publications Series No. 25, World Meteorological Organization, 61-120.
- Byers, Horace Robert 1944: *General Meteorology*; McGraw-Hill, New York, 645pp.
- Carpenter, Thomas H., Ronald L. Holle, Jose J. Fernandez-Partagas 1972: Observed relationship between lunar tidal cycles and formation of hurricanes and tropical storms; *Mon. Weather Rev.* **100** (6), 451-460.
- Carr, L. E., III and R. T. Williams 1989: Barotropic vortex stability to perturbations from axisymmetry; *J. Atmos. Sci.* **46** (20), 3177-3191.
- Carr, L. E., III and Russell L. Elsberry 1990: Observational evidence for predictions of tropical cyclone propagation relative to environmental steering; *J. Atmos. Sci.* **47** (4), 542-546.
- Carrier, G. F. 1971a: Swirling flow boundary layers; *J. Fluid Mech.* **49** (1), 133-144.
- Carrier, G. F. 1971b: The intensification of hurricanes; *J. Fluid Mech.* **49** (1), 145-158.
- Carroll, Lewis 1876: *The Hunting of the Snark*; 83pp.
- Ceselski, B. F. 1974: Cumulus convection in weak and strong tropical disturbances; *J. Atmos. Sci.* **31** (5), 1241-1255.
- Challa, Malakondayya and Richard L. Pfeffer 1984: The effect of cumulus momentum mixing on the development of a symmetric model hurricane; *J. Atmos. Sci.* **41** (8), 1312-1319.
- Challa, Malakondayya and Richard L. Pfeffer 1990: Formation of Atlantic hurricanes from cloud clusters and depressions; *J. Atmos. Sci.* **47** (7), 909-927.
- Chandrasekhar, S. 1961: *Hydrodynamic and Hydromagnetic Stability*; Oxford Univ., Oxford, 654pp.
- Chang, Chih-Pei 1971: On the stability of low-latitude quasi-geostrophic flow in a conditionally unstable atmosphere; *J. Atmos. Sci.* **28**, 270-274.

- Chang, C.-P. and R. T. Williams 1974: On the short-wave cutoff of CISK; *J. Atmos. Sci.* **31**, 830-833.
- Charney, J. G. 1973a: Planetary fluid dynamics; in P. Morel, ed., *Dynamical Meteorology*, Reidel, Dordrecht, 97-351. (See especially section XIII, p. 331-344.)
- Charney, Jule G. 1973b: Moveable CISK; *J. Atmos. Sci.* **30** (1), 50-52.
- Charney, J. 1974: Reply to Holton 1974 (Comments on "Moveable CISK"); *J. Atmos. Sci.* **31** (3), 834-835.
- Charney, J. G. and P. D. Drazin 1961: Propagation of planetary scale disturbances from the lower into the upper atmosphere; *J. Geophys. Res.* **66** (1), 83-109.
- Charney, J. G. and A. Eliassen 1949: A numerical method for predicting the perturbation of the middle latitude westerlies; *Tellus* **1** (2), 38-54.
- Charney, Jule G. and Arnt Eliassen 1964a: On the growth of the hurricane depression, a summary; *Geof. Int.* **4** (3), 223-230.
- Charney, Jule G. and Arnt Eliassen 1964b: On the growth of the hurricane depression; *J. Atmos. Sci.* **21** (1), 68-75.
- Cheng, Ming-Dean 1989: Effects of downdrafts and mesoscale convection on the heat and moisture budgets of tropical cloud clusters. Part I: A diagnostic cumulus ensemble model; *J. Atmos. Sci.* **46** (11), 1517-1538.
- Cheng, Ming-Dean and Michio Yanai 1989: Effects of downdrafts and mesoscale convection on the heat and moisture budgets of tropical cloud clusters. Part III: Effects of mesoscale convective organization; *J. Atmos. Sci.* **46** (11), 1566-1588.
- Cho, Han-Ru and Yoshimitsu Ogura 1974: A relationship between cloud activity and the low-level convergence as observed in Reed-Recker's composite easterly waves; *J. Atmos. Sci.* **31** (8), 2058-2065.
- Coddington, Earl A. and Norman Levinson 1955: *Theory of Ordinary Differential Equations*; McGraw-Hill, New York, 429pp.
- Dampier, William 1699: *Voyages and Descriptions*; vol. 2 of *A New Voyage round the World*, Part I. Supplement of the Voyage round the World, Part III. A Discourse on the Trade-Winds, Breezes, Storms, Seasons of the Year, Tides and Currents in the *Torrid Zone*, Knapton, London. [Volume 1 was originally published under the title *A Voyage round the World* in 1697 and contains a description of a typhoon passing directly over Dampier's ship, including the eye.]

- Davies, H. C. and R. A. de Guzman 1979: On the preferred mode of Ekman-CISK; *Tellus* **31**, 406–412.
- DeMaria, Mark and John D. Pickle 1988: A simplified system of equations for simulation of tropical cyclones; *J. Atmos. Sci.* **45** (10), 1542–1554.
- Deppermann, Charles E. 1938: Typhoons originating in the China Sea; Weather Bureau, Commonwealth of the Philippines, 51pp.
- Deppermann, Charles E. 1939a: Typhoons and depressions originating to the near east of the Philippines; Weather Bureau, Commonwealth of the Philippines, 44pp.
- Deppermann, Charles E. 1939b: Some characteristics of Philippine typhoons; Weather Bureau, Commonwealth of the Philippines, 143pp.
- Dobrysham, E. M. 1982: Theoretical studies of tropical waves; ch. 5 of *GARP* [Global Atmospheric Research Programme] *Atlantic Tropical Experiment (GATE) Monograph*, GARP Publications Series No. 25, World Meteorological Organization, 121–181.
- Dunn, Gordon E. 1949: Cyclogenesis in the tropical Atlantic; *Bull. Amer. Met. Soc.* **21** (6), 215–229.
- Durst, C. S. and R. C. Sutcliffe 1938: The importance of vertical motion in the development of tropical revolving storms; *Quart. J. Roy. Met. Soc.* **64** (273), 75–84; with addendum on p. 240.
- Ekman, V. Walfrid 1905: On the influence of the Earth's rotation on ocean-currents; *Arkiv för Matematik, Astronomi och Fysik* **2** (11), 1–52, +1 plate.
- Eliassen, Arnt 1951: Slow thermally or frictionally controlled meridional circulation in a circular vortex; *Astrophys. Norv.* **5** (2), 19–60.
- Eliassen, A. 1971: On the Ekman layer in a circular vortex; *J. Met. Soc. Japan* (Ser. II) **49** (Special issue), 784–789. (This issue may be difficult to locate, but the citation is correct.)
- Eliassen, Arnt and Magne Lystad 1977: The Ekman layer of a circular vortex. A numerical and theoretical study; *Geophysica Norvegica* **31** (7), 1–16.
- Eliot, T. S. 1934: all selection can be found in *The Waste Land and Other Poems*; Harcourt, Brace, New York, 88pp.
- Elsberry, Russel L. 1987: Observation and analysis of tropical cyclones; in Russel L. Elsberry (ed.), William M. Frank, Greg J. Holland, Jerry D. Jarrell, Robert L. Southern 1987: *A Global View of Tropical Cyclones*; based largely on material prepared for the International Workshop on Tropical Cyclones, Bangkok,

- Thailand, November 25–December 5, 1985; published privately Russell L. Elsberry, Naval Postgraduate School, Monterey, California, 1–12.
- Elsberry, Russell L. (ed.), William M. Frank, Greg J. Holland, Jerry D. Jarrell, Robert L. Southern 1987: *A Global View of Tropical Cyclones*; based largely on material prepared for the International Workshop on Tropical Cyclones, Bangkok, Thailand, November 25–December 5, 1985; published privately Russell L. Elsberry, Naval Postgraduate School, Monterey, California, 185pp.
- Emanuel, Kerry A. 1983a: The lagrangian parcel dynamics of moist symmetric instability; *J. Atmos. Sci.* **40** (10), 2368–2376.
- Emanuel, Kerry A. 1983b: Elementary aspects of the interaction between cumulus convection and the large-scale environment; in D. K. Lilly and T. Gal-Chen, eds., *Mesoscale Meteorology—Theories, Observations and Models*, Reidel, Dordrecht, Holland, 551–575.
- Emanuel, Kerry A. 1986: An air-sea interaction theory for tropical cyclones. Part I: Steady-state maintenance; *J. Atmos. Sci.* **43** (6), 585–604.
- Emanuel, K. A. 1987a: The dependence of hurricane intensity on climate; *Nature* **326** (6112), 483–485.
- Emanuel, Kerry A. 1987b: An air-sea interaction model of intraseasonal oscillations in the tropics; *J. Atmos. Sci.* **44** (16), 2324–2340. See also Comment by Bin Wang, *J. Atmos. Sci.* **45** (22), 3521–3525; Reply by J. David Neelin, 3526–3527; and Reply by Kerry A. Emanuel, 3528–3530.
- Emanuel, Kerry A. 1989a: Negative influences on axisymmetric tropical cyclones; *Eighteenth Conference on Hurricanes and Tropical Meteorology, May 16–19, 1989 (extended abstracts)*, American Meteorological Society, Boston, Massachusetts, 85–86.
- Emanuel, Kerry A. 1989b: The finite-amplitude nature of tropical cyclongenesis; *J. Atmos. Sci.* **46** (22), 3431–3456.
- Emanuel, Kerry A. and Richard Rotunno 1989: Polar lows as arctic hurricanes; *Tellus* **41A**, 1–17.
- Emanuel, Kerry A., Maurizio Fantini and Alan J. Thorpe 1987: Baroclinic instability in an environment of small stability to slantwise moist convection. Part I: Two-dimensional models; *J. Atmos. Sci.* **44** (12), 1559–1573.
- Erickson, C. O. 1963: An incipient hurricane near the west African coast; *Mon. Weather Rev.* **91**, 61–68.

- Espy, J. P. 1835: Theory of rain, hail, snow and the water spout, deduced from the latent caloric of vapour and the specific caloric of atmospheric air; *Trans. Geol. Soc. Penn.* **1** (2), 342–346.
- Espy, James P. 1841: *Philosophy of Storms*; Little and Brown, Boston, Massachusetts, 552pp.
- Farrell, Brian 1988: Optimal excitation of neutral Rossby waves; *J. Atmos. Sci.* **45** (2), 163–172.
- Ferrel, W. 1856: An essay on the winds and the currents of the ocean, *Nashville J. Medicine and Surgery* **9** (4, 5). Reprinted in 1882: *Professional Papers of the Signal Service* **12**, U.S. War Dept., Washington, D.C., 7–19.
- Fett, Robert W. 1968a: Typhoon formation within the zone of intertropical convergence; *Mon. Weather Rev.* **96** (2), 106–117.
- Fett, Robert W. 1968b: Some unusual aspects concerning the development and structure of typhoon Billie—July 1967; *Mon. Weather Rev.* **96** (9), 637–648.
- Fisher, Edwin L. 1958: Hurricanes and the sea-surface temperature field; *J. Meteor.* **15** (3), 328–333.
- Foster, I. J. and T. J. Lyons 1984: Tropical cyclogenesis: a comparative study of two depressions in the northwest of Australia; *Quart. J. Roy. Met. Soc.* **110**, 105–119.
- Fraedrich, Klaus and John L. McBride 1988: The physical mechanism of CISK and the free-ride balance; *J. Atmos. Sci.* **46** (17), 2642–2648.
- Frank, Neil L. and Gilbert Clark 1979: Atlantic tropical systems of 1978; *Mon. Weather Rev.* **107** (8), 1035–1041.
- Frank, Neil L. and Paul J. Hebert 1974: Atlantic tropical systems of 1973; *Mon. Weather Rev.* **102** (4), 290–295.
- Frank, William M. 1977a: Structure and energetics of the tropical cyclone: I. Storm structure; *Mon. Weather Rev.* **105** (9), 1119–1135.
- Frank, William M. 1977b: Structure and energetics of the tropical cyclone: II. Dynamics and energetics; *Mon. Weather Rev.* **105** (9), 1136–1150.
- Frank, William M. 1977c: Convective fluxes in tropical cyclones; *J. Atmos. Sci.* **34**, 1554–1568.
- Frank, William M. 1984: A composite analysis of the core of a mature hurricane; *Mon. Weather Rev.* **112** (12), 2401–2420.

- Frank, William M. 1987: Tropical cyclone formation; in Russel L. Elsberry (ed.), William M. Frank, Greg J. Holland, Jerry D. Jarrell, Robert L. Southern 1987: *A Global View of Tropical Cyclones*; based largely on material prepared for the International Workshop on Tropical Cyclones, Bangkok, Thailand, November 25–December 5, 1985; published privately Russell L. Elsberry, Naval Postgraduate School, Monterey, California, 53–90.
- Frank, William M. and Charles Cohen 1987: Simulation of tropical convective systems. Part I: A cumulus parameterization; *J. Atmos. Sci.* **44** (24), 3787–3799.
- Frank, William M. and Charles Cohen 1989: Lapse rate adjustment in the tropical atmosphere; *Eighteenth Conference on Hurricanes and Tropical Meteorology, May 16–19, 1989 (extended abstracts)*, American Meteorological Society, Boston, Massachusetts, 159–160.
- Gentry, R. Cecil, Edward Rogers, Joseph Steranka, and William E. Shenk 1980: Predicting tropical cyclone intensity using satellite-measured equivalent blackbody temperatures of cloud tops; *Mon. Weather Rev.* **108**, 445–455.
- Gill, A. 1982: Spontaneous growing hurricanelike disturbances in a simple baroclinic model with latent heat release; appendix by J. M. Smith, in L. Bengtsson and J. Lighthill, eds., *Intense Atmospheric Vortices*, Springer-Verlag, 111–130.
- Gray, William M. 1968: Global view of the origin of tropical disturbances and storms; *Mon. Weather Rev.* **96** (10), 669–700.
- Gray, W. M. 1973: Cumulus convection and larger scale circulations, I: Broadscale and mesoscale considerations; *Mon. Weather Rev.* **101**, 839–855.
- Gray, William M. 1975: Tropical cyclone genesis; Dept. Atmospheric Sci. Paper No. 234, Colorado State University, Fort Collins, 121pp.
- Gray, William M. 1979: Hurricanes: Their formation, structure and likely role in tropical circulation; in D. B. Shaw, ed., *Meteorology over the Tropical Oceans*, Royal Meteorological Society, Bracknell, Berkshire, England, 155–218.
- Gray, William M. and Dennis J. Shea 1973: The hurricane's inner core region. II. Thermal stability and dynamic characteristics; *J. Atmos. Sci.* **30** (8), 1565–1576.
- Greenspan, H. P. and L. N. Howard 1963: On a time-dependent motion of a rotating fluid; *J. Fluid Mech.* **17**, 385–404.
- Grube, P. G. 1979: Convection induced temperature change in GATE; Dept. Atmospheric Sci. Paper No. 305, Colorado State University, Fort Collins, 128pp.

- Gyakum, John R. 1983a: On the evolution of the QE II storm. I: Synoptic aspects; *Mon. Weather Rev.* **111** (6), 1137–1155.
- Gyakum, John R. 1983b: On the evolution of the QE II storm. II: Dynamic and thermodynamic structure; *Mon. Weather Rev.* **111** (6), 1156–1173.
- Hack, James J. and Wayne H. Schubert 1986: Nonlinear response of atmospheric vortices to heating by organized cumulus convection; *J. Atmos. Sci.* **43** (15), 1559–1573.
- Handel, Mark David 1990: On the asymmetry of tropical cyclone outflows; MS, Center for Meteorology and Physical Oceanography, Massachusetts Institute of Technology, Cambridge, Massachusetts (in preparation).
- Haque, S. M. A. 1952: The initiation of cyclonic circulation in a vertically unstable stagnant air mass; *Quart. J. Roy. Met. Soc.* **78**, 394–406.
- Hawkins, Harry F. and Stephen M. Imbembo 1976: The structure of a small intense hurricane—Inez 1966; *Mon. Weather Rev.* **104** (4), 418–442.
- Hawkins, Harry F. and Daryl T. Rubsam 1968a: Hurricane Hilda, 1964. I. Genesis as revealed by satellite photographs, conventional and aircraft data, *Mon. Weather Rev.* **96** (7), 428–452.
- Hawkins, Harry F. and Daryl T. Rubsam 1968b: Hurricane Hilda, 1964. II. Structure and budgets of the hurricane on October 1, 1964, *Mon. Weather Rev.* **96** (9), 617–636.
- Hawkins, Harry F. and Daryl T. Rubsam 1968c: Hurricane Hilda, 1964. III. Degradation of the hurricane; *Mon. Weather Rev.* **96** (10), 701–707.
- Hebert, Paul J. 1978: Intensification criteria for tropical depressions of the western North Atlantic; *Mon. Weather Rev.* **106** (6), 831–841.
- Holland, G. J. 1982: Lagrangian angular momentum transports in tropical cyclogenesis; in L. Bengtsson and J. Lighthill, eds., *Intense Atmospheric Vortices*, Springer-Verlag, 51–59.
- Holland, Greg J. 1987: Mature structure and structure change; in Russel L. Elsberry (ed.), William M. Frank, Greg J. Holland, Jerry D. Jarrell, Robert L. Southern 1987: *A Global View of Tropical Cyclones*; based largely on material prepared for the International Workshop on Tropical Cyclones, Bangkok, Thailand, November 25–December 5, 1985; published privately Russell L. Elsberry, Naval Postgraduate School, Monterey, California, 13–52.
- Holton, James R. 1974: Comments on “Moveable CISK”; *J. Atmos. Sci.* **31** (3), 833–834.

- Holton, James R. 1979: *An Introduction to Dynamic Meteorology, 2nd ed.*; Academic, New York, 391pp.
- Houze, Robert J., Jr. 1982: Cloud clusters and large-scale vertical motions in the tropics; *J. Met. Soc. Japan* (Ser. II) **60** (1), 396–410.
- Ince, E. L. 1926: *Ordinary Differential Equations*; reprinted 1956 by Dover, New York, 558pp.
- Jordan, C. L. 1958: Mean soundings of the West Indies area; *J. Meteor.* **15** (1), 91–97.
- Iribarne, J. V. and W. L. Godson 1981: *Atmospheric Thermodynamics, 2nd ed.*; Reidel, Dordrecht, Holland, 259pp.
- Jorgensen, David P. 1984a: Mesoscale and convective-scale characteristics of mature hurricanes. Part I: General observations by research aircraft; *J. Atmos. Sci.* **41** (8), 1268–1285.
- Jorgensen, David P. 1984b: Mesoscale and convective-scale characteristics of mature hurricanes. Part II: Inner core structure of Hurricane Allen (1980); *J. Atmos. Sci.* **41** (8), 1287–1311.
- Jorgensen, David P., Edward J. Zipser and Margaret A. LeMone 1985: Vertical motions in intense hurricanes; *J. Atmos. Sci.* **42** (8), 839–856.
- Juster, Norton 1961: *The Phantom Tollboth*; Jules Feiffer, illus., Epstein & Carroll Assoc., republished by Random House, New York, 256pp.
- Kasahara, A. 1954: Supplementary notes on the formation and the schematic structure of typhoons; *J. Met. Soc. Japan* (Ser. II) **32** (2), 31–52.
- Kasahara, Akira 1961: A numerical experiment on the development of a tropical cyclone; *J. Meteor.* **18**, 259–282.
- Kleinschmidt, E., jun. 1951: Grundlagen einer theorie der tropischen zyklonen; *Archiv Meteor. Geophys. Bioklim.* **A 4**, 53–72. Anonymous unpublished translation by British Meteorological Office as “Principles of the theory of tropical cyclones”.
- Koss, W. J. 1976: Linear stability of CISK-induced disturbances: Fourier component analysis; *J. Atmos. Sci.* **33** (7), 1195–1222.
- Krishnamurti, Ruby 1968: Finite amplitude convection with changing mean temperature. Part 1. Theory; *J. Fluid Mech.* **33** (3), 445–455.
- Krishnamurti, T. N. and D. Oosterhof 1989: Prediction of the life cycle of a supertyphoon with a high-resolution global model; *Bull. Amer. Met. Soc.* **70** (10), 1218–1230.

- Kuo, H. L. 1959: Dynamics of convective vortices and eye formation; in Bert Bolin, ed., *The Atmosphere and the Sea in Motion* (also referred to as *The Rossby Memorial Volume*), Rockefeller Inst. Press with Oxford Univ. Press, New York, 413–424.
- Kuo, H. L. 1964: On formation and intensification of tropical cyclones by deep cumulus convection; *Geof. Int.* **4** (3), 199–205.
- Kurihara, Yoshio 1975: Budget analysis of a tropical cyclone simulated in an axisymmetric numerical model; *J. Atmos. Sci.* **32** (1), 25–59.
- Kurihara, Yoshio and Robert E. Tuleya 1981: A numerical study on the genesis of a tropical storm; *Mon. Weather Rev.* **109**, 1629–1653.
- Kutzbach, Gisela 1979: *The Thermal Theory of Cyclones*; American Meteorological Society, Boston, Massachusetts, 255pp.
- Lee, Cheng-Shang 1986: An observational study of tropical cloud cluster evolution and cyclogenesis in the western North Pacific; Dept. Atmospheric Sci. Paper No. 403, Colorado State University, Fort Collins, 250pp.
- Lee, Cheng Shang 1989a: Observational analysis of tropical cyclogenesis in the western North Pacific. Part I: Structural evolution of cloud clusters; *J. Atmos. Sci.* **46** (16), 2580–2598.
- Lee, Cheng Shang 1989b: Observational analysis of tropical cyclogenesis in the western North Pacific. Part II: Budget analysis; *J. Atmos. Sci.* **46** (16), 2599–2616.
- Lee, Cheng-Shang, Roger Edson and William M. Gray 1989: Some large-scale characteristics associated with tropical cyclone development in the north Indian Ocean during FGGE; *Mon. Weather Rev.* **117** (2), 407–426.
- Liebmann, Brant and Harry Hendon 1989: Easterly waves along the equator; *Eighteenth Conference on Hurricanes and Tropical Meteorology, May 16–19, 1989 (extended abstracts)*, American Meteorological Society, Boston, Massachusetts, 22–23.
- Lilly, Douglas K. 1960: On the theory of disturbances in a conditionally unstable atmosphere; *Mon. Weather Rev.* **88** (1), 1–19.
- Lindzen, R. S. 1974: Wave-CISK in the tropics; *J. Atmos. Sci.* **31** (1), 156–179.
- Lopez, R. E. 1973: Cumulus convection and larger scale circulations, II: Cumulus and mesoscale interactions; *Mon. Weather Rev.* **101**, 856–870.
- Lord, Stephen J., Hugh E. Willoughby and Jacqueline M. Piotrowicz 1984: Role of a parameterized ice-phase microphysics in an axisymmetric, nonhydrostatic tropical cyclone model; *J. Atmos. Sci.* **41** (19), 2836–2848.

- Lorenz, Edward N. 1955: Available potential energy and the maintenance of the general circulation; *Tellus* **7** (2), 157–167.
- Love, Geoff 1985: Cross-equatorial interactions during tropical cyclogenesis; *Mon. Weather Rev.* **113** (9), 1499–1509.
- Ludlam, David M. 1963: *Early American Hurricanes 1492–1870*; American Meteorological Society, Boston, Massachusetts, 198pp.
- Ludlam, David M. 1969: The Espy-Redfield dispute; *Weatherwise* **22**, 224–229, 245, 261.
- Lunney, Patrick A. 1988: Environmental and convective influences on tropical cyclone development vs. non-development; Dept. Atmospheric Sci. Paper No. 436, Colorado State University, Fort Collins, 105pp.
- Lyons, Walter A, Monique G. Venne, Peter G. Black, R. Cecil Gentry 1989: Hurricane lightning: a new diagnostic tool for tropical storm forecasting?"; *Eighteenth Conference on Hurricanes and Tropical Meteorology, May 16–19, 1989 (extended abstracts)*, American Meteorological Society, Boston, Massachusetts, 113–114.
- Mak, M. 1981: An inquiry on the nature of CISK. Part I; *Tellus* **33**, 531–537.
- Malkus, J. S. and H. Riehl 1960: On the dynamics and energy transformations in steady-state hurricanes; *Tellus* **12** (1), 1–20.
- Malkus, W. V. R. and G. Veronis 1958: Finite amplitude cellular convection; *J. Fluid Mech.* **4**, 225–260.
- Marks, Frank D., Jr. and Robert A. Houze, Jr. 1987: Inner core structure of Hurricane Alicia from airborne Doppler radar observations; *J. Atmos. Sci.* **44** (9), 1296–1317.
- Mass, Clifford 1979: A linear primitive equation model of African wave disturbances; *J. Atmos. Sci.* **36** (11), 2075–2092.
- McBride, John L. 1981a: Observational analysis of tropical cyclone formation. Part I: Basic description of data sets; *J. Atmos. Sci.* **38** (6), 1117–1131.
- McBride, John L. 1981b: Observational analysis of tropical cyclone formation, Part III. Budget analysis; *J. Atmos. Sci.* **38** (6), 1152–1166.
- McBride, J. L. and T. D. Keenan 1982: Climatology of tropical cyclone genesis in the Australian region; *J. Climatology* **2** (1), 13–33.
- McBride, John L. and Raymond Zehr 1981: Observational analysis of tropical cyclone formation. Part II: Comparison of non-developing versus developing systems; *J. Atmos. Sci.* **38** (6), 1132–1151.

- McWilliams, James Cyrus 1971: *The Boundary Layer Dynamics of Symmetric Vortices*; thesis, Harvard University, Cambridge, Massachusetts, 89pp.
- McWilliams, J. C. 1984: The emergence of isolated coherent vortices in turbulent flow, *J. Fluid Mech.* **146**, 21–43.
- Melander, M. V., J. C. McWilliams, and N. J. Zabusky 1987: Axisymmetrization and vorticity-gradient intensification of an isolated two-dimensional vortex through filamentation, *J. Fluid Mech.* **178**, 137–159.
- Merceret, Francis J. 1976: The turbulent microstructure of hurricane Caroline (1975); *Mon. Weather Rev.* **104** (10), 1297–1307.
- Merrill, Robert T. 1984: A comparison of large and small tropical cyclones; *Mon. Weather Rev.* **112** (7), 1408–1418.
- Merrill, R. T. 1988a: Characteristics of the upper-tropospheric environmental flow around hurricanes; *J. Atmos. Sci.* **45** (11), 1665–1677.
- Merrill, R. T. 1988b: Environmental influences on hurricane intensification; *J. Atmos. Sci.* **45** (11), 1678–1687.
- Middlebrooke, Mike and William M. Gray 1987: Comparison of low-level aircraft observations between early stage developing and non-developing tropical disturbances in the Northwest Pacific; *Seventeenth Conf. on Hurricanes and Tropical Meteorology, April 7–10, 1987 (extended abstracts)*, American Meteorological Society, Boston, Massachusetts, 200–203.
- Miller, Banner I., Peter P. Chase, and Brian R. Jarvinen 1972: Numerical prediction of tropical weather systems; *Mon. Weather Rev.* **100** (12), 825–835.
- Miller, Ronald Lindsay 1990: Topics of Shear Instability: a: Viscous Destabilization of Stratified Shear Flow, b: Organization of Rainfall by an Unstable Jet Aloft; thesis, Massachusetts Institute of Technology, Cambridge, Massachusetts, 153pp.
- Molinari, John and Steven Skubis 1985: Evolution of the surface wind field in an intensifying tropical cyclone; *J. Atmos. Sci.* **42** (24), 2865–2879.
- Molinari, John and David Vollaro 1989: External influences on hurricane intensity. Part I: Outflow layer eddy angular momentum fluxes; *J. Atmos. Sci.* **46** (8), 1093–1105.
- Moss, Michael S. and Francis J. Merceret 1976: A note on several low-layer features of Hurricane Eloise (1975); *Mon. Weather Rev.* **104** (7), 967–971.
- Neelin, J. David, Isaac M. Held and Kerry H. Cook 1987: Evaporation-wind feedback and low-frequency variability in the tropical atmosphere; *J. Atmos. Sci.* **44** (16), 2341–2348.

- Norquist, Donald C., Ernest E. Recker, and Richard J. Reed 1977: The energetics of African wave disturbances as observed during Phase III of GATE; *Mon. Weather Rev.* **105** (3), 334–342.
- Nuss, Wendell A. 1989: Air-sea interaction influences on the structure and intensification of an idealized marine cyclone; *Mon. Weather Rev.* **117** (2), 351–369.
- Ogura, Y. 1964: Frictionally controlled, thermally driven circulations in a circular vortex with applications to tropical cyclones; *J. Atmos. Sci.* **21** (6), 610–621.
- Ooyama, Katsuyuki 1964: A dynamical model for the study of tropical cyclone development; *Geof. Int.* **4** (3), 187–198.
- Ooyama, Katsuyuki 1969: Numerical simulation of the life cycle of tropical cyclones; *J. Atmos. Sci.* **26** (1), 3–40.
- Ooyama, K. V. 1982: On basic problems in theory and modeling of the tropical cyclone, in L. Bengtsson and J. Lighthill, eds., *Intense Atmospheric Vortices*, Springer-Verlag, 21–34. Reprinted with only minor changes as: Conceptual evolution of the theory and modeling of the tropical cyclone; *J. Met. Soc. Japan* (Ser. II) **60** (1), 369–380.
- Orszag, Steven A. and Anthony T. Patera 1983: Secondary instability of wall bounded shear flow; *J. Fluid Mech.* **128**, 347–385.
- Palmén, Erik 1948: On the formation and structure of tropical hurricanes; *Geophysica* **3**, 26–38.
- Palmén, E. 1956: Formation and development of tropical cyclones; *Proc. Tropical Cyclone Symp., Brisbane, Australia*, 213–231.
- Palmén, E. and C. W. Newton 1969: Tropical cyclones, hurricanes, and typhoons; ch. 15 of *Atmospheric Circulation Systems*, Academic, New York, 603pp.
- Paluch, Ilga R. 1979: The entrainment mechanism in Colorado cumuli; *J. Atmos. Sci.* **36** (12), 2467–2478.
- Pedersen, Torben Strunge and Erik Rasmussen 1985: On the cut-off problem in linear CISK models; *Tellus* **37A** (Polar low special issue), 394–402.
- Pelroth, Irving 1962: Relationship of central pressure of Hurricane Esther (1961) and the sea surface temperature field; *Tellus* **14** (4), 403–408.
- Pelroth, Irving 1967: Hurricane behavior as related to oceanographic environmental conditions; *Tellus* **19** (2), 258–268.
- Pelroth, Irving 1969: Effects of oceanographic media on equatorial Atlantic hurricanes; *Tellus* **21** (2), 230–244.

- Pfeffer, Richard L. 1958: Concerning the mechanics of hurricanes; *J. Meteor.* **15** (1), 113–120.
- Pfeffer, Richard L. and Malakondayya Challa 1981: A numerical study of the role of eddy fluxes of momentum in the development of Atlantic hurricanes; *J. Atmos. Sci.* **35** (11), 2392–2398.
- Piersig, Walter 1944: The cyclonic disturbances of the sub-tropical eastern North Atlantic; *Bull. Amer. Met. Soc.* **25** (1), 2–69. Adapted from Parts II and III of 1936: Schwankungen von Luftdruck und Luftbewegung sowie ein Beitrag zum Wettergeschehen in Passategebeit des ostlichen Nord-atlantischen Ozeans (Variations of pressure and wind: A treatise on the weather of the trade wind region of the eastern North Atlantic); *Archiv der deutschen Seewarte* **54** (6).
- Ramage, C. S. 1959: Hurricane development; *J. Meteor.* **16** (3), 227–237.
- Randel, William J., Duane E. Stevens, John L. Stanford 1987: A study of planetary waves in the southern winter troposphere and stratosphere. Part II: Life cycles; *J. Atmos. Sci.* **44** (6), 936–949.
- Rasmussen, E. 1979: The polar low as an extratropical CISK disturbance; *Quart. J. Roy. Met. Soc.* **105**, 531–549.
- Rasmussen, Erik 1985: A case study of a polar low development over the Berents Sea; *Tellus* **37A** (Polar low special issue), 407–418.
- Rasmussen, Erik and Magne Lystad 1987: The Norwegian polar lows project: A summary of the International Conference on Polar Lows; 20–23 May 1986, Oslo, Norway; *Bull. Amer. Met. Soc.* **68** (7), 801–816.
- Redfield 1831: Remarks on the prevailing storms of the Atlantic coast of the North American States; *Am. J. Sci. Arts* **20** (1), 17–51.
- Reed, Richard J. and Mark D. Albright 1986: A case study of explosive cyclogenesis in the eastern Pacific; *Mon. Weather Rev.* **114** (12), 2297–2319.
- Reed, Richard J. and Warren Blier 1986: A further study of comma cloud development in the eastern Pacific; *Mon. Weather Rev.* **114** (9), 1696–1708.
- Reed, Richard J. and E. E. Recker 1971: Structure and properties of synoptic-scale wave disturbances in the equatorial western Pacific; *J. Atmos. Sci.* **28** (7), 1117–1133.
- Reeves, Robert W., Chester F. Ropelewski, Michael D. Hudlow 1979: Relationships between large-scale motion and convective precipitation during GATE; *Mon. Weather Rev.* **107** (9), 1154–1168.
- Riehl, Herbert 1948a: On the formation of typhoons, *J. Meteor.* **5** (6), 247–264.

- Riehl, Herbert 1948b: On the formation of west Atlantic hurricanes; *Studies of the Upper-Air Conditions in Low Latitudes*, Part I, Miscellaneous Reports No. 24 of the Department of Meteorology of the University of Chicago, University of Chicago Press, 1-67.
- Riehl, Herbert 1950: A model of hurricane formation; *J. Appl. Phys.* **21**, 917-925.
- Riehl, Herbert 1954: *Tropical Meteorology*; McGraw-Hill, New York, 392pp.
- Riehl, Herbert 1975: Further studies on the origin of hurricanes; Dept. Atmospheric Sci. Paper No. 235, Colorado State University, Fort Collins, 8pp., 25 figs.
- Riehl, Herbert and Joanne Malkus 1961: Some aspects of Hurricane Daisy, 1958; *Tellus* **13** (2), 181-213.
- Rodenhuis, David 1971: A note concerning the effect of gravitational stability upon the CISK model of tropical disturbances; *J. Atmos. Sci.* **28**, 126-129.
- Rotunno, Richard and Kerry A. Emanuel 1987: An air-sea interaction theory for tropical cyclones. Part II: Evolutionary study using a nonhydrostatic axisymmetric numerical model; *J. Atmos. Sci.* **44** (3), 542-561.
- Rosenthal, Stanley L. 1961: Concerning the mechanics and thermodynamics of the inflow layer of the mature hurricane; National Hurricane Research Project Report No. 47, National Hurricane Research Laboratory, Miami, Florida, 31pp.
- Rosenthal, Stanley L. 1962: A theoretical analysis of the field of motion in the hurricane boundary layer; National Hurricane Research Project Report No. 56, National Hurricane Research Laboratory, Miami, Florida, 12pp.
- Rosenthal, Stanley L. 1978: Numerical simulation of tropical cyclone development with latent heat release by the resolved scales. I: Model description and preliminary results; *J. Atmos. Sci.* **35**, 258-271.
- Sadler, James C. 1976: A role of the tropical upper tropospheric trough in early season typhoon development; *Mon. Weather Rev.* **104** (10), 1266-1278.
- Sadler, James C. 1978: Mid-season typhoon development and intensity changes and the tropical upper tropospheric trough; *Mon. Weather Rev.* **106** (8), 1137-1152.
- de Saint Exupéry, Antoine 1943, *Le Petit Prince*; Harcourt-Brace, New York, 113pp.
- Sawyer, J. S. 1947: Notes on the theory of tropical cyclones; *Quart. J. Roy. Met. Soc.* **73**, 101-126.

- Schlüter, A., D. Lortz and F. Busse 1965: On the stability of finite amplitude convection; *J. Fluid Mech.* **28**, 223–239.
- Schubert, Wayne H. and James J. Hack 1982: Inertial stability and tropical cyclone development; *J. Atmos. Sci.* **39** (8), 1687–1697.
- Schubert, Wayne H. and James J. Hack 1983: Transformed Eliassen balanced vortex model; *J. Atmos. Sci.* **40**, 1571–1583.
- Schubert, Wayne H., James J. Hack, Pedro L. Silva Dias and Scott R. Fulton 1980: Geostrophic adjustment in an axisymmetric vortex; *J. Atmos. Sci.* **37** (7), 1464–1484.
- Scofield, Edna 1938: On the origin of tropical cyclones; *Bull. Amer. Met. Soc.* **19**, 244–256.
- Sears, Francis W. and Gerhard L. Salinger 1975: *Thermodynamics, Kinetic Theory, and Statistical Mechanics*, third ed.; Addison-Wesley, Reading, Massachusetts, 454pp.
- Shapiro, Lloyd J. 1977: Tropical storm formation from easterly waves: A criterion for development; *J. Atmos. Sci.* **34**, 1007–1021.
- Shapiro, L. 1982a: Hurricane climatic fluctuations, Part I: Patterns and cycles; *Mon. Weather Rev.* **110**, 1007–1013.
- Shapiro, L. 1982b: Hurricane climatic fluctuations, Part II: Relation to large-scale circulation; *Mon. Weather Rev.* **110**, 1014–1023.
- Shapiro, Lloyd J. and Hugh E. Willoughby 1982: The response of balanced hurricanes to local sources of heat and momentum; *J. Atmos. Sci.* **39** (2), 378–394.
- Shea, Dennis J. and William M. Gray 1973: The hurricanes's inner core region. I. Symmetric and asymmetric structure; *J. Atmos. Sci.* **30** (8), 1544–1564.
- Sheets, R. C. 1979: Some aspects of tropical cyclone modification; *Aust. Meteor. Mag.* **27** (4), 259–280.
- Shutts, G. J., M. Booth, and J. Norbury 1988: A geometric model of balanced, axisymmetric flows with embedded penetrative convection; *J. Atmos. Sci.* **45** (19), 2609–2621.
- Shutts, Glenn J. and Alan J. Thorpe 1978: Some aspects of vortices in rotating, stratified fluids; *PAGEOPH* **116**, 993–1006.
- Simpson, Joanne, Michael Garstang, Edward J. Zipser and Gordon A. Dean 1967: A study of a non-deepening tropical disturbance; *J. Appl. Met.* **6** (2), 237–254.
- Simpson, R. H. 1954: Structure of an immature hurricane; *Bull. Amer. Met. Soc.* **35** (8), 335–350.

- Simpson, R. H. 1974: The hurricane disaster potential scale; *Weatherwise* **27**, 169, 186.
- Simpson, R. H., Neil Frank, David Shideler, and J. M. Johnson 1969: Atlantic tropical systems of 1968; *Mon. Weather Rev.* **97** (3), 240–255.
- Simpson, Robert H. and Herbert Riehl 1981: *The Hurricane and Its Impact*; Louisiana State University Press, Baton Rouge, Louisiana, 398pp.
- Solberg, H. 1936: Le mouvement d'inertie de l'atmosphère stable et son rôle dans la théorie des cyclones; *Procès-verbaux de l'assoc. de Meteorolog. Un. Geod. Geophys. Int.*, Edinbourg, 66–82.
- Southern, R. L. 1979: The global socio-economic impact of tropical cyclones; *Aus. Meteor. Mag.* **27** (4), 175–195.
- Spar, Jerome 1964: A survey of hurricane development; *Geof. Int.* **4**, 169–178.
- Stossmeister, Greg J. and Gary M. Barnes 1989: Low-level structure of a non-developing tropical storm: Isabel (1985); *Eighteenth Conference on Hurricanes and Tropical Meteorology, May 16–19, 1989 (extended abstracts)*, American Meteorological Society, Boston, Massachusetts, 83–84.
- Steranka, J., E. B. Rogers and R. C. Gentry 1986: The relationship between satellite measured convective bursts and tropical cyclone intensification; *Mon. Weather Rev.* **114**, 1539–1546.
- Stevens, Duane E., Richard S. Lindzen and Lloyd J. Shapiro 1977: A new model of tropical waves incorporating mixing by cumulus convection; *Dynam. Atmos. Oceans* **1** (5), 365–425.
- Sundqvist, Hilding 1970: Numerical simulation of the development of tropical cyclones with a ten-level model. Part I.; *Tellus* **22** (4), 359–390.
- Syōno, S. 1953: On the formation of tropical cyclones; *Tellus* **5** (2), 179–195.
- Syōno, S., Y. Ogura, K. Gambo and A. Kasahara 1951: On the negative vorticity in a typhoon; *J. Met. Soc. Japan* (Ser. II) **29** (12), 397–415.
- Syōno, S. and M. Yamasaki 1966: Stability of symmetrical motions by latent heat released by cumulonimbus convection under the existence of surface friction; *J. Met. Soc. Japan* (Ser. II) **44** (6), 353–375.
- Takahashi, T., T. Watanabe, S. Kubota, T. Ando and N. Nakamura 1951: The structure and energy of typhoons; *J. Met. Soc. Japan* (Ser. II) **29** (3), 69–85.
- Tannehill, I. R. 1935: A relation between temperature and cyclone-frequency in the tropics; *Trans. Amer. Geophys. Un.* **16** (1), 121–124.

- Thompson, Owen E. and JoAnna Miller 1976: Hurricane Carmen: August–September 1974 — Development of a wave in the ITCZ; *MWR* **104** (9), 1194–1199.
- Thompson, Robert M., Jr., Steven W. Payne, Ernest E. Recker and Richard J. Reed 1979: Structure and properties of synoptic-scale wave disturbances in the intertropical convergence zone of the eastern Atlantic; *J. Atmos. Sci.* **36** (1), 53–72.
- Thorpe, A. J. 1985: Diagnosis of balanced vortex structure using potential vorticity; *J. Atmos. Sci.* **42** (4), 397–406.
- Tuleya, Robert E. 1988: A numerical study of the genesis of tropical storms observed during the FGGE year; *Mon. Weather Rev.* **116** (5), 1188–1208.
- Tuleya, R. E. and Y. Kurihara 1981: A numerical study on the effects of environmental flow on tropical storm genesis; *Mon. Weather Rev.* **109**, 2487–2506.
- Venne, Monique G., Walter A. Lyons, Cecil S. Keen, Peter G. Black, R. Cecil Gentry 1989: Explosive supercell growth: A possible indicator for tropical storm intensification?; *Twenty-fourth Conf. on Radar Meteorology, March 24–31, 1989, Talahasee, Florida*, American Meteorological Society, Boston, Massachusetts, 545–548.
- Veronis, George 1981: A theoretical model of Henry Stommel; in Bruce A. Warren and Carl Wunsch, eds., *Evolution of Physical Oceanography*, MIT Press, Cambridge, Massachusetts, xix–xxiii.
- Vincent, Dayton G. and Robert G. Waterman 1979: Large-scale atmospheric conditions during the intensification of Hurricane Carmen (1974): I. Temperature, moisture and kinematics; *Mon. Weather Rev.* **107** (3), 283–294.
- Wada, Misuzu 1989: The effects of ice phase on cumulus organization; *Eighteenth Conference on Hurricanes and Tropical Meteorology, May 16–19, 1989 (extended abstracts)*, American Meteorological Society, Boston, Massachusetts, 133–134.
- Wang, Bin 1987: The nature of CISK in a generalized continuous model; *J. Atmos. Sci.* **44** (10), 1411–1426.
- Warner, C., J. Simpson, G. Van Helvoirt, D. W. Martin, D. Suchman, G. L. Austin 1980: Deep convection on day 261 of GATE; *Mon. Weather Rev.* **108** (2), 169–194.
- Weatherford, Candis L. and William M. Gray 1988a: Typhoon structure as revealed by aircraft reconnaissance. Part I: Data analysis and climatology; *Mon. Weather Rev.* **116** (5), 1032–1043.

- Weatherford, Candis L. and William M. Gray 1988b: Typhoon structure as revealed by aircraft reconnaissance. Part II: Structural variability; *Mon. Weather Rev.* **116** (5), 1044–1056.
- Weatherford, Candis L. 1989: The structural evolution of typhoons; Dept. Atmospheric Sci. Paper No. 446, Colorado State University, Fort Collins, 198pp.
- Wendland, Wayne M. 1977: Tropical storm frequencies related to sea surface temperature; *J. Appl. Met.* **16**, 477–481.
- Willheim, Ernst 1980: A legal regime for artificial cyclone modification; *Aust. Meteor. Mag.* **28** (1), 1–6.
- Willoughby, H. E. 1990: Temporal changes of the primary circulation in tropical cyclones; *J. Atmos. Sci.* **47** (2), 242–264.
- Willoughby, H. E., J. A. Clos and M. G. Shoreibah 1982: Concentric eye walls, secondary wind maxima and the evolution of the hurricane vortex; *J. Atmos. Sci.* **39** (2), 395–411.
- Willoughby, Hugh E. and Han-Liang Jim, Stephen J. Lord and Jacqueline M. Piotrowicz 1984a: Hurricane structure and evolution as simulated by an axisymmetric, nonhydrostatic model; *J. Atmos. Sci.* **41** (7), 1169–1188.
- Willoughby, Hugh E., Frank D. Marks, Jr. and Robert J. Feinberg 1984b: Stationary and moving convective bands in hurricanes; *J. Atmos. Sci.* **41** (22), 3189–3211.
- Willoughby, H. E., D. P. Jorgensen, R. A. Black, and S. L. Rosenthal 1985: Project STORMFURY: A scientific chronicle, 1962–1983; *Bull. Amer. Met. Soc.* **66** (5), 505–514.
- WMO 1966: *International Meteorological Vocabulary*; WMO/OMM/BMO–No. 182. TP. 91, World Meteorological Organization, Geneva, 276pp.
- Wright, Stanley 1976: The comparable development of Tropical Storm Hallie with a gulf tropical disturbance; *Mon. Weather Rev.* **104**, 1451–1454.
- Xu, Kuanman 1987: Vertical structure and the convective characteristics of the tropical atmosphere; M.S. thesis, Dept. of Earth, Atmospheric, and Planetary Sciences, Massachusetts Institute of Technology, Cambridge, Massachusetts, 121pp.
- Xu, Kuanman and Kerry A. Emanuel 1989: Is the tropical atmosphere conditionally unstable?; *Mon. Weather Rev.* **117**, 1471–1479.
- Yamasaki, Masanori 1968a: Numerical simulation of tropical cyclone development with the use of primitive equations; *J. Met. Soc. Japan* (Ser. II) **46** (3), 178–201.

- Yamasaki, Masanori 1968b: A tropical cyclone model with parameterized vertical partition or released latent heat; *J. Met. Soc. Japan* (Ser. II) **46** (3), 202–214.
- Yamasaki, Masanori 1977: A preliminary experiment of the tropical cyclone without parameterizing the effects of cumulus convection; *J. Met. Soc. Japan* (Ser. II) **55** (1), 11–31.
- Yanai, Michio 1961a: A detailed analysis of typhoon formation; *J. Met. Soc. Japan* (Ser. II) **39** (4), 187–214.
- Yanai, Michio 1961b: Dynamical aspects of typhoon formation; *J. Met. Soc. Japan* (Ser. II) **39** (5), 282–309.
- Yanai, Michio 1964: Formation of tropical cyclones; *Rev. Geophys.* **2** (2), 367–414.
- Yanai, Michio 1968: Evolution of a tropical disturbance in the Caribbean Sea region; *J. Met. Soc. Japan* (Ser. II) **46** (2), 86–109.
- Yanai, Michio, Steven Esbensen and Jan-Hwa Chu 1973: Determination of bulk properties of tropical cloud clusters from large-scale heat and moisture budget; *J. Atmos. Sci.* **30** (4), 611–627.
- Yanai, M., J.-H. Chu, T. E. Stark, Tsuyoshi Nitta 1976: Response of deep and shallow tropical maritime cumuli to large-scale processes; *J. Atmos. Sci.* **33** (6), 976–991.

... et Pangloss disait quelquefois à Candide: "Tous les événements sont enchaînés dans le meilleur des mondes possibles; car enfin si vous n'aviez pas été chassé d'un beau château à grands coups de pied dans le derrière pour l'amour de Mlle Cunégonde, si vous n'aviez pas été mis à l'inquisition, si vous n'aviez pas couru l'Amérique à pied, si vous n'aviez pas donné un bon coup d'épée au baron, si vous n'aviez pas perdu tous vos moutons du bon pays d'Eldorado, vous ne mangeriez pas ici des cédrats confits et des pistaches.— Cela est bien dit, répondit Candide, mais il faut cultiver notre jardin."

Mr. le Docteur Ralph [Voltaire]
Candide, ou l'Optimisme